

Study of variables determining the engraftment and homing of  
human acute myeloid leukemia samples in the NSG mouse  
model

Inauguraldissertation

zur

Erlangung der Würde eines Doktors der Philosophie

vorgelegt der

Philosophisch-Naturwissenschaftlichen Fakultät

der Universität Basel

von

Pauline Hanns

Basel, 2023

Originaldokument gespeichert auf dem Dokumentenserver der Universität Basel

[edoc.unibas.ch](https://edoc.unibas.ch)



Genehmigt von der Philosophisch-Naturwissenschaftlichen Fakultät  
auf Antrag von

Prof. Dr. Claudia Lengerke

Prof. Dr. Markus Affolter

Prof. Dr. César Nombela-Arrieta

Basel, den 19.10.2021

Prof. Dr. Marcel Mayor  
Dekan der Philosophisch-  
Naturwissenschaftlichen Fakultät



# Table of content

<b>Acknowledgments</b> .....	<b>8</b>
<b>Abbreviations</b> .....	<b>11</b>
<b>1. ....</b>	<b>Introduction</b>
.....	<b>18</b>
<b>1.1. Healthy Hematopoiesis</b> .....	<b>18</b>
<b>1.2. Acute Myeloid Leukemia</b> .....	<b>20</b>
1.1.1. Incidence.....	21
1.1.2. Risk factors.....	21
1.1.3. Diagnosis of AML .....	22
1.1.4. AML classification and risk stratification .....	23
1.1.5. Treatment strategies .....	25
1.1.6. Monitoring disease response and eventual relapse.....	26
<b>1.3. Investigation of AML in laboratory settings</b> .....	<b>27</b>
1.1.1. Murine models of AML.....	28
1.1.2. Limitations and factors influencing leukemia induction in the NSG xenotransplantation model	31
<b>1.4. Bone marrow microenvironment in health and disease</b> .....	<b>33</b>
1.1.3. The healthy HSCs niche.....	34
1.1.4. The BM niche in hematological malignancies.....	35
1.1.5. Circadian and adrenergic regulation of the BM niche .....	39
1.1.6. Impact of adrenergic regulation in tumorigenesis .....	44
1.1.7. Cancer cells use similar molecular cues than HSPCs to colonize the BM niche.....	48
<b>2. ....</b>	<b>Aim of this study</b>
.....	<b>54</b>
<b>3. ....</b>	<b>Identification and study of human AML samples' characteristics influencing disease</b>
<b>induction and homing in the NSG mouse model</b> .....	<b>56</b>
<b>1.1. Background of the study</b> .....	<b>56</b>
<b>1.2. Results</b> .....	<b>57</b>
1.1.1. Patient's cohort description .....	57
1.1.2. Vast majority of AML samples lead to disease induction in the year follow mice transplantation	59
1.1.3. Times improves the detection rate of human AML engraftment in NSG mice .....	65
1.1.4. High proportions of human AML cells in the BM at week 16 correlates with reduced survival of the murine recipients.....	67
1.1.5. Intermediate and adverse risk group patient's samples have higher homing rates .....	69
1.1.6. Expression of the CD34+ marker in the AML samples is not affecting the engraftment nor the homing in the murine recipient .....	72
1.1.7. Identification of further patient's characteristics determining the engraftment potential of primary AML cells into the murine recipient .....	77
<b>1.3. Discussion</b> .....	<b>79</b>

<b>4. ....</b>	<b><i>Transplantation at night promotes leukemogenesis via enhanced adrenergic activity</i></b>	<b>90</b>
.....		
1.1.	<b>Manuscript in preparation</b>	<b>90</b>
1.2.	<b>Additional data (not included in the manuscript)</b>	<b>119</b>
1.1.1.	The expression of ARs is heterogenous between AML samples	119
1.1.2.	The number of colony forming unit cells (CFU-C) is not influenced by our time-point of transplantation nor by EPI treatment	120
1.1.3.	EPI treatment does not affect Vcam-1 expression in the murine BM	123
1.1.4.	In vitro adhesion of AML cells but not HSPCs is influenced by EPI treatment	124
1.1.5.	Effect of EPI treatment on the transcriptome of MS-5 stromal cell line	127
1.1.6.	Investigation of EPI treatment on the transcriptome of a primary AML sample and a CB-derived HSPCs sample	130
1.1.7.	EPI particularly influences endothelial cells within the BM microenvironment cells	131
1.3.	<b>Discussion</b>	<b>135</b>
<b>5. ....</b>	<b><i>Materials and Methods</i></b>	<b>144</b>
.....		
1.1.	<b>Primary AML cells and healthy HSPCs</b>	<b>144</b>
1.2.	<b>Cell lines and cell culture</b>	<b>144</b>
1.3.	<b>Xenotransplantation assays</b>	<b>145</b>
1.4.	<b>Bone marrow puncture</b>	<b>146</b>
1.5.	<b>Syngeneic mouse models</b>	<b>147</b>
1.6.	<b>Day/Night transplantation settings</b>	<b>148</b>
1.7.	<b>EPI and propranolol treatment</b>	<b>148</b>
1.8.	<b>CXCR4 and VLA-4 blocking</b>	<b>148</b>
1.9.	<b>Flow cytometry</b>	<b>148</b>
1.10.	<b>Histopathology</b>	<b>150</b>
1.11.	<b>qPCR</b>	<b>151</b>
1.12.	<b>Enzyme-Linked Immunosorbent assays (ELISA)</b>	<b>153</b>
1.13.	<b>VLA-4 affinity assay</b>	<b>154</b>
1.14.	<b>Adhesion assay</b>	<b>154</b>
1.15.	<b>CFU assay from murine PB</b>	<b>154</b>
1.16.	<b>RNA sequencing</b>	<b>155</b>
1.17.	<b>Statistical analysis</b>	<b>157</b>
<b>6. ....</b>	<b><i>Contribution to Publications</i></b>	<b>158</b>
.....		
1.1.	<b>Stress and catecholamine modulate the bone marrow microenvironment to promote tumorigenesis</b>	<b>158</b>
1.2.	<b>Absence of NKG2D ligands defines leukaemia stem cells and mediates their immune evasion</b>	<b>159</b>
1.3.	<b>Modeling hematopoietic disorders in zebrafish.</b>	<b>161</b>

1.4. Acute myeloid leukemia stem cells: the challenges of phenotypic heterogeneity.....162

1.5. SRP54 mutations induce congenital neutropenia via dominant-negative effects on XBP1 splicing 163

**REFERENCES ..... 166**

**APPENDIX: CV..... 202**

# Acknowledgments

I would like to thank everyone who supported me all the way during my PhD. In particular, I would like to particularly thank the following people that were especially important for me during this time:

Claudia, thank you very much for giving me the opportunity to pursue this work in your lab. I started my scientific career as a master student in your team and was happy to stay for my PhD. Thank you very much for your always helpful scientific advices concerning the exciting projects I had the chance to work on during the last years.

Martina, there are so many aspects in which I want to thank you, on a professional and very importantly also on personal level. You always supported me during these years even in the worse moments I sometimes went through. I've learned so much from you in experimental planning, in writing, in good scientific practice and also especially from your figure making expertise. You were also always there and motivated to organize outings outside the lab and we shared so many good moments.

Of course, I also would like to thank my colleagues and friends in the lab: Chris, Joëlle, Ronja, Marcelle, Marlon, Elsa, Alain and Henrik for all the good times in and outside the lab. Especially, I was very happy to share our wedding with all of you and we really enjoyed the mouse Pinata.

A special thanks to you Marlon, that helped me a lot during my pregnancy and took great care of my mice during my maternity leave.

Also, Anna, I thank you for sharing your mouse expertise with me and for your help.

Markus, César and Jürg, thank you very much for being part of my PhD committee and for giving me input and support during my committee meetings and of course for evaluating this work.

Bien sûr, je voudrais aussi remercier mes parents et ma petite sœur Emilie pour le soutien durant ces années de PhD mais aussi depuis bien plus longtemps. C'est grâce à vous que j'en suis ici aujourd'hui et j'en suis reconnaissante. Merci de m'avoir aidé



à déménager plusieurs fois même si ce n'était pas la porte à côté et d'être venus nous voir les week-end quand nous ne pouvions pas retourner dans le Bas-Rhin car les souris avaient urgemment besoin de moi.

Pour finir naturellement, un énorme merci à toi Antoine. Merci d'avoir été mon bio-informaticien personnel mais aussi et surtout d'être devenu mon mari. Ces dernières années n'auront pas été un long fleuve tranquille mais tu m'as toujours soutenu, et je savais qu'importe la décision que je prendrais, ce serai toujours la meilleure à tes yeux. Merci pour ces soirées de jogging ou de vélo après des moments de stress, pour ces moments de détente après des journées difficiles et pour ces fous rires après les larmes. Et puis surtout.... Merci de m'avoir récemment accompagné sur un nouveau projet, surement le plus beau et le plus important de notre vie. Merci à notre petite Madeline, née à la fin de ce PhD, et qui dès que nous la retrouvons illuminent notre journée de ses sourires malicieux. Tu n'es parmi nous que depuis quelques mois mais déjà tu m'as appris tant de choses et je suis si fière de la famille que nous formons.



# Abbreviations

7-AAD: 7-aminoactinomycin D

AECs: arteriolar endothelial cells

AF700: Alexa Fluor 700

ALL: acute lymphoblastic leukemia

AML: acute myeloid leukemia

APC: allophycocyanin

ARs: adrenergic receptors

ASXL1: ASX transcription regulator 1

BAD: Bcl-2-associated death promoter

BCL-2: B-cell lymphoma 2

BCL-xL: B-cell lymphoma-extra large

BM: bone marrow

Bmal1: brain and muscle Arnt-like protein-1)

BMI1: B-cell specific Moloney murine virus integration site 1)

BMP: bone marrow puncture

BSA: bovine serum albumin

BV605: Brilliant Violet 605

cAMP : cyclic adenosine monophosphate

CAR: CXCL12-abundant reticular

CB: cord blood

CBF: core binding factor

CD: cluster of differentiation

CEBPA: CCAAT enhancer binding protein

CFSE: carboxyfluorescein succinimidyl ester

CFU-C: colony forming unit cell

CLL-1: C-type lectin-like receptor

Clock: circadian locomotor output cycles kaput

CML: chronic myeloid leukemia

COX-2: cyclooxygenase-2

CR: complete remission

CRi: complete remission with incomplete hematologic

Cry: crystal protein  
CXCL: C-X-C motif chemokine  
CXCR: C-X-C chemokine receptor  
DA: dopamine  
DAPI: 4',6-diamidino-2-phenylindole  
DARC: duffy antigen receptor for chemokines  
DEG: differentially expressed gene  
DNMT3A: DNA-methyltransferase 3A  
EDTA: ethylenediamine tetraacetic acid  
ELISA: enzyme-linked immunosorbent assay  
ELN: European leukemia net  
EPI: epinephrine  
ESMO: European society for medical oncology  
ETO: eight twenty one  
FAB: french-american-british  
FAK: focal adhesion kinase  
FC: flow cytometry  
FCS: fetal calf serum  
FGF1: fibroblast growth factor 1  
FITC: fluorescein isothiocyanate  
FLT3: fms-like tyrosine kinase 3  
GAPDH: glyceraldehyde 3-phosphate dehydrogenase  
GCSF: granulocyte colony stimulating factor  
GFP: green fluorescent protein  
GM-CSF: granulocyte-macrophage colony-stimulating factor  
gp130: glycoprotein 130  
HEPES: 4-(2-hydroxyethyl)-1-piperazineethanesulfonic acid  
HSCs: hematopoietic stem cells  
HSPCs: hematopoietic stem and progenitor cells  
HSCT: hematopoietic stem cell transplantation  
IDH: isocitrate dehydrogenase  
IF: intrafemoral  
IL: interleukin  
ITD: internal tandem duplication

IV: intravenous  
JAK2: janus kinase 2 gene  
KIT: tyrosine protein kinase  
LIC: leukemia-initiating cell  
LMO2: lim domain only 2  
LSC: leukemia stem cell  
MACS: magnetic-activated cell sorting  
MDS: myelodysplastic syndrome  
M-CSF: macrophage colony-stimulating factor  
MLL: Mixed lineage leukemia  
MPN: myeloproliferative neoplasm  
MRD: minimal residual disease  
MSCs: mesenchymal stem cells  
NCAM: neural adhesion molecule  
NCCN: national comprehensive cancer network  
NGS: next generation sequencing  
NK: natural killer  
NKG2D: natural killer group D  
NMP1: nucleophosmin  
Npas2: neuronal PAS domain protein 2  
NOD/SCID: non obese diabetic/ severe combined immunodeficient mice  
NOR: norepinephrine  
NSG: NOD/SCID/IL2R $\gamma$ <sup>null</sup>  
PB: peripheral blood  
PBlu: Pacific Blue  
PBGD: phorphobilinogen deaminase  
PBMC: peripheral blood mononuclear cells  
PBS: phosphate-buffered saline  
PD-L1: programmed death ligand 1  
PE: phycoerythrin  
PECy7: phycoerythrin-cyanine 7  
Per: period circadian protein  
PerCP: peridinin-chlorophyll-protein

PFA: paraformaldehyde  
PKA: protein kinase A  
PR: partial remission  
P/S: penicillin/streptavidin  
RANK: receptor activator of NF- $\kappa$ B  
RANKL: receptor activator of NF- $\kappa$ B ligand  
RAS: Rat Sarcoma  
RD: resistant disease  
RT-qPCR: reverse transcription quantitative polymerase chain reaction  
RUNX1: Runt-related transcription factor 1  
SCID: severe combined immunodeficient mice  
SCF: stem cell factor  
SDF-1: stromal-cell derived factor 1  
SECs: sinusoidal endothelial cells  
SIRP $\alpha$ : signal recognition particule  $\alpha$   
SNS: sympathetic nervous system  
Spp1: osteopontin  
t-AML: therapy-related AML  
TEL/ETV6: Ets family transcription factor  
TET: ten-eleven translocation protein  
TF: transcription factors  
TGFbeta: transforming growth factor beta  
TIE2: angiopoietin-1 receptor  
TPO: thrombopoietin  
TP53: tumor protein 53  
USA: United States of America  
VCAM-1: vascular cell adhesion molecule 1  
VEGF: vascular endothelial growth factor  
VLA-4: very late antigen 4  
WBC: white blood cells  
WHO: world health organization  
WT: wild-type  
ZT: zeitgeber



# Summary

Acute myeloid leukemia (AML) is the most frequent hematopoietic malignancy in adults, causing death of about 90% of elderly patients. Cytogenetic and molecular abnormalities are used to categorize AML in favorable, intermediate and adverse risk groups. The classification in one of these groups will directly affect clinical decision-making. Although molecular criteria have significantly improved prognostication and thus AML patient stratification and treatments, they still do not allow full risk prediction. AML is a complex disease with a very high heterogeneity which makes it challenging to accurately reproduce patient phenotypes in murine models. Patient-derived xenografts can reproduce this heterogeneity but display inherent limitations including the long-latency until AML develops in those models.

In this thesis, we aimed to study the variables that determine the *in vivo* leukemogenesis in a xenotransplantation model of human AML samples into NOD/SCID/IL2R $\gamma$ <sup>null</sup> (NSG) mice. We aimed to better understand the impact of the characteristics of the human AML cells, as well as the effect of modulation of the bone marrow (BM) microenvironment of the recipient mice on the homing and engraftment of human AML cells.

Firstly, we could show that the latency of symptomatic AML induction in mice as well as the homing of transplanted AML cells into the murine BM depends on the molecular risk group established in patients. We also gained insights in the kinetics of disease induction by screening for human AML cells in the mice with regular BM biopsies. Moreover, correlation between some AML patient characteristics (expression of some particular surface markers, remission status and Flt3 (Fms-like tyrosine kinase 3) mutational status) and the behavior of the corresponding transplanted AML was observed. This suggests that this mouse model accurately depicts the clinical course of the disease and reproduces important features of human AML.

Furthermore, we observed that xenotransplantation performed at night, together with disturbance of the circadian rhythm in NSG mice, accelerated engraftment and enhanced homing of transplanted human and murine AML cells compared to corresponding procedures performed in the late afternoon. Our work suggests that observed pro-oncogenic effects are mediated by catecholamines and we could prevent them by beta-blocker treatment. Therefore, varying the transplantation time-



point or inducing a stress response may optimize AML xenograft models and these observations might be important for the knowledge about the tumor-initiation processes in murine models and could possibly be transferred to humans.

# 1. INTRODUCTION

## 1.1. HEALTHY HEMATOPOIESIS

Hematopoiesis is the process of blood production throughout the lifespan of an organism. Mature blood cells are short-lived, which explains why it is estimated that an adult generates around  $4 \times 10^{11}$  differentiated hematopoietic cells per day, including erythrocytes, megakaryocytes, myeloid cells (monocytes, macrophages and neutrophils) and lymphocytes (Orkin and Zon, 2008; Stevenson et al., 1988). Hematopoiesis is a tightly regulated process, organized hierarchically and dominated by hematopoietic stem cells (HSCs) that are characterized by their ability to self-renew (Figure 1a). HSCs give rise to a hierarchy from multipotent to more committed progenitors that have only limited self-renewal properties and a restricted lineage differentiation potential (Figure 1a)(Pinho and Frenette, 2019).

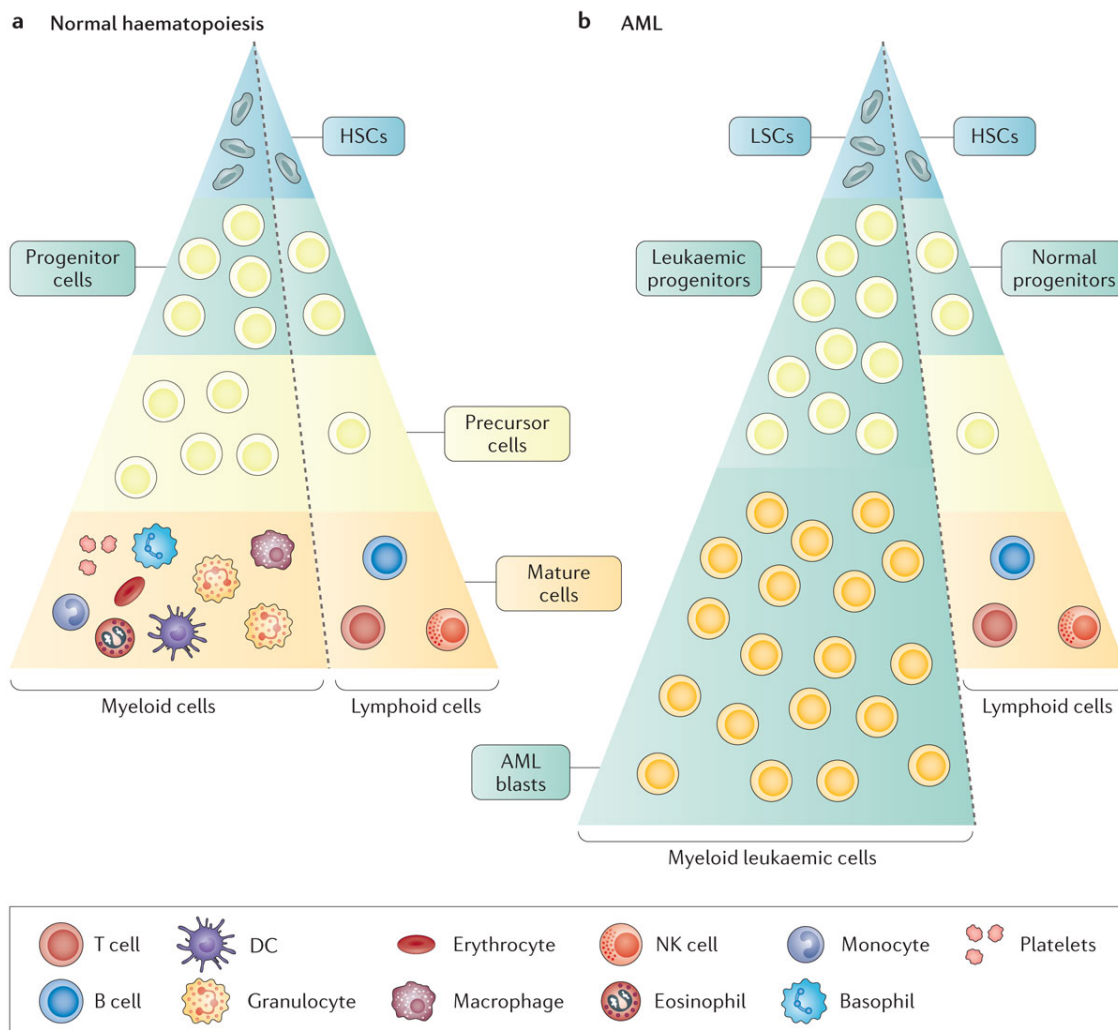


**Figure 1: Normal and leukemic hematopoiesis (adapted from Khwaja et al.)**

a) Normal hematopoiesis is organized as a hierarchy. At the top, the HSCs have extensive self-renewal properties and give rise to more committed hematopoietic progenitors cells. These progenitors will produce precursor cells and then mature hematopoietic cell types.

b) In a similar way, AML is also organized as a hierarchy, with leukemic stem cells residing at the top of the pyramid. These stem cells will give rise to leukemic progenitors and mature myeloid blasts. The lymphoid part of hematopoiesis is relatively preserved in comparison to the impaired production of myeloid cells.

*HSCs, hematopoietic stem cells; LSCs, leukemic stem cells; DC, dendritic cells; NK, natural killer*

In adults, HSCs are primarily found in the BM, but this differs during the distinctive stages of development. The sequential sites of hematopoiesis in mammals include the yolk sac, the aorta-gonad mesonephros, the fetal liver and finally the BM. The placenta has also been described as an additional site for hematopoiesis during development (Orkin and Zon, 2008). Interestingly, the properties of HSCs residing in each niche are disparate indicating the important role of the microenvironment in the HSCs characteristics at each stage of development. For example, HSCs in the fetal liver are cycling much more than adult HSCs which are mainly quiescent (Orkin and Zon, 2008). Within the BM, the regulation between quiescence and self-renewal is also of particular importance, in order to balance between dormancy and differentiation of blood cells, either for a basal production of blood or in “emergency” situations, as for example in the context of an infection or inflammation. Therefore, regulation of HSCs can occur either via extrinsic signals of the BM niche or through intrinsic regulation. Extrinsic regulation of HSCs through interactions with niche cells will be detailed later in this work.

Beyond the external regulation driven by the niche, HSCs are also regulated by some intrinsic factors including transcription factors (TF) or epigenetic mechanisms. Transcription factors are key players in the regulation of HSCs development during development and embryogenesis as well as for the process of lineage-restricted differentiation (Orkin and Zon, 2008). The implication of TF in hematopoiesis has been studied using several model organisms including mice but also zebrafish, chicken or drosophila (Orkin and Zon, 2008). Interestingly, important TF involved in healthy

hematopoiesis are also connected with hematopoietic malignancies upon undergoing genetic events such as translocations or somatic mutations. Examples of these TF include MLL (Mixed Lineage Leukemia), RUNX1 (Runt-related transcription factor 1), TEL/ETV6 (Ets family transcription factor) or LMO2 (Lim Domain only 2) (Orkin and Zon, 2008). Epigenetic modulation, defined as all types of modifications of the chromatin that are involved in transcriptional activity, is also of particular interest for the intrinsic regulation of HSCs, especially given the fact that most of these modulations are not permanent and thus can be targeted more easily. DNA methylation is one epigenetic mechanism and is driven by DNA methyltransferase enzymes. Mutations in methyltransferases are found in hematological diseases with DNMT3A (DNA methyltransferase 3A) being frequently targeted. Beyond methyltransferases, other genes implicated in DNA methylation have also been described both in healthy hematopoiesis and malignant transformation, including mutations in TET (ten-eleven translocation protein) and IDH (isocitrate dehydrogenase) (Haladyna et al., 2015; Han et al., 2015; Shi et al., 2015).

## 1.2. ACUTE MYELOID LEUKEMIA

AML is a group of leukemia affecting both children and adults for whom it is described as the most common malignant myeloid disorder. The pathophysiology of AML consists in genetic abnormalities in healthy hematopoietic progenitors that lead to the proliferation of malignant myeloblasts that accumulate in the BM and the peripheral blood (PB), but that can also manifest in extramedullary tissues (Khwaja et al., 2016). The expansion of malignant immature myeloid cells goes in pair with abnormal production of blood and differentiated hematopoietic cells including red blood cells, platelets and leukocytes (Khwaja *et al.*, 2016). Consequently, patients with AML exhibit typical BM failure symptoms such as frequent infections due to neutropenia, uncontrolled bleeding due to thrombocytopenia, as well as fatigue and shortness of breath due to anemia (Khwaja *et al.*, 2016; Levine, 2013). Similar to normal hematopoiesis, AML has a general hierarchical structure. Leukemic stem cells (LSCs), which exhibit self-renewal properties, reside at the top of the pyramid and give rise to more differentiated cells, including leukemic progenitors and AML blasts (Figure 1b) (Khwaja *et al.*, 2016).

### **1.1.1. Incidence**

Age is a very important factor in the development of AML. The median age at diagnosis is approximately 70 years, with an incidence of 20.1 per 100.000 persons affected by year in adults older than 65 years in comparison to 2.0 per 100.000 persons for those younger than 65 years old (Howlader et al., 2019; Khwaja *et al.*, 2016). A partial explanation to the age-related difference can be found in a worse tolerance to therapy and to aggregation of several poor risk factors. Furthermore, older patients are often excluded from clinical trials because of the very strict criteria applied for the inclusion of patients in those studies (Khwaja *et al.*, 2016).

Gender differences also exist, with males over 50 years being 1.2 to 1.6 times more likely to get sick from this disease during their lifetime than females (Howlader *et al.*, 2019; Shallis et al., 2019)

AML also exhibits important incidence differences regarding the ethnic origin of the patients. As such, Asian countries show a lower incidence rate than Western countries including Europe and the United States of America (USA) (Khwaja *et al.*, 2016).

The clinical course of AML is aggressive with an overall five-year survival rate of approximately 25% (Narayanan and Weinberg, 2020). Over the last 30 years, survival of patients with AML younger than 60 years has significantly improved, but unfortunately this does still not hold true for older patients (Khwaja *et al.*, 2016).

### **1.1.2. Risk factors**

For the majority of patients diagnosed with AML, no predisposition risk factor can be identified. Nevertheless, clinicians have made a list of factors that could in some cases reasonably increase the risk of developing AML. Those include, as already described in the previous paragraph of this work, older age and male gender, but also exposure to DNA-damaging substances (chemicals, cigarette smoke, irradiation e.g. during therapeutic radiotherapy), chemotherapeutic drugs, genetic syndromes (e.g. Fanconi anemia, Down syndrome, Bloom syndrome, Diamond-Blackfan anemia, Schwachman-Diamond syndrome, severe congenital neutropenia) and family history of AML (Khwaja *et al.*, 2016; Narayanan and Weinberg, 2020).

*De novo* AML, that arises in the absence of known exposure to DNA damaging agents, is to oppose to secondary AML that occurs either due to exposure to chemotherapy or radiotherapy, and is then called therapy-related AML (t-AML), or evolves from previous hematological disorders such as myelodysplastic syndrome (MDS), myeloproliferative neoplasm (MPN) or aplastic anemia (Kim et al., 2020; Shallis *et al.*, 2019). 10-30% of all AML are secondary AML, however this proportion might be underestimated, as numbers of MDS leading to AML may stay undiagnosed (Leone et al., 1999).

### **1.1.3. Diagnosis of AML**

The previously mentioned symptoms of AML are similar to those observed for other hematopoietic malignancies like MDS and acute lymphoblastic leukemia (ALL). In contrast, chronic myeloid leukemia (CML) does not display the mentioned features of BM failure but rather exhibits high levels of circulating differentiated myeloid cells as well as splenomegaly (Khwaja *et al.*, 2016).

In addition to clinical presentation and history of the patients, the diagnosis of AML also includes important biological laboratory and pathology studies including morphological analysis of BM aspirates or biopsies, immunohistochemistry, flow cytometry (FC), cytogenetic tests and molecular mutation analysis (Narayanan and Weinberg, 2020). The goal of these studies is not only to diagnose AML over other hematological malignancies, but also to identify the AML subtype in order to predict prognosis, define the risk group of the patient and formulate the best treatment strategy (Narayanan and Weinberg, 2020).

In order to make the diagnosis of AML, one criterion amongst the two following needs to be fulfilled:

- The detection of myeloid blasts counts superior or equal to 20% in the BM or the PB. Blasts are identified based on morphology and enumeration (manual counting on slides and/or FC analysis of BM aspirate samples). The morphological features of a majority of myeloblasts consist in high nuclear/cytoplasmic ratios, round-to-oval nuclei, immature nuclear chromatin, presence of nucleoli and of cytoplasmic granules (Narayanan and Weinberg, 2020) even if this can be different for some AML subtypes. As nicely summarized in the work of Narayanan et al., clinicians and pathologists have

established a very precise list of morphological features of myeloblasts depending on the different AML subtypes.

- The detection of the following specific cytogenetic abnormalities: t(8;21)(q22;q22.1), inv(16)(p13.1q22) or t(15;17)(q24.1;q21.2). Cytogenetic studies can be performed with conventional karyotyping and/or fluorescence *in situ* hybridization (Narayanan and Weinberg, 2020).

#### **1.1.4. AML classification and risk stratification**

In order to unify the classification of AML and to draw appropriate guidelines in treatment strategies, expert panels have worked together to publish recommendations.

Amongst organizations that have worked on the diagnosis and management of AML, one can of course cite the World Health Organization (WHO), as well as the European LeukemiaNet (ELN), the National Comprehensive Cancer Network (NCCN) and the European Society for Medical Oncology (ESMO). Even though differences exist between these classifications, the proposed risk-stratification is always based on cytogenetic abnormalities and mutations. (Narayanan and Weinberg, 2020)

As described in the previous part of this work, AML can be defined on the basis of specific cytogenetic abnormalities, and those, in addition with others can also be used for prognosis association as described in table 1.

Besides cytogenetic rearrangements and abnormalities, a large next generation sequencing (NGS) study performed in more than 1540 patients has identified 5234 mutations in 76 genes (Papaemmanuil et al., 2016). Mutations in genes with different functional consequences have been identified to be associated with AML:

- Modulation of epigenetic mechanisms such as DNA methylation (e.g. DNMT3A, TET2, IDH1 and IDH2 (Isocitrate Dehydrogenase 1 and 2) and chromatin modification (e.g. ASXL1, ASX transcription regulator 1)
- Promotion of cell survival and proliferation (e.g. FLT3 , KIT (Tyrosine Protein Kinase) and RAS (Rat Sarcoma))
- Impairment of differentiation and apoptosis of hematopoietic cells (e.g. CEBPA (CCAAT enhancer binding protein), RUNX1 and NMP1 (Nucleophosmin))
- Suppression of tumor (e.g. TP53, tumor protein 53)

(Almosailleakh and Schwaller, 2019; Narayanan and Weinberg, 2020; Papaemmanuil *et al.*, 2016)

Most of the time patients with AML display more than one mutation, and certain mutations or combinations of mutations are more frequently seen in specific AML subtypes. For example, AML patients with mutated NPM1 as well as those with biallelic mutations of CEBPA alone can most of the time be classified as favorable prognosis AML. Patients with mutations in RUNX1 or ASXL1 alone, however, rather have a poor prognosis. Furthermore, mutations in CEBPA together with FLT3 mutations are also associated with poor prognosis (Narayanan and Weinberg, 2020). With emerging technological advances such as NGS, the prognostic relevance of some AML-specific mutations and karyotypes has been more and more studied, which were amongst others incorporated in the WHO AML classification in their update from 2016 (Arber *et al.*, 2016). This is the major difference to the French-American-British (FAB) classification that is only based on the degree of maturation and differentiation of the cells, but is not including immunophenotypic or genetic parameters (Aberger *et al.*, 2017).

In the 2017 ELN publication, AML are classified in favorable, intermediate and adverse risk groups according to molecular and cytogenetic criteria (Döhner *et al.*, 2017).

<b>Risk Category</b>	<b>Genetic Abnormality</b>
<b>Favorable prognosis</b>	t(8;21)(q22;q22.1) ; RUNX1-RUNX1T1 inv(16)(p13.1q22) or t(16 ;16)(p13.1 ;q22) ; CBFB-MYH11 Mutated NPM1 without FLT3-ITD (Internal Tandem Duplication) or with FLT3-ITD low allelic ratio (<0.5) Biallelic mutation of CEBPA
<b>Intermediate prognosis</b>	Normal karyotype t(9;11)(p21.3;q23.3);MLLT3-KMT2A Mutated NPM1 and FLT3-ITD high allelic ratio (≥0.5) Wild-type NPM1 without FLT3-ITD or with FLT3-ITD low allelic ratio (<0.5), without adverse risk genetic lesion Cytogenetic abnormalities not classified as favorable or poor prognosis indicators



<b>Poor prognosis</b>	Complex* and monosomal karyotype t(6:9)(p23;q34.1) ; DEK-NUP-214 t(v;11q23.3) ; KMT2A rearranged t(9;22)(q34.1;q11.2) ; BCR-ABL1 inv(3)(q21.3;q26.2) or t(3 ;3)(q21.3 ;q26.2) ;GATA2MECOM(EVI1) -5 or del(5q);-7;-17/abn(17p) Wild-type NPM1 and FLT3-ITD <sup>high</sup> Mutated RUNX1 Mutated ASXL1 Mutated TP53
-----------------------	---

**Table1: 2017 ELN risk stratification by genetics (adapted from (Döhner *et al.*, 2017))**

*ITD (internal tandem duplication)*

*\*Complex karyotype: three or more unrelated chromosome abnormalities in the absence of 1 of the WHO-designated recurring translocations or inversions, that is, t(8;21), inv(16) or t(16;16), t(9;11), t(v;11)(v;q23.3), t(6;9), inv(3) or t(3;3); AML with BCR-ABL1.*

### 1.1.5. Treatment strategies

Given the heterogeneity of AML patients, treatment strategies include several aspects that may be considered when choosing the treatment strategy. For example, the dose intensity of chemotherapy or hematopoietic stem cell transplantation (HSCT) is adapted to the general health of the patient, thus being directly linked to age. Treatment strategies for patients with AML include:

- Cytotoxic chemotherapy: standard protocols consist in 7 to 10 days of cytarabine combined with 3 days of an anthracycline (usually daunorubicin or idarubicin), which can be improved/completed by adding other drugs (e.g. granulocyte colony-stimulating factor, GCSF) (Narayanan and Weinberg, 2020).
- HSCT: in allogeneic HSCT, blood or BM obtained from a donor is infused into the patient that received a priori conditioning to allow engraftment and avoid host-versus-graft and graft-versus-host reactions. In autologous HSCT, stem

cells from the patient itself are harvested and re-infused after chemotherapy, in order to favor hematopoietic recovery.

- Antibody therapy: even though AML seems to be an ideal target for antibody therapy, given the localization of malignant cells in the blood, BM, liver and spleen that are easily accessible for large antibodies, antibody therapies for AML encounter several difficulties due to the high similarities with normal hematopoietic cells making it difficult to identify antigens specific for leukemic cells (Arnone et al., 2020). Furthermore, to be effective there is a need of an effective immune cell being able to kill the target cell, which is not necessary the case in *de novo* AML patients that often present with an impaired immune system. Consequently, most of the antibodies used for treating leukemia serve as a carrier of chemotherapy or radioimmunotherapy to which they are conjugated (Narayanan and Weinberg, 2020).
- Kinase inhibitors: recent understanding of signaling pathways that are dysregulated in AML as well as of kinase mutations promoting the proliferation and survival of blasts opened new treatment perspectives. Inhibitors to kinase activity of FLT3, RAS, KIT and JAK2 (Janus Kinase 2 gene) are the most commonly used, but it is still unknown whether their effect is limited to patients with identified mutations in these kinases or if they could also be applied to patients with constitutive activation of signaling pathways (Narayanan and Weinberg, 2020).

Prognosis factors established as previously described by the ELN or the WHO are impacting the choice of the treatment strategy. For example, adverse risk group patients will be included into clinical trials rather than receiving standard protocols. Allogeneic HSCT during remission phase might also be advised for patients of intermediate or adverse risk groups rather than receiving more courses of chemotherapy, but is not indicated for favorable-risk AML (Döhner *et al.*, 2017; Narayanan and Weinberg, 2020)

### **1.1.6. Monitoring disease response and eventual relapse**

Monitoring of AML patients is of major importance both during the treatment phase to follow therapy response and to prevent disease progression and after remission to

prevent relapse. A myeloblast count of 5% is the standard threshold used for diagnosing relapse or persistence of the disease. The classical detection method used to monitor disease response remains manual enumeration of blasts and FC counting. Besides the classical 5% blast threshold, minimal residual disease (MRD) consists in identifying residual disease far below this threshold and has shown its importance to detect imminent relapse and thus enables early intervention (Schuurhuis et al., 2018). For MRD testing more sensitive detection techniques can be used, including reverse transcription polymerase quantitative polymerase chain reaction (RT-qPCR) and FC (Narayanan and Weinberg, 2020).

Importantly, chemotherapy can give rise to expansion of cell populations that have mutations unrelated to the initial AML. One hypothesis concerning the origin of these clones would be that those consist in therapy-resistant subpopulations that were below the level of detection during the initial phase of diagnosis. Their expansion increases the risk of relapse and are a real challenge in the monitoring of the disease (Arnone et al., 2020; Klco et al., 2014; Narayanan and Weinberg, 2020).

### 1.3. INVESTIGATION OF AML IN LABORATORY SETTINGS

As we can see from the previous chapter, AML is a very complex disease with a very high heterogeneity amongst patients both at a mutational level and at the genomic landscape.

Despite improvement in the *ex vivo* culturing of primary AML cells, there are still some major challenges remaining in the expansion of primary AML blasts during a long period of time without losing their characteristics at different levels of metabolism, mutational and genetic profiles, or stemness properties. Modeling AML in a way that recapitulates what clinicians observe in their routine work will bring significant insights in a better understanding of the disease pathogenesis, the identification of genetic markers and how to link them with prognosis as well as the study of the effectiveness of different treatment strategies according to disease characteristics. Complex interactions between malignant cells and the BM microenvironment as well as regulation mechanism at even an organism-wide level make it currently impossible to recapitulate the disease complexity even in the most sophisticated *in vitro* culture systems.

### 1.1.1. Murine models of AML

*In vivo* murine models are of particular importance to reach a higher level of complexity in the study of leukemia. In order to develop currently used mouse leukemia models several technics have been used:

- Carcinogen-induced tumors are generated via exposure of the animals to chemicals, viruses or irradiation, thus leading to spontaneous AML development
- Transgenic animals are engineered either in a more classical way by insertion of DNA into the genome (in embryonic stem cells or into fertilized oocytes) or by the transfer method of modified murine hematopoietic stem and progenitor cells (HSPCs) (by retroviral transduction or by genome editing techniques) into irradiated recipient.
- Xenograft models are based on the transplantation of patient-derived primary AML blasts or *in vitro* modified HSPCs into irradiated immune-compromised mice.

(Almosailleakh and Schwaller, 2019)

All of the above described models display specific advantages and drawbacks, and the choice of the one over the others has to be done regarding the purpose of each single study.

For the purpose of the work presented here, we have chosen to mainly focus on xenograft models of human AML, since we were particularly interested in the disease heterogeneity amongst patients and these models represent an elegant way to recapitulate a single patients' features in murine models. Over the past decades, xenograft models have rapidly evolved and have shown effectiveness in the engraftment of both primary healthy HSPCs and AML cells. Back in the 90's, Lapidot *et al.* nicely described engraftment of AML cells from all of the FAB subtypes into severe combined immunodeficient (SCID) mice (Lapidot, 1994). These mice have a mutation in *Prkdc<sup>scid</sup>* and are thus lacking functional B and T lymphocytes (website, consulted 30.07.2021). In their work, the authors described many similar morphological and dissemination features and characteristics between the AML patient and the SCID-leukemia mice. Leukemia cells from the engrafted murine BM showed an identical immunophenotype compared to donor leukemia cells and – for

some specific AML subgroups – were able to disseminate in the liver, spleen, kidney and lungs (Lapidot, 1994).

Further studies also confirmed the successful use of SCID and non-obese diabetic - SCID (NOD/SCID) mice to study morphological and biological characteristics of human AML (Ailles et al., 1999; Bonnet and Dick, 1997; Lapidot et al., 1997). Although representing a major advance in the study of primary AML material *in vivo*, these models display low levels of engraftment classically ranging from 0.1 to 5% of human leukemic cells within the murine BM, as well as a reduced life span upon these low levels of engraftment (Ailles *et al.*, 1999). More potent models have consequently been developed, which provided an improved microenvironment for the growth and development of human AML cells. First, a mouse strain with targeted deletion of the beta2-microglobulin gene within the NOD/SCID genetic background (also known as NSB mice) was engineered, leading to additional decreased natural killer (NK) cell function in comparison to classical NOD/SCID. Transplantation of AML samples in this model demonstrated significantly increased engraftment rates (up to 70-fold increase 8-12 weeks post transplantation) as well as engraftment of samples that failed to engraft in the standard NOD/SCID strain (Feuring-Buske et al., 2003). Furthermore, adding an IL(Interleukin)-2 receptor gamma chain deficiency in the NOD/SCID background gave rise to the NOD/LsSz-scid IL2 $\gamma$ c null (NSG) mouse strain, lacking mature T, B and functional NK cells and being deficient in cytokine signaling. Importantly, these mice have an improved life span and their very high immunodeficiency provides a suitable microenvironment for growth and expansion of human AML cells with significantly higher levels of engraftment up to 90% of the mouse BM. Sanchez and colleagues investigated the engraftment of 35 primary human AML samples in NSG mice and were able to conclude that 40% of primary leukemia samples transplanted intravenously engrafted to an extent of 10% or more in the murine BM 12 weeks after transplantation. Engraftment was maintained in secondary and tertiary recipients, thus confirming that this model retains the consistent engraftment of leukemia initiating cells over multiple passages (Sanchez et al., 2009). A recent study by our group furthermore showed that the use of NSG mice for xenotransplantation permitted to engraft a much higher proportion (up to 95%) of AML cases, simply by extending the follow-up period until one year. Interestingly, by looking at the engraftment rate at the standard end-point of 16 weeks post transplantation via

BM puncture could detect human leukemic cells in only a minority (less than 40%) of patients used in the study, indicating that leukemia cells can persist at undetectable levels without losing their disease-initiating properties (Paczulla et al., 2017). In addition, AML samples from all subgroups showed robust engraftment, including those from the favorable subgroup that were initially considered as non-engrafters. Moreover, a correlation was observed between the risk group of the patient and the time for detecting engraftment, with cells from favorable AML patients needing longer than those from intermediate and adverse risk groups (Paczulla et al., 2017). All together this shows that xenotransplantation of human AML cells in NSG mice could nicely recapitulate the human disease, both concerning the conservation of the phenotype and functional properties of leukemia-initiating cells, and the maintenance of disease kinetics according to the determined risk group of the patient.

Nevertheless, xenotransplantation models using immunodeficient mice are still limited in some aspects. Given that components of the niche in these murine models cannot faithfully recapitulate the human niche, these models are not the preferential ones to study the interplay between human leukemia blasts and the niche cells or the immune system (Almosaillekh and Schwaller, 2019). In addition, cytokines, that are known as being key regulators of several process in leukemia initiation and development, differ between mouse and human.

To overcome these limitations and mimic the human BM niche, some humanized mouse strains have emerged. For example, transgenic expression of human SCF (Stem Cell Factor), GM-CSF (granulocyte-macrophage colony stimulating factor) and IL-3 into NOD/SCID or NSG mice significantly improved the expansion of normal myeloid cells and the engraftment of patients usually considered as difficult to study *in vivo* (e.g. those harboring AML1 (RUNX1) -ETO (Eight-Twenty-One) or CBF $\beta$  (Core Binding Factor) -MYH11). However, high levels of human cytokines in these models cause the exhaustion of human HSCPs (Abarrategi et al., 2018; Nicolini et al., 2004; Wunderlich et al., 2010). To overcome such issues and to obtain more physiological levels of human cytokines, knock-in mice were generated, such as MITRG (encoding human M-CSF (macrophage colony stimulating factor), IL-6/GM-CSF and TPO (thrombopoietin)) in Rag2<sup>-/-</sup>Il2rg<sup>-/-</sup> immunodeficient mice or MISTRG (which encode in addition human SIRP $\alpha$  (Signal Recognition Particule  $\alpha$ ), thus reducing phagocytosis and allowing better engraftment of xenogeneic cells). Expression of human cytokines

in the background of an immunodeficient mouse nicely allows the presence of a functional human innate immune system, and hematopoietic engraftment was successfully confirmed in these models (Abarrategi *et al.*, 2018; Rongvaux *et al.*, 2014). Engraftment of HSPCs was higher than in conventional NSG mice and also supported robust engraftment of AML patient samples including favorable risk-group AML patients (Ellegast *et al.*, 2016).

In addition, synthetic material was also used to create biological inserts and scaffolds in order to create a humanized microenvironment in the mouse that is able to support growth and differentiation of transplanted cells without affecting their normal function (Almosaillekh and Schwaller, 2019). Many similar models coexist, in which different types of human stromal cells can be seeded. For example, coating of a polyurethane scaffold with freshly isolated human BM-derived mesenchymal stem cells (MSCs) in NOD-SCID mice showed nice engraftment rates (Almosaillekh and Schwaller, 2019; Vaiselbuh *et al.*, 2010).

Of course, none of the models presented in this chapter fully recapitulate the patient complexity, but they were nevertheless particularly useful for the investigation of several aspects of AML such as the hierarchy of leukemic stem cells, linking genetic aberrations to AML initiation and progression, as well as in the development of many drugs used to fight against AML (Almosaillekh and Schwaller, 2019).

Besides these murine models, one powerful and easy-to-handle model to study hematopoiesis *in vivo* consists in using transgenic zebrafish lines, because of the high conservation of the hematopoietic organization between zebrafish and mammals. Without going into the details of this model organism here, zebrafish are particularly valuable because of their high proliferation rates, the external fertilization allowing easy embryo study, the small size and transparency of the embryos and the well-established live-imaging studies. Zebrafish also allow the study of hematopoietic malignancies. Similarly to murine models, they can e.g. also serve as recipient for xenotransplantation experiments, in which both embryos and adult zebrafish can be transplanted with human leukemia cells (Konantz *et al.*, 2019; Zizioli *et al.*, 2019)

### **1.1.2. Limitations and factors influencing leukemia induction in the NSG xenotransplantation model**

The engraftment of human AML cells in NSG recipient mice is highly depend on factors that can be either intrinsic to AML cells that are used, linked to the recipient animal or to technical experimental settings.

First of all, if considering the 16 weeks post transplantation time-point which is standardly used as a final analysis endpoint, only a limited proportion of transplanted AML samples (66%) were reported to induce leukemia. Amongst them, favorable risk group samples were underrepresented and those harboring the ITD in the FLT3 gene had an enhanced potential to engraft in recipient mice (Rombouts *et al.*, 2000a; Rombouts *et al.*, 2000b; Sanchez *et al.*, 2009). Several patient parameters were also shown to be involved in the engraftment rate. For examples, patient samples derived from secondary AML have been reported to engraft better in a NOD/SCID xenograft model when compared to primary AML samples (Rombouts *et al.*, 2000b). Furthermore, the same study also indicated that the most important clinical parameter for correlation with engraftment in xenograft models were the white blood cells (WBC) counts at diagnosis (Rombouts *et al.*, 2000b).

Moreover, recipient animals also play an important role in the engraftment capacity. The age and the gender of the recipient mice impact transplantation efficiency. Standardly, NSG mice are used between 6 to 10 weeks of age (Paczulla *et al.*, 2017; Sanchez *et al.*, 2009), but transplantation into newborn mice (up to 3 days after birth) has been shown to be more efficient, even though it is technically more difficult and might impact several other parameters such as hormone or cytokines levels, since at this time-point mice are not mature yet (Traggiati *et al.*, 2004). Differences were also observed in engraftment depending on the gender of recipient mice. These gender-linked variations have already been described in the context of healthy human HSPCs, as well as for human ALL transplantation, and their translation to AML is currently under investigation in our group (Konantz *et al.*, 2013; Notta *et al.*, 2010).

A more technical point affecting the engraftment of transplanted AML cells consists in the experimental settings used for mouse transplantations. For example, irradiation of the mice before injection of the cells is an important parameter to consider. Standardly, mice are sublethally irradiated within the 24 hours preceding the transplantation procedure (Paczulla *et al.*, 2017; Sanchez *et al.*, 2009). Nevertheless, one could also consider avoiding this irradiation step in order to favor the study of the BM microenvironment that would thus be less affected (Klco *et al.*, 2014). Even though necessary for more relevant studies of the interaction of AML cells with components



of the healthy BM niche, transplantation without prior conditioning of the mice could be challenging for some hard-to-transplant samples and could also necessitate a longer follow up time until detectable engraftment. The transplantation route can also impact engraftment. Indeed, in past and present work, we were able to notice that intrafemoral (IF) transplantation was more effective than intravenous (IV) transplantation and allowed to either lower the cell dosage or reduce the time-to-leukemia induction (Paczulla *et al.*, 2017). Nevertheless, the choice of one or the other method also impacts several other experimental parameters and should consequently be discussed in regard of the experimental purpose. For example, IF transplantation is an invasive procedure inside the bone and is thus highly disturbing the BM niche organization. It also necessitates an anesthesia step which can also affect the whole mouse organism. Furthermore, the homing step of the AML cells from the circulation to the BM is occurring mainly when IV transplantation is used and not upon IF transplantation, hence rendering useless processing such as chemoattraction or intravasation. The time point of analysis is also a very important parameter to consider when looking at engraftment. Indeed, many studies consider 16 weeks, or even 12 weeks as a final analysis endpoint (Eppert *et al.*, 2011; Sanchez *et al.*, 2009). Nevertheless, work published by our laboratory in 2017 could show that prolonging the observation time for a longer time (up to one year) could lead to engraftment of most of the patients tested, even those derived from patients that were considered as difficult to engraft (e.g. favorable risk group patients with inv(16)) (Paczulla *et al.*, 2017).

Last but not least, the time-point of transplantation of the cells is of particular interest. In fact, the BM niche and endogenous HSCs are highly regulated by circadian oscillations and the period of the day when transplantation occurs might thus impact engraftment rates (Méndez-Ferrer *et al.*, 2009). Correlations between time-point of transplantation and AML cells homing and engraftment were indeed investigated in this thesis.

#### 1.4. BONE MARROW MICROENVIRONMENT IN HEALTH AND DISEASE

As already described above, the BM naturally harbors HSCs that are responsible for blood production by giving rise to all types of mature hematopoietic cells. In order to fulfill this function, HSCs alternate between dormancy and self-renewal either for a

basal production of blood cells or for an “on demand” production in case of e.g. infections or inflammation (Hanns et al., 2019). There is increasing evidence that this very finely regulated balance between dormancy and production is highly dependent on the interaction between HSCs and the surrounding BM microenvironment (Kumar et al., 2018).

The concept of the niche was first described by R. Schofield back in the 70’s, which he described as «the stem cell is seen in association with other cells which determine its behavior» (Schofield, 1978). Since then, advances in genetic tools, imaging techniques and the knowledge of HSCs markers have enabled better insights into the HSCs niche (Pinho and Frenette, 2019). It is now of common knowledge that the niche is composed of complex interactions between several different types of cells in order to provide molecular signaling as well as physical interactions that are crucial for HSCs localization, maintenance and differentiation (Pinho and Frenette, 2019). One reason for this complexity lies in the high heterogeneity found among HSCs themselves, which offers the possibility that distinct niches could support distinct subsets of stem cells (Morrison and Scadden, 2014; Pinho and Frenette, 2019).

### **1.1.3. The healthy HSCs niche**

The various components of the HSC niche have been extensively studied using transgenic mouse models, e.g. upon depletion of regulatory factors or certain cell types. Both non-hematopoietic cell types and the progeny of HSCs themselves are part of the HSC niche (Pinho and Frenette, 2019).

Among non-hematopoietic cells, osteolineage cells were the first to be implicated in HSC regulation, primarily due to their colocalization with HSCs in the endosteal region. (Pinho and Frenette, 2019; Schofield, 1978) However, more recent imaging techniques have shown that HSPCs, although preferentially localized in endosteal zones, are not significantly associated with osteoblasts (Kunisaki et al., 2013; Nombela-Arrieta et al., 2013). Nonetheless, more committed hematopoietic progenitors could be regulated by cells from the osteolineage (Pinho and Frenette, 2019).

In addition to the endosteum, HSCs were also found near sinusoids in a so-called perivascular niche. Amongst perivascular cells, MSCs—rare multipotent cells wrapped around sinusoids and able to differentiate into bone, fat, muscle and cartilage—have

been described as an integral part of the HSCs niche (Méndez-Ferrer et al., 2010b; Pittenger et al., 1999). MSCs are indeed spatially associated with HSCs and highly express HSCs maintenance genes including vascular cell adhesion molecule 1 (Vcam1), CXCL12 (C-X-C motif chemokine 12) or osteopontin (Spp1) (Méndez-Ferrer et al., 2010b). In addition to MSCs, CXCL12-abundant reticular (CAR) stromal cells are also part of the perivascular niche. They consist of adipo-osteogenic progenitors and wrap around sinusoids as well as arterioles and also play an important role in the HSC niche (Baccin et al., 2020).

A lot of blood vessels are entering the BM, thus enabling both differentiated blood cells and HSCs to enter and leave the bloodstream. This high vascularization goes in pair with high numbers of BM endothelial cells that are lining the inner part of the blood vessels. Apart from perivascular cells, endothelial cells themselves also produce factors involved in the regulation of the activity of HSCs, such as Notch ligands, CXCL12 and SCF (Pinho and Frenette, 2019). Amongst endothelial cells arteriolar endothelial cells (AECs) and sinusoidal endothelial cells (SECs) can be distinguished by their specific surface membrane marker expression. Interestingly, AECs and SECs display different roles in the regulation of HSCs and express different levels of SCF and CXCL12 (Pinho and Frenette, 2019). For example, endothelial SCF is almost exclusively produced by AECs and the genetic depletion of Scf in AECs but not in SECs leads to a significant reduction of functional HSCs (Xu et al., 2018).

Differentiated adipocytes, that are more and more present when people age, also affect HSCs, but more negatively, with adipocytes-rich BM containing fewer HSPCs than adipocyte-poor BM (Pinho and Frenette, 2019). One more component that is playing an important role consists in the nerve fibers that innervate the skeletal system. This aspect will be discussed in more details later in this introduction.

Next to the stromal cells mentioned above that are involved in HSC regulation, some HSC-derived hematopoietic cells, such as megakaryocytes, macrophages or regulatory T cells, also regulate HSC activity in a feedback loop (Pinho and Frenette, 2019).

#### **1.1.4. The BM niche in hematological malignancies**

The most relevant microenvironment for malignant cells from hematopoietic cancer is of course the BM, which is also where healthy HSCs locate. Similar to normal

hematopoiesis, leukemia also displays a hierarchical organization. On the top of the system, a small population of leukemia-initiating cells (LIC) presents stem-cell like functions, repopulation capacity and is thus considered as being the major cause of leukemia relapse (Huntly and Gilliland, 2005). LIC have been described to have the potential to corrupt the BM niche component in order to hijack the normal homeostatic processes and to use niche cells to their advantage, thus supporting their survival and proliferation but also maintaining their quiescence and resistance to chemotherapy (Backhovens et al., 1987; Lane et al., 2009). Several niche related pathways and cell types are involved in leukemia progression and can consequently open therapeutic windows (Figure 2).

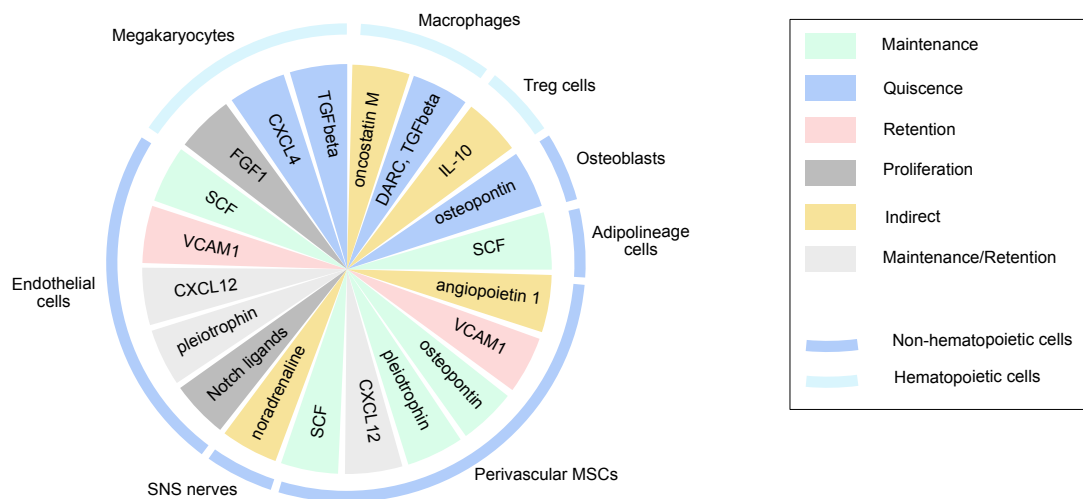


**Figure 2: Leukemic blast interactions with the perivascular niche. (adapted from Behrmann et al.)**

Secreted factors and cell-cell interactions regulate the survival, proliferation and resistance of AML cells in the perivascular niche.

*AML, acute myeloid leukemia; EC, endothelial cells; MSC, mesenchymal stromal cells; CXCL12, C-X-C motif chemokine 12, C-X-C chemokine receptor 4; VLA-4, very late antigen 4; VCAM-1, vascular cell adhesion molecule 1.*

First of all, the vasculature has been described to be in close relationship with leukemic cells. As such, the proangiogenic factor VEGF (vascular endothelial growth factor) is expressed by many leukemia patients, leading to the induction of angiogenesis and reduction of apoptosis (Figure 3) (Backhovens et al., 1987).

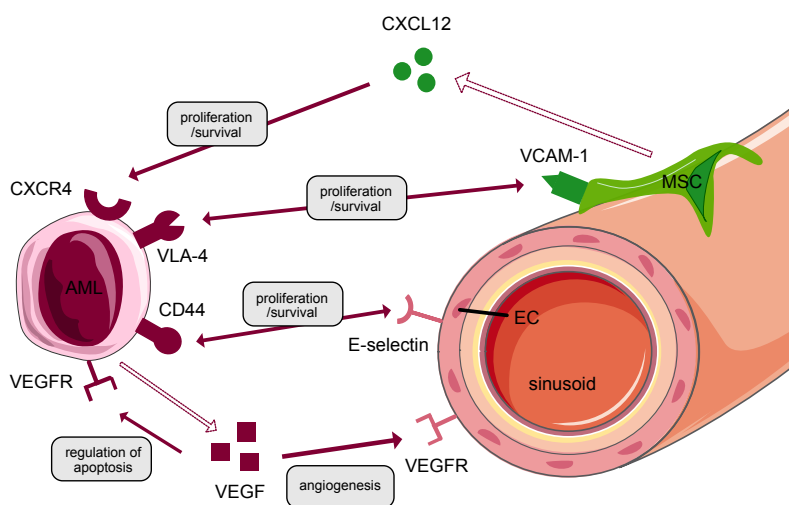


**Figure 3: Cellular and molecular constituents of the HSC niche (adapted from Pinho et al.)**

Various cell types from both non-hematopoietic cells and hematopoietic cells are implicated in the regulation of the HSC activity. The target plot illustrates some of these cell types and the niche factors (cell bound or secreted molecules) involved directly or indirectly in the processes of maintenance, quiescence, retention, proliferation.

*DARC, duffy antigen receptor for chemokines; FGF1, fibroblast growth factor 1; gp130, glycoprotein 130; IL-10, interleukin-10; SCF, stem cell factor; VCAM1, vascular cell adhesion molecule 1.*

Additionally, MSCs, for which the tight interaction with HSCs has been outlined previously, are also important in oncogenic processes. Indeed, their ability to differentiate in different types of stromal cells is disturbed by leukemia cells, which induce osteoblastic but inhibit adipogenic differentiation, thereby promoting AML expansion (Battula et al., 2017).

The BM microenvironment is also the residence for various immune cell types, e.g. T and B cells, dendritic cells and macrophages. One could easily hypothesize that this immunological microenvironment is detrimental for leukemic cells that would be recognized and eliminated by immune cells. Unfortunately, leukemic cells have the capacity to escape immune surveillance e.g. by creating a BM microenvironment in which immune responses are dysregulated. It has e.g. been shown that leukemic cells express PD-L1 (programmed death ligand 1), the ligand to PD-1 usually expressed on

antigen-presenting cells and for which the binding to its receptor leads the reduction of the activation of T-cells. PD-L1 expression on leukemic cells thus contributes to their immune escape (Zhang et al., 2009). Another interesting mechanism of immune evasion has recently been described by our laboratory. NKG2D (Natural Killer Group D) ligand expressing cells are usually recognized and cleared by NK cells. We could however show that LSCs, in contrast to more differentiated leukemic blasts, lack the expression of NKG2D ligands, hence allowing them to escape cell killing by NK cells and favoring later relapse of the disease (Paczulla et al., 2019).

Beyond all the described cells types involved in leukemic processes, many molecules and signaling pathways are also of major importance. Among these, adhesion molecules such as very late antigen 4 (VLA-4), CD (Cluster of differentiation) 44 and E-selectin, are of particular interest since the adhesion of malignant cells to the BM niche is necessary for leukemia engraftment and development (Figure 3) (Backhovens *et al.*, 1987). VLA-4 is an integrin expressed by both HSPCs and leukemic stem cells (LSCs) and serves as a ligand for VCAM-1 that is expressed by BM niche cells, including endothelial cells and MSCs (Figure 2 and 3) (Levesque, 2016). Importantly, higher VLA-4 expression level have been correlated with poor prognosis in AML patients (Matsunaga, 2003). The interaction between the VLA-4 integrin and its receptor VCAM-1 has been shown to be beneficial for the survival and the stroma, thus leading to chemotherapy resistance (Jacamo et al., 2014). Similarly, CD44 is also highly expressed on leukemic cells and is able to bind its receptor, E-selectin, which is expressed by endothelial cells. CD44 blockade has been shown to lead to reduced leukemic engraftment, mediated by the inhibition of the homing capacity of LSCs, and to increased blast differentiation (Figure 3) (Jin et al., 2006).

Besides these adhesion molecules, BM niche cells secrete soluble factors that directly impact leukemic cells. (Backhovens *et al.*, 1987) Amongst them, CXCL12, also known as SDF-1 (stromal-cell derived factor 1), is secreted by MSCs and plays a chemotactic role to attract CXCR (C-X-C motif receptor) 4-expressing cells, including leukocytes, HSCs and leukemic cells (Figure 2 and 3)(Backhovens *et al.*, 1987; Villatoro et al., 2020). In healthy hematopoiesis, the CXCR4/CXCL12 axis regulates leukocyte trafficking in and out of the BM niche. In myeloid malignancies, CXCR4 expression has been directly linked to poor prognosis in leukemic patients, and chemotherapy has been shown to upregulate CXCR4 expression (Rombouts et al., 2004; Sison et al., 2013; Spoo et al., 2007). Thus, inhibition of CXCR4 and consequent release of

leukemic cells out of the BM protective niche, sensitizes them to chemotherapy via anti-apoptotic mechanisms. Several inhibitors of CXCR4, e.g. AMD3100, ulocuplumab and BL-8040 are currently studied in clinical trials and may show beneficial for patients with leukemia (Backhovens *et al.*, 1987; Villatoro *et al.*, 2020).

Interestingly, interactions between the CXCL12/CXCR4 axis and both adhesion interactions presented above exist. For example, CXCL12 activates VLA-4 expression on HSCs and triggers its firm interaction with VCAM-1 expressing cells (Peled, 2000). Cooperation between CD44 and CXCL12 has also been observed in human HSPCs homing to the BM (Avigdor *et al.*, 2004).

### **1.1.5. Circadian and adrenergic regulation of the BM niche**

Most of the literature overview that will be presented in this part is derived from a recent review published by our laboratory with me as the first author. Some parts are consequently directly derived of this publication (Hanns *et al.*, 2019).

#### **1.1.1.1. Catecholamines and adrenergic signaling**

Stress is defined as the relationship between a person and her/his environment when latter is perceived as endangering to her/his well-being. While the stimulus-based definition understands stress as the sum of effects that emerge after exerting acute or a chronic external discomfort on a subject, the response-based definition proposes stress as part of the physiological alert reaction activated by the body to better master a dangerous situation (King, 1993). On the physiological and biochemical level, stress involves the sympathetic nervous system (SNS) and the release of catecholamine neurotransmitters (epinephrine (EPI), norepinephrine (NOR), dopamine (DA)) from SNS fibers. Catecholamine release may differ in acute compared to chronic stress: whereas acute and chronic stress both induce EPI as well as NOR (Moreno-Smith *et al.*, 2010; Rupp, 1994; Rupp, 1995; Schmidt, 1996), brain concentrations of DA were instead found elevated in acute but however reduced in chronic stress (Imperato, 1992; Moreno-Smith *et al.*, 2010; Puglisi-Allegra, 1991). The downstream adrenergic signaling responses activated by stress are furthermore dependent on the expression of specific adrenergic receptors (ARs) on various organs and tissues participating in

the alert reaction (Elenkov et al., 2000; Esler et al., 2008). ARs belong to the class of G protein-coupled receptors and are subdivided into  $\alpha$ - and  $\beta$ -ARs. Activation of  $\alpha$ 1-ARs (comprising  $\alpha$ 1a,  $\alpha$ 1b,  $\alpha$ 1d-ARs) increases intracellular calcium levels and induces vasoconstriction, while  $\alpha$ 2-AR (comprising  $\alpha$ 2a,  $\alpha$ 2b,  $\alpha$ 2c-ARs) activation inhibits intracellular cAMP (cyclic adenosine monophosphate), insulin, acetylcholine and NOR release (Chakroborty et al., 2009). Stimulation of  $\beta$ -ARs (comprising  $\beta$ 1,  $\beta$ 2,  $\beta$ 3-ARs) elevates cytosolic cAMP levels and activates PKA (protein kinase A) leading to smooth muscle relaxation and lipolysis (Hein and Kobilka, 1995; Hieble et al., 1995; Molinoff, 1984). While  $\beta$ 3-ARs bind EPI and NOR with the same affinity,  $\alpha$ 2 and  $\beta$ 2-ARs are more potently stimulated by EPI and  $\alpha$ 1 and  $\beta$ 1-ARs by NOR (Ariëns and Simonis, 1983; Orenberg et al., 1983; Rang et al., 2007). ARs can be pharmacologically modulated by drugs with selectivity for certain receptors, e.g. “selective” blockers targeting  $\alpha$ 1-ARs (e.g. prazosin),  $\alpha$ 2-ARs, (e.g. yohimbine),  $\beta$ 1-ARs (e.g. acebutolol) or by so-called “unselective” blockers targeting for example all types of  $\alpha$ -ARs (e.g. phenoxybenzamine), or all types of  $\beta$ -ARs (e.g. propranolol). AR-blockers are in routine clinical use especially for the treatment of patients with hypertension and cardiovascular disorders.

#### **1.1.1.2. Circadian regulation and catecholamine signaling**

Circadian rhythms are used by living organisms to anticipate their daily needs and consequently adapt their behavior and physiology to daily changes in light and temperature. These adaptations have significant impact on organism’s ability to decide when is the appropriate time for them to reproduce, to store food, to hide, or at the contrary to hunt. All these aspects are critical for the survival of the organisms and thus explain why the regulatory mechanisms of the circadian clock have been conserved throughout evolution (Bhadra et al., 2017).

In mammals, day-night cycling is sensed through light signals detected from the retina and will affect important processes including sleep, hormone secretion, cell cycle and immunity (Méndez-Ferrer *et al.*, 2009). In a very simplified way, at the molecular level, circadian rhythms are sustained by the expression, mostly in the suprachiasmatic nucleus (localized in the anterior hypothalamus), of clock genes (*Bmal1 (Brain and muscle Arnt-like protein-1)*, *Clock (Circadian Locomotor Output Cycles Kaput)*, *Npas2 (Neuronal PAS domain protein 2)*). The system operates as a feedback loop, as the



expression of these clock genes occurs asynchronously with the transcription of other genes of the *Cry* (*Crystal protein*), *Per* (Period circadian protein) and *Rev-erb* families (Méndez-Ferrer *et al.*, 2009).

Within the SNS, EPI and NOR blood levels have been described to follow diurnal patterns, indicating that the activity of the SNS undergoes circadian rhythms (Méndez-Ferrer *et al.*, 2009). As shown in a murine model, also in the BM microenvironment the release of NOR and DA, but not EPI is peaking during the night phase. Higher levels of catecholamines in the BM space correlates with the proportion of BM in the G2/M and S phase (Maestroni *et al.*, 1998; Méndez-Ferrer *et al.*, 2009).

### **1.1.1.3. The BM regulation by catecholamines**

The BM naturally harbors HSCs responsible for sustaining blood production. In order to fulfill this function over the whole life-span of an organism, HSCs balance dormancy and self-renewal activity with basal or demand-oriented proliferation and differentiation. HSCs reside in so-called BM niches, which are embedded in complex cellular networks that intensively communicate via molecular, biophysical (e.g. oxygen levels, blood pressure) and structural (e.g. extracellular matrix) signals (Guilak *et al.*, 2009; Rieger *et al.*, 2009; Zhang and Lodish, 2008). Different BM niches have been described and reported to support the unique requirements of HSCs (as elegantly reviewed in (Birbrair and Frenette, 2016; Pinho and Frenette, 2019)). Osteoblasts producing among others osteopontin (Nilsson *et al.*, 2005) were initially considered major regulators of HSCs shown to reside in proximity of the endosteum (Gong, 1978; Lord and Hendry, 1975; Nilsson and Coverdale, 2001; Taichman and Emerson, 1996). More recent studies have questioned the importance of molecular signals deriving from osteoblasts for the regulation of HSCs quiescence and rather pointed out roles of osteoblasts in the maintenance of more committed hematopoietic progenitors, particularly in B-cell lymphopoiesis (Asada *et al.*, 2017b; Ding and Morrison, 2013; Greenbaum *et al.*, 2013; Kunisaki *et al.*, 2013; Nilsson *et al.*, 2005; Nombela-Arrieta *et al.*, 2013; Visnjic *et al.*, 2004). More recently there is instead increasing evidence for the existence of the so-called vascular HSCs niche. HSCs were shown to localize in proximity of sinusoids enriched for MSCs activity (Kiel *et al.*, 2005; Yu *et al.*, 2015) and endothelial cells lining the BM vasculature and MSCs to secrete factors sustaining the maintenance and activation of HSCs and derived progenitors (Asada *et al.*, 2017a;

Ding et al., 2012; Greenbaum *et al.*, 2013; Morrison and Scadden, 2014). The influence of the vascular niche on HSCs fate is nicely summarized in (Kunisaki and Frenette, 2014; Pinho and Frenette, 2019).

Sympathetic nerve fibers are an additional critical component of the BM niche. Already back in 1925, they were described by De Castro to enter the bone with blood vessels and branch to form rings around osteoblasts and osteocytes, as described in (Mach et al., 2002). Next to a baseline routine secretion, these fibers release catecholamines to the BM space (Nadri et al., 2008) in response to circadian rhythm oscillations with especially NOR levels peaking during night and EPI release less dependent on circadian oscillations (Maestroni *et al.*, 1998). As shown by Heidt et al., chronic stress applied to mouse models induces a surplus release of NOR, which then reduces CXCL12 levels in the BM through activation of  $\beta$ 3-ARs. Chronic stress as a consequence activates HSCs and increased their proliferation and differentiation, thereby causing increased output of inflammatory cells and inducing a functional decline of HSCs (Heidt et al., 2014). Neural regulation of the BM as well as the interplay of the nerve system with the bone, BM and immunity has been recently reviewed in (Maryanovich et al., 2018). Several other cell types residing in the BM (e.g. immune cells (Cosentino et al., 2013), mast cells (Freeman et al., 2001), HSPCs (Kuci et al., 2006)) were also shown to produce catecholamines, which adds another layer of complexity to the regulation of adrenergic signaling in the BM.

Various cell types in the BM – among which niche cells as well as HSPCs themselves – are known to express ARs and respond to catecholamines as part of their baseline regulatory program or of demand reactions (Table 2) (Hoggatt and Scadden, 2012; Méndez-Ferrer et al., 2008; Seidel et al., 2007; Spiegel et al., 2007). The circadian rhythm influences the release of HSPCs from the BM into circulation (with a maximum of mobilized HSPCs at five hours after light onset and another five hours after the onset of darkness), partially via catecholamine secretion. This cyclic release of HSPCs is in antiphase with the expression of the chemokine CXCL12 responsive for HSPCs homing and retention to the BM (Méndez-Ferrer *et al.*, 2008). Interestingly, latter are regulated by core genes of the molecular clock through circadian NOR secretion by the SNS. Nerve fibers locally deliver these adrenergic signals to the BM where  $\beta$ 3-ARs expressing stromal cells respond with CXCL12 downregulation (Méndez-Ferrer

*et al.*, 2008) Furthermore, G-CSF produced in response to systemic bacterial infections, mobilizes HSPCs by suppressing CXCL12 secretion from osteoblasts via NOR/EPI release (Asada *et al.*, 2017a; Hoggatt and Scadden, 2012; Kropfl *et al.*, 2014; Méndez-Ferrer *et al.*, 2008). NOR release also reinforces the egress of HSPCs from the BM by acting on CAR cells expressing  $\beta$ 3-ARs, in which exposure to NOR leads to degradation of Sp1 (specificity protein 1), a protein required for CXCL12 expression (Dar *et al.*, 2011; Méndez-Ferrer *et al.*, 2010a; Méndez-Ferrer *et al.*, 2009). Consistently, low catecholamine levels associate with enhanced CXCL12 levels and enhanced homing and retention of CXCR4 expressing HSPCs in BM niches (Dar *et al.*, 2011). Thus, one major role of catecholamines in the BM is to regulate the HSPCs pool via controlling their egress (Dar *et al.*, 2011)(reviewed in more detail in (Asada, 2018; Costa *et al.*, 2018; Doron *et al.*, 2018; Morrison and Scadden, 2014; Sarkaria *et al.*, 2018; Shafat *et al.*, 2017; Wei and Frenette, 2018). Furthermore, adrenergic signals were associated with circadian leukocyte recruitment to the BM. Perivascular SNS fibers acting on  $\beta$ -ARs that are expressed on non-hematopoietic cells lead to differential circadian oscillations in the expression of adhesion cell molecules and chemokines, thus governing CXCR4-independent leukocyte recruitment to the BM (Scheiermann *et al.*, 2012). The influence of catecholamines on cancer cells and the roles of such processes on the BM colonization by cancer cells are still understudied.

BM cell type	Type of adrenergic receptors expressed									Reference
	$\alpha$ 1a-AR	$\alpha$ 1b-AR	$\alpha$ 1d-AR	$\alpha$ 2a-AR	$\alpha$ 2b-AR	$\alpha$ 2c-AR	$\beta$ 1-AR	$\beta$ 2-AR	$\beta$ 3-AR	
Adipocytes							+	+	+	(Scheller <i>et al.</i> , 2018)
Fibroblast like cells		+		+				+	+	(Méndez-Ferrer <i>et al.</i> , 2008)
HSPCs	+	+	+	+	+	+		+		(Muthu <i>et al.</i> , 2007)
Macrophages				+	+	+	+	+		(Shen <i>et al.</i> , 1994)

MSCs	+	+		+		+	+	+	+	(Méndez-Ferrer <i>et al.</i> , 2008)
Osteoblasts	+	+	+					+		(Méndez-Ferrer <i>et al.</i> , 2008)
Osteoclasts	+	+		+	+	+		+		(Méndez-Ferrer <i>et al.</i> , 2008)
T lymphocytes								+		(Sanders and Kohm, 2002)

**Table 2: Expression of ARs on the surface of different BM cell type in rodents**

## 1.1.6. Impact of adrenergic regulation in tumorigenesis

### 1.1.1.1. Epidemiologic studies

The relationships between stress, catecholamine levels, AR-blocker use and cancer incidence or outcome were investigated by several epidemiological studies with in part controversial results. Enhanced perceived stress (measured by self-assessment via a questionnaire) was identified as a risk factor for rectal cancer in a prospective study involving 61,563 Japanese men and women followed-up for 21 years (Kikuchi *et al.*, 2017). Furthermore, elevated intra-tumor NOR levels determined by high performance liquid chromatography were associated with advanced stage and high-grade histology in ovarian carcinoma (Lutgendorf *et al.*, 2011). Consistently, retrospective studies indicated treatment with  $\beta$ -blocker to associate with increased overall and progression-free survival in patients with prostate (Grytli *et al.*, 2014; Kaapu *et al.*, 2016), breast (Barron *et al.*, 2011; Botteri *et al.*, 2013; Choy *et al.*, 2016; Melhem-Bertrandt *et al.*, 2011; Montoya *et al.*, 2017; Powe *et al.*, 2010) ovarian cancer (Diaz *et al.*, 2012) or melanoma (De Giorgi *et al.*, 2011; Lemeshow *et al.*, 2011), and treatment with propranolol to reduce the incidence of head and neck, esophagus, stomach, colon, and prostate carcinoma in an analysis of 24,000 people followed-up for twelve years (Chang *et al.*, 2015). Finally, a meta-analysis of 20,898 patients with cancer (including patients from twelve studies published between 1993 and 2013, among which the studies mentioned above) indicated that  $\beta$ -blocker usage may associate with

prolonged survival in early stage cancer patients undergoing surgical resection (Choi et al., 2014).

In contrast, other reports – also involving patients with a variety of different tumors (e.g. breast cancer (Cardwell et al., 2013), renal carcinoma (Parker et al., 2017), AML (Chae et al., 2014), melanoma (Livingstone et al., 2013; McCourt et al., 2014) as well as a retrospective meta-analysis with more than 88,000 cancer patients from approximately thirty studies failed to reproduce these associations (Weberpals et al., 2016). We hypothesize that these controversial results may derive from the heterogeneity among the analyzed patient groups and tumor types, stages and therapies, as well as the differences in employed  $\beta$ -blockers. Different types of stress may induce different catecholamine compositions (e.g. acute or chronic stress, versus exercise-induced, see also below) that influence results. Selected tumor subtypes or phases during tumorigenesis might be more or less responsive to pro-tumorigenic effects mediated by catecholamines and large meta-analyses may not sufficiently capture such effects. Prospective randomized trials focusing on defined patient subgroups, disease stages and medications are required to obtain conclusive results. Epidemiologic studies investigating  $\beta$ -blocker treatment in patients with cancer were recently comprehensively reviewed by Yap *et al.* (Yap et al., 2018).

#### **1.1.1.2. Pre-clinical studies**

Experimental data indicate that stress and catecholamines promote tumor growth and metastasis via both cell autonomous and non-autonomous mechanisms (Behrenbruch et al., 2018; Chang et al., 2016; Chen et al., 2018; Hulsurkar et al., 2017; Kim et al., 2016; Kim-Fuchs et al., 2014; Lin et al., 2013; Madden et al., 2013; Magnon et al., 2013; Partecke et al., 2016; Qin et al., 2015; Sloan et al., 2010; Thaker et al., 2006; Zhang et al., 2016) (see also the recent review by Qiao et al. (Qiao et al., 2018)). In an ovarian cancer animal model, restraint stress enhanced NOR and EPI levels and thereby promoted malignant cell growth by suppressing anoikis and enhancing phosphorylation of FAK (focal adhesion kinases) (Sood et al., 2010). Elevated housing temperature enhanced NOR levels in an orthotopic pancreatic carcinoma model thereby up-regulating the expression of anti-apoptotic BCL-2 (B-cell lymphoma 2), BCL-xL (B-cell lymphoma-extra large) and induced myeloid leukemia cell

differentiation proteins, suppressing the pro-apoptotic BAD (Bcl-2-associated death promoter) protein and inducing apoptosis resistance (Eng et al., 2015). Similarly, in a prostate cancer xenograft model, behavioral stress increased EPI levels, induced  $\beta$ 2-AR signaling activation and accelerated tumor progression by enhancing anti-apoptotic responses in tumor cells (Hassan et al., 2013). Finally, recent work has pointed out that catecholamines induce cytoskeleton alterations and expression of genes mediating invasive properties thereby enhancing the aggressiveness of tumor cells (Kim *et al.*, 2016). Molecularly,  $\beta$ -AR activation by catecholamines activated cAMP and downstream PKA signaling, resulting in higher  $\text{Ca}^{2+}$  efflux from the endoplasmic reticulum and finally in modulation of cadherins and actin (Kim *et al.*, 2016).

Consistent with this, expression of different ARs has been documented on different cancer cell types and linked to cancer progression ( $\beta$ 1: (Hu et al., 2008; Rains et al., 2017),  $\beta$ 2: (Chang *et al.*, 2016; Hu *et al.*, 2008; Rains *et al.*, 2017),  $\beta$ 3: (Calvani et al., 2018; Calvani et al., 2015; Perrone et al., 2008; Rains *et al.*, 2017), and targeting of catecholamine signaling by treatment with specific  $\beta$ -AR inhibitors has been proposed as a potential therapeutic approach for cancer (Cole et al., 2015; Dal Monte et al., 2013; Rains *et al.*, 2017). In fact, treatment with specific  $\beta$ 3-AR antagonists was shown to reduce proliferation and activate cell death in tumor cells, thereby inhibiting melanoma progression in a mouse model (Dal Monte *et al.*, 2013).

Non-cell autonomous catecholamine-mediated pro-tumorigenic mechanisms include effects on blood and lymphatic vessels, fibroblasts, immune cells as well as different subtypes of BM cells and are thus even more complex. For example, daily restraint stress was shown to activate cancer-associated fibroblasts to produce extracellular matrix components favoring ovarian cancer growth (Nagaraja et al., 2017). Chronic psychological stress (induced by different types of stressors) furthermore facilitated breast cancer cell metastasis to the lung by modulating macrophage responses and the pre-metastatic niche (Chen *et al.*, 2018). Additionally, chronic restraint stress promoted angio- and lymphangiogenesis (Hulsurkar *et al.*, 2017; Le et al., 2016) and the re-organization of lymphatic networks within and around the primary tumor via induction of tumor-derived VEGF (vascular endothelial growth factor)-C, which in turn was found to depend on COX-2 (cyclooxygenase-2) mediated inflammatory signaling

from macrophages (Le *et al.*, 2016). Furthermore, in a prostate cancer mouse model, NOR release in the stroma was shown to activate an angiogenic switch fueling tumor growth via the endothelial  $\beta$ -AR signaling pathway (Zahalka *et al.*, 2017). Consistently,  $\beta$ -adrenergic-mediated chronic restraint stress also enhanced leukemic burden in an ALL mouse xenograft model. Interestingly, the pro-leukemogenic effect of catecholamines in this setting was not mediated by adrenergic signaling in leukemic cells themselves but rather by pro-leukemogenic modulation of host cells that interact with human ALL cells. The effects could potentially be mediated by SNS regulation of anti-tumor immune response (e.g. involving NK cell-mediated killing of leukemia cells) and of BM stromal cells, including osteoblasts that play a key role in the maintenance of healthy hematopoietic cells (Lamkin *et al.*, 2012). In response to stress, tumor cells furthermore showed increased release of pro-inflammatory prostaglandin E2 (Nagaraja *et al.*, 2016). Further studies demonstrated that NOR induced activation of  $\beta$ 3-ARs in both melanoma cells and cells of the tumor microenvironment and enhanced the response of stromal macrophages and fibroblasts by inducing pro-inflammatory cytokine secretion and de novo angiogenesis in the tumor, thus sustaining tumor growth and aggressiveness (Calvani *et al.*, 2015). Interestingly, pharmaceutical blockade of  $\beta$ 3-AR could significantly decrease the tumor vasculature by activating apoptosis signaling pathways of endothelial cells in tumor blood vessels, thus reducing melanoma malignancy (Dal Monte *et al.*, 2013).

The pro-tumorigenic effects of stress summarized above were obtained in models studying the effects of catecholamine release associated with physical or psychological stress, or a combination of both. Interestingly, different results were observed when catecholamines released upon exercise were analyzed. Mice given the voluntary opportunity to run in an environmentally enriched cage also showed enhanced catecholamine levels, but these did not promote tumor growth (Westwood *et al.*, 2013). Interestingly, suppressive effects on tumor growth were instead observed upon such exercise in different murine cancer models (e.g. of breast (Dethlefsen *et al.*, 2017), pancreas (Song *et al.*, 2017), lung and melanoma (Pedersen *et al.*, 2016)). There is no definitive molecular explanation for the different impact of stress- versus exercise-induced catecholamine increase on tumorigenesis. Possible explanations include (a) that different types of catecholamines are released in exercise compared to stress (e.g. higher induction of NOR and DA in exercise (Devalon *et al.*, 1989) and

of EPI in stress conditions, perhaps due to the fact that exercise preferentially induces a response of the SNS, while stress primarily triggers an adrenal response (Dimsdale and Moss, 2018)), (b) different catecholamine dynamics (intensive peaks upon exercise versus more constant enrichment under “chronic” stress with latter perhaps being only permissive for modeling of a pro-tumorigenic environment (Hanson et al., 2018) and (c) confounding non-catecholamine related physiological and biochemical processes associated with exercise versus stress. Exercise-induced cancer protection could also be linked to the activation of the immune system. For example, high EPI levels induced by voluntary wheel running mobilized NK cells to the tumor site thereby reducing incidence and growth of melanoma, liver and lung tumors (Pedersen *et al.*, 2016). The effects of catecholamines on the immune system are reviewed in detail elsewhere (Kohm and Sanders, 2000; Qiao *et al.*, 2018; Sanders and Kohm, 2002; Scanzano and Cosentino, 2015).

#### **1.1.7. Cancer cells use similar molecular cues than HSPCs to colonize the BM niche**

Homing and retention of HSPCs to the BM is regulated by the CXCL12/CXCR4 molecular axis (Campbell et al., 2012; Shiozawa et al., 2015). As discussed above, this pathway is regulated by adrenergic signals, which in part are released under the influence of circadian rhythms (Asada *et al.*, 2017b; Hoggatt and Scadden, 2012; Méndez-Ferrer *et al.*, 2008). While these molecular cues are best characterized for healthy HSPCs, some data suggest that they are also co-used by cancer cells. As such, cancer cells may also express the CXCR4 receptor and migrate towards BM osteoblasts releasing CXCL12 (Figure 4) (Kan et al., 2016). Consistently, BM areas showing metastasis also display enhanced CXCL12 expression (Roccaro et al., 2014). In experimental mouse models, inhibition of CXCL12 was furthermore shown to reduce BM homing of injected multiple myeloma cells and thereby affecting disease progression. (Kan *et al.*, 2016; Roccaro *et al.*, 2014) Another molecular axis promoting the colonization of bones by cancer cells is the receptor activator of NF- $\kappa$ B (RANK)/receptor activator of NF- $\kappa$ B ligand (RANKL) pathway (Jones et al., 2006; Kan *et al.*, 2016). RANKL released by osteoblasts was shown to promote BM colonization and retention of metastatic cancer cells expressing the RANK receptor. RANK expression on tumor cells furthermore promotes their migration to the bones, while



inhibition of RANKL/RANK signaling resulted in reduced bone metastasis in an experimental breast cancer model (Figure 4) (Jones *et al.*, 2006; Kan *et al.*, 2016). Notably, RANKL producing osteoblasts are the main source responsive to sympathetic nerves in bones, because of their very high expression of  $\beta$ 2-AR. The stimulation of these receptors by NOR was indeed shown to induce RANKL synthesis (Elefteriou, 2016) and thereby promoting BM metastasis (Campbell *et al.*, 2012). Another less-well studied pathway is the CXCR6/CXCL16 molecular axis, which has recently been shown to be involved in the colonization of prostate cancer cells to the bones. While mainly expressed by antigen-presenting cells, CXCL16 is also produced by bone tissues including osteocytes and was thus shown to be involved in the migration of CXCR6 expressing prostate cancer cells to this site (Figure 4) (Hu *et al.*, 2008; Kan *et al.*, 2016). Cancer cells may also reach the BM without specific cues, as disseminated tumor cells that are part of the circulating blood flow. Enhanced sympathetic activity in the bone microenvironment increases the density of blood vessels, which may contribute to BM colonization in patients with circulating DTCs (disseminated tumor cells)(Mulcrone *et al.*, 2017). In line, EPI and NOR were shown to increase the synthesis of pro-angiogenic factors such as VEGF thereby stimulating angiogenesis and the formation of abnormal vessels with higher permeability (Figure 4) as reviewed by Chakroborty and colleagues (Chakroborty *et al.*, 2009). Mulcrone *et al.* for example recently also showed that stimulation of  $\beta$ 2-AR-expressing osteoblasts using the non-selective  $\beta$ -adrenergic agonist isoproterenol effectively induced VEGF-a expression thereby increasing the vascular density in the mouse BM and promoting BM metastasis (Figure 4) (Mulcrone *et al.*, 2017). Importantly, specific blockade of the VEGF-a/VEGF-R axis abrogated the stimulatory effect of isoproterenol on tumor seeding in bones (Mulcrone *et al.*, 2017), which suggests a direct involvement of this molecular axis in the pro-metastatic effect of catecholamines at this site.

In addition to the mechanisms discussed above, the retention of cancer cells in BM niche structures may be promoted by the expression of specific adhesion molecules such as cadherins, integrins or annexins, which promote the binding of tumor cells to BM stromal cells and the bone matrix (Roodman, 2004). For example, osteoblasts and endothelial cells were shown to produce annexin II, the receptor of which is widely expressed in cancer cells (Shiozawa *et al.*, 2015; Zhang *et al.*, 2017). Adhesion can also be mediated by E-cadherin, which was found to be expressed by cancer cells and

to form adherent junctions with N-cadherin from osteogenic cells. Furthermore,  $\alpha V\beta 3$  and  $\alpha V\beta 5$  integrins expressed by tumor cells mediate binding to bone extracellular matrix proteins such as fibronectin, vitronectin or osteopontin as nicely reviewed in (Kan *et al.*, 2016). Interestingly, stress behavior and associated increased levels of catecholamines have been described to regulate the expression of adhesion molecules in cancer cells. For example, high levels of NOR induced a  $\beta 1$ -integrin-mediated increase of the adhesion of human breast carcinoma cells with the vascular endothelium in an *in vitro* model of human breast cancer. Importantly, this effect was mediated by  $\beta$ -ARs and could be abrogated by  $\beta$ -blockers (Strell *et al.*, 2012). Furthermore, restraint stress and the associated increases in catecholamines induced elevated levels of FAK (Focal adhesion kinase) in an orthotopic mouse model of human ovarian cancer, thereby affecting adhesion of tumor cells to the extracellular matrix, which contributed to cancer progression (Sood *et al.*, 2010). Very recently, Obradovic *et al.* showed that an increase in stress hormone levels during breast cancer progression mediated activation of glucocorticoid receptors in tumor cells and promoted breast cancer metastasis through induction of signaling networks and protein kinases known to facilitate breast cancer progression (Obradović *et al.*, 2019). Whether catecholamines regulate adhesion of disseminated tumor cells to the BM matrix is still under-investigated.

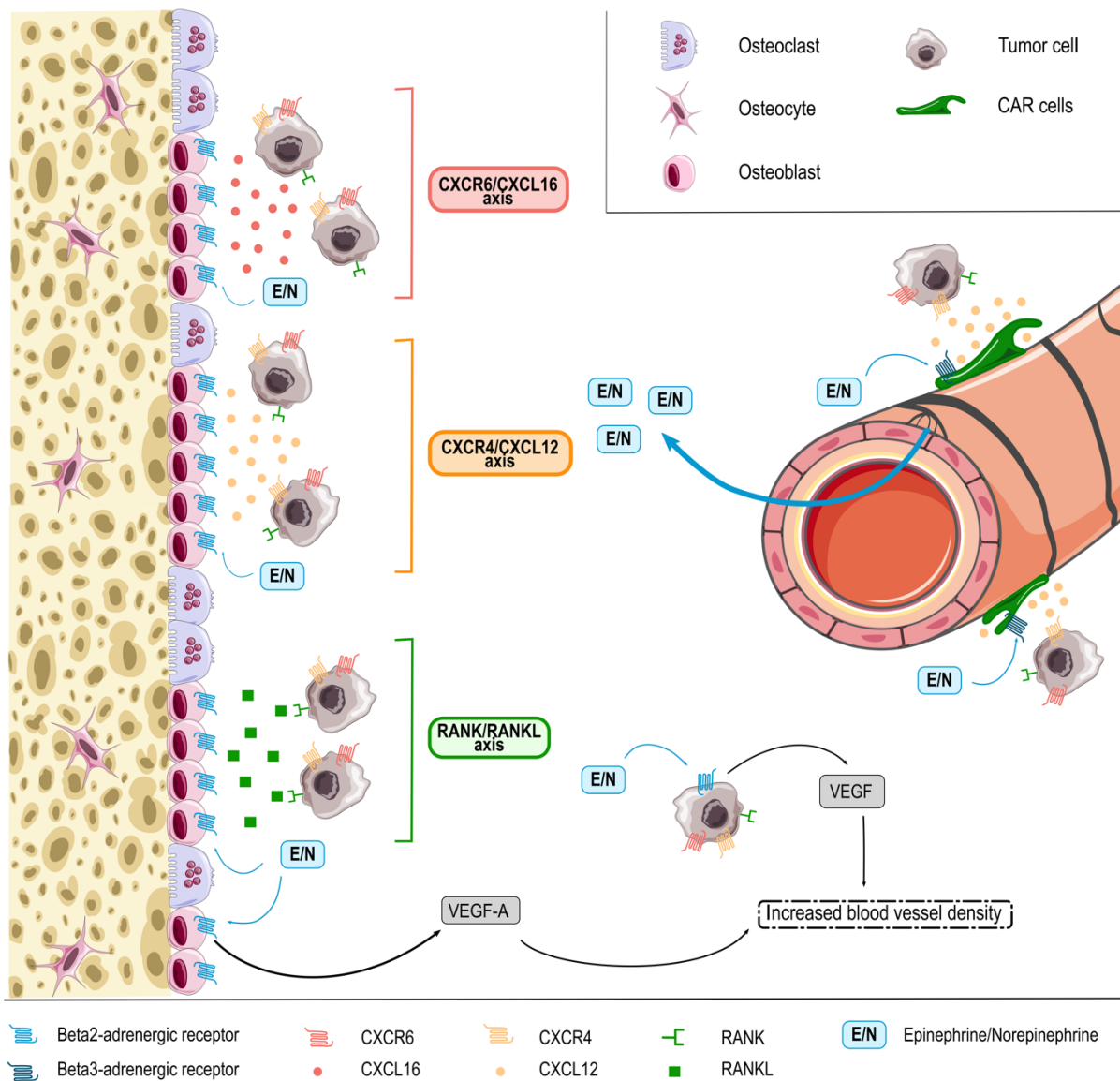


**Figure 4: Adrenergic regulation of the BM niche and how it impacts bone metastasis (from (Hanns et al., 2019))**

EPI and NOR (E/N, blue square) are released in the BM microenvironment from SNS fibers entering the bone with blood vessels. EPI and NOR influence interaction of tumor cells with AR-expressing BM niche cells, e.g. CAR cells, osteoblasts and osteoclasts through different axis. In response to adrenergic signaling, niche cells release (1) CXCL16 chemokine (red) that interacts with CXCR6 expressed on the surface of several tumor cells types, (2) CXCL12 (orange) that chemoattracts CXCR4 expressing cancer cells and (3) RANKL (green) protein that binds RANK-expressing malignant cells. In addition, adrenergic signaling in osteoblasts and also directly in

tumor cells themselves can promote release of angiogenic factors thus promoting BM colonization by tumor cells through increased blood vessel density.

As discussed above, healthy HSCs reside in specific BM niches, which however neoplastic cells modify to better serve their own requirements. As demonstrated by imaging experiments, leukemic cells specifically engraft in microvascular BM domains displaying high E-selectin and CXCL12 expression levels, where HSCs are also known to localize, indicating a possible competition between malignant and healthy cells (Sipkins et al., 2005). Furthermore, transplantation of MLL-AF9 AML cells in immunodeficient mice transformed the HSC niche by reducing the density of the SNS nerve network and remodeling of the BM microenvironment by depleting niche cells required for the maintenance of healthy HSCs (e.g. arteriole associated stromal cells) and expanding leukemia-supportive cells (e.g. more differentiated mesenchymal progenitors). Thus, manipulation of the adrenergic system could provide a strategy to re-install conditions favoring healthy HSCs over LSCs (Hanoun et al., 2014). This notion is further supported by the work from Arranz et al. who showed a disturbed niche consisting in reduced numbers of sympathetic nerve fibers, supporting nestin+ MSCs and Schwann cells in the BM of myeloproliferative neoplasia patients as well as in mouse models. Sympathetic regulation of nestin+ MSCs was restored by pharmacological treatment with a  $\beta$ 3-adrenergic agonist leading to improvement in BM fibrosis and restoration of healthy over malignant hematopoiesis (Arranz et al., 2014).

Neoplastic cells from solid tumors may also outcompete healthy HSPCs from niches via selected molecular cues. Both the endosteal zone and the perivascular niche, known to harbor healthy HSPCs, are also colonization sites for tumor cells (Reagan and Rosen, 2016; Zhang *et al.*, 2017). This is perhaps due to the fact that neoplastic cells co-use molecular signals regulating healthy homing and retention of HSPCs to the BM, as mentioned above. Metastatic prostate cancer cells for example were shown to use CXCR4/CXCL12 (Sun et al., 2007; Sun et al., 2005), Annexin II/Annexin II receptor (Shiozawa et al., 2008) as well as CXCR7 (Asri et al., 2016) pathways to establish themselves in the bone (Asri *et al.*, 2016; Jung et al., 2007; Sharma et al., 2011). Prostate cancer cells, for example, were shown to co-localize with HSCs in the BM niche, both with a preferred binding to annexin-2 expressing osteoblasts (Shiozawa et al., 2011). However, prostate cancer cells also demonstrated a superior

ability to bind to common receptors, giving them an advantage over HSCs (Shiozawa *et al.*, 2010). Interestingly, there is no direct link between the size of the primary tumor and the prevalence of disseminated tumor cells in the BM of cancer patients. A limited number of available niche sites in the BM was discussed as possible cause for this phenomenon (Shiozawa *et al.*, 2011). Of note, HSCs derived from animals with disseminated prostate carcinoma were found to express lower levels of niche adhesion molecules and receptors (e.g. NOTCH, TIE2 (angiopoietin-1 receptor)) and TF such as BMI1 (B-cell specific Moloney murine virus integration site 1) and inhibitors of CDK4 A (cyclin-dependent kinases 4), regulating HSC self-renewal and proliferation (Shiozawa *et al.*, 2011). This again suggests that these aggressive prostate carcinoma cells actively alter HSCs to vacate the niche. On the other side, as described above, disseminated tumor cells take advantage of the RANKL/RANK signaling pathway induced by sympathetic activation to migrate to the BM and liberation of a few niche spaces by mechanisms described above would further give the cancer cells an advantage to settle in their new microenvironment.

## 2. AIM OF THIS STUDY

The heterogeneity and complexity of AML, regarding molecular and cytogenetic characteristics makes this hematopoietic malignancy particularly challenging to study in laboratory settings. Even though molecular and genetic criteria have improved prognostication, categorization in adequate risk groups and further clinical decision-making, they still do not allow full risk prediction. Thus, the study of xenotransplantation models of human AML samples into immunosuppressed mice are particularly valuable since they can very nicely reproduce phenotype heterogeneity of patients. However, very little is known about the variables influencing the development of transplanted human AML cells in the murine recipient.

In regard to these observation and problematics, the purpose of the projects presented in this thesis is to optimize the xenotransplantation model of human AML into NSG mice in order to understand the processes regulating leukemia induction in this model and to use them to study mechanistic aspects of AML.

We aimed to contribute to the identification of both, variables intrinsic to the transplanted primary AML cells, i.e. surface marker expression on leukemic blasts, genetic aberrations, as well patient characteristics, i.e. sex, age, outcome, risk group classification, and to understand how they may or may not influence the kinetics of disease induction, engraftment and homing rates of the murine immunocompromised recipient.

Moreover, the results presented in a second part of this work aimed to identify and understand the impact of modulating transplantation conditions. To this end, the role of the circadian rhythm and stress molecule levels on AML induction and homing in the murine recipient BM, maybe through modulation of the interaction of AML cells with the BM environment, was assessed.

The results presented in this thesis promise not only a better understanding and improved efficacy of the xenotransplantation model, but might also open new insights for the classification and treatment of human AML patients.



### 3. IDENTIFICATION AND STUDY OF HUMAN AML SAMPLE CHARACTERISTICS INFLUENCING DISEASE INDUCTION AND HOMING IN THE NSG MOUSE MODEL

#### 1.1. BACKGROUND OF THE STUDY

As described in the introduction, cytogenetic and molecular abnormalities are used to categorize AML in favorable, intermediate and adverse molecular risk groups. Classification in one of these groups will directly affect clinical decision-making. Although molecular criteria have significantly improved prognostication and thus AML patient stratification and risk-based treatment, they still do not allow full risk prediction. In this project, we used a xenotransplantation model of human AML samples into NSG mice. This work is based on previous preliminary findings from our lab that have shown that favorable risk AML engraft NSG mice after longer latency when compared to intermediate or adverse risk AML, suggesting that this mouse model accurately depicts important features of human AML. The same paper reports that extending the follow-up beyond the standard analysis endpoint of 16 weeks after transplantation permits to reach engraftment of about 95% of the xenotransplanted cases of AML. Furthermore, the xenogeneic leukemic cells showed conserved immune phenotypes and genetic signatures in NGS analysis compared to the corresponding pre-transplant cells (Paczulla *et al.*, 2017). The described work has been performed using a relatively small cohort of n=19 AML patients (n=2 acute promyelocytic leukemia samples, n= 4 favorable AML samples, n=10 intermediate AML samples, n=3 adverse AML samples). Preliminary findings using n=3 AML samples per group also allowed to show a tendency of an inferior homing to the BM for the leukemic cells engrafting after a prolonged latency (Paczulla *et al.*, 2017).

To further investigate the relationship between *in vivo* leukemia induction in NSG mice and AML outcome in patients, we have expanded our analyses to a cohort of n= 34 favorable, n=34 intermediate and n=15 adverse AML patient samples with diverse cytogenetic and molecular features. We hypothesize that the time-to-leukemia induction in mice correlates with the capacity of homing to the BM as well as with the clinical outcome in patients. One highlight of this study is to determinate whether the



rapid homing assay would give us solid prediction of further evolution of the disease (kinetics, aggressiveness) both in the mouse model and in patients

One expectation concerning the investigation of the large set of data generated by the analysis of this cohort of patients would reside in gaining more insight into the kinetics and mechanisms of engraftment of human AML cells into the NSG xenotransplantation model, by taking advantage of several measurements including survival time, engraftment at final analysis time-points, engraftment at the time point of the bone marrow puncture (BMP) as well as homing rates.

## 1.2. RESULTS

The results presented in this work include transplantations (about 40%) and end analyses (about 25%) of mice performed by Marcelle Baer and Anna Paczulla Stanger. Marlon Arnone also helped me with some transplantations and end analysis.

### 1.1.1. Description of the patient cohort

A cohort of a total of 83 AML patients (43 male patients {51.81%}, 34 female patients {40.96%}, 6 for which the sex was unknown {7.23%}, median age 62 years {range 21-83 years}) of various genetic backgrounds was used in this work (see Table 3). The percentage of blasts in the PB was highly variable between patients in this cohort (median 80% blasts in PB {range 14-100% blasts}).

For the classification of AML, we used the 2017 ELN risk stratification, that consists in allocating the AML cases into favorable, intermediate and adverse prognosis by molecular and cytogenetic criteria (Döhner *et al.*, 2017).

Amongst the favorable risk group cases, the majority (20/34) were mutated in *NPM1* without *FLT3-ITD* or with *FLT3-ITD<sup>low</sup>*, 6/34 patients were harboring *inv(16)* or *t(16;16)* genetic abnormalities and one sample a *t(15;17)* translocation. Moreover, 10/34 intermediate samples were mutated in *NPM1* and were *FLT3-ITD<sup>high</sup>*, while 19/34 samples were wild-type *NPM1* without *FLT3-ITD* or with *FLT3-ITD<sup>low</sup>*. Last, amongst adverse risk group samples, 7/15 were considered as patients with a complex karyotype, i.e. harboring three or more unrelated chromosome abnormalities in the absence of one of the WHO-designated recurring translocations or inversions (Döhner



Table summarizing the characteristics (risk group classification, % of blasts, white blood cell (WBC) counts, age at first diagnosis, gender, remission status after first treatment induction, CD34 marker expression, genetic profile) of the patients cohort used in this project. Favorable patients are represented in green, intermediate patients in yellow and adverse patients in red.

*ELN: European LeukemiaNet; FAB: French American-British; FLT3: Fms related receptor tyrosine kinase 3; ITD: internal tandem duplication CR: Complete remission; RD: resistant disease; CRi: Complete remission with incomplete hematologic recovery; PR: Partial remission; n.c.: data was not collected; WT: wild-type; MUT: mutated.*

### **1.1.2. Most AML samples lead to disease induction in the year following transplantation in mice**

Mice transplanted intrafemorally with human AML cells from the patient cohort described above were assessed at defined time-points (week 16, week 26 and week 39) for the engraftment of leukemic cells and were also screened regularly for signs of disease (Figure 5). Euthanazation and final analysis was performed after fulfillment of the following requirements:

- Determination of  $\geq 80\%$  human CD33+ cells after BMP
- Evident sign of disease (according to precise scoring, sacrifice after 2 days with a score of 5 or immediately with a score of 6).

If none of the two conditions was fulfilled 52 weeks post transplantation, mice were anyway sacrificed at this time-point.

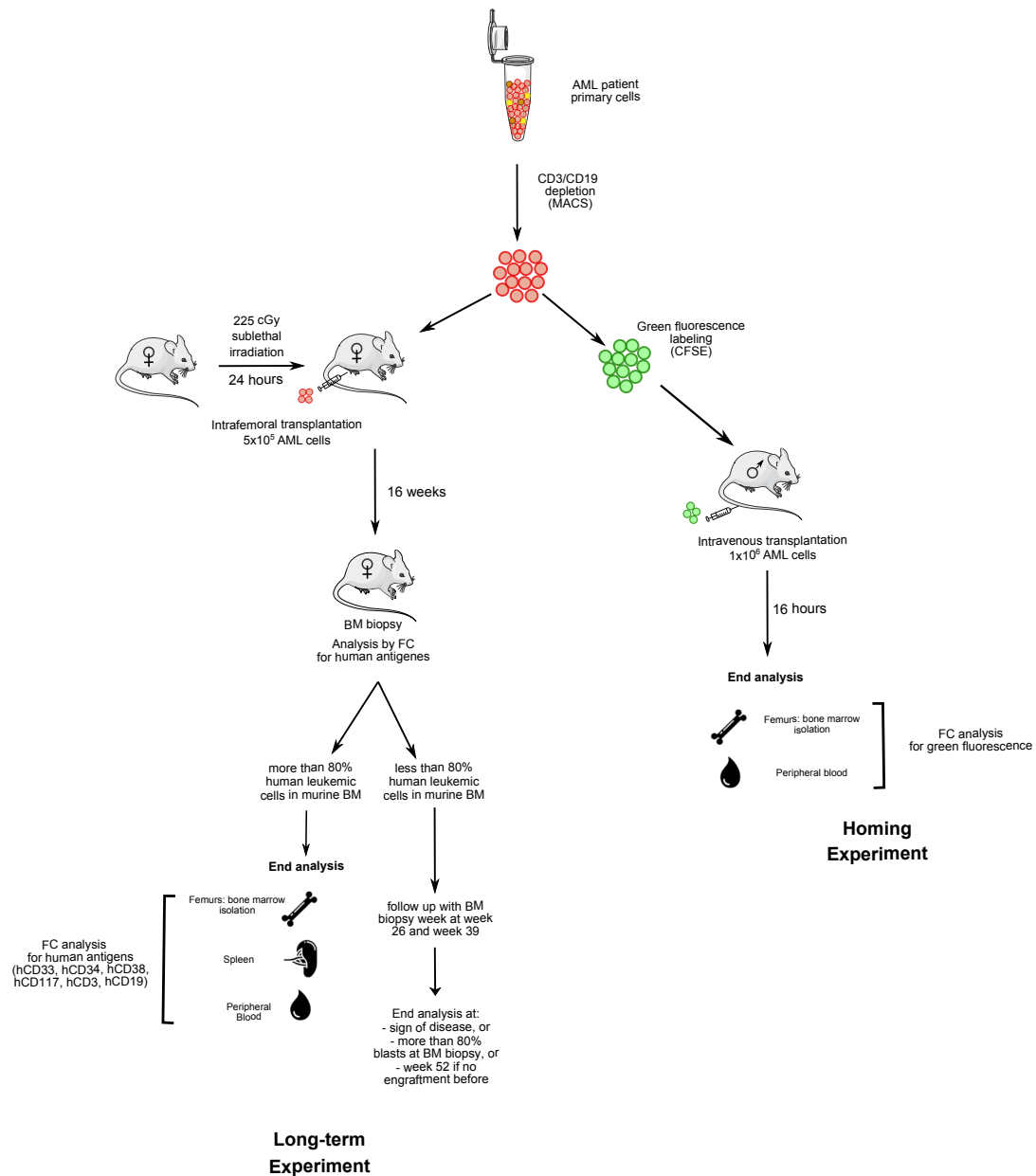


**Figure 5: Experimental workflow**

Primary AML cells were first depleted for T and B cells when the blast purity was inferior to 90%. For long-term experiments, sublethally irradiated female mice were intrafemorally transplanted with 500'000 primary AML cells. Mice were then regularly screened for signs of disease or for the presence of human AML cells in the murine BM. BM biopsies were performed at week 16, 26 and 39. Final analysis was performed if the punctured mouse was showing more than 80% blasts, if the animal was showing signs of distress necessitating its sacrifice or 52 weeks post transplantation if none of the two previously mentioned conditions was achieved. For homing experiments, male

mice without irradiation were intravenously transplanted with  $1 \times 10^6$  fluorescently labeled primary AML cells. 16 hours later, mice were sacrificed and BM and PB were analyzed for green fluorescence.

In previous studies, in which mice transplanted with human AML cells were assessed at latest at week 16, a considerable proportion of AML cases were considered as non-engraftable (Sanchez *et al.*, 2009). In our previous studies, we could already demonstrate that late analysis at 1 year after transplantation revealed better engraftment than earlier time points (week 8-10, week 12-14 and week 16), and that only 37% of transplanted AML cases were showing engraftment in the first 16 weeks after transplantation, whereas this proportion raised to 95% when increasing the follow-up time to 1 year. In this work, the standard definition of engraftment was used, i.e.  $\geq 1\%$  leukemic blasts in the murine BM (Paczulla *et al.*, 2017).

Here, we first categorized the engraftment of mice transplanted with samples from the three different risk groups according to the percentage of human CD33+ cells in the BM at final analysis time-point. Note that the “non-engrafted” category consists of mice that were analyzed at week 52 (since they did neither show engraftment nor signs of disease). Interestingly, a considerable number of mice had very low engraftment percentage but still showed evident signs of disease that lead to their sacrifice. Those mice were categorized in the “ $<1\%$ ” group. For the rest of the mice, engraftment was subdivided into three groups, low engraftment (1-5%), medium engraftment (5-20%) and high engraftment (20-100%). First, we note that a vast majority of the mice were considered as engrafted at the final analysis time-point, in all three risk groups. Not surprisingly, the proportions of non-engrafted mice is higher for the favorable risk group (13.8% of the mice, corresponding to 4 favorable AML cases) than for the intermediate (12.5% of the mice, corresponding to 4 intermediate AML cases) and for the adverse (9.1% of the mice, corresponding to 1 adverse AML case) risk groups (Figure 6A and Table 4).

Patient designation	ENL 2017 cytogenetic risk group	BM	PB	spleen	splenomegaly	tumor
M1	intermediate	+++	+++	+++	no	no
M3	adverse	++	++	low	no	no
M4	intermediate	+++	+	+	no	no
M5	adverse	+++	++	++	yes	no
M6	adverse	low	low	low	no	no
M7	favorable	not engrafted	not engrafted	not engrafted	no	no
M8	intermediate	low	low	low	no	no
M10	intermediate	low	low	low	no	no
M13	favorable	low	low	low	no	leg
M14	favorable	low	low	low	no	no
M15	favorable	+++	+	+	no	no
M16	favorable	not engrafted	not engrafted	not engrafted	no	no
M17	adverse	low	+	low	no	no
M18	favorable	+++	low	+	no	no
M19	adverse	+++	n.a.	n.a.	no	no
M22	intermediate	+++	low	+	no	leg
M24	favorable	++	n.a.	n.a.	no	no
M25	intermediate	+	+	+	no	no
M28	adverse	low	low	low	no	leg
M29	favorable	+	low	low	no	no
M30	favorable	+	n.a.	n.a.	no	no
M32	intermediate	+++	++	++	no	no
M34	intermediate	++	n.a.	n.a.	no	no
M36	favorable	n.a.	n.a.	n.a.	no	no
M37	favorable	+	+	low	no	no
M38	intermediate	not engrafted	not engrafted	not engrafted	no	no
M39	intermediate	n.a.	n.a.	n.a.	no	no
M40	intermediate	+	+	+	no	no
M41	intermediate	+++	++	+	no	no
M42	favorable	+++	+++	n.a.	no	no
M43	favorable	not engrafted	not engrafted	not engrafted	no	no
M44	intermediate	++	++	+	no	leg
M45	intermediate	++	low	+	no	no
M46	adverse	n.a.	n.a.	n.a.	no	no
M49	adverse	not engrafted	not engrafted	not engrafted	no	no
M50	adverse	n.a.	n.a.	n.a.	no	no
M51	favorable	++	low	low	no	no
M52	intermediate	+++	++	++	no	no
M53	favorable	+++	+++	+++	no	no
M54	favorable	+++	+++	++	no	no
M55	favorable	+++	low	low	no	no
M56	intermediate	low	+	low	no	no
M57	intermediate	+++	++	++	no	no
M58	intermediate	++	low	++	no	no
M59	favorable	+++	+	+	no	no
M62	favorable	+++	+	n.a.	no	no
M63	adverse	+++	++	+	no	leg
M64	intermediate	+++	+	++	no	no
M65	favorable	+++	++	+++	no	no
M66	favorable	+++	+++	+++	no	no
M69	intermediate	low	+	++	no	no
M70	intermediate	+++	+++	+++	yes	no
M71	favorable	low	n.a.	n.a.	no	no
M72	favorable	+++	+++	+++	no	no
M73	intermediate	+	+	++	no	no
M74	favorable	+++	+++	++	no	no
M75	intermediate	low	low	low	no	no
M76	favorable	+	n.a.	n.a.	no	no
M77	adverse	low	low	+	no	no
M78	adverse	n.a.	n.a.	n.a.	no	no
M79	intermediate	n.a.	n.a.	n.a.	no	no
M80	intermediate	not engrafted	not engrafted	not engrafted	no	no
M82	favorable	not engrafted	not engrafted	not engrafted	no	no
M84	intermediate	++	low	low	no	no
M85	intermediate	low	+	low	no	leg
M89	intermediate	+++	n.a.	n.a.	no	no
M90	adverse	+++	+++	+++	no	leg
M94	favorable	+	low	low	no	no
M95	intermediate	not engrafted	not engrafted	not engrafted	no	no
M96	favorable	low	low	low	no	no
M98	favorable	low	low	low	no	no
M99	adverse	+++	low	low	no	no
M100	intermediate	not engrafted	not engrafted	not engrafted	no	no
M101	favorable	low	low	low	no	no
M122	intermediate	++	+	+	no	no
M123	intermediate	+++	++	+	no	no
M124	intermediate	+	low	+	no	no
M125	intermediate	low	low	low	no	no

**Legend**

not engrafted	no symptoms after one year
low	<1%
+	1-5%
++	5-20%
+++	>20%

**Table 4: Engraftment table**

Table summarizing the engraftment in the BM, PB, spleen of mice transplanted with the respective patient sample. Splenomegaly and the presence of occurring tumors are also indicated in the table. Favorable patients are represented in green,

intermediate patients in yellow and adverse patients in red. Please note that a small number of mice from this project were reallocated for another project and were consequently not analyzed for final engraftment. In this case, the value of the last BMP was used to consider them as engrafted.

The high engraftment group represents the majority of the mice in all three risk groups, with nonetheless the highest proportion visible in the adverse risk group (41.4% of mice transplanted with cells from favorable risk group patients, 34.4% of mice transplanted with samples from intermediate risk group patients, 45.5% of mice transplanted with cells of adverse risk group patients). Remarkably, the mice transplanted with cells from adverse risk group patients displayed a particularly higher proportion of mice with very low (<1%) engraftment (Figure 6A).

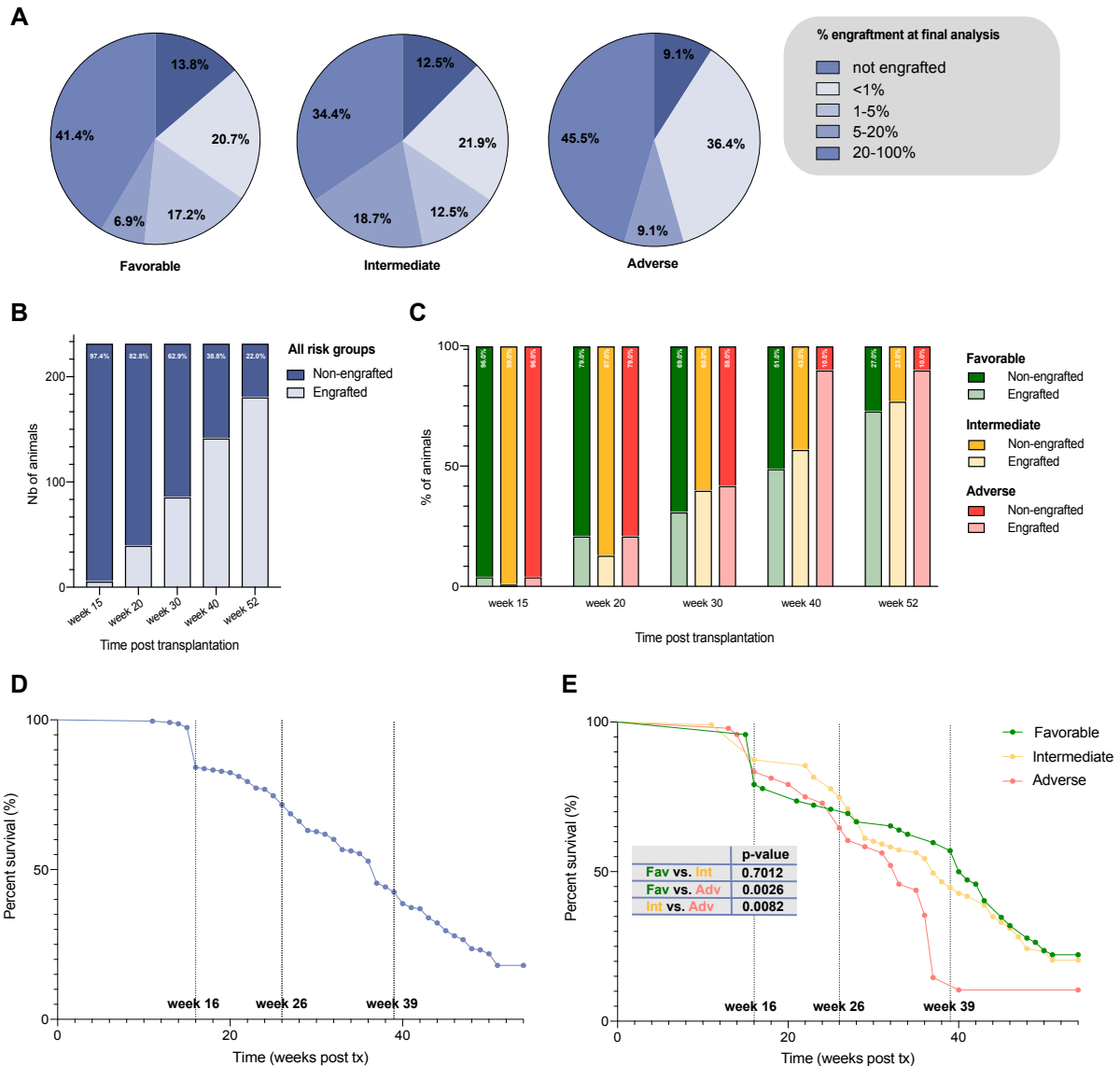


**Figure 6: AML engraftment in mice and survival correlate to the risk group classification of patients**

(A) Pie charts representing the engraftment of mice transplanted with AML patient samples from the different risk groups. Engraftment was categorized into five different categories according to the percentage of CD33 positive human AML blasts found in the murine femurs at the time point of final analysis. The category defined as “not engrafted” consists in the mice in which no blasts were detected in none of the BMP performed and for which no signs of disease were visible until the one-year endpoint. N.B.: Mice with very low engraftment percentage that were sacrificed because of signs of distress are classified into the <1% engraftment category (favorable, n= 81 mice from n=29 AML cases; intermediate, n= 103 mice from n= 32 AML cases; adverse, n= 48 mice from 15 AML cases). (B) Number of animals engrafted at different time points



post transplantation, independently of the AML patient risk groups (n= 232 mice from n=76 AML cases). Animals were considered as engrafted as soon as they were either showing engraftment after BMP or exhibiting a disease score leading to their sacrifice. Indicated in white are the percentages that represent the proportion of non-engrafted animals for each time-point. **(C)** Number of animals engrafted at the different time points post transplantation, patients were classified per AML risk group (favorable (green), n= 81 mice; intermediate (yellow), n= 103 mice; adverse (red), n= 48 mice). Indicated in white are the percentages that represent the proportion of non-engrafted animals for each time-point. **(D)** Kaplan-Meier survival analysis of mice transplanted with AML samples. All mice were plotted, independently of the AML patient risk group. Highlighted time points (week 16, week 26 and week 39) are the time points of the three BMP (n= 232 mice). **(E)** Kaplan-Meier survival analysis of mice transplanted with AML samples per risk group (favorable (green), n= 81 mice; intermediate (yellow), n= 103 mice; adverse (red), n= 48 mice). Table indicates the p-value of the comparisons between the different risk groups. Log-rank (Mantel-Cox) tests for Kaplan-Meier analyses were performed.

### 1.1.3. Time improves the detection rate of human AML engraftment in NSG mice

In our previous study published by Paczulla et al., our lab could nicely show that analysis at week 16 already improved engraftment when compared to week 10-12 and week 14-16, but late analysis at one year revealed higher engraftment rates than any these earlier time-points (Paczulla *et al.*, 2017). To gain insights into the kinetics of engraftment, we compared the three intermediate time-points (week 20, week 30 and week 40) to each other. As shown in Figure 6B, at week 15 a very small proportion of the transplanted mice were engrafted (2.5%). This proportion increased gradually at week 20, week 30 and week 40 to reach 78% at one year, thus confirming the observation of the previous study, and also reinforcing the finding that follow-up time matters and that for some patients a long time is necessary for disease induction (Figure 6B). A more detailed analysis of the kinetics of engraftment in the different risk groups shows that until week 30, the proportions of engrafted animals are similar in all three risk groups whereas at week 40, we can clearly see a significantly higher proportion of engrafted animals from the adverse risk group in comparison to both

favorable and intermediate risk groups (Figure 6C). This difference is still visible at the final analysis time point (week 52), but to a lesser extent, since the proportion of engrafted animals of the adverse risk groups did not evolve between week 40 and week 52, whereas the proportion of engrafted mice in the favorable and intermediate risk groups were still increasing (Figure 6C).

Consistently, when comparing survival rates, we can clearly see that the vast majority of the mice were still alive at week 16 post-transplantation but still developed AML progressively within the next months (Figure 6D). Of note, the time-to-leukemia induction was also very heterogenous between patients, as we can see from the very regular survival curve. Only the week 16 time-point depicts a break in the curve, certainly due to the first BMP time-point that takes place at this precise time-point (Figure 6D). Time-to-leukemia induction also correlates with the risk group stratification, but mice transplanted with favorable and intermediate risk group patient samples behave very similarly when considering disease induction upon transplantation into NSG mice, whereas mice that obtained patient samples from the adverse risk group are significantly different and showed lower survival rates especially at the time-point of the third BMP, i.e. week 39 (Figure 6E), indicating an effect of the risk group of the patient.

Importantly, in all described data, engraftment was determined according to the percentage of human CD33 positive cells within the BM of the transplanted mice. As described in the experimental procedure (Figure 5), we also analyzed the PB and the spleen at the designated endpoints. Of note, we also tried to analyze liver cells, however, data will not be shown here since after cell preparation, these cells were mainly dead when analyzed by FC. This led to hardly interpretable data and we thus decided to exclude these data from our analyses. Nevertheless, various degrees of leukemic cells within the PB and spleen were observed between patients (Table 4). For all analyzed transplanted patient samples, the BM was the organ where most engraftment was detected and none of the sample showed engraftment only in the PB or the spleen. This indicates that within our cohort, the colonization of the BM by human leukemic cells seems to be a prerequisite for the establishment of these cells in the spleen or for their detection in the PB. The presence and the proportion of AML cells found in those two reservoirs also seems independent of the risk group (Table 4). Of note, some patient samples also lead to other remarkable phenotypes, such as splenomegaly (1 intermediate and 1 adverse AML sample) or tumors (1 favorable, 3

intermediate and 3 adverse AML samples) (Table 4). The tumors were all located in the legs, close to the femurs, and analysis of cells from these tumors by FC revealed for the majority the presence of human CD33 positive cells (data not shown). Notably, all mice from the same patient that was likely to cause splenomegaly or tumor development had the same phenotype, indicating that this is an intrinsic property of the patient sample and not a hazardous event.

#### **1.1.4. High proportions of human AML cells in the BM at week 16 correlates with reduced survival of the murine recipients**

As already mentioned, week 16 was often used as a standard endpoint for analysis of mice xenotransplanted with human AML cells. Consequently, we decided to set the first BMP at this important intermediate time-point. In order to analyze the different engraftment levels, we first classified the mice according to the percentage of human CD33 positive cells in the BM into five different categories (<0.1%, 0.1-1%, 1-5%, 5-20% and 20-100%). Consistently with the observations presented in Figure 6, a very high proportion of the analyzed mice had no or very low amounts of detectable human AML cells (64.8%, Figure 7A). Notably, the repartition of the transplanted mice in each engraftment category was similar in each AML risk group (Figure 7B and 7C). Interestingly, mice showed mainly either very low (<1%) or high (>20%) proportions of human leukemic cells, with only 19.1% of the mice displaying medium (1-20% engraftment) levels of human AML cells (Figure 7B and 7C). This might indicate a rapid expansion of the leukemic cells once a certain level of colonization of the BM is achieved in these mice, an observation that seems to be valid for AML cases from all three risk groups.

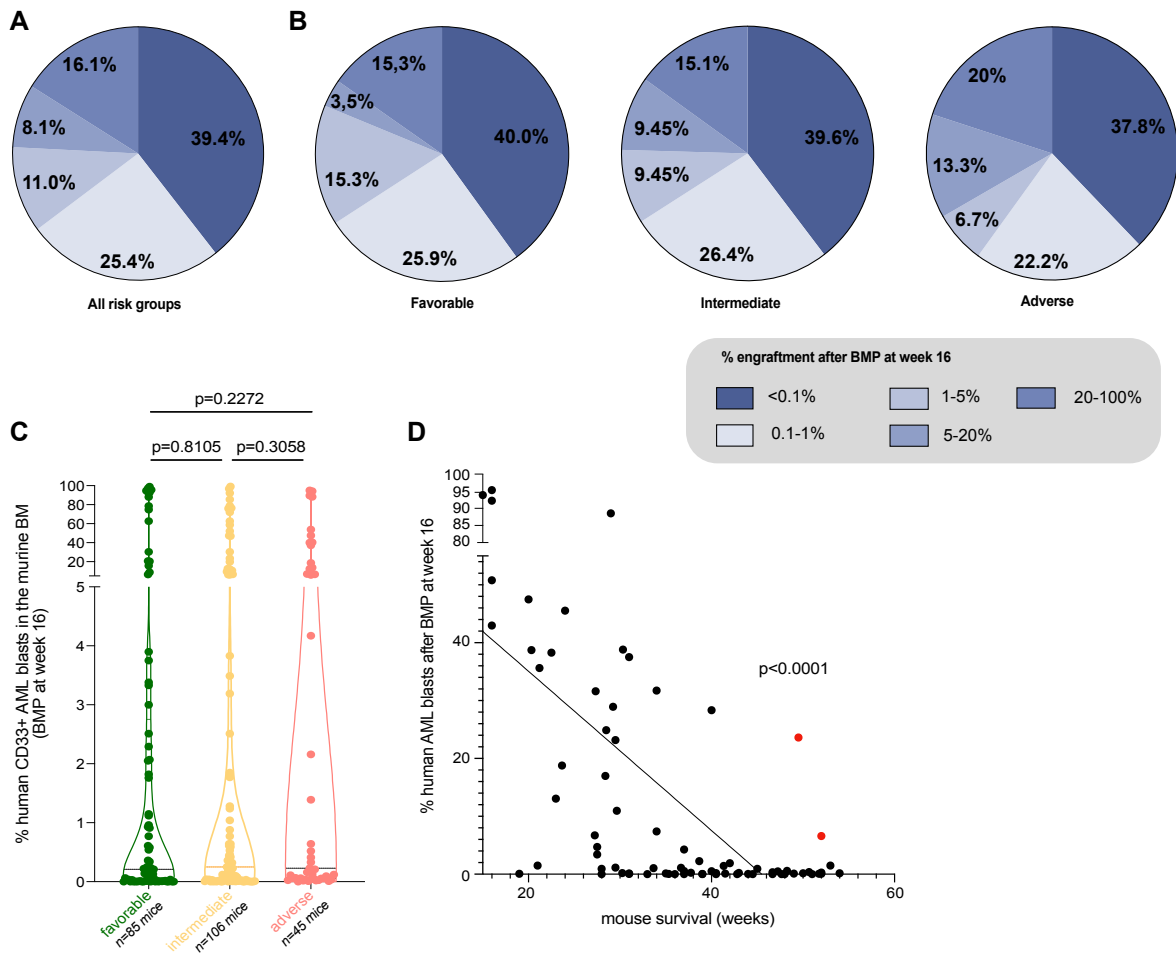


**Figure 7: % Engraftment at week 16 correlates with long-term mouse survival**

(A) Pie charts representing the engraftment at week 16 BMP of the mice transplanted with AML patient samples, independently of the different risk groups (n=236 mice from n=76 AML cases). Engraftment was divided into five different categories according to the percentage of CD38 positive human AML blasts detected in murine femurs at the time point of the puncture. (B) Pie charts representing the engraftment at week 16 BMP of the mice transplanted with AML patient samples per risk group (favorable, n= 85 mice from n= 29 AML cases; intermediate, n= 106 mice from n= 32 AML cases; adverse, n= 45 mice from 15 AML cases). Please note that the numbers of AML cases and mice here are not exactly the same than in Figure 6 since some animals were already sacrificed before week 16. (C) Percentage of engraftment at week 16 of mice from all different risk groups (favorable, n= 85 mice from n= 29 AML cases; intermediate, n= 106 mice from n= 32 AML cases; adverse, n= 45 mice from 15 AML cases). (D) Scatter plot and linear regression analyzing displaying the relationship between the percentage of engraftment at week 16 BMP and survival of the mice. One

dot represents one AML sample for which the mean of the engraftment and survival of all mice transplanted with respective patient cells are used (n= 76 AML patients, n=2-6 mice per AML sample). Best fit values for the line: slope -1.376, Y-intercept 62.60, X-intercept 45.49, R square 0.3923.

In (C), data are represented as violin plot with the lines representing median and quartiles. In (D), linear regression was performed to investigate the correlation between both sets of value. P-value defines whether the slope is significantly different from zero.

Shapiro-Wilk test for normality, Student-t-test, Mann-Whitney-U-test.

Moreover, we were interested in correlating the percentage of engraftment at week 16 with mouse survival after transplantation of the respective patient samples (Figure 7D). Interestingly, there is a significant negative correlation between high level of engraftment of patient samples detected at week 16 and the survival of mice transplanted with the same patient sample. Of note, only very few AML samples (2/14) induced disease in less than 26 weeks post-transplantation but displayed low (<5%) engraftment levels at week 16. Nevertheless, certain AML cells with very low (<0.1%) proportions detected cells at week 16 still engrafted at a later time-point (Figure 7D). This leads to the question of what is driving long-latency disease induction in these patients. We speculate that.... Of note, two AML samples (in red), for which BMP showed elevated engraftment levels at week 16, only showed profound leukemia induction after more than 47 weeks after transplantation (Figure 7D). This begs the question of whether the 1% threshold used to define engraftment in previous studies using leukemia xenotransplantation models, is sufficiently accurate, and highlights once again the necessity of long-term observations in these models.

#### **1.1.5. Intermediate and adverse risk group patient samples show higher homing rates**

In previous studies from our lab we could show that homing was reduced in long-latency versus standardly engrafting AML, with the lowest percentage of homing cells observed in one AML case that did not engraft at all (Paczulla *et al.*, 2017). However, this interesting observation was only made with a total of n=6 AML cases leading us to repeat this experiment with a much bigger cohort. Importantly, we do not observe a

significant difference between long-latency and standardly engrafting AML samples, maybe because of the big difference in the number of samples that fall in each group, with a vast majority of the samples being long-latency engrafters (Figure 8A, n= xx AML samples). We were thus also interested in exploring the homing rates of mice transplanted with samples from the three different risk groups. Interestingly, we found that mice transplanted with AML samples from the favorable risk group show homing rates that are significantly different from those transplanted with intermediate and adverse risk group patients, with the two latter groups behaving very similar (Figure 8B-C). Remarkably, in all three groups, we were able to observe some mice displaying particularly high homing rates ( $>0.02\%$ ) compared to the majority of the animals. Importantly, homing rates within each group transplanted with the same AML sample (n=2-5 mice per group) were very similar, thus, mice showing high homing rates are consequently mice that were transplanted with cells from only a limited number of AML cases (n=2 favorable, n=3 intermediate and n=1 adverse risk group patient sample, respectively; Figure 8D). We investigated the characteristics of these deviating patients, in particular whether they had similar characteristics or differences compared to other patient samples from the group, but the reason remains unclear (Figure 8D). Since we also observed a clear correlation between risk group classification and the homing rate, we were next interested to see whether we could correlate the mean homing rate determined for an AML case with the mean survival of the mice transplanted with the same AML sample (Figure 8E). It would be a very helpful tool if homing rates correlated with mouse survival, since the homing assay is a rapid assay with a readout time of less than 24 hours, and would thus allow prediction for the long-term behavior of an AML sample in murine recipients. Unfortunately, however, we were not able to observe any correlation between the homing rate and the survival for the same AML patient (Figure 8E).

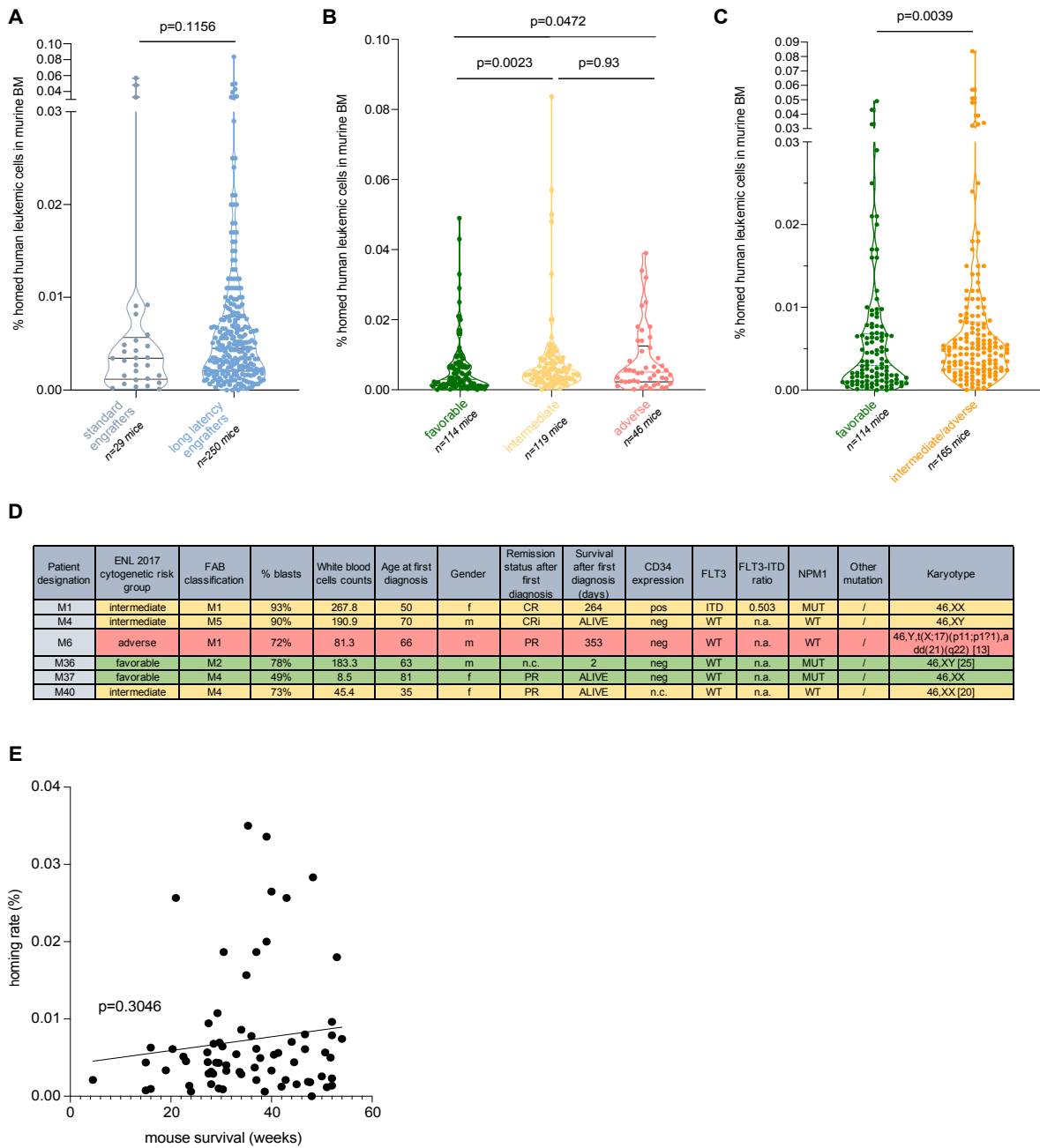


**Figure 8: Homing rates of AML patient cells are higher in intermediate/adverse compared to favorable risk groups.**

**(A)** Percentage of CFSE labeled human leukemic cells found in the murine BM, 16 hours post transplantation. AML samples were categorized in standard engrafters (grey blue, n=30 mice from n=9 AML cases), i.e. end analysis before week 20 post transplantation and long-latency engrafters (blue, n=257 mice from n=80 AML cases) i.e. end analysis after week 20 post transplantation. **(B-C)** Percentage of fluorescently labeled homed human leukemic cells found in the murine BM, 16 hours post

transplantation. Data are plotted per risk group (B, favorable, green, n=114 mice, n= 35 AML cases; intermediate, yellow, n=119 mice, n= 39 AML cases; adverse, red, n=46 mice, n= 15 AML cases), or with intermediate and adverse patients together (C, favorable, green, n=114 mice, n= 35 AML cases; intermediate/adverse, orange, n=165 mice, n= 54 AML cases). **(D)** Table summarizing the characteristics of the patient samples with high homing rates (>0.02%). **(E)** Scatter plot and linear regression analyzing the relationship between the homing rate and the long-term survival of transplanted mice. One dot represents one AML patient for which the mean of the homing rate and survival of all mice transplanted with the same patient cells are depicted (n= 72 AML cases, n=3-5 mice per AML sample). Please note that we did not investigate the survival of mice for all AML samples used for homing experiments, explaining why we only plotted the data for 72 AML cases.

Best fit values for the line: slope  $8.89 \times 10^{-5}$ , Y-intercept 0.004137, X-intercept -46.54, R square 0.01527.

In (A-C), data are represented as violin plot with lines representing median and quartiles. In (E), linear regression was performed to investigate the correlation between both data sets. P-value defines whether the slope is significantly different from zero.

Shapiro-Wilk test for normality, Student-t-test, Mann-Whitney-U-test.

#### 1.1.6. **CD34+ surface marker expression on AML samples has no influence on the engraftment or the homing in murine recipients**

We next wanted to investigate if surface marker expression influences homing or engraftment of our patient samples. Therefore, the expression of standard cell-surface markers used for the diagnosis of AML (precursors markers: CD33, CD34, CD117; (Döhner *et al.*, 2017) was analyzed. It is important to point out here, that even though the HSPC antigen CD34 is a well-established surface marker for LSCs, about 30% of AML cases lack robust CD34 expression in AML blasts (these samples will be termed “CD34 non-expressing AML” in the rest of this work) (Arnone *et al.*, 2020; Quek *et al.*, 2016; Sarry *et al.*, 2011; Taussig *et al.*, 2010).



Furthermore, we also explored the expression of markers known to be important for AML prognostication and for which the expression in our AML samples has been determined (CD56 and CD38; (Keyhani et al., 2000; Raspadori et al., 2001) (Plesa et al., 2017)).

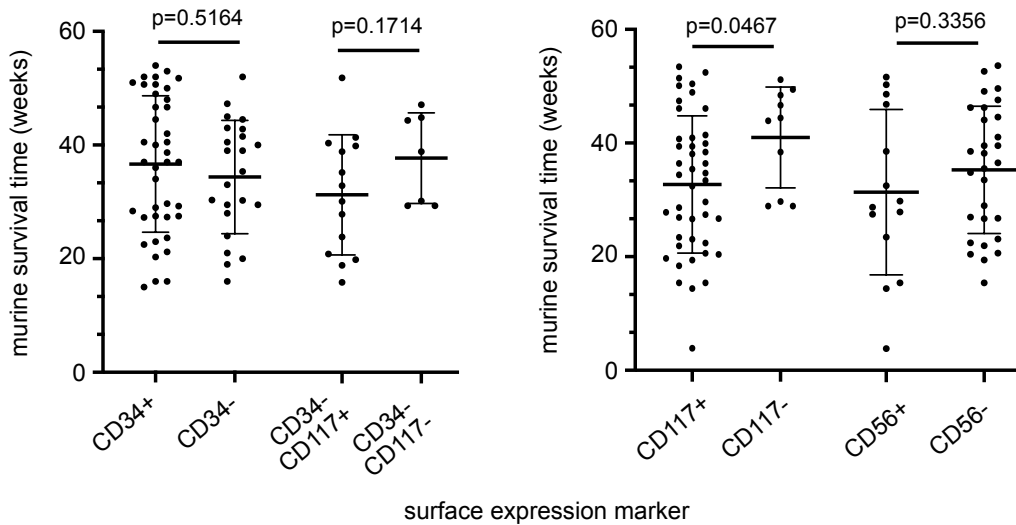
AML samples from the intermediate and adverse risk groups show higher CD34 and CD117 surface expression compared to favorable risk group AML samples. Not surprisingly, we were able to detect CD33 and CD38 expression on the cell surface independently of the risk group in all patient samples, the reason why we chose CD33 for the determination of engrafted cells in our BMP experiment. In addition, surface expression of CD56 is quite similar in all three risk groups (Figure 8A). We then compared marker expression (CD34, CD117, CD56, as well as the expression of CD117 amongst CD34 non-expressing patient samples) with mouse survival (Figure 8B) and the homing rate (Figure 8C) after transplantation. We were not able to detect differences in the survival rate or the homing capacity between CD34-expressing or -non-expressing patient samples (Figure 8B-C). Since LSCs can be further enriched through the expression of CD117 (Arnone *et al.*, 2020), we wanted to analyze if there is a difference between patients that express CD117 (CD34-CD117+) or not (CD34-CD117-). Here again we were not able to see any significant difference between the two groups (Figure 8B-C). Interestingly, however, by only looking at CD117 marker expression regardless of CD34, we saw that CD117-expressing AML patient samples were more aggressive upon xenotransplantation in NSG mice, as shown by both survival (Figure 8B, right) and homing to the BM (Figure 8C, right).

Finally, we also wanted to investigate if CD56 surface expression influences homing and engraftment. The survival of murine recipients was slightly but not significantly increased in mice that obtained AML patient blasts expressing CD56 (Figure 8B, right), while we surprisingly saw a significantly increased homing capacity for AML samples that do not express this marker (Figure 8C). CD56 is also known as neural cell adhesion molecule and its expression on leukemic blasts has been correlated to bad prognosis for AML patients (Sun et al., 2021; Van Acker et al., 2017; Xu et al., 2015). In regard to our results, we speculate that this might be linked to an increased homing of AML cells. Moreover, the marker has also been described as involved in migration processes and consequently to be associated with extramedullary infiltrates of AML (Chang et al., 2004).

**A**

Marker	Favorable risk group	Intermediate risk group	Adverse risk group	Positive rate (%)
CD34	12/25 (48%)	24/30 (80%)	8/13 (61.5%)	64.7
CD33	25/25 (100%)	32/32 (100%)	13/13 (100%)	100
CD38	24/24 (100%)	25/25 (100%)	13/13 (100%)	100
CD56	14/18 (77.8%)	13/22 (59.1%)	9/12 (75%)	69.2
CD117	17/22 (77.3%)	23/24 (95.8%)	11/14 (78.6%)	85

**B**



**C**

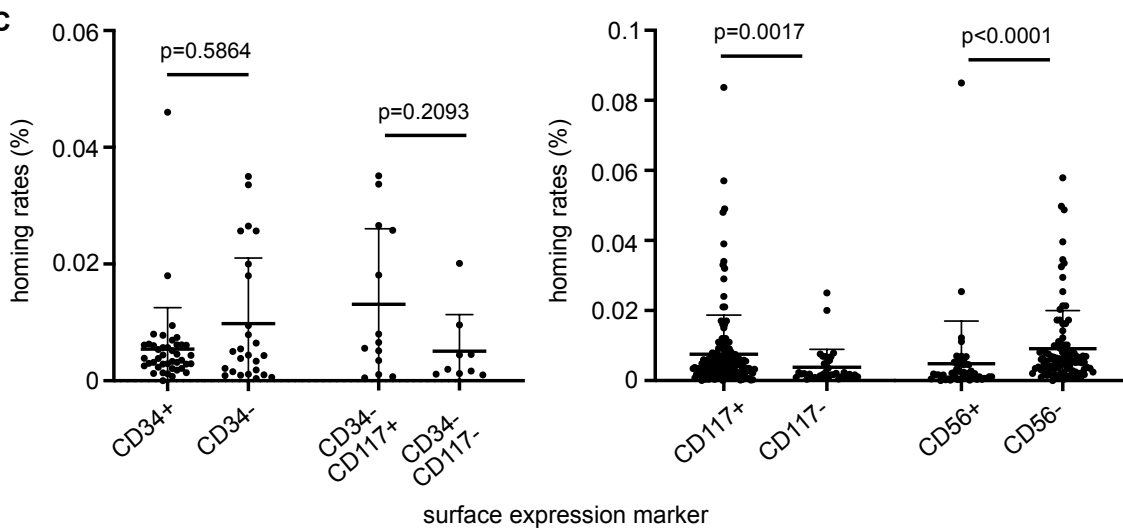


**Figure 8: AML samples marker expression is neither correlated with the mouse survival, nor the homing rate**

**(A)** Table summarizing the expression of surface markers in the different AML samples. Indicated are the number of positive over the total number of AML samples

for which specific marker expression was investigated, as well as the percentage of positive cells. Last column indicates the positive rate in the patient cohort, independently of the risk group. **(B)** Comparison of mouse survival according to surface marker expression. Patients with AML blasts positive for CD34, CD117 and CD56 expression were compared to those negative for the respective marker. Similarly, amongst CD34 non-expressing patients, AML samples expressing CD117 were compared to those that were not expressing this marker. Each dot represents one AML patient for which the mean of the survival time is plotted. **(C)** Comparison of homing rates according to surface marker expression. Each dot represents one AML patient for which the mean of the homing rates is plotted.

In (B-C) lines represent mean with standard deviation.

Shapiro-Wilk test for normality, Student-t-test, Mann-Whitney-U-test.

Furthermore, we also analyzed surface expression of CD34, CD38 and CD117 in the BM, spleen and PB of transplanted mice at final analysis (Table 5). Marker expression was similar in all compartments at final analysis in the majority of transplanted AML samples. However, we observed that for some CD34-expressing AML samples we could not retrieve this marker in any of the compartments in the transplanted animals. This was also the case for CD38 and to a lesser extend for CD117 marker expression (Table 5). This is a surprising observation that differs to what was described in several previous papers, i.e. that the phenotype of human AML cells was maintained upon transplantation into murine recipient, and even remained unaltered after serial retransplantations (Ailles *et al.*, 1999; Her *et al.*, 2017; Paczulla *et al.*, 2017; Sanchez *et al.*, 2009). We speculate that this might be due the very long time of follow up of the mice that contrasts with many of the previous studies and that could induce more differentiation of AML cells. Another explanation could be linked to technical issues with the multi-color FC analysis of the murine recipients.

Patient	%CD34+				%CD38+				%CD117+			
	pre-transplant	BM	spleen	PB	pre-transplant	BM	spleen	PB	pre-transplant	BM	spleen	PB
M1	neg	low	low	+	pos	+	low	low	pos	++	low	low
M3	pos	+	++	+++	pos	+++	+++	++	pos	+++	+++	+++
M4	neg	low	low	low	pos	low	low	low	pos	low	low	low
M5	pos	low	low	low	pos	+++	++	low	pos	+++	+++	low
M6	neg	low	+	+	pos	+	++	++	pos	low	+++	+
M7	neg	not engrafted	not engrafted	not engrafted	pos	not engrafted	not engrafted	not engrafted	neg	not engrafted	not engrafted	not engrafted
M8	pos	low	low	low	pos	low	low	low	pos	low	low	low
M10	pos	low	low	low	pos	low	low	low	pos	low	+	low
M12	pos	+	++	++	pos	+++	+++	+++	pos	+++	++	+++
M13	neg	low	low	low	pos	low	++	low	n.c.	low	+	low
M14	n.c.	low	low	low	pos	low	low	low	n.c.	low	low	low
M15	neg	low	low	low	pos	+++	++	++	low	+++	++	+
M16	neg	not engrafted	not engrafted	not engrafted	pos	not engrafted	not engrafted	not engrafted	neg	not engrafted	not engrafted	not engrafted
M17	n.c.	low	++	++	pos	+	++	++	n.c.	low	low	+
M18	pos	+++	+	low	pos	+++	low	low	pos	+++	low	low
M22	n.c.	low	low	low	pos	+++	++	+	n.c.	+++	+	+
M25	pos	low	low	low	pos	low	low	low	n.c.	low	low	low
M29	n.c.	low	++	low	pos	low	+	low	pos	low	++	+
M32	pos	+++	+++	+++	pos	+++	+++	++	n.c.	+++	++	+++
M34	n.c.	low	low	low	pos	low	low	low	n.c.	+	low	low
M37	neg	low	low	low	pos	low	low	+	pos	low	low	+
M38	pos	not engrafted	not engrafted	not engrafted	pos	not engrafted	not engrafted	not engrafted	pos	not engrafted	not engrafted	not engrafted
M40	n.c.	low	++	low	pos	low	low	low	n.c.	+	low	++
M41	pos	+	low	low	pos	+++	++	++	pos	+++	+	+
M42	pos	low	low	low	pos	+++	+++	+++	pos	+++	+++	+++
M43	pos	not engrafted	not engrafted	not engrafted	pos	not engrafted	not engrafted	not engrafted	pos	not engrafted	not engrafted	not engrafted
M44	neg	low	+	low	pos	++	++	low	pos	low	+++	low
M45	pos	low	low	low	pos	+++	++	low	pos	+	low	low
M46	pos	low	low	low	pos	low	low	low	pos	low	low	low
M49	pos	not engrafted	not engrafted	not engrafted	pos	not engrafted	not engrafted	not engrafted	neg	not engrafted	not engrafted	not engrafted
M51	pos	+	+	+	pos	+	low	+	pos	++	+	+
M52	pos	low	low	low	pos	low	++	low	pos	low	+	low
M53	neg	++	++	++	pos	+++	+++	+++	pos	+++	+++	+++
M55	pos	low	++	+	pos	+++	+++	+	pos	++	low	+
M56	neg	low	low	low	pos	low	low	low	pos	n.c.	n.c.	n.c.
M57	pos	low	+	low	pos	low	low	low	pos	low	low	low
M58	pos	low	low	low	pos	++	+	low	pos	++	++	+
M59	pos	+	low	low	pos	low	low	low	pos	+++	low	+
M62	pos	+	+	++	pos	+++	++	++	pos	+++	low	++
M63	pos	+++	+	+	pos	+++	low	low	pos	++	low	low
M64	pos	+++	+	+	pos	+++	+	low	pos	+++	+	low
M65	neg	+	low	low	pos	+	low	low	pos	+	low	low
M66	n.c.	low	++	+	pos	+++	+++	+++	n.c.	++	+	++
M69	pos	+	n.c.	n.c.	pos	+	n.c.	n.c.	pos	n.c.	n.c.	n.c.
M70	pos	+	+	+++	pos	+++	+++	+	pos	+++	++	low
M72	n.c.	+	+	low	pos	+++	++	+++	n.c.	+++	+++	+++
M73	neg	low	low	low	pos	++	++	+	pos	+	+	low
M74	pos	+	low	+	pos	+++	+	++	pos	+++	++	++
M75	n.c.	low	++	low	pos	low	++	low	n.c.	+	++	low
M80	n.c.	not engrafted	not engrafted	not engrafted	pos	not engrafted	not engrafted	not engrafted	n.c.	not engrafted	not engrafted	not engrafted
M82	pos	not engrafted	not engrafted	not engrafted	pos	not engrafted	not engrafted	not engrafted	n.c.	not engrafted	not engrafted	not engrafted
M84	n.c.	low	low	low	pos	low	low	low	n.c.	low	low	low
M85	pos	low	low	low	pos	+	+	+	n.c.	low	+	+
M90	neg	low	low	low	pos	+++	+++	+++	pos	+++	+++	+++
M94	neg	low	low	low	pos	low	low	low	pos	low	low	low
M95	pos	not engrafted	not engrafted	not engrafted	pos	not engrafted	not engrafted	not engrafted	pos	not engrafted	not engrafted	not engrafted
M96	pos	low	low	low	pos	low	low	low	pos	low	++	low
M98	n.c.	low	low	low	pos	low	low	low	n.c.	low	low	low
M99	neg	low	low	low	pos	++	low	low	pos	++	low	low
M100	pos	not engrafted	not engrafted	not engrafted	pos	not engrafted	not engrafted	not engrafted	neg	not engrafted	not engrafted	not engrafted
M101	neg	low	++	low	pos	low	+	low	low	low	low	low
M122	pos	++	+	+	pos	++	++	+	pos	++	low	low
M123	pos	low	+	low	pos	+++	+	+	low	n.c.	n.c.	n.c.
M124	neg	low	+	low	pos	low	low	low	pos	low	low	low

**Table 5: Marker expression pre- and post-transplantation**

Table summarizing the expression of CD34, CD38 and CD117 in the AML samples pre-transplantation, in the bone marrow (BM), spleen and peripheral blood (PB).

Please note that the animals that were not analysis at the final endpoint due to reallocation to other experiments (c.f. legend table 4) are not indicated in this table.

Please note that the CD33 expression is not included in this table since this marker is the one used for the definition of the engraftment percentage and the proportions in the expression at final analysis time-point is already summarized in table 2.

*Low: <1% marker expression; +: 1-5% marker expression; ++: 5-20% marker expression; +++: >20%; n.c.: data was not collected*

### 1.1.7. Identification of further patient characteristics determining the engraftment potential of primary AML cells in the murine recipient

In addition to the risk group classification, we also had a look at other known characteristics of our cohort and their potential influence on engraftment or homing. First, we wanted to investigate if the survival of the patient (survival status, Figure 9A and survival time, Figure 9B) correlates with the survival time of the murine recipient transplanted with the respective AML sample. In Figure 9A, we classified all AML cases according to whether patients died or were still alive two years after the time-point of first diagnosis. Although the difference is not significant, we were able to observe a slightly higher survival rate of mice transplanted with samples for which the patient survived longer than two years. Within the group of patients that survived less than two years after first diagnosis, we had a closer look at the correlation between the survival time of the patient and the corresponding murine recipients, however, we were not able to observe a correlation between the two variables (Figure 9B). Furthermore, we could also observe a clear, but not significant enhanced survival time of the mice transplanted with samples of patients that achieved complete remission in response of initial treatment, in comparison to those that did not (Figure 9C). This is in accordance with a previous study, in which the authors showed enhanced engraftment of the population who failed to achieved a complete remission in a NOD/SCID human chimera model of human AML (Rombouts *et al.*, 2000b). Moreover, we were not able to observe correlations between the age, sex or WBCs of patients and mouse survival after transplantation (data not shown), which was also the case for homing rates (data not shown).

It has furthermore been described before that AML samples from patients with an internal tandem duplication in the Flt3 gene (Flt3/ITD) displayed a greatly enhanced potential to engraft in immunodeficient mice (Rombouts *et al.*, 2000a). We thus split the AML cases from our cohort into three different groups: ITD high: ratio >0.5, ITD low: ratio <0.5 and WT. In accordance to this previous study we could observe a reduced survival time for the mice transplanted with AML samples with high Flt3/ITD ratio versus mice with a low ITD ratio and a significant reduction compared to WT mice group. No difference was observed between the ITD low ratio and the WT group. (Figure 9D). We next also analyzed homing rates of patient samples from these three

groups. Interestingly, we were also able to observe a clear but not significant increase in the homing of the cells derived from patients with high Flt3/ITD ratio (Figure 9E). Moreover, we were interested if mutations in NPM1, which is also a very frequent genetic aberration found in AML patients, might influence disease induction and homing in the murine recipients. Unfortunately, we were not able to find any correlation between these variables (data not shown).

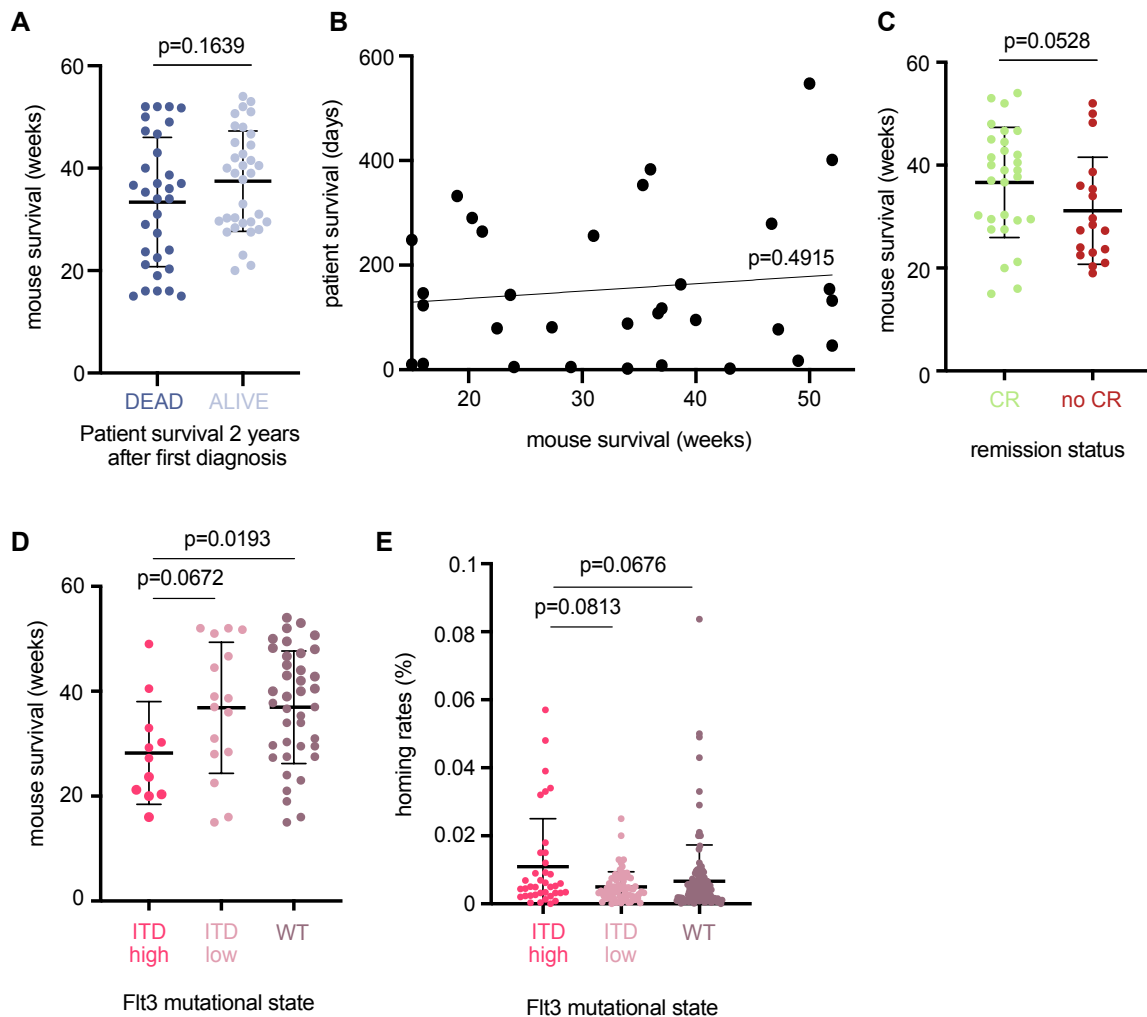


**Figure 9: Analysis of additional patient characteristics determining the engraftment potential of primary AML cells in murine recipients.**

**(A)** Comparison of mouse survival according to the status of the patient two years after first diagnosis (dead,  $n=32$  AML cases,  $n=2-5$  mice per AML samples, blue; alive,  $n=34$  AML cases,  $n=2-5$  mice per AML sample, light blue). Each dot represents one AML patient for which the mean of the survival time is plotted. **(B)** Scatter plot and

linear regression analyzing the relationship between patient and mouse survival. One dot represents one AML patient for which the mean of the survival in the murine recipient transplanted with the respective patient cells is shown. Only patient samples for the “dead” category displayed in Figure 6A are represented in this plot. Best fit values for the line: slope 1.410, Y-intercept 108.1, X-intercept -76.67, R square 0.01591. **(C)** Comparison of mouse survival according to the remission status of the patient (CR, complete remission, n=29 AML cases, n=2-5 mice per AML sample, green; no CR, n=18 AML cases, n=2-5 mice per AML sample, red). Each dot represents one AML patient for which the mean of the survival time is plotted. **(D)** Comparison of mouse survival according to the Flt3 mutation status (ITD<sup>high</sup>, n=12 AML samples, n=2-5 mice per AML sample, red; ITD<sup>low</sup>, n=17 AML samples, n=2-5 mice per AML sample, pink; WT, n=40 AML samples, n=2-5 mice per AML sample, brown). Each dot represents one AML patient for which the mean of the survival time is plotted. **(E)** Comparison of homing rates according to the Flt3 mutation status (ITD<sup>high</sup>, n=38 mice from n=11 AML cases, red; ITD<sup>low</sup>, n= 72 mice from n=21 AML cases, pink; WT, n=131 mice from n=40 AML cases, brown).

In (A, C, D and E) lines represent mean with standard deviation.

In (B), linear regression was performed to investigate the correlation between both data sets. P-value defines whether the slope is significantly different from zero.

Shapiro-Wilk test for normality, Student-t-test, Mann-Whitney-U-test.

### 1.3. DISCUSSION

The understanding of the basic biology of AML as well as the development of new strategies to cure this disease relies on the availability of reliable *in vivo* models. Over the last decades, our lab as well as many others have used xenotransplantation models for these purposes and could demonstrate the ability of AML cells to engraft in immunodeficient mice, including the NSG mouse strain that we have used in this work. However, the main disadvantage described for this model has been the complexity to predict engraftment as well as the low and long-lasting engraftment in this assay. We aimed to improve the prediction of engraftment in the NSG xenotransplantation model by using a large cohort of AML samples from various genetic backgrounds. Moreover, we describe some parameters (risk group of the

patient, genetic and molecular markers) that can influence the time needed for engraftment in this model.

Our results confirm data previously published by our lab (Paczulla et al, ...) by using a larger cohort of patient samples that, in contrast to several previous publications (Eppert *et al.*, 2011; Sanchez *et al.*, 2009), included samples from favorable risk group patients, that routinely engrafted NSG mice as well. Importantly, in this work, we used intrafemoral transplantation for any long-term experiments, since we were previously able to show that both IV and IF transplantation lead to comparable engraftment when starting with a 2-fold reduced cell number for the IF transplantation. This is very important since for some rare AML samples only low levels of cells were available, which would not allow to achieve a sufficient number of animal replicates in the IV transplantation setting. Nevertheless, we cannot completely exclude the possibility of a different mechanism of engraftment and disease induction in the two methods, since we also show in chapter 4 that circadian rhythm and stress molecule levels strongly affect engraftment and homing of transplanted human AML cells via IV transplantation. It is not clear if engraftment and homing are similarly affected after IF transplantation, when the animals are completely anesthetized upon transplantation.

Despite previous reports, in which experiments were usually stopped latest at week 16 we were able to show that at each investigated time point (week 15, week 20, week 30, week 40, week 52), a substantial proportion of AML samples could be added to the list of patients that were capable to engraft and to induce symptomatic leukemia in our NSG xenotransplantation model. Importantly, the proportion of engrafted adverse AML samples reach the maximum at week 40, in contrast to favorable and intermediate AML samples for which the proportion engrafted samples still increases between weeks 40 and 52 post transplantation. Consequently, the follow-up time for mice transplanted with cells of the adverse risk group of patients could eventually be reduced to 40 weeks.

An important and puzzling observation we made in this work concerns a small proportion (around 25%) of mice showing signs of disease that, according to our scoring system, lead to their sacrifice, even though further analysis of hematopoietic compartments shows only very low proportions (<1%) of engrafted human leukemic cells. This is mostly true for mice transplanted with patient samples from the adverse risk group. We hypothesize that for some AML cases only a few leukemia cells are sufficient to provoke strong symptoms, which could also explain why so many adverse



risk group patients, that are known for the particularly high aggressiveness (Paczulla *et al.*, 2017)(Döhner *et al.*, 2017), fall into this engraftment category. Nevertheless, the reasons why those mice display symptoms is still unknown and could be either leukemia dependent or linked to leukemia-independent factors such as age, infections or other unrelated diseases.

Several previous studies demonstrated that the level of engraftment was linked to the FAB subtype of the AML patient (Rombouts *et al.*, 2000b) (Ailles *et al.*, 1999) when mice were analyzed at a defined time-point (set to respectively 30 days and 8 weeks post-transplantation). Here we could confirm results from a previous study by our laboratory (Paczulla *et al.*, 2017), indicating that survival rates of transplanted animals with samples from the different risk groups nicely recapitulated observations made in the patient, such as longer survival for patients from the favorable and intermediate risk groups when compared to adverse groups. We also observed high similarities between mice transplanted with patient cells from the favorable and intermediate risk group. A previous study already described that the engraftment of intermediate-risk group samples was difficult to be anticipated (Griessinger *et al.*, 2018). However, we were able to show that in our experimental settings, the survival time for mice transplanted with patient samples from this group behave similarly to those from the favorable risk group which can help anticipating the course of the disease in the recipient animal.

Interestingly, even though the survival curve we draw is very linear over time, we observe, independently of the risk group, a rupture corresponding to the week 16 time-point, when the first BMP is performed. After this first BMP, a high number of mice had to be sacrificed since they were harboring more than 80% human AML blast in the BM even though they did not show signs of disease. This situation was much less frequent for the two subsequent BMP (week 26 and week 39), which is why we could not observe large drops of survival rates at these time-points. One hypothesis is that this is again due to the aggressiveness of some AML cases, which require more to lead to symptomatic disease induction. Another possibility could be that this is linked to the young age of the mice that can consequently resist to higher numbers of infiltrated blasts in the BM without showing symptoms. In order to prove this assumption, transplantations in older mice could be performed to see potential changes.

As mentioned in the result part of this thesis, we were able to detect human leukemic cells not only in the BM, but to a lesser extent also in the PB and spleen, thus indicating

that the colonization of the BM seems to be a prerequisite for further infiltration of the spleen and retrieval of human cells in the circulation. Importantly, concerning leukemic circulating cells, it might be possible that these cells first settle to the BM (or the spleen) and enter circulation using the same in and out mechanism than healthy HSPCs (Méndez-Ferrer *et al.*, 2008). As we described before, this mechanism of release into the circulation involves circadian oscillations and it would be interesting to see if the proportions of circulating leukemic cells in the PB would vary if the the final analysis of engrafted mice were performed at different times of the day. Noteworthy, in this work, mice were all sacrificed and analyzed around the same time of the day, and the comparison of the proportion of AML cells in the circulation might thus not be biased by circadian oscillations. Nevertheless, the profound differences in the proportions of leukemic cell residing in the BM and the PB show that screening of the PB is not sufficient to monitor the engraftment reliably.

Moreover, we show that in most cases, leukemic cells also colonized the spleen of the murine recipient. The spleen is a site for extramedullary hematopoiesis in mice and humans under hematopoietic stress (Inra *et al.*, 2015) and splenomegaly is observed in many AML patients. However, very little is known about the colonization of this organ in xenotransplantation models (Her *et al.*, 2017). A few years ago, it was shown that AML cells repopulated the BM at greater frequency and absolute counts, followed by spleen and PB, when the cells were injected into newborn NSG pups intrahepatically (Her *et al.*, 2017). It would be of particular interest to study the kinetics of the infiltration of the spleen and for example determine when the colonization of this organ starts, which is impossible in our currently used experimental settings but could be conducted using methods such as *in vivo* bioluminescence imaging (Vick *et al.*, 2015). Of particular interest, two transplanted AML samples led to splenomegaly in recipient mice, which has already been described for some AML cases in such xenotransplantation models (Her *et al.*, 2017) (Paczulla *et al.*, 2017) (Agliano *et al.*, 2008).

In addition, we also observed tumor development in mice transplanted with cells from five different AML samples. Notably, in most of these cases, all the mice that were transplanted with the same AML sample show tumor development, thus meaning that this observation is not due to hazard or to intrinsic properties of the recipient mouse, but rather to the material being transplanted. Interestingly, these tumors were all located along the animals' legs. One might suspect that the development of these

tumors may have been driven by the BMP procedure, in which some AML cells “escaped” from the femur marrow and settled along the bone. Supporting this hypothesis, human CD33 positive cells were detected in the tumor of almost all analyzed mice. We could unfortunately not find any common characteristics between the different patients that developed these leg tumors upon transplantation and consequently could not find a molecular or genetic marker that would cause the cells of some particular AML samples to survive and emerge from the BM. Similarly, 2-8% of patients with AML exhibit myeloid sarcoma, which is an extramedullary proliferation of blasts (Avni and Koren-Michowitz, 2011). Unfortunately, we do not have any information about a possible myeloid sarcoma in the patients for which we observe these murine leg tumors.

Furthermore, our data also show that in a high proportion of the samples (64.8%), the BM puncture performed 16 weeks after transplantation showed less than 1% human leukemic cells in the BM. We have chosen this time-point for the first puncture because this was for a long time widely considered as the final analysis time-point for AML xenograft experiments, with all the samples that did not induce leukemia at this time-point being considered as non-engrafters (Eppert *et al.*, 2011; Sanchez *et al.*, 2009). The percentage of colonization of the BM at this 16 week time point was not significantly different when comparing the samples according to the risk group classification. In all three groups, we were able to observe a similar distribution regarding the percentage of engraftment in the analyzed mice, with the majority of the mice showing low or very low levels of engraftment, as well as considerable number of animals with high engraftment rates. Interestingly, we could observe medium engraftment rates only for very few samples at the week 16 BMP time-point. We hypothesize that this is due to the expansion of human AML cells in the murine BM, which increases rapidly after reaching a certain threshold. Interestingly, we observed differences between the engraftment seen in the mice at the BMP (regardless of the time of the puncture) and that seen in the same mouse at the analysis endpoint (which is lower in most cases), although final analysis usually occurs within 24 hours after BM engraftment higher than 80% was detected. This observed difference is most likely due to the difference in the method, since during the BM puncture, mainly marrow is collected, while at final analysis, all bones were crushed, thus leading to a mixture of BM with components of the bone structure such as the endosteum, periosteum and

cartilage and consequently a greater dilution of human AML cells at the moment of analysis. In line with this hypothesis and observation, it is important to carefully consider the BMP method, since mice are anesthetized repeatedly but more importantly also because of the introduction of the needle into the bone cavity that might disturb its structure. It is well known that transplanted AML cells need important interactions with their microenvironment (Reinisch et al., 2016) (Ishikawa et al., 2007) (Schepers et al., 2015) and this disturbance is certainly not without consequence.

Moreover, another important point to consider is the impact of the extraction of a certain quantity of human AML cells present in the murine bone, especially during advanced courses of the disease. The effects might not be the same when cells are extracted from a mouse with very low numbers of AML cells in the bone or another that is fully engrafted. To optimize the BMP procedure, answering these questions with imaging technologies for example, would be of particular interest.

In this work, we were able to find a correlation between the BMP engraftment rate with long-term survival of the transplanted mice, showing that the majority of transplanted AML samples detected at high levels during the week 16 BMP had lower survival time. This is of particular interest, because the read-out at this time-point allows a prediction of the later survival of the mice and could thus be used for certain purposes (e.g. therapy development) instead of the “long-term” follow-up of the transplanted animals. Nevertheless, the correlation is not perfect and some AML samples behave differently. For example, we observed some AML cases where the engraftment rate was low or absent at week 16, but the mice that were transplanted with these samples still showed signs of disease at early time points, and less frequently vice versa. In view of these findings, careful evaluation of this method is necessary. These exceptions also raise questions about the commonly used 0.1 or 1% threshold for the definition of engraftment (Sanchez *et al.*, 2009) (Eppert *et al.*, 2011). For each experimental setup, it is thus important to carefully consider which threshold shall be used in the experimental setup, since we could show that an animal does not necessarily develop a symptomatic disease even though 0.1% or 1% of leukemic cells were detected.

Another interesting finding is the fact, that in our work, we see that the vast majority of animals develop leukemia at a later time point after transplantation, even though they harbor very low levels of human leukemic cells at week 16. This opens new insights in what eventually drives the transplanted AML cells to expand and proliferate at a later time point. Answers may reside in the selection of specific clones that require a

specific time to expand and drive symptomatic leukemia, or in *de novo* acquisition of permissive mutation. Consequently, it would be particularly interesting to look at genetic patterns of the human cells derived from BM of mice at final analysis and compare them to those of the matched samples before transplantation.

In addition, homing experiments showed a significant correlation with patient risk group stratification, i.e. intermediate and adverse risk group patients showed higher homing rates than favorable AML cells. Of note, while in the long-term experiments intermediate risk group AML samples behaved similarly favorable AML, they were more similar to adverse AML samples in this homing assay. In contrast our previously published data on a smaller data set (Paczulla et al...), we were however not able to see any difference in the homing rates between standard and long-latency engrafters. However, Pearce and colleagues showed that homing of AML cells into NOD/SCID animals was the same between engrafters and nonengrafters (Pearce et al., 2006). Not surprisingly, we were unfortunately also unable to correlate the homing rate for a patient sample with the survival of the mouse transplanted with the same AML sample, making it impossible to use the homing assay as a predictive assay for the later behavior of the patient sample in the murine recipient. Also, the homing assay relies on the detection of very few (often less than 30) fluorescent cells using FC. In my opinion, this makes this assay particularly difficult to interpret and very sensitive to small variations that can make a big difference in the read-out. Importantly to mention, the number of blasts from our samples were also very different, ranging from 14-100%, which may also explain these differences and highlight the necessity of transplanting 100% blasts to be eventually able to reach consistency in this assay. Even though we depleted human T and B cells from the sample before each transplantation, there are most probably remaining human healthy hematopoietic cells that may contaminate the AML sample. These cells might also home to the BM similar to malignant cells and might consequently distort the results. Unfortunately, removing these cells is also particularly challenging if not impossible as they share most of the surface markers with AML cells (Arnone *et al.*, 2020).

The diversity of the marker expression amongst the different patients of the cohort lead us to investigate whether their expression would correlate with the disease course in the murine recipient. CD34 is a well-described marker for both HSPC and LSC in

AML. In our previously published paper we showed that when CD34+ or CD34- AML blasts with inv(16) were transplanted in NSG mice, leukemia initiation was observed only from transplanted CD34+ blasts even after prolonged follow-up time (Paczulla *et al.*, 2017). Another study demonstrated that only a minority of NSG mice injected with CD34- cells showed significant engraftment (Sarry *et al.*, 2011) when samples with robust CD34 positivity were sorted based on their CD34 expression. In the work presented here, we sorted our AML samples based on their CD34 expression, which did not result in worse survival or increased homing rates. A recent work by Griessinger *et al.* also wanted to prove the hypothesis of a lower frequency of leukemia initiating cells in the samples that they describe as “nonengrafting”, but could not find a difference in the proportion of CD34+ or CD34+CD38- in “engrafter” and “nonengrafting” samples (Griessinger *et al.*, 2018). A similar observation was described by Sarry *et al.* who could show that CD34 is not necessary for engraftment potential but rather that amongst CD34 expressing samples, only the positive fraction is capable of engraftment (Sarry *et al.*, 2011). It would have been particularly interesting to investigate both the engraftment potential of the CD34 negative and positive fractions and maybe also to use this cohort to investigate if similar observations could be made independently of the patient risk group classification. Notably, it is also important to mention that in our analysis we do not consider the “strength” of CD34 positivity, and some samples might have been classified as CD34 expressing even though CD34 expression is low in these patients. In fact, in the study by Sarry *et al.* the authors noted that the majority of specimens show only low CD34 expression (Sarry *et al.*, 2011). Without considering the percentage of expression of the markers used, since they are unknown for the majority of samples, analyzing these samples before transplantation would have cost a lot of material that we did not have, this could skew the analysis and has to be kept in mind in the following paragraphs. Amongst CD34 non-expressing samples, we could also see a broad heterogeneity, both in the murine survival time and the homing rates. We wondered if using the CD117 marker, which is well known to be associated with LSCs within the CD34- population (Arnone *et al.*, 2020), we could detect differences in engraftment and/or homing. Unfortunately, we could not see any significant difference between patients that were CD34-CD117+ and those that were negative for both markers. However, when studying the impact of CD117 expression in patients, independently of CD34, we could see a significant worse prognosis in mice that were transplanted with cells

from patients that were expressing CD117. In line with this we could also show increased homing of samples from these patients. It was previously shown that high expression of CD117 mRNA predicts unfavorable outcome in AML patients (Gao et al., 2015), but to our knowledge we are the first to describe CD117 expression influences leukemia initiation and kinetics in a xenotransplantation model.

CD117 is of course not the only marker that was described for LSC enrichment in CD34 negative populations such as CD244 or CLL-1 (C-type lectin-like receptor) (Arnone *et al.*, 2020). It would be very interesting to similarly investigate these markers either alone or in combination in larger cohorts. Lastly, we also investigated the effect of CD56 surface expression. Contrarily to the other investigated markers, CD56 is not necessarily associated with LSCs, but was identified as an isoform of the neural adhesion molecule NCAM (Lanier et al., 1989). CD56 has been found to be expressed in several lympho-hematopoietic neoplasms, including AML, and was described as an important adverse prognostic factor (Raspadori *et al.*, 2001). In our xenotransplantation settings, we could not see any significant correlation between the expression of CD56 in patient samples and the survival of the transplanted mice. However, surprisingly, homing rates were significantly increased in mice that obtained CD56 non-expressing AML cells. Since CD56 belongs to the class of adhesion molecules, we assumed that patient samples expressing this marker would have home better to the BM, but interestingly almost all patient samples with high homing rates in the murine model did not express CD56. These findings might indicate a difference between the xenotransplantation model and what has been observed in human patients, maybe at the level of NCAM expression and/or regarding interactions within the BM.

Finally, in regard to a recent publication from our group identifying the absence of NKG2D ligands as a reliable marker for LSC identification, it would be particularly interesting to study a potential correlation between the level of these ligands expression – or rather their absence – on the investigated AML samples from our cohort regarding outcome and homing in recipient mice. Furthermore, it would also be interesting to study the expression of NKG2D ligands (possibly also in combination with other markers) in the BM, spleen and PB of engrafted recipient animal at final analysis in comparison to the proportion of NKG2D ligand expressing cells in the transplanted sample. Including this novel marker could also add one more important

variable in patient risk stratification and prognostication according to surface marker expression.

Lastly, we also tried to correlate patient characteristics (other than risk group and molecular marker expression) with the course of the disease in the murine recipient. We were however not able not correlate patient survival with the survival time of mice transplanted with the respective patient sample. This is certainly due to the many parameters that can influence the survival of the AML patients (age, treatment, transplantation etc.). We could also not find any correlation between the age or the gender of the patients with neither survival nor homing in the NSG recipient. This is similar to what was observed in a recent study in NOD/SCID animals (Rombouts *et al.*, 2000b). More elaborated statistical analyses would be necessary to incorporate or exclude different variables when studying the correlation between two parameters. Another important information that we investigated in our patient cohort was the remission status and its impact on homing and engraftment. In line with previously published work, we could show a worse survival of the mice transplanted with cells from patients that did not achieve complete remission after first therapy. This integrates to the observation we previously described, i.e. that the survival of recipient mice is worse when transplanted with samples of patients with a bad prognosis. Last but not least, we could confirm findings from another study in our settings and show that patient samples with an ITD in the *Flt3* gene had an enhanced potential to engraft (Rombouts *et al.*, 2000a). We can furthermore add to these already described findings that patient samples with ITD<sup>low</sup> (ratio <0.5) behave very similarly to the ones that are *Flt3* wildtype. This is of particular importance since *Flt3* mutational status is an important parameter for the classification of the patient risk group categories. In the ELN 2017 classification, *FLT3*-ITD<sup>low</sup> mutational status and *FLT3*-WT are grouped together and opposed to *FLT3*-ITD<sup>high</sup>. Furthermore, we also made similar findings when looking at homing rates, which were higher for AML samples that were *FLT3*-ITD<sup>high</sup>. This is particularly interesting since it was previously shown that in comparison to *FLT3*-WT, AML cells with *Flt3*/ITDs are less proliferative *in vitro* (Rombouts *et al.*, 1999)., which cannot explain the higher homing rates observed for samples with an ITD in the *Flt3* gene in our cohort. A more plausible mechanism that has been described and may correlate with our findings is an antiapoptotic effect of mutated *Flt3* (Lisovsky *et al.*, 1996). Additional molecular characterization of both WT and mutant



*Flt3* would be required to proof, which mechanisms are involved in the observed behavior of AML samples with *Flt3*-ITD<sup>high</sup>.

Taken together, in this work we could confirm that a vast majority of primary AML samples transplanted in NSG mice was able to engraft and to induce symptomatic disease by using a bigger and more heterogenous patient cohort compared to the 19 patient samples analyzed in our previous study (Paczulla...). To reach this high proportion of engrafted samples, long follow-up time (more than 40 weeks) of the transplanted mice, especially for patients samples from favorable and intermediate risk groups, is needed. Analyzing the colonization of the BM with human leukemic cells at an intermediate time-point (week 16), even though the prediction is not perfectly accurate, can already give insights in the subsequent course of the disease, i.e. survival time.

These findings also provide proof-of-principle data for a prospective clinical study analyzing correlation of both kinetics of leukemia induction in mice and AML cell homing capacity with the molecular risk group classification of the AML samples. Some molecular and genetic markers of the used AML samples, including CD117 expression as well as high ratio of ITD mutations in the *Flt3* gene, also influenced survival and homing rates of and in the recipient mice.

The identification of parameters determining the homing, the outgrowth and the kinetics of engraftment of AML samples in NSG mice may help to select patient samples that are better suited for each individual experimental design as well as for therapy development in these immunodeficient mice.

## 4. TRANSPLANTATION AT NIGHT PROMOTES LEUKEMOGENESIS VIA ENHANCED ADRENERGIC ACTIVITY

### 1.1. MANUSCRIPT IN PREPARATION

This project was a shared project between Anna Paczulla Stanger (APC) and Pauline Hanns (PH). APS performed the majority of day and night transplantations as well as EPI and propranolol conditions (long-term and homing) for primary AML cells. She also significantly participated in the conception of the project. PH performed all experiments (day and night as well as EPI and propranolol) with the syngeneic murine model, murine and human healthy HSPCs as well as AML cell lines. She also performed homing experiments investigating the role of CXCR4 and VLA-4 as well as *in vitro* experiments.

#### **Transplantation at night promotes leukemogenesis via enhanced adrenergic activity**

Pauline Hanns<sup>1\*</sup>, Anna M. Paczulla Stanger<sup>1\*</sup>, Martina Konantz<sup>1</sup>, Marcelle Baer<sup>2</sup>, Christoph Schürch<sup>1</sup>, Marlon Arnone<sup>1</sup>, Pontus Lundberg<sup>2</sup>, Stephan Dirnhofer<sup>3</sup>, Claudia Lengerke<sup>1,4</sup>

<sup>1</sup> University of Basel and Univeristy Hospital Basel, Department Biomedicine, Basel, Switzerland

<sup>2</sup> University Hospital Basel, Diagnostic Hematology, Basel, Switzerland

<sup>3</sup> University of Basel, Department for Pathology, Basel, Switzerland

<sup>4</sup>University of Basel and Univeristy Hospital Basel, Division of Hematology, Basel, Switzerland

\* These authors contributed equally to this work

**Key words:** acute myeloid leukemia, circadian rhythm, catecholamines, epinephrine

#### **Abstract**

Patient-derived xenografts (PDX) are routinely used for *in vivo* studies on human acute myeloid leukemia (AML). However, a significant proportion of primary AML samples require a particularly long time to show detectable engraftment or fails completely to show repopulation in this model. Here we report that changing the transplantation timepoint from day to night promotes leukemic cell homing to the bone marrow (BM) accelerating *in vivo* leukemogenesis in NOD/SCID/IL2Rg<sup>null</sup> (NSG) xenografts as well as in a syngeneic MLL-PTD/FLT3-ITD leukemia mouse model. When compared to mice receiving leukemic cells at day time, mice transplanted at night showed behavioral abnormalities and higher levels of epinephrine, norepinephrine and corticosterone in plasma and BM, indicating an enhanced stress response. Blockade of beta-adrenergic signaling with the non-selective beta-blocker propranolol prior to night transplantation decreased pro-leukemogenic effects, whereas stimulation of mice with epinephrine prior to day transplantation enhanced leukemic engraftment, mimicking night transplantation. Interestingly, these stress-induced pro-leukemogenic effects were molecularly mediated by the VLA-4/VCAM-1 axis and selectively observed with leukemic but not with healthy hematopoietic stem and progenitor cells (HSPCs). In sum, we identified modulation of transplantation timepoints and catecholamine activities as important variables that selectively influence the *in vivo* engraftment of leukemic but not healthy hematopoietic cells.

## **SUMMARY**

When compared to day times, transplantation at night induces catecholamine activity thereby promoting leukemic cell homing and long-term leukemogenesis in xenograft and mouse syngeneic acute myeloid leukemia models. Healthy hematopoietic cells are not similarly affected by stress conditions.

## ***Introduction***

Human acute myeloid leukemia (AML) is a complex disease with a very high intra- and inter-patient heterogeneity, which makes it challenging to accurately reproduce patient phenotypes in genetic mouse models. Patient-derived xenografts (PDX) can reproduce this heterogeneity, but display inherent limitations particularly relevant to certain AML subsets (Lapidot, 1994). As such, only ca. 40% of human AML samples were shown to engraft as expected within 12-16 weeks after transplantation in

NOD/SCID/IL2Rg<sup>null</sup> (NSG) mice (Eppert *et al.*, 2011). In contrast, other AML samples, specifically those of favorable molecular risk, required up to one year to be detected in mice or respectively could not at all repopulate xenograft models (Paczulla *et al.*, 2017; Rombouts *et al.*, 2000b). The development of methods accelerating leukemia induction can facilitate studies with such long-latency engrafters to further enable functional studies.

The proliferation and survival of AML cells is influenced by largely unexplored microenvironmental cues. For example, circadian oscillations identified to be important for the regulation of the egress of hematopoietic stem and progenitor cells (HSPCs) from the bone marrow (BM) (Méndez-Ferrer *et al.*, 2008), have been recently also implicated in the biology of hematopoietic neoplasms (He *et al.*, 2018; Puram *et al.*, 2016). Healthy circulating HSPCs are regulated by core genes of the molecular clock, which are guided by activation of stress pathways (Méndez-Ferrer *et al.*, 2008). The catecholamine neurotransmitters and stress response molecules epinephrine (EPI) and norepinephrine (NOR) were directly linked to circadian oscillations and egress of HSPCs through activation of  $\beta$ -2- and  $\beta$ -3-adrenergic receptors with rapid effects on the CXCR4/SDF-1 axis, a major player in the homing of HSPCs (Méndez-Ferrer *et al.*, 2010a; Méndez-Ferrer *et al.*, 2008). The interplay between stress and cancer development has been intensively investigated and associations reported in epidemiologic studies as well as in experimental data sets (Barron *et al.*, 2011; Botteri *et al.*, 2013; Chang *et al.*, 2015; Choi *et al.*, 2014; Choy *et al.*, 2016; Grytli *et al.*, 2014; Melhem-Bertrandt *et al.*, 2011; Powe *et al.*, 2010). Moreover, links between adrenergic signaling and leukemogenesis have been suggested. (Kim *et al.*, 2016; Lamkin *et al.*, 2012). In fact, it has been for example shown that chronic stress can accelerate the progression of acute lymphoblastic leukemia via  $\beta$ -adrenergic signaling involving the BM microenvironment (Lamkin *et al.*, 2012).

Here, we observed that xenotransplantations performed at night (with disturbance of the circadian rhythm) induced stress responses in NSG mice and accelerated engraftment when compared to corresponding procedures performed in the late afternoon. Therefore, varying the transplantation timepoint or inducing a stress response may optimize AML xenograft models.

Interestingly, the accelerated leukemia induction observed after night transplantation in PDX models could also be reproduced in a syngeneic murine AML model. However, effects were only observed with leukemic but not with healthy cells, suggesting

important differential regulatory pathways that could be potentially therapeutically explored in the future.

## Results

### Transplantation at night accelerates leukemogenesis in PDX models and a syngeneic MLL-PTD/FLT3-ITD leukemia model

Primary AML blasts (see Table S1 for patient characteristics) were transplanted into NSG mice at equal numbers and following identical procedures at “night” (4 am) or “day” (5 pm) times, respectively (Figure 1A). Interestingly, transplantation at night resulted in a reduced survival of mice when compared transplantations at daytime. Mice transplanted at night showed shorter times to leukemia induction and strikingly, all of these mice developed leukemia even after receiving low numbers of cells. In contrast, mice transplanted at daytimes often failed to develop disease (7/10 engrafted mice per transplanted mice for  $5 \times 10^5$  cells/mouse and respectively 3/10 for  $1 \times 10^5$  cells/mouse) when transplanted with these low cell numbers (Figure 1B).

Patient	% blasts	age	sex	AML type	karyotype	mutations		markers
						FLT3	NPM1	
Patient #1	95	68	m	n.a.	46XY, add (17) und (8) p(11-2), 46 XY (15)	ITD	MUT	n.a.
Patient #2	71	56	m	n.a.	n.a.	n.a.	n.a.	CD11b-, CD13+, CD14-, CD15-, CD33+, CD34+, CD38+, CD45-, CD65-, 36%CD71, CD117+, CD133+, HLA-DR+, MPO-
Patient #3	87	51	f	n.a.	n.a.	ITD	WT	CD11b-, CD13+, CD14-, CD15-, CD33+, CD34+, CD38+, CD56-, CD65-, 14%CD71, CD117+, CD133-, HLA-DR+, MPO-
Patient #4	72	83	m	M2 intermediate	46, XXY	ITD	WT	CD11b-, CD13+, CD14-, 23%CD15, CD33+, CD34-, CD38+, CD45+, CD56-, CD65-, CD71-, CD117+, CD133-, HLA-DR+, MPO-
Patient #5	96.5	69	f	M0 intermediate	46, XX	n.a.	n.a.	CD11b+, CD13+, CD14+, CD15+, CD34-, CD38+, CD56-, CD65+, CD117-, HLA-DR+, MPO-
Patient #6	51	58	f	M2	n.a.	n.a.	n.a.	CD11b+, CD13+, CD14+, CD15+, CD34-, CD38+, CD56-, CD65+, CD117-, HLA-DR+, MPO-
Patient #7	80.5	66	m	M5	n.a.	WT	WT	CD11b+, CD13+, CD14+, CD15+, CD34-, CD38+, CD56-, CD65+, CD117-, HLA-DR+, MPO-
Patient #8	67	81	f	M7	n.a.	WT	WT	CD11b-, CD13+, CD14-, CD15-, CD33-, CD34+, CD38+, CD56-, CD65-, 20% CD71, CD117+, CD133+, HLA-DR+, MPO-
Patient #9	82	72	m	M4/M5	n.a.	n.a.	n.a.	CD11b+, CD13+, CD14+, CD33+, CD34-, CD56+, CD71-, CD117-, HLA-DR+, MPO-
Patient #10	26	50	f	M2 de novo favorable	46, XX	ITD	MUT	CD11c+, CD13+, CD14-, CD15+, CD33+, CD34+, CD38+, CD45+, CD56-, CDw65+, CD71+, CD117+, CD133+, HLA-DR+, FLT3+, MPO+
Patient #11	86	43	f	M4 de novo favorable	46, XX	WT	MUT	CD11c+, CD13+, CD14+, CD15+, CD33+, CD34-, CD38+, CD45+, CD56-, CDw65+, CD71+, CD117-, CD133-, HLA-DR+, FLT3+, MPO+
Patient #12	92	74	m	M5 de novo adverse	46, XY	ITD	WT	CD11c+, CD13+, CD14+, CD15+, CD33+, CD34+, CD38+, CD45+, CD56+, CDw65+, CD71+, CD117-, CD133-, HLA-DR+, FLT3+, MPOlow

**Table S1**

*Characteristics of the AML patient samples: percentages of leukemic blasts, molecular risk group, age, sex, karyotype, leukemia-specific mutations and surface markers.*

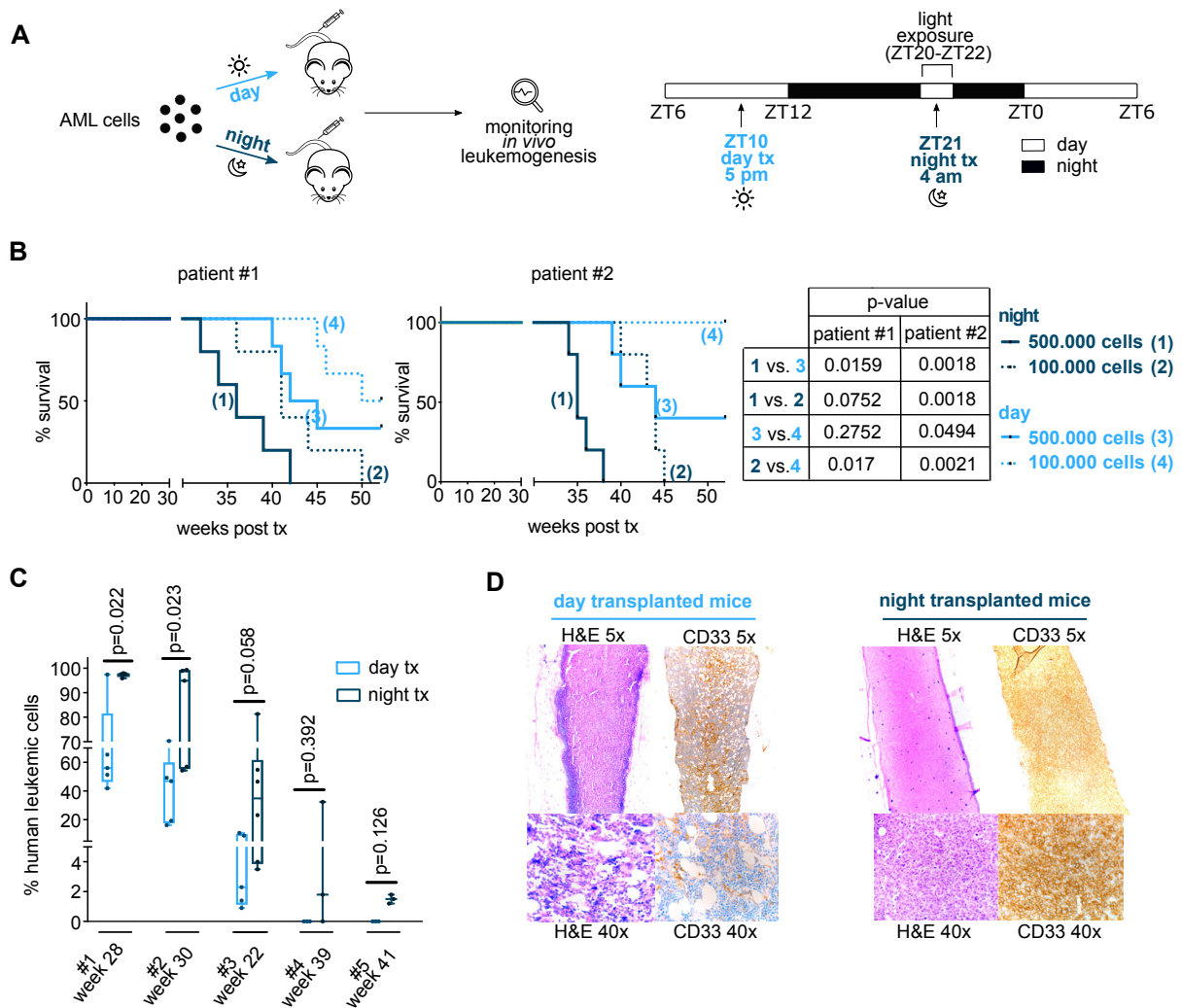


**Figure 1: Night transplantation promotes leukemogenesis in human AML xenotransplantation models**

**(A)** Schematic overview of experimental set-up for day/night transplantations. Leukemic cells isolated from patients with AML were freshly thawed before each transplantation time-point and intravenously injected into sublethally irradiated NSG mice at 5.00 pm (“day”) or respectively at 4.00 am (“night”). Of note, mice were exposed to light one hour prior to transplantation at night and one hour afterwards as well (right panel; ZT20-22 light exposure). **(B)** Kaplan-Meier survival analysis of mice transplanted with 500.000 (full line) vs. 100.000 (dotted line) cells from two patients with AML at day (blue) and night (dark blue) (patient #1, left; patient #2, right, n=3-5 mice per group). **(C)** All mice transplanted (at day, blue, or at night, red) with cells from one patient were analyzed for longterm engraftment when the signs of disease were

detected at any mouse in these groups. Engraftment in the BM was quantified as a percentage of CD33+ cells amongst BM cells (n=5 different AML cases n=3-6 mice per AML case and condition). **(D)** Representative histopathological images of femurs of day (left) and night (right) transplanted mice. 5x magnification was used for upper panel sections (left, hematoxylin and eosin staining, H&E; right anti-human CD33 staining) and 40x magnification was used on bottom panel.

Data are represented as boxes that extend from the 25<sup>th</sup> to the 75<sup>th</sup> percentiles. Line in the middle represents the median and the whiskers extend from the minimum to the maximum.

Student-t-test or Mann-Whitney-U-test for long-term analyses and Log-rank (Mantel-Cox) test for Kaplan-Meier analysis.

When analyzed for engraftment at the same time points after transplantation, mice transplanted at night showed significant more robust engraftment than mice that were transplanted with the same leukemic blasts at day time (n=20 mice per group from n=5 different patients; night: 54.34 ± 40.94% vs. day: 26.92 ± 30.10%, human leukemic cells in BM, p=0.0172; Figure 1C). Remarkably, 2 of the 5 transplanted AML patient samples engrafted only in mice transplanted at night (5/5 engrafted AML and 20/20 engrafted mice) but not at day time (3/5 engrafted AML and 14/20 engrafted mice; Figure 1C and Table S2). Of note, these findings were confirmed in analyses of spleen and peripheral blood (PB) which also showed higher infiltrations with leukemic cells in night versus day transplanted mice (Table S2 and Figure S1A-B).

Leukemic cells	% blasts	transplantation route	injected cell number	transplantation time-point	treatment	engrafted/transplanted mice	Analysis time-point	% human leukemic cells in BM	% human leukemic cells in PB	% human leukemic cells in spleen	% human leukemic cells in liver
Patient #1	95.0%	i.v.	1 x 10 <sup>6</sup>	day	none	5/5	week 28	66.42±23.75	13.56±10.74	3.64±1.10	7.18±6.13
				night	none	5/5	week 28	97.26±0.80	35.80±12.81	5.30±2.60	43.84±11.07
Patient #2	87.0%	i.v.	1 x 10 <sup>6</sup>	day	none	5/5	week 30	40.38±22.61	7.40±6.85	12.14±7.29	38.24±28.19
				night	none	5/5	week 30	80.86±23.14	21.10±10.23	36.24±19.83	79.72±16.8
Patient #3	n.a.	i.v.	1 x 10 <sup>6</sup>	day	none	5/5	week 22	4.86±4.63	1.8±1.29	1.42±0.92	4.12±2.60
				night	none	6/6	week 22	35.57±30.86	9.85±11.21	13.03±13.51	19.97±22.14
Patient #4	80.5%	i.v.	1 x 10 <sup>6</sup>	day	none	0/3	week 39	0	0	0	0
				night	none	2/3	week 39	11.40±18.21	0	0	0.97±0.15
Patient #5	52.0%	i.v.	1 x 10 <sup>6</sup>	day	none	0/2	week 41	0	0	0	0
				night	none	2/2	week 41	1.50±0.42	0	0	1.55±1.06
Patient #1	95.0%	i.v.	1 x 10 <sup>6</sup>	day	control	4/4	week 24	94.50±4.41	43.73±3.25	28.18±8.15	47.98±3.64
				night	propranolol	4/4	week 24	42.08±13.30	26.03±8.52	12.87±0.58	20.33±6.88
Patient #8	68.0%	i.v.	1 x 10 <sup>6</sup>	day	control	3/3	week 20	85.73±8.00	14.90±2.81	7.06±0.95	0.57±0.18
				night	propranolol	4/4	week 20	53.30±5.17	8.97±2.82	3.46±0.61	0.50±0.09
EOL-1 (cell line)	n.a.	i.v.	5 x 10 <sup>4</sup>	day	control	3/3	week 3	19.69±12.04	1.115±0.85	1.727±1.01	n.a.
				night	propranolol	2/3	week 3	9.685±14.21	0.525±0.26	5.950±8.52	n.a.
Patient #8	68.0%	i.v.	1 x 10 <sup>6</sup>	day	control	4/4	week 12	70.63±14.91	26.03±8.52	17.58±10.80	33.53±8.08
				day	epinephrine	4/4	week 12	90.33±2.25	43.73±3.26	28.7±4.80	47.98±3.64
EOL-1 (cell line)	n.a.	i.v.	5 x 10 <sup>4</sup>	day	control	4/4	week 3	4.83±3.69	2.39±1.72	0.22±0.20	0.54±0.42
				day	epinephrine	5/5	week 3	11.99±6.12	7.58±6.28	1.38±2.36	1.70±1.13

**Table S2**

*Transplantation procedures and treatments, analysis time-points and engraftment percentages for each AML case.*

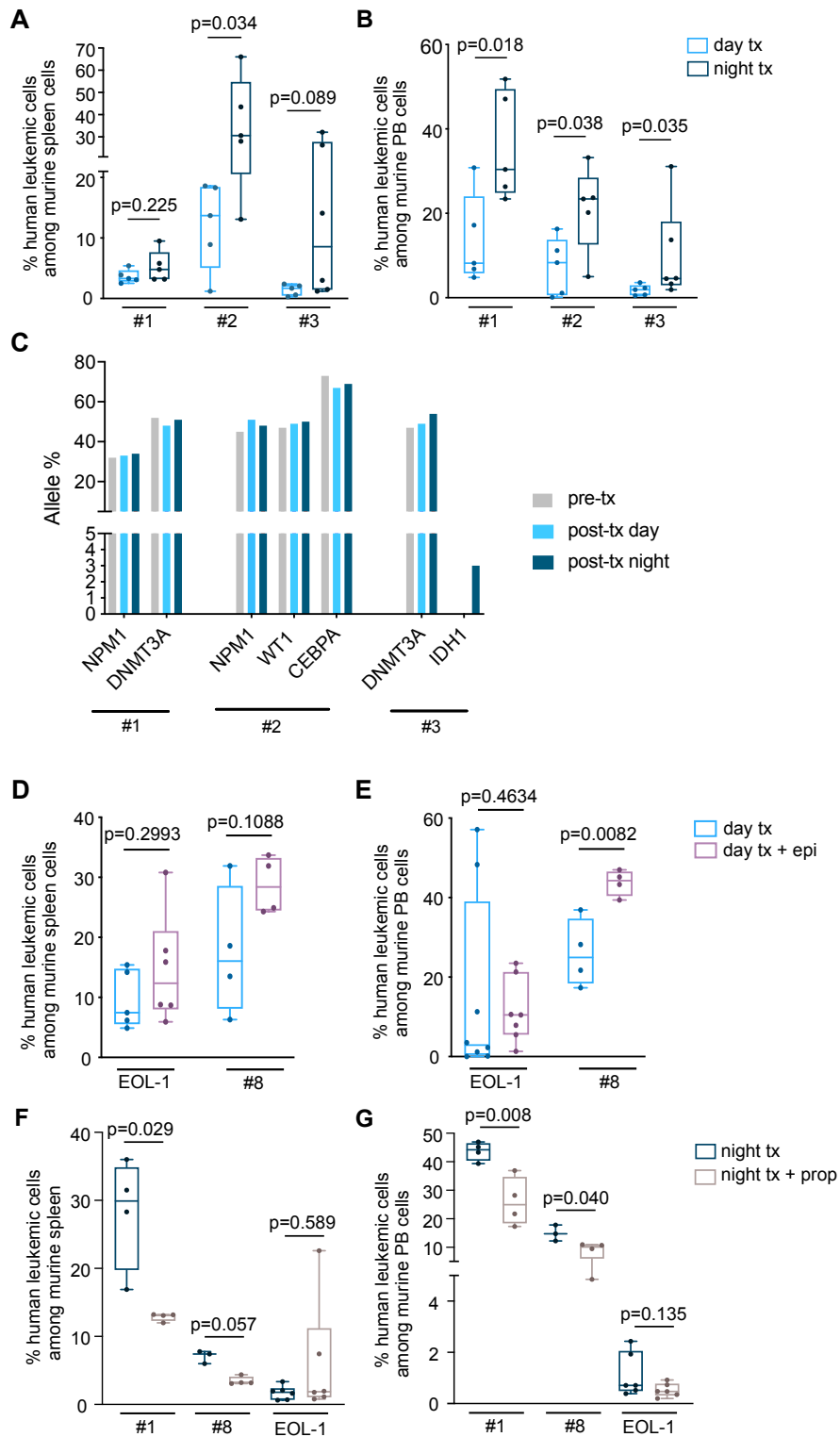




### **Figure S1**

**(A-B)** Mice were analyzed at first signs of disease for long-term engraftment after day (blue) vs. night (dark blue) transplantation. Shown are percentages of leukemic cells in the spleen (**A**) and PB (**B**;  $n=5$  different AML cases with  $n=3-6$  mice each per AML case and condition). No engraftment was detected in the spleen nor the PB for patients #4 and #5. **(C)** Targeted next generation sequencing of BM samples before transplantation into recipient mice (grey), after day (blue) or night (dark blue) transplantation. Leukemia-related individual mutations identified are indicated for each of the three patients tested ( $n=3$  AML samples).

**(D-E)** Mice were analyzed at first signs of disease for long-term engraftment after day control (blue) vs. day + epinephrine treatment (purple). Shown are percentages of leukemic cells in the spleen (**D**) and PB (**E**,  $n=1$  cell line in 3 independent experiments and  $n=1$  primary patient sample,  $n=3-4$  mice per AML case and condition).

**(F-G)** Mice are analyzed at first signs of disease for long-term engraftment after night control (dark blue) vs. night + propranolol treatment (brown). Shown are percentages of leukemic cells in the spleen (**F**) and PB (**G**,  $n=1$  cell line in 3 independent experiments and  $n=2$  primary patient samples,  $n=3-4$  mice per AML case and condition).

Data are represented as boxes that extend from the 25<sup>th</sup> to the 75<sup>th</sup> percentiles. Line in the middle represents the median and the whiskers extend from the minimum to the maximum.

Student-t-test or Mann-Whitney-U-test for statistical analysis.

Consistently, histopathological analyses showed micro-leukemic infiltrations in the BM of mice transplanted during day, while mice transplanted during night analyzed at the same time points showed much more aggressive leukemic infiltration (Figure 1D).

To analyze whether night and day transplantation favors engraftment from cells with specific leukemic mutations we performed targeted Next Generation Sequencing (NGS) comparing allele frequencies in samples collected from day and respectively night transplanted mice. Similar patterns were revealed except for one patient (patient 3) for which the mutation in isocitrate dehydrogenase 1 (IDH1) was only present when AML cells were transplanted at night (Figure S1C). Latter indicates that cells displaying such a mutation might be more permissive for engraftment in the night settings.

To further consolidate these data generated in PDX models, we further investigated whether findings hold true also in a syngeneic MLL-PTD/FLT3-ITD mouse AML model. Similar numbers of MLL-PTD/FLT3-ITD leukemic cells were transplanted at the same timepoints as described in Figure 1A and lead indeed to earlier disease induction in night compared to day transplanted mice (n=12 mice per group, longer survival time observed 38 days for day transplantation vs. 34 days for night transplantation; median survival night: 30 days vs. day: 35 days, p= 0.0004, Figure 2A) accompanied by higher spleen weight (n=15 mice per group, night:  $348.5 \pm 173.6$  mg vs. day:  $196.3 \pm 170.5$  mg, p=0.0396, Figure 2B and S2A) and overall more pronounced organ engraftment. These results were further confirmed by histopathological analyses where at daytimes transplanted animals showed only few malignant amongst healthy hematopoietic cells while at night transplanted mice showed high infiltration rates (Figure 2C). Consistently, blood counts showed enhanced numbers of white blood cells mice (n=14-15 mice per group, night:  $42.37 \pm 35.64$  ( $\times 10^9$ ) cells/L vs. day:  $15.01 \pm 23.17$  ( $\times 10^9$ ) cells/L, p=0.0019 ; Figure 2D), and decreased numbers of red blood cells (n=13-15 mice per group, night:  $6.683 \pm 2.478$  ( $\times 10^{12}$ ) cells/L vs. day:  $8.094 \pm 1.428$  ( $\times 10^{12}$ ) cells/L, p=0.0006; Figure 2D) going along with decreased hemoglobin (n=13-15 mice per group, night:  $103.1 \pm 39.92$  g/L vs. day:  $125.7 \pm 19.61$  g/L, p=0.0001; Figure 2D) but also platelets (n=13 mice per group, night:  $396.6 \pm 233.1$  ( $\times 10^9$ ) cells/L vs. day:  $580.1 \pm 182.0$  ( $\times 10^9$ ) cells/L, p=0.0019; Figure 2D) and in night vs. day transplanted, indicating highly impaired hematopoiesis in these mice.

Taken together, these data indicate that night transplantation accelerates disease induction and increases leukemic burden in both PDX and syngeneic mouse models.

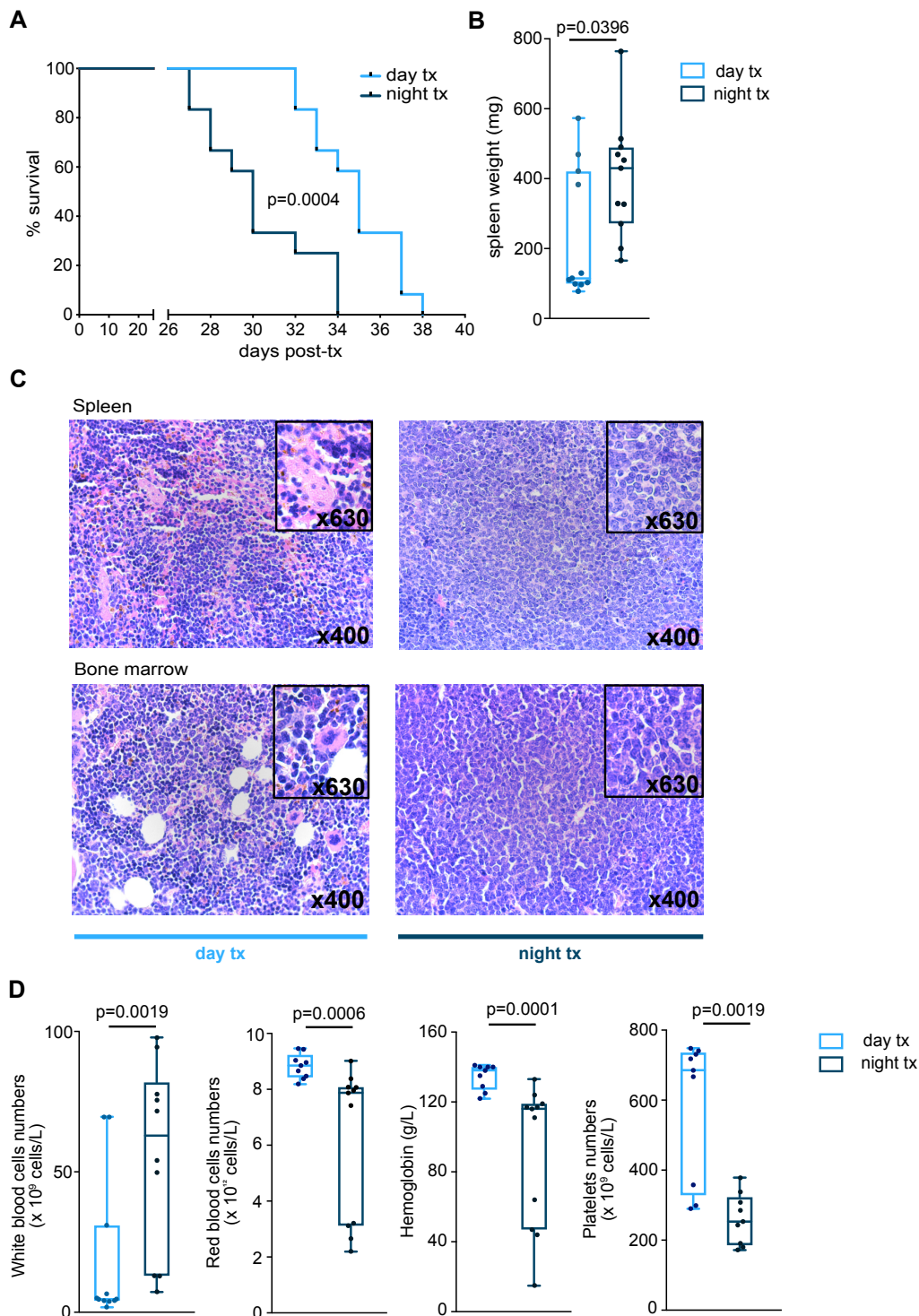


**Figure 2: Conserved effects in syngeneic mouse models: Night transplantation promotes leukemia induction in mice transplanted with MLL-PTD/FLT3-ITD leukemic cells.**

**(A)** Kaplan-Meier survival analysis of day (blue) vs. night (dark blue) mice transplanted with 50,000 MLL-PTD/FLT3-ITD cells (n=9 mice in total per condition with n=3 mice

each in 3 independent experiments). **(B-D)** Day and night transplanted mice were sacrificed and analyzed for long-term engraftment at first sign of disease (i.e. 27 days post transplantation). **(B)** Spleen weight taken from day (blue) vs. night (dark blue) transplanted mice. ( $n=9$  mice in total per condition with  $n=3$  mice each in 3 independent replicates). **(C)** Representative histopathological images of spleens (upper panel) and BM (lower panel) of day (blue, left) vs. night (dark blue, right) transplanted mice (400x and 630x magnification; H&E staining). **(D)** Blood counts (white blood cells, left; red blood cells, middle left; hemoglobin levels, middle right and platelets, right) were analyzed in the PB of mice transplanted at day (blue) vs. night (dark blue) time-points ( $n=9$  mice in total per condition with  $n=3$  mice each in 3 independent replicates).

Data are represented as boxes that extend from the 25<sup>th</sup> to the 75<sup>th</sup> percentiles. Line in the middle represents the median and the whiskers extend from the minimum to the maximum.

Student-t-test or Mann-Whitney-U-test for spleen weights and blood counts, and Log-rank (Mantel-Cox) test for Kaplan-Meier analysis.

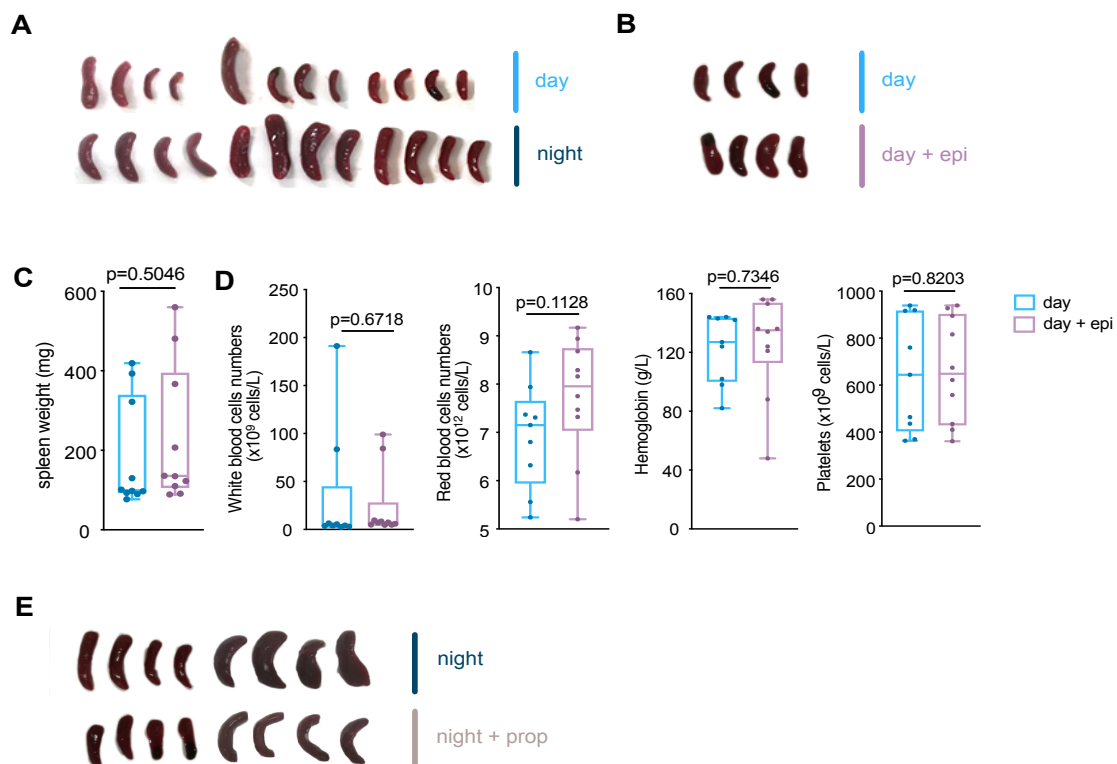


## **Figure S2**

**(A)** Representative picture of the increased spleen sizes observed after night transplantation (dark blue) vs. day (blue). Shown are spleens from  $n=12$  mice per group in  $n=3$  independent experiments. **(B)** Representative picture of the increased spleen sizes observed after epinephrine treatment during day transplantation (purple) vs. day control transplantation (blue). Shown are spleens from  $n=4$  mice per group. **(C)** Spleen weight quantification of mice transplanted at day (blue) or at day after epinephrine (purple) treatment ( $n=10$  mice in total, performed in 3 independent replicates). **(D)** Analysis of blood counts (white blood cells, left; red blood cells, middle left; hemoglobin, middle right and platelets, right) of mice transplanted at day (blue) or at day after epinephrine (purple) treatment ( $n=10$  mice in total, performed in 3 independent replicates). **(E)** Representative picture of decreased spleen sizes observed after propranolol treatment during night transplantation (brown) vs. night control transplantation (dark blue).

Data are represented as boxes that extend from the 25<sup>th</sup> to the 75<sup>th</sup> percentiles. Line in the middle represents the median and the whiskers extend from the minimum to the maximum.

Student-t-test or Mann-Whitney-U-test for statistical analysis.

### **Higher catecholamine levels during night enhance leukemic burden**

Mice are naturally more active at nighttime and we observed that mice showed more distress due to interruption by light exposure for two hours and transplantation during night compared to standard procedures performed during day time (Movies S1 and S2). To further explore the role of stress behavior in leukemia induction, we measured levels of stress hormones in the plasma and femur fluids at these different transplantation timepoints and found enhanced levels of epinephrine, nor-epinephrine and corticosterone ( $n=3$  mice per group, Figure 3). Of note, amongst other epinephrine levels were significantly higher in both plasma and femur extracts derived from mice analyzed at night compared to daytime (for epinephrine: night  $0.321 \pm 0.017$  ng/ml vs. day  $0.102 \pm 0.012$  ng/ml in plasma,  $p=0.023$  and night  $21.080 \pm 1.038$  ng/ml vs day  $13.15 \pm 3.573$  ng/ml in femur fluids,  $p=0.021$ ; Figure 3).

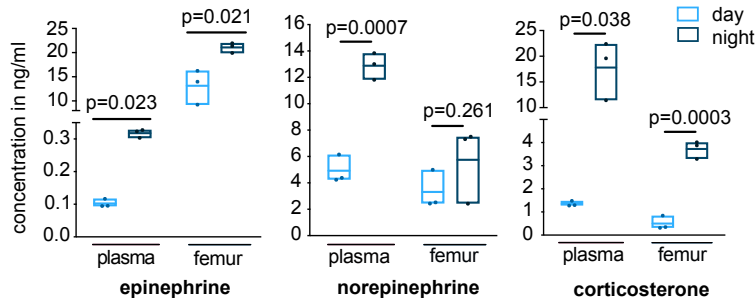


**Figure 3: Night transplantation associates with enhanced epinephrine, norepinephrine and corticosterone levels.**

Epinephrine (left), norepinephrine (middle) and corticosterone (right) levels measured in the plasma and femur fluids of NSG mice at day (blue) vs. night (dark blue) time-points ( $n=3$  mice per group) using an ELISA approach.

Data are represented as boxes that extend from the 25<sup>th</sup> to the 75<sup>th</sup> percentiles. Line in the middle represents the median and the whiskers extend from the minimum to the maximum.

Student-t-test.

To test if catecholamine and adrenergic signaling pathways are involved in the observed “night effect” enhancing leukemia induction, we performed additional *in vivo* experiments with single-dose epinephrine treatment prior to daytime transplantations (Figure 4A). Mimicking the stress situation via catecholamine treatment before daytime transplantation accelerated disease-related death of mice compared to vehicle-treated animals as observed upon transplantation of MLL-PTD/FLT3-ITD cells in the syngeneic model ( $n=12$  mice per group; longer survival time observed 28 days for day transplantation vs. 25 days for day with catecholamine treatment; median survival day untreated 27.5 days vs. day + epinephrine 24 days,  $p=0.0035$ ; figure 4B) and even more pronounced in the xeno-setting upon transplantation of the human AML EOL-1 cell line in NSG mice ( $n=11-15$  mice per group; longer survival time observed 38 days for day transplantation vs. 32 days for day with catecholamine treatment; median survival day untreated 37 days vs. day + epinephrine 32 days,  $p=0.0055$ ; Figure 4C). This reduced overall survival upon epinephrine treatment prior to transplantation correlates with significantly increased long-term engraftment of the EOL-1 cell line but also primary patient cells (EOL-1 cell line  $n=10-11$  mice per group, epinephrine:  $29.49 \pm 23.22$  % vs. untreated:  $15.22 \pm 16.92$  % leukemic cells in BM,

p=0.064 and patient #8 primary AML cells n=4 mice per group, epinephrine  $90.33 \pm 2.251\%$  vs.  $70.63 \pm 14.91\%$ , p=0.029; Figure 4D). Interestingly, epinephrine treatment also led to enhanced engraftment of leukemia cells in the spleen, and higher levels of malignant cells were found in the PB in comparison to control animals (Figure S1D-E). Similar results were obtained in the syngeneic model, which displayed splenomegaly after epinephrine treatment (n=10 mice per group, control  $182.0 \pm 137.9$  mg vs. epinephrine  $229.9 \pm 174.5$  mg, p=0.5046; Figure S2B-C) but only showed minor effects in blood counts of the PB (Figure S2D).

Taken together, these data indicate that increased catecholamine levels measured at night play an important role in the enhanced engraftment observed with our transplantation method.

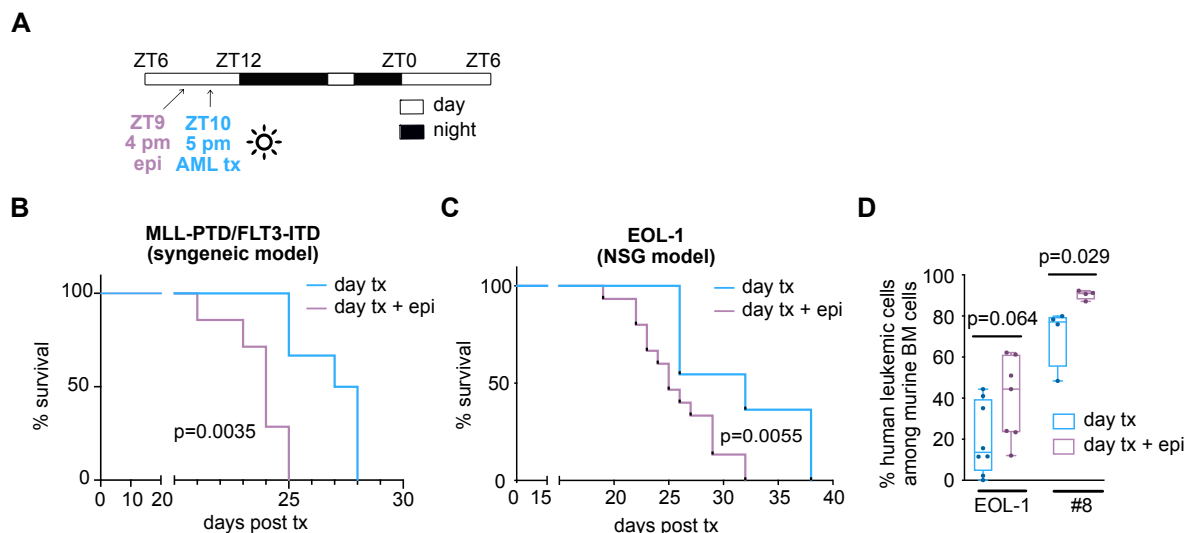


**Figure 4: Pre-treatment with epinephrine promotes leukemogenesis from transplanted leukemic cells.**

**(A)** Schematic overview of epinephrine treatment before day transplantation. Mice were given 2 mg/kg epinephrine intraperitoneally one hour before day transplantation of leukemia cells in order to mimic the “night effect”. **(B)** Kaplan-Meier survival analysis of mice transplanted at day (blue) vs. transplanted at day with prior epinephrine treatment (violet) with  $5 \times 10^4$  MLL-PTD/FLT3-ITD cells (n=6-7 mice per group in total, experiments performed in 3 independent replicates). **(C)** Kaplan-Meier survival analysis of NSG mice transplanted at day (blue) vs. transplanted at day with epinephrine treatment (violet) with  $5 \times 10^4$  EOL-1 leukemia cells (n=9 mice per group in

*total, experiment performed in 3 independent replicates). (D) NSG mice were analyzed at first signs of disease for long-term engraftment of leukemia cells in the BM after day (blue) vs. epinephrine treatment during day (violet, n=1 AML cell line in 3 independent replicates with n=9 mice in total; and n=1 primary AML sample, n=3-4 mice per group and condition).*

*Data are represented as boxes that extend from the 25<sup>th</sup> to the 75<sup>th</sup> percentiles. Middle line represents the median and the whiskers extend from the minimum to the maximum.*

*Student-t-test or Mann-Whitney-U-test for long-term analyses, and Log-rank (Mantel-Cox) test for Kaplan-Meier analysis.*

### **Blocking adrenergic signaling pathways can decrease the observed “night effect”**

In line with the enhanced stress hormone levels measured during night, we found that treating mice with the beta1/2 blocker propranolol could reverse the stress phenotype during night, leading to less active animals as expected (Movie S3). Following this observation, we established a beta-blocker treatment protocol, in which mice received a single dose of propranolol or respectively vehicle control one hour before night transplantation (Figure 5A). In contrast to epinephrine treatment, chemical blockade of beta-adrenergic signaling during night resulted in increased survival rates of NSG mice injected with the EOL-1 cell line (longer survival time observed 25 days for night transplantation vs. 32 days for night with propranolol treatment; median survival night control solution 23 days vs. night propranolol 28 days,  $p=0.0002$ ; Figure 5B) further confirmed by reduced leukemic burden upon transplantation of EOL-1 but also primary AML cells to the BM compared to control mice injected and sacrificed at the same timepoint ( $n=17-18$  mice per group, propranolol:  $27.36 \pm 17.47$  % vs. untreated:  $53.46 \pm 38.13$  % leukemic cells,  $p=0.0146$ ; Figure 5C). Consistently, propranolol treatment also led to reduced leukemic infiltration in the spleen and lower number of malignant cells circulating in the PB in comparison to control animals (Figure S1F-G).

To further consolidate these findings, we repeated this experimental setting with the MLL-PTD/FLT3-ITD syngeneic mouse leukemia model to investigate if this again is a general effect, not only limited to PDX models. Transplantation of similar numbers of leukemia cells in animals treated with propranolol before transplantation at the night



timepoint significantly prolonged the overall survival compared to control treated animals (n= 9 mice per group, longer survival time observed 34 weeks for night control vs. 40 weeks for night propranolol; median survival night control: 33 days vs. night propranolol 34 days,  $p = 0.0402$ ; Figure 5D). Mice treated with propranolol before night transplantation furthermore displayed reduced leukemic burden compared to control treated mice when analyzed at first signs of disease (Figure 5E-F). Indeed, splenomegaly was less pronounced in propranolol treated mice (n=11-12 mice per group, night control:  $744.9 \pm 105.1$  mg vs. night + propranolol:  $559.5 \pm 70.90$  mg,  $p=0.0025$ ; Figures 5E and S2E) and these mice also displayed reduced white blood cell numbers (night control:  $299.7 \pm 107.1$  vs. night propranolol:  $127.5 \pm 43.77$  ( $\times 10^9$ ) cells,  $p=0.0002$ ; Figure 5F), increased red blood cells (night control:  $4.923 \pm 0.9673$  vs. night propranolol:  $6.738 \pm 0.8921$  ( $\times 10^{12}$ ) cells,  $p=0.0007$ ; Figure 5F) and hemoglobin levels (night control:  $85.25 \pm 14.91$  vs. night propranolol:  $114.8 \pm 14.23$  g/L,  $p<0.0001$ ; Figure 5F) as well as platelets numbers (night control:  $222.3 \pm 28.19$  vs. night propranolol:  $370.9 \pm 96.83$  ( $\times 10^9$ ) cells,  $p=0.0023$ ; Figure 5F) when compared to control animals, indicating a less advanced disease.

Altogether, these data demonstrate that blocking adrenergic signaling using a common clinically used beta-blocker can counteract the effect of stress behavior on *in vivo* leukemogenesis observed at night-time in mice.

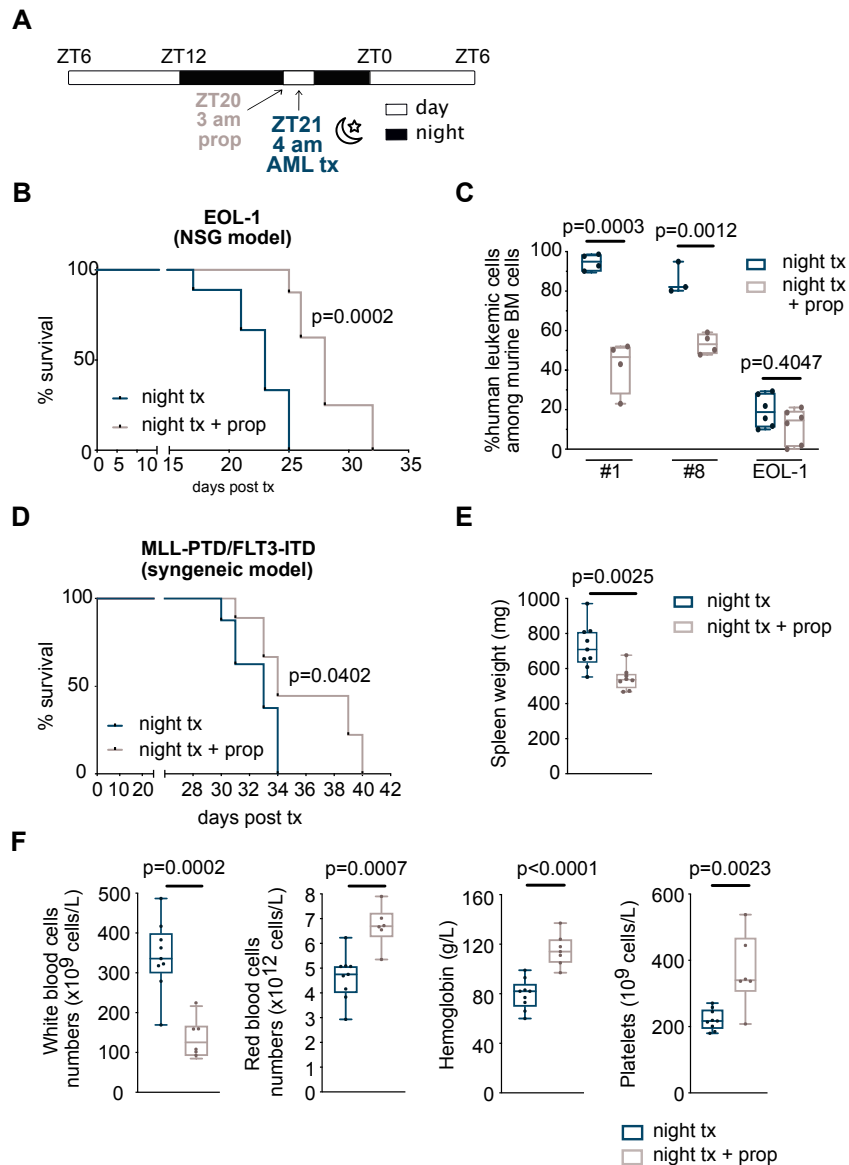


**Figure 5: Pro-leukemogenic effects induced by night transplantation are reduced by pre-treatment with propranolol.**

**(A)** Schematic overview of experimental set-up for propranolol treatment. Mice transplanted at night were injected with propranolol (10mg/kg) or control treatment (0.9M NaCl) intraperitoneally one hour before transplantation. **(B)** Kaplan-Meier survival analysis of NSG mice transplanted at night with  $5 \times 10^4$  EOL-1 human AML cells, after pre-treatment with vehicle control (dark blue) vs. propranolol (brown) ( $n=9$  mice per group in total, experiments performed in 3 independent replicates). **(C)** Mice were analyzed for long-term engraftment at first signs of disease of any mouse of the experiment (night transplantation and vehicle control, dark blue, or respectively

propranolol, brown) ( $n=2$  patient samples and  $n=1$  AML cell line,  $n=3-5$  mice per condition). **(D)** Kaplan-Meier survival analysis of mice transplanted with  $5 \times 10^4$  murine MLL-PTD/FLT3-ITD leukemia cells at night transplantation with vehicle control (dark blue), vs. at night with propranolol (brown) ( $n=9$  mice per condition, experiments performed in 3 independent replicates). **(E)** Kaplan-Meier survival analysis of mice transplanted with 50.000 murine MLL-PTD/FLT3-ITD leukemia cells at night with vehicle control treatment (dark blue) vs. propranolol treatment (brown) ( $n=8-9$  mice per group, performed in 3 independent replicates). **(F)** Spleen weight taken from control (dark blue) and propranolol treated (brown) night mice. Mice from both groups were sacrificed and analyzed for long-term engraftment at the same time-point ( $n=9$  mice in total per group, performed 3 independent experiments, sacrificed 27 days post transplantation). **(F)** Blood counts (white blood cells, left; red blood cells, middle left; hemoglobin, middle right and platelets, right) levels were analyzed in the PB of mice transplanted at night (dark blue) or at night after propranolol (brown) treatment ( $n=9$  mice in total per group, performed in 3 independent experiments, sacrificed 27 days post transplantation).

Data are represented as boxes that extend from the 25<sup>th</sup> to the 75<sup>th</sup> percentiles. Line in the middle represents the median and the whiskers extend from the minimum to the maximum.

Student-t-test or Mann-Whitney-U-test for long-term analyses, spleen weights and blood counts, and Log-rank (Mantel-Cox) test for Kaplan-Meier analysis.

### **Adrenergic signaling pathways influence the homing of leukemic cells to the BM**

An important physiological process, which happens directly after IVtransplantation is the migration (“homing”) of transplanted cells from the PB into the BM, a process that is shared by both healthy HSPCs and also malignant cells. We hypothesized that the homing process would be particularly influenced by the timepoints of transplantation. Therefore, in order to investigate the mechanisms underlying the difference in survival and long-term engraftment in day vs. night settings, we performed homing assays with AML cells. Leukemic cells were fluorescently labeled with CFSE prior to transplantation in order to facilitate their detection afterwards. Labeled cells were then intravenously transplanted at different timepoints with different treatment conditions

(Figure 6A), and mice were analyzed 12 hours post transplantation for CFSE positive cells in BM, PB and spleen.

Interestingly, cells from the same primary AML sample showed higher homing rates upon transplantation at night compared to day time (n=32 mice per group from n= 7 AML patient samples, night:  $0.2906 \pm 0.199\%$  vs. day:  $0.1188 \pm 0.1030\%$ ,  $p=0.0002$ ; Figure 6B and S3C). Of note, higher homing rates were also observed in the spleen (Figure S3A and S3C). Consistently, lower numbers of labeled cells were detected circulating in the PB upon night transplantation (Figure S3B and S3C).

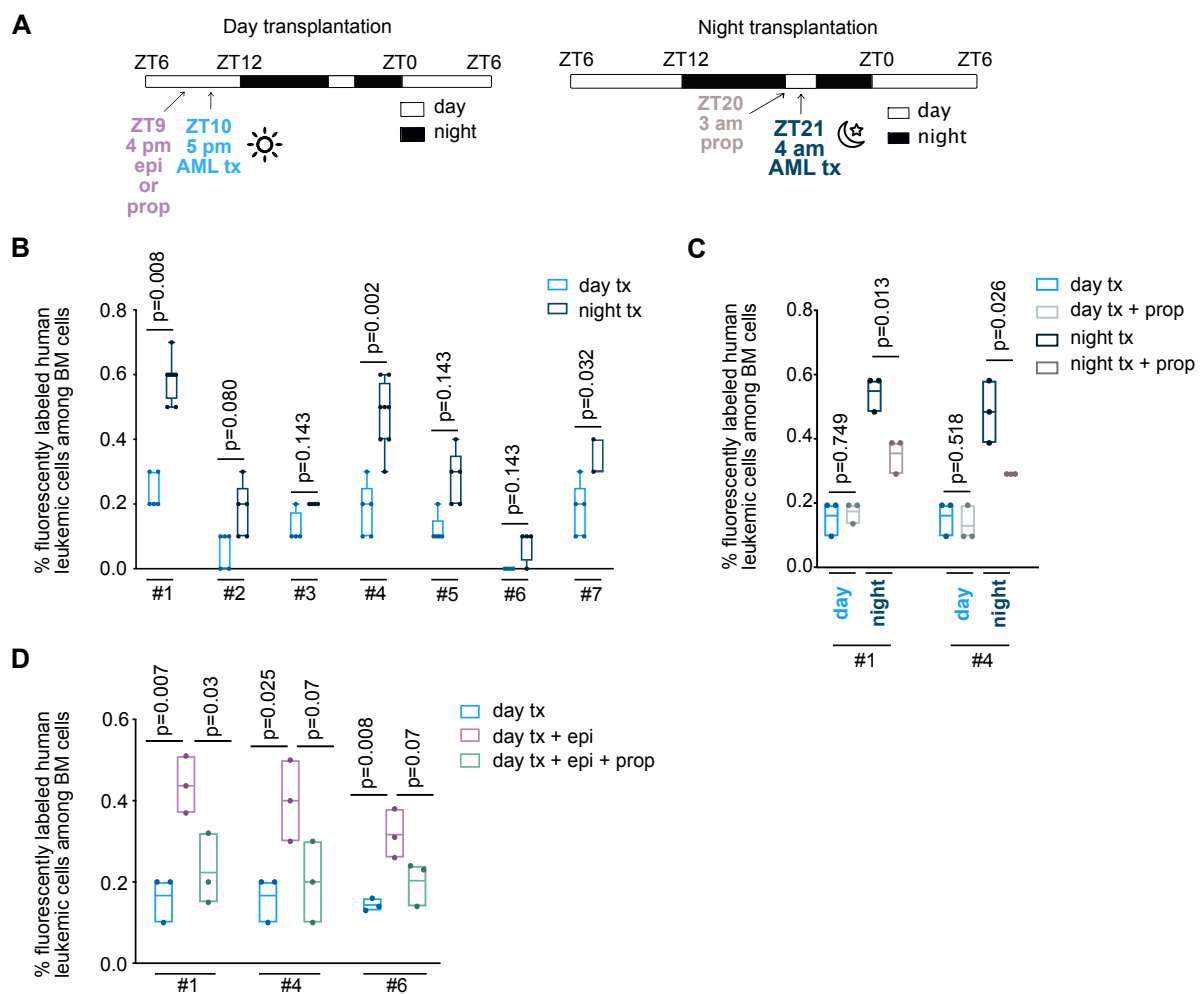


**Figure 6: Modulation of adrenergic signaling pathways influence leukemic cell homing**

**(A)** Schematic overview of experimental set-up for epinephrine and propranolol treatment. Mice were injected with epinephrine (2mg/kg), propranolol (10mg/kg) or control treatment (0.9M NaCl) intraperitoneally one hour before transplantation.

**(B)** Homing rates of CFSE stained leukemic cells within the BM of mice transplanted at day (blue) or night (dark blue) timepoints (n=4-5 mice per AML case and condition, n=7 different AML samples). **(C)** Homing rates of CFSE stained leukemic cells within the BM of mice transplanted at day (blue) vs. night (dark blue) with and without propranolol pre-treatment (respectively grey and brown) (n=3 AML samples, n=3 mice per condition). **(D)** Homing rates of CFSE stained leukemic cells within the BM of mice transplanted at day time-points after pre-treatment with vehicle control (blue), epinephrine (purple) or propranolol plus epinephrine (green) (n=3 different AML samples, n=3 mice per condition). Note that data points presented for the day condition in B and C are the same due to optimization of animal numbers in regard to the 3R principle.

Data are represented as boxes that extend from the 25<sup>th</sup> to the 75<sup>th</sup> percentiles. Line in the middle represents the median and the whiskers extend from the minimum to the maximum.

Student-t-test or Mann-Whitney-U-test for statistical analysis.

The night transplantation effect on the homing of primary AML cells was also—at least partially—counteracted by pre-treatment of mice with propranolol (n=6 mice per group from n=2 AML patient samples, propranolol:  $0.3333 \pm 0.05164$  % vs. untreated:  $0.5333 \pm 0.08165$  % leukemic cells in BM,  $p=0.0533$ ; Figure 6C and S3F). Importantly, the effect of beta-blocker treatment on leukemia induction and homing was also observed in the spleen and again on the number of circulating malignant cells (Figure S3D-F). Additionally, propranolol treatment during day transplantation had no effect on homing of leukemia cells when compared to control animals transplanted at daytimes (n=6 mice per group from n=2 AML patient samples, day + propranolol:  $0.1567 \pm 0.04967$  % vs. untreated:  $0.1667 \pm 0.05164$  % leukemic cells in BM,  $p>0.9999$ , Figure 6C and S3D-F).

Furthermore, epinephrine treatment significantly increased homing of malignant cells to the BM (n=9 mice per group, epinephrine:  $0.384 \pm 0.086$  vs. untreated:  $0.159 \pm 0.043$  % leukemic cells,  $p<0.0001$  ; Figure 6D and S3I) as well as to the spleen (Figure S3H), while propranolol treatment was able to partially counteract the enhanced homing rates observed upon epinephrine treatment (Figure 6D and S3G-I).

These data indicate that homing is also highly influenced by the timepoint of transplantation as well as by adrenergic signaling pathway activation suggesting that the observed long-term and survival phenotype might be due to different homing rates.

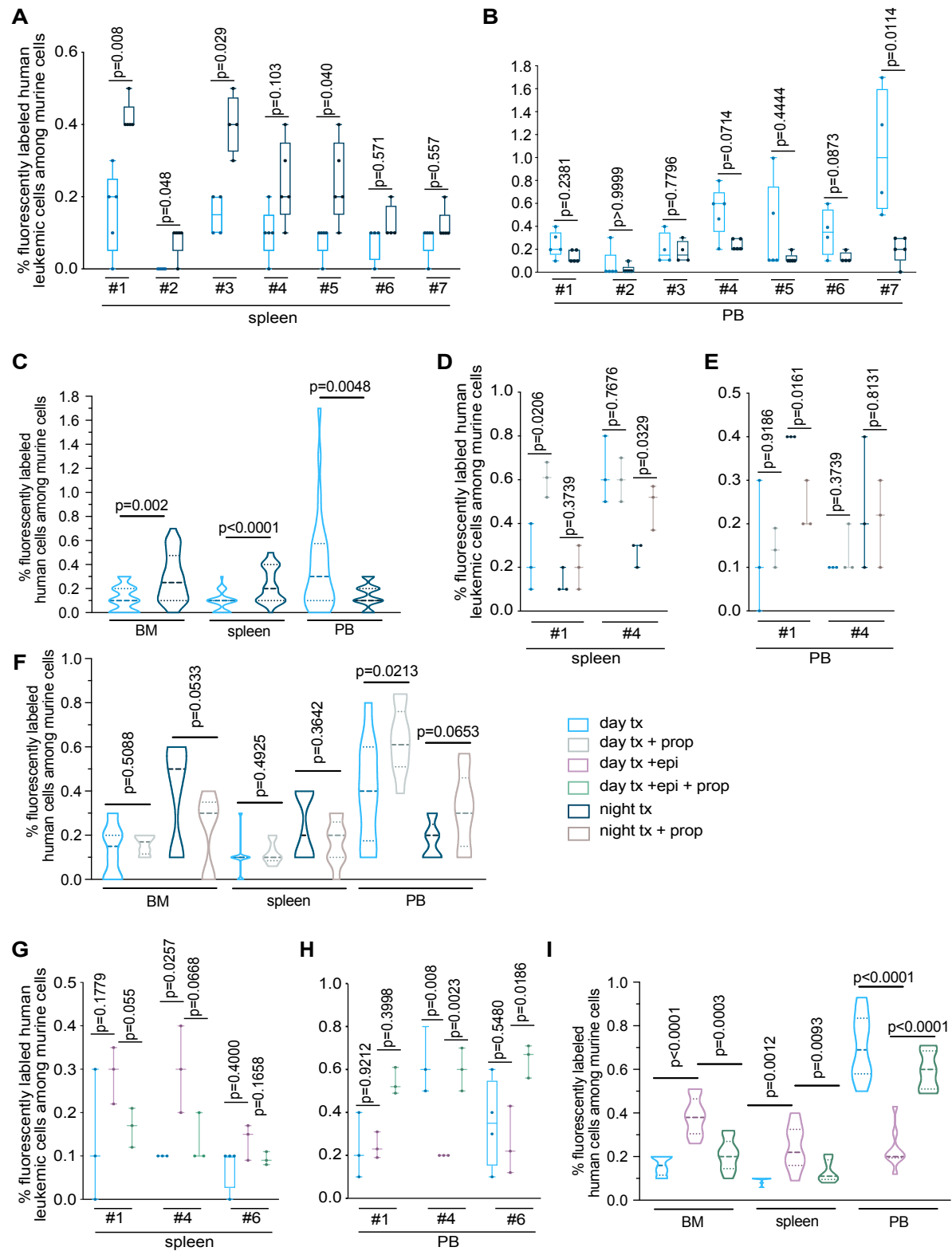


### **Figure S3**

**(A-B)** Homing of CFSE stained leukemic cells in the spleen **(A)** and the PB **(B)** of mice transplanted during day (blue) vs. night (dark blue;  $n=3-5$  mice per condition and  $n=7$  different AML samples). **(C)** Homing of leukemic cells in the BM, spleen and PB of mice transplanted during day (blue) vs. night (dark blue). Results from all AML samples shown in Figure 6B and S3A-B were pooled together. **(D-E)** Homing of CFSE stained leukemic cells in the spleen **(D)** and PB **(E)** of mice transplanted at day control (blue), day with propranolol treatment (grey), night control (dark blue) or night with propranolol treatment (brown;  $n=3$  mice per group,  $n=2$  different AML samples). **(F)** Homing of leukemic cells in the BM, spleen and PB of mice transplanted during day (blue) day with propranolol treatment (grey), night control (dark blue) or night with propranolol treatment. Results from all AML samples shown in Figure 6C and S3D-E were pooled together. **(G-H)** Homing of CFSE stained leukemic cells in the spleen **(G)** and PB **(H)** of mice transplanted at day control (day), day with epinephrine treatment (purple) or day with epinephrine and propranolol treatment (green,  $n=3$  mice per condition and  $n=3$  different AML samples). **(I)** Homing of leukemic cells in the BM, spleen and PB of mice transplanted during day (blue), day with epinephrine treatment (purple) or day with epinephrine and propranolol treatment. Results from all AML samples shown in Figure 6D and S3G-H were pooled together.

Note that data points presented for the day condition in C and E as well in D and F are the same due to optimization of animal numbers in regard to the 3R principle.

Data are represented as boxes that extend from the 25<sup>th</sup> to the 75<sup>th</sup> percentiles. Line in the middle represents the median and the whiskers extend from the minimum to the maximum.

Student-t-test or Mann-Whitney-U-test for statistical analysis.

### **Malignant cells are less sensitive to CXCR4 blockade than healthy HSPCs, which are also not impacted by the timepoint of transplantation**

Given that CXCR4/SDF-1 is a major axis involved in the homing of HSPCs (Aiuti, 1997; Méndez-Ferrer *et al.*, 2008; Sugiyama, 2006), but also reported to play a role in leukemia-stroma interactions in AML (Cho, 2017; Fiegl, 2009; Sison *et al.*, 2013; Tavor, 2004; Voermans, 2002), we next wanted to analyze whether the epinephrine-driven effect was also dependent on this axis or another underlying mechanism. By using flow cytometry, we first confirmed that all tested AML samples (12 primary AML

samples and 3 AML cell lines used in *in vivo* studies) express CXCR4 and found heterogenous surface expression varying between 8.37% (patient 13) and 93.9% (patient 4) of CXCR4 positive cells (Figure S4A).

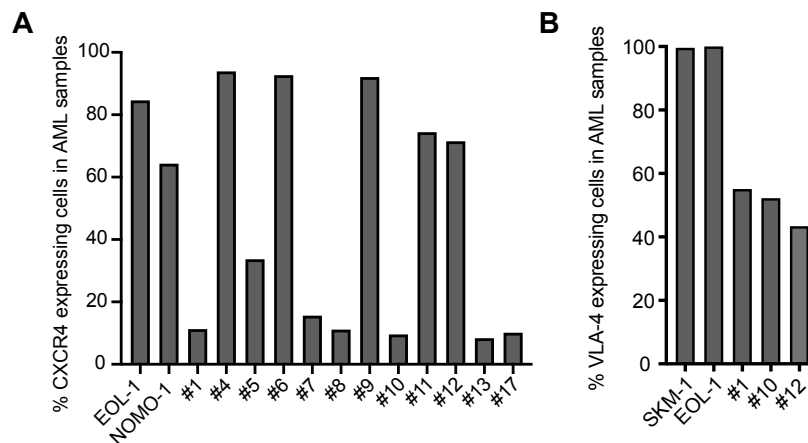


#### Figure S4

**(A)** CXCR4 surface expression on AML samples was measured using flow cytometry ( $n=2$  AML cell lines and  $n=12$  primary AML samples). **(B)** VLA-4 surface expression on AML samples was measured using flow cytometry ( $n=2$  AML cell lines and  $n=3$  primary AML samples). Data represent % positive cells within the bulk of living single cells.

We next performed homing assays and incubated AML cells with anti-CXCR4 blocking antibody prior to day transplantation. Mice received vehicle or epinephrine treatment as previously described. CXCR4 blockade slightly reduced the homing of AML cells both after control day transplantation, as well as after epinephrine treatment ( $n=19-21$  mice per group, untreated:  $0.009965 \pm 0.006382$  vs. CXCR4 blockade alone:  $0.008786 \pm 0.007968$ ,  $p=0.6068$  vs. epinephrine treated:  $0.01342 \pm 0.009374$  vs. CXCR4 blockade and epinephrine treatment:  $0.01237 \pm 0.01066$  % human leukemic cells,  $p=0.7398$ ; Figure 7A). Hence, we performed similar homing experiment with cord blood derived CD34+ HSPCs. Of note, we could observe a stronger effect upon CXCR4 blockade in comparison to leukemic cells, indicating that leukemia might be less sensitive to CXCR4 blockade ( $n=9$  mice per group, CXCR4 blockade:  $0.0008822 \pm 0.0009612$  vs. untreated:  $0.00323 \pm 0.002517$  % human cells,  $p=0.0188$ ; Figure 7A).



Interestingly, homing of healthy HSPCs was neither increased by epinephrine treatment nor upon night transplantation (n=8-9 mice per group, epinephrine:  $0.003482 \pm 0.002888$  vs. untreated:  $0.00323 \pm 0.002517$  % leukemic cells,  $p=0.25$ ; Figure 7A and B).

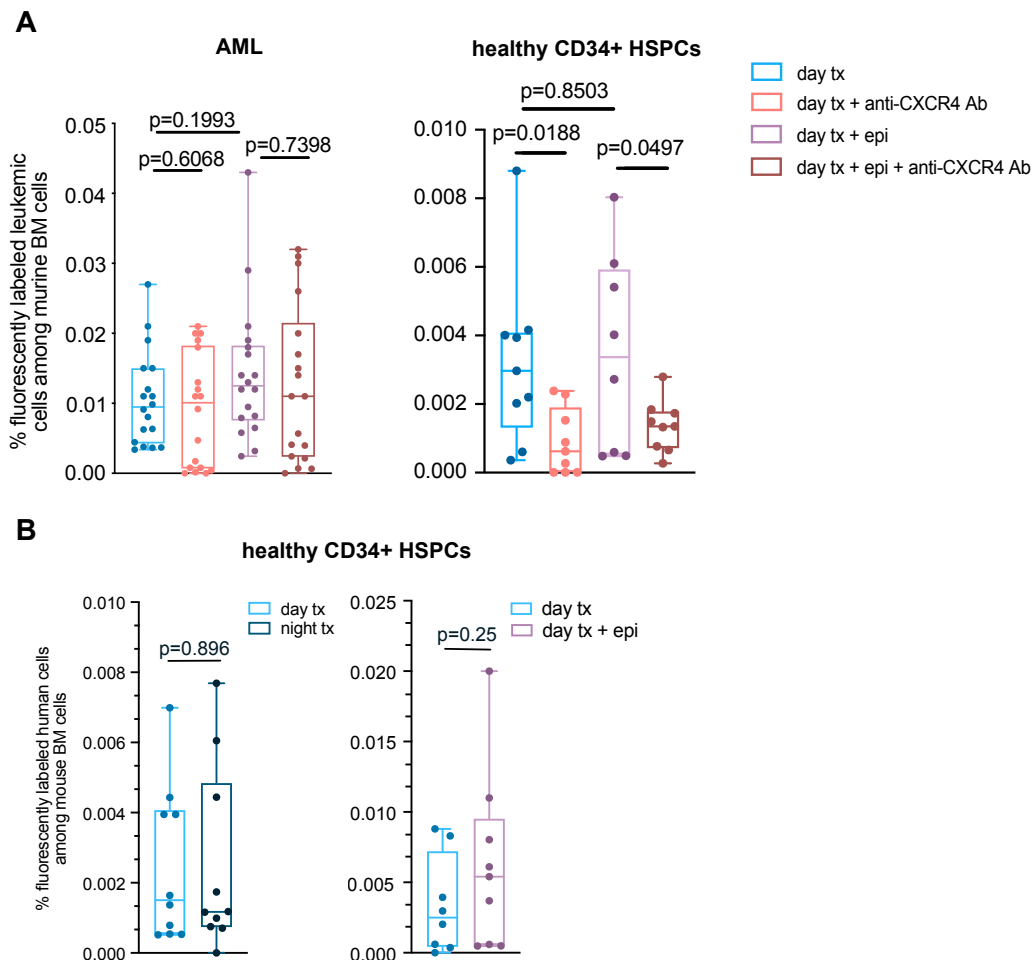


**Figure 7: Malignant cells are less sensitive to CXCR4 blockade than healthy HSPCs which in turn are not impacted by the time-point of transplantation**

**(A)** BM homing rates of CFSE stained leukemic cells (left, n=3-15 mice per AML case and condition, n=1 AML cell line and n=2 AML samples) and respectively healthy HSPCs (right, n=2-3 mice per healthy donor sample and condition, n=3 different donor samples) after treatment with an anti-CXCR4 antibody (orange and dark red) or respectively vehicle control (blue and purple). Transplantations were performed at day in mice pre-treated with epinephrine (purple and dark red) or respectively vehicle control (blue and orange). Note that data points presented for day and day + epi conditions in 7A and 8A are the same due to optimization of animal numbers in regard to the 3R principle.

**(B)** Homing rates of CFSE stained healthy HSPCs within the BM of mice transplanted either during day (blue), night (dark blue, (n=3-4 mice per donor and condition, n=3 different donor samples) or during day with epinephrine control (n=3-4 mice per donor and condition, n=3 different donor samples).

Data are represented as boxes that extend from the 25<sup>th</sup> to the 75<sup>th</sup> percentiles. Line in the middle represents the median and the whiskers extend from the minimum to the maximum.

Student-t-test or Mann-Whitney-U-test for statistical analysis.

Furthermore, human CD34<sup>+</sup> HSPCs were also transplanted in recipient mice at day and night time points. Chimerism of human CD45<sup>+</sup> cells among all peripheral blood mononuclear cells (PBMCs) showed no significant difference between day and night transplantation settings neither at the intermediate timepoint of 16 weeks nor at the final analysis endpoint at week 30 (week 16 day  $13.59 \pm 13.72$  % vs. night  $20.87 \pm 19.95$  % of hCD45<sup>+</sup> cells, p=0.2351 and week 30 day  $38.96 \pm 18.84$  % vs. night  $37.33 \pm 17.94$  % of hCD45<sup>+</sup> cells, p=0.2351; Figure S5A). Similar results were obtained upon analysis of the expression of human CD3<sup>+</sup>, CD19<sup>+</sup> and CD33<sup>+</sup> cells (Figure S5A). We could consolidate these observations in a syngeneic mouse model, in which UBC-GFP lineage negative cells were transplanted into sublethally irradiated wildtype recipients. Donor GFP<sup>+</sup> cells were observed in similar amounts in day vs. night transplanted mice (n=9 mice per group, day:  $4.051 \pm 4.791$  % vs. night  $5.8 \pm 6.59$  % donor GFP<sup>+</sup> cells amongst BM cells, p=0.8456; figure S5B) further confirmed by similar percentages of donor CD3<sup>+</sup>, CD19<sup>+</sup> and CD45<sup>+</sup> cells (Figure S5B). Taken together, these data indicate that the effect of night transplantation and epinephrine treatment is leukemia-specific and does not affect healthy HSPCs.

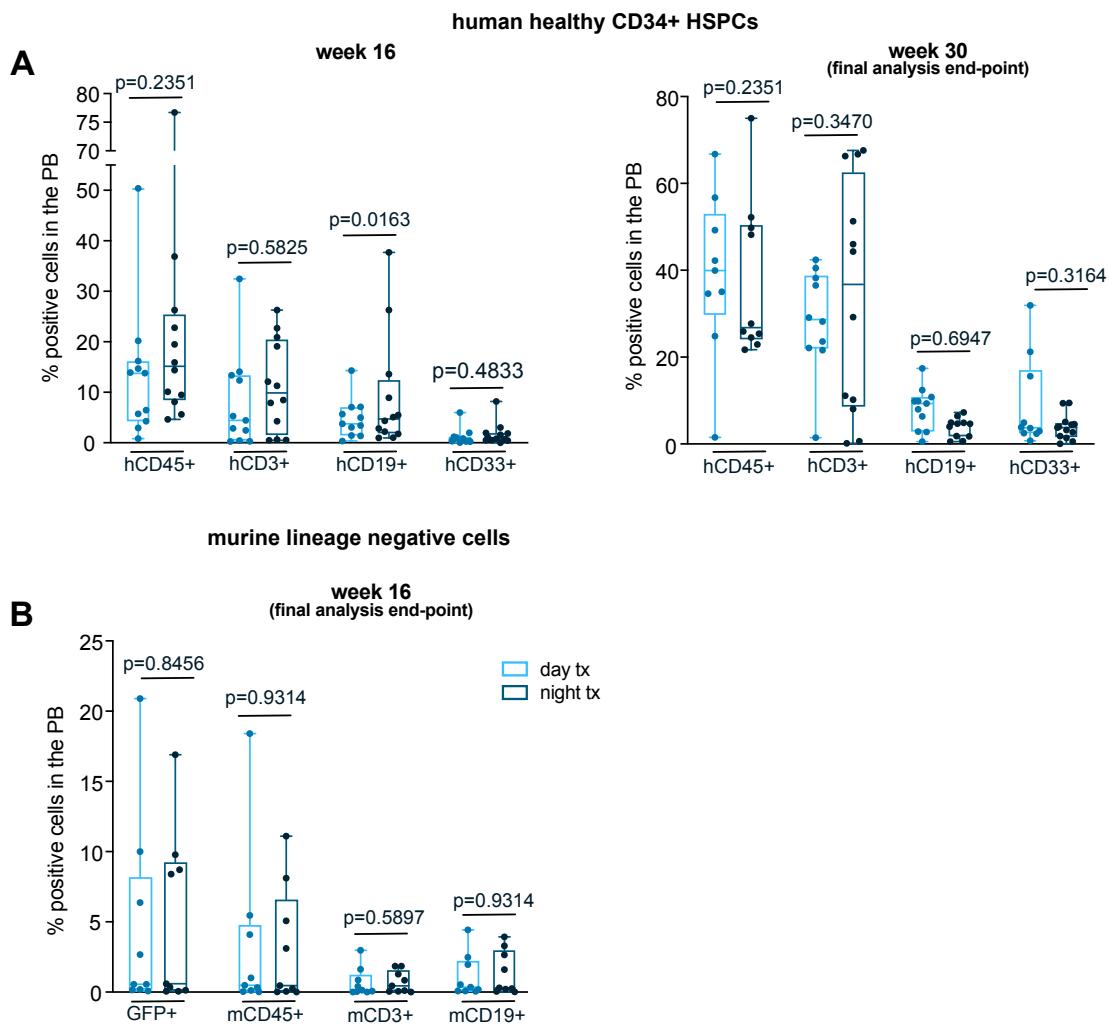


### Figure S5

**(A)** Infiltration of PB of recipient NSG mice with human hematopoietic cells, 16 weeks (left panel) or 30 weeks (final analysis endpoint, right) after transplantation with  $1.5 \times 10^5$  cord blood derived CD34<sup>+</sup> cells at day (blue) vs. night (dark blue). Percentages of human donor CD45<sup>+</sup>, CD3<sup>+</sup>, CD19<sup>+</sup> and CD33<sup>+</sup> cells were assessed in murine PB ( $n=11-12$  mice per condition from  $n=3$  healthy cord blood samples). **(B)** Infiltration of PB of recipient WT mice with UBC-GFP murine donor hematopoietic cells, 16 weeks after transplantation (final analysis end-point) with  $5 \times 10^5$  GFP<sup>+</sup> Lin<sup>-</sup> at day (blue) or night (dark blue) timepoints. Percentages of murine donor GFP<sup>+</sup> cells, CD45<sup>+</sup>, CD3<sup>+</sup> and CD19<sup>+</sup> cells assessed in the PB ( $n=9$  mice per condition from  $n=3$  different UBC-GFP donor mice).

Data are represented as boxes that extend from the 25<sup>th</sup> to the 75<sup>th</sup> percentiles. Line in the middle represents the median and the whiskers extend from the minimum to the maximum.

*Student-t-test or Mann-Whitney-U-test for statistical analysis.*

### **VLA-4 is involved in adrenergic driven enhanced homing, likely due to enhanced affinity of VLA-4 to its receptor**

It was previously shown that the transmigration of human CD34<sup>+</sup>/CXCR4<sup>+</sup> cells through BM endothelial cells was highly dependent on the interaction with VLA-4/VCAM-1 (Peled, 2000), hence we next investigated the importance of this integrin molecule in our model. We were particularly interested in studying VLA-4 in our epinephrine treatment condition, since it was reported to be functionally activated on immature CD34<sup>+</sup> cells by CXCL12, whose levels are in turn increased during night and under stress conditions in mice (Méndez-Ferrer *et al.*, 2010a; Méndez-Ferrer *et al.*, 2008; Peled, 2000). We found heterogeneous but high VLA-4 surface expression in both AML cell lines and primary samples (3 primary AML samples, 2 AML cell lines, Figure S4B). Even though all analyzed samples expressed high levels of VLA-4, AML cell lines displayed higher proportions of VLA-4 expressing cells (99.6 and 100% for SKM-1 and EOL-1 cell lines respectively) in comparison to primary AML cell lines (55.1, 52.2 and 43.4% for patient 1, 10 and 12 respectively, Figure S4B).

Consequently, we used an anti-VLA-4 blocking antibody to treat both AML and healthy HSPCs in homing assays prior to injection in combination with epinephrine treatment of NSG mice. Interestingly VLA-4 blockade could partially counteract the effect of epinephrine and decrease the homing rate of AML cells even though it had no significant effect on their homing capacity in basal conditions (n=17-18 mice per group, day control  $0.00344 \pm 0.001866$  vs. day VLA-4 blockade  $0.003687 \pm 0.002112$  % leukemic cells, p=0.8386 and day epinephrine  $0.0085 \pm 0.00401$  vs. day epinephrine + VLA-4 blockade  $0.005574 \pm 0.002853$  % leukemic cells, p=0.0191; Figure 8A left panel). In contrast to this, their healthy counterparts HSPCs were highly sensitive to VLA-4 blockade in basal homing (n=8-9 mice per group, day control  $0.00323 \pm 0.002517$  % vs. day VLA-4 blockade  $0.0006936 \pm 0.002888$  % human cells, p= 0.0098 and day epinephrine  $0.003482 \pm 0.002888$  % vs. day epinephrine and VLA-4 blockade  $0.0008308 \pm 0.0007209$  % human cells, p=0.0174; Figure 8A). We next explored whether epinephrine was increasing the affinity of VLA-4 to its receptors. In an *in vitro* binding assay, we could show enhanced affinity of VLA-4 when expressed

on the surface of AML (n=25-26 technical replicates, control  $1.306 \pm 0.1873$  vs. epinephrine  $1.577 \pm 0.4951$  relative binding quantification,  $p=0.0025$ ; Figure 8B-C left panel) in contrast to healthy CD34<sup>+</sup> HSPCs, for which epinephrine treatment had no impact (n=15 technical replicates, control  $1.206 \pm 0.2224$  vs. epinephrine  $1.279 \pm 0.2021$  relative binding quantification,  $p=0.1982$ ; Figure 8B-C).

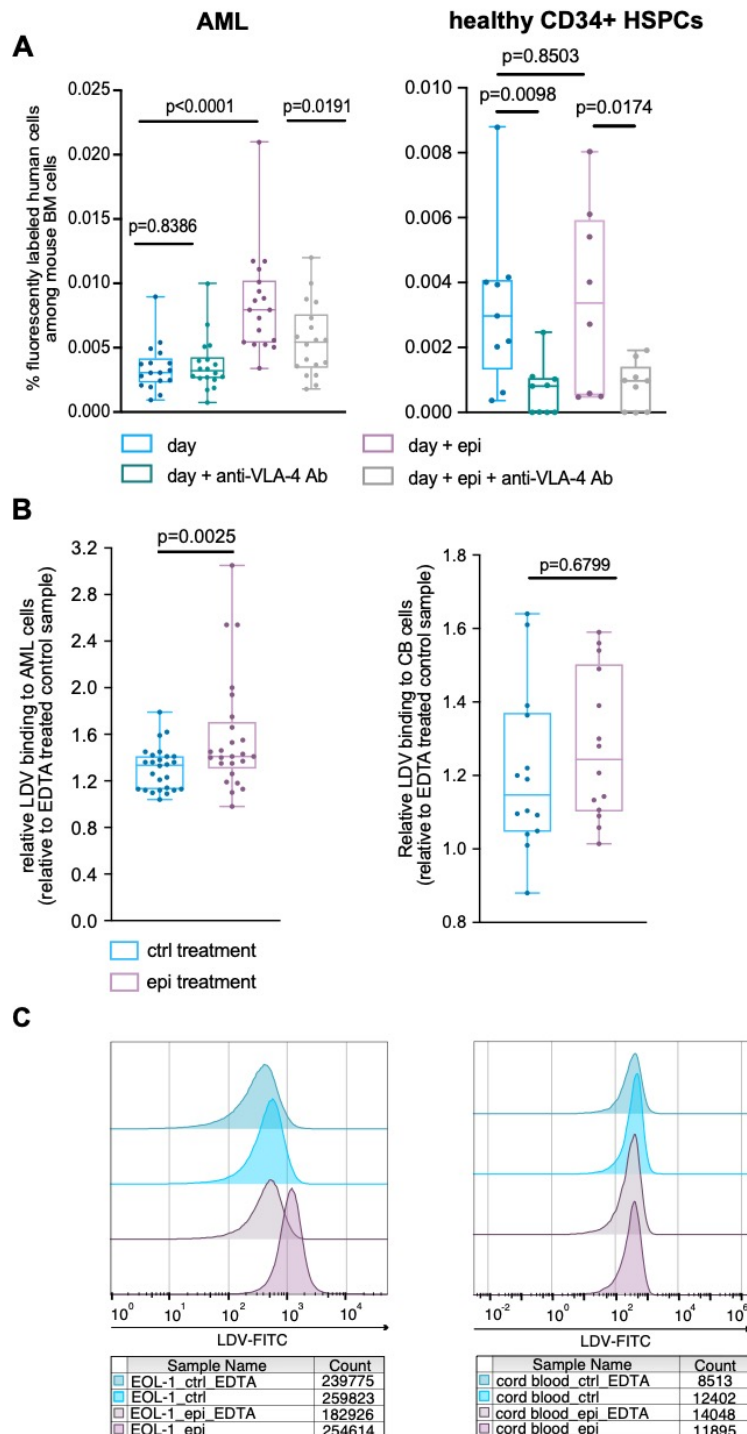


**Figure 8: VLA-4 is involved in adrenergic-driven enhanced homing, likely due to enhanced affinity of VLA-4 to its receptor**

**(A)** Homing rates of CFSE stained leukemic cells (left panel) or healthy HSPCs (right panel) pre-treated with either anti-VLA-4 antibody (petrol blue and grey) or vehicle control (blue and purple). Cells were transplanted at day time in mice pre-treated with epinephrine (purple and grey) or vehicle control (blue and petrol blue). Note that data points presented for day and day + epi conditions in 7A and 8A are the same due to optimization of animal numbers in regard to the 3R principle. **(B)** In vitro affinity assay showing relative LDV peptide binding to AML cells (left panel, n=2 AML cell lines and n=1 AML sample, n=6-11 technical replicates per AML case and condition) or healthy HSPCs (right panel, n=15 healthy donor samples) upon epinephrine (purple) or vehicle control treatment (blue). Data are shown relative to EDTA treated control samples. Data are represented as boxes that extend from the 25<sup>th</sup> to the 75<sup>th</sup> percentiles. Line in the middle represents the median and the whiskers extend from the minimum to the maximum.

Student-t-test or Mann-Whitney-U-test for homing experiments and ratio paired t-test for in vitro affinity assays for statistical analysis.

Altogether these data show that in the case of leukemia cells, VLA-4 is involved in epinephrine-driven enhanced homing to the BM, certainly via enhanced affinity of the integrin to its receptors, thus increasing the transmigration through the BM endothelial cell layer.

N.B.: The discussion and Material and Method parts have been included with respectively the discussion of the chapter 4 and the general Material and Method part of this thesis.

### **Acknowledgements**

We would like to thank the flow cytometry and animal facility at the Department of Biomedicine in Basel, Dr. Parimala Sonika Godavarthy and Antoine Devisme for proofreading the manuscript as well as Ronja Wieboldt and Joëlle Müller for the help with respectively affinity assay and isolation of cord blood derived HSPCs.

We also would like to thank Prof. Dr. Robert Zeiser for providing MLL-PTD/FLT3-ITD cells for the syngeneic leukemia model, Prof. Dr. Tsvee Lapidot for giving great

suggestions concerning VLA-4 and CXCR-4 signaling and for providing the protocol for affinity assay, and Prof. Dr. Gerd Klein for proofreading and critical comments on the several aspects of the manuscript.

This work was funded by grants of the Swiss Cancer League (KFS-4013-08-2016-R) to C.L.

### **Author contributions**

A.M.P.S, P.H. and C.L. designed the study, analyzed the data and wrote the manuscript. A.M.P.S, P.H., M.K., M.B., C.S. and M.A. performed experiments and interpreted data. P.L. performed Next Generation Sequencing experiments and interpreted data. S.D. performed histopathology experiments and interpreted data. All authors contributed to the writing and approved the final version of the manuscript.

## 1.2. ADDITIONAL DATA (NOT INCLUDED IN THE MANUSCRIPT)

### 1.1.1. **The expression of ARs is heterogenous between AML samples**

To investigate the possibility of an adrenergic regulation of the engraftment and homing of AML cells, we explored mRNA expression of the nine different ARs ( $\alpha$ 1a-AR,  $\alpha$ 1b-AR,  $\alpha$ 1d-AR,  $\alpha$ 2a-AR,  $\alpha$ 2b-AR,  $\alpha$ 2c-AR,  $\beta$ 1-AR,  $\beta$ 2-AR,  $\beta$ 3-AR) in four primary AML samples and three AML cell lines used in our *in vivo* studies (Figure 10A-B). The expression of ARs has been observed along all analyzed samples but at different levels. In general, we observed a higher expression in the cell lines, especially in the SKM-1 cell line (Figure 10B) in comparison to AML patients samples (Figure 10A). Amongst the different types of receptors. Next to AR $\beta$ 2, the  $\alpha$ 2-AR category is the most represented amongst all AML samples in the majority of the analyzed samples. Two AML cell lines, EOL-1 and NOMO-1 behave differently, since they almost exclusively express mRNA for  $\beta$ 3-AR (Figure 10B).

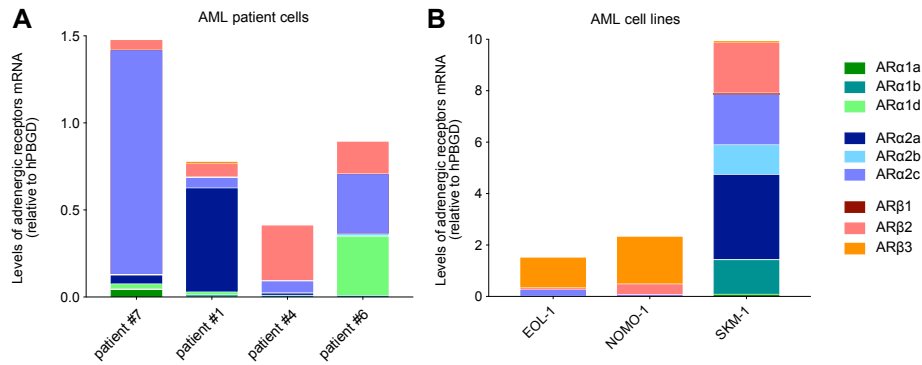


**Figure 10: ARs expression on AML cells.**

mRNA expression of the different types of ARs (AR  $\alpha$ 1 subtypes ( $\alpha$ 1a-AR,  $\alpha$ 1d-AR,  $\alpha$ 1d-AR) in green, AR  $\alpha$ 2 subtypes ( $\alpha$ 2a-AR,  $\alpha$ 2b-R,  $\alpha$ 2c-AR) in blue and ARs of the  $\beta$  subtype ( $\beta$ 1-AR,  $\beta$ 2-AR,  $\beta$ 3-AR) in orange) was determined by qRT-PCR in four primary AML samples and three AML cell lines (EOL-1, SKM-1 and NOMO-1). Data are represented as levels of mRNA relative to the housekeeping gene PBGD (Porphobilinogen deaminase).

### 1.1.2. The number of colony forming unit cells (CFU-C) is neither influenced by our time-point of transplantation nor by EPI treatment

It is well established that the levels of SDF-1 and the related CFU-C numbers, which inform about the number of circulating HSPCs, from PB of mice are influenced by circadian regulations. We were interested to investigate whether this was the case in our transplantation settings, namely between the two different time-points of injection. We first compared levels of *Sdf-1* mRNA in samples collected at day (5 pm) and night (4 am) time-points of transplantation. We observed significantly higher levels of *Sdf-1* at night in comparison to day in the BM of transplanted mice (Figure 11A). We also looked at the capacity of the peripheral blood mononuclear cells (PBMCs) isolated from the PB of the mice to form CFU-C. We could not see a difference in the CFU-C numbers between the PB collected at day and at night (Figure 11B). Similarly, we also analyzed the levels of *Sdf-1* mRNA in the BM of mice at two different time-points (one hour and two hours) after epinephrine treatment (Figure 11C). Of note, similarly to the *in vivo* experiments, EPI treatment was performed during day (at 4:00 pm). EPI treatment did not influence the expression of *Sdf-1* mRNA in the murine BM in any of



the analyzed time-point (Figure 11C). The number of circulating HSPCs was also not impacted by epinephrine treatment (Figure 11D). As it was published and confirmed that both *Sdf-1* levels and HSPCs numbers in circulation are influenced by circadian rhythms (Méndez-Ferrer *et al.*, 2008), we decided to analyze these two variables at 7 different time-points between midnight and 10 am under classical light conditions (Figure 11E) and also under what we term “transplantation” light conditions (Figure 11F), i.e. switch on of the light for 2 hours between 3 and 5 am. Under steady-state conditions, i.e. when mice were exposed to a classical cycle of 12 hours light and 12 hours darkness, we could recapitulate the previously published data and show that the numbers of circulating HSPCs is clearly oscillating in the investigated timeframe with a peak around light onset (Figure 11E). In parallel, *Sdf-1* mRNA levels also markedly oscillated and reached the nadir around light onset (Figure 11E). Interestingly, the oscillation pattern was very different when the classical cycle of light and darkness was disturbed. 2 hours of light input during darkness was sufficient to shift the peak of circulating HSPCs around this unusual time point of light onset (3-4 am) and to break the usual peak in *Sdf-1* mRNA, which dropped very rapidly after light onset (Figure 11F). Of note, the CFU-C peak observed under these light conditions is less pronounced than the usual peak and substitutes the latter (Figure 11F).

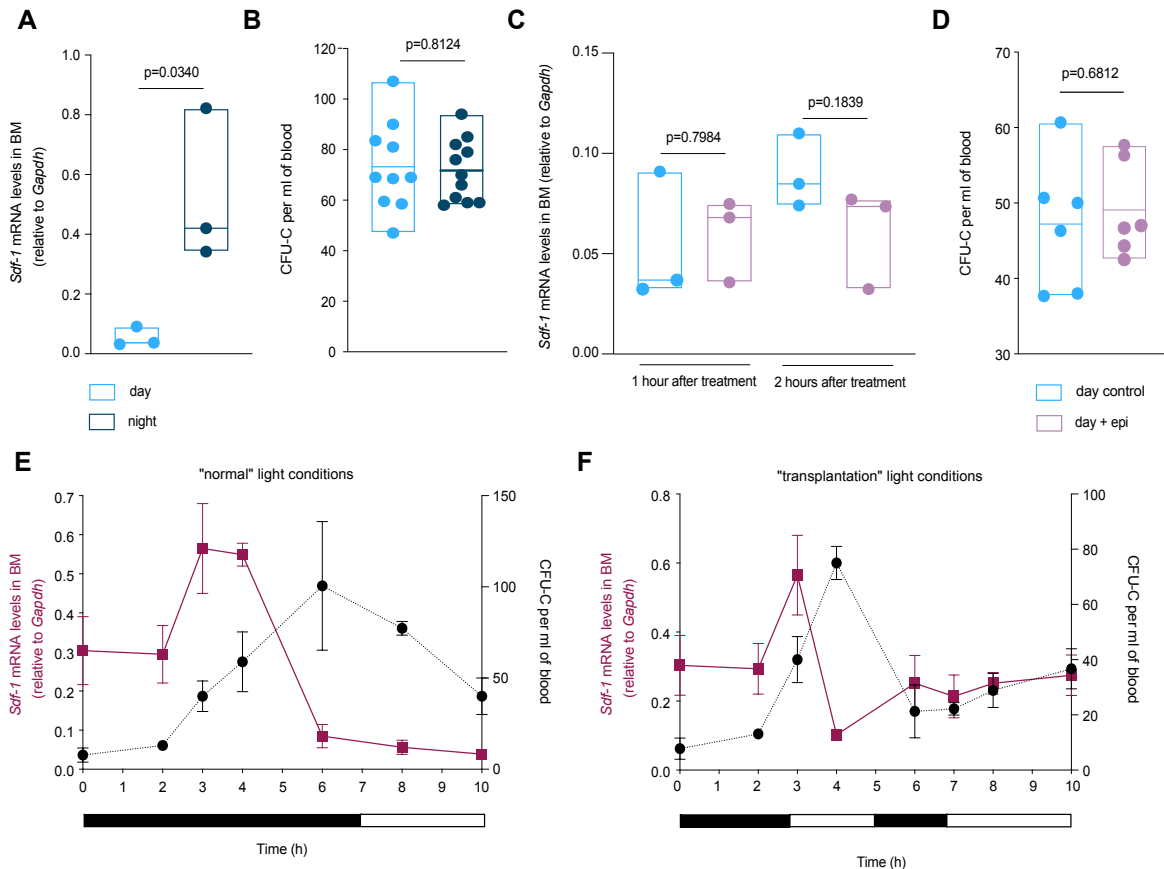


**Figure 11: Influence of the circadian rhythm and EPI treatment on the levels of *Sdf-1* and the number of circulating progenitors.**

**(A)** *Sdf-1* mRNA levels in the BM of the mice analyzed at day (blue) and night (dark blue) time-points were determined by qRT-PCR ( $n=3$  mice per group). Data are represented as levels of mRNA relative to the housekeeping gene GAPDH (Glyceraldehyde 3-phosphate dehydrogenase). **(B)** The number of circulating progenitors was determined via a CFU assay. The total number of CFU-C (independent of the type of colony) was determined in the PB of mice at day (blue) and night (dark blue) time-points ( $n=10-11$  mice per group). Data are represented as CFU-C per ml of murine blood. **(C)** *Sdf-1* mRNA levels in the BM of mice treated during day with control (blue) or EPI (purple) were analyzed by qRT-PCR. Mice were either analyzed one hour or two hours after treatment ( $n=3$  mice per group). Data are represented as levels of mRNA relative to the housekeeping gene GAPDH. **(D)** The total number of CFU-C was determined in the PB of mice one hour after control (blue) or EPI (purple) treatment performed during day ( $n=6$  mice per group). Data are represented as CFU-C per ml of murine blood. **(E-F)** *Sdf-1* levels in the BM and CFU-C numbers in the PB were determined in mice at seven different time points between

midnight and 10 am (0 am, 2 am, 3 am, 4 am, 6 am, 8 am and 10 am) under classical light/darkness conditions (**E**, 12 hours light/ 12 hours darkness cycle, switch on of the light at 7 am) and under “transplantation” light conditions (**F**, 2 hours of light during the classical darkness period, from 3 to 5 am). Data for *Sdf-1* levels are represented as levels of mRNA relative to the housekeeping gene *GAPDH* and data for circulating progenitors as CFU-C per ml of murine blood ( $n=3$  mice per group and condition). In (A, B, C and D) lines represent means with standard deviation. Shapiro-Wilk test for normality, Student-t-test, Mann-Whitney-U-test.

### 1.1.3. EPI treatment does not affect *Vcam-1* expression in the murine BM

We next investigated if EPI treatment has an impact on the expression of the *Vcam-1* adhesion molecule in the murine BM. The analysis of three control and three EPI-treated mice one hour after the induction of treatment did not reveal any impact of the catecholamine treatment of the mRNA level of *Vcam-1* within the murine BM (Figure 12).

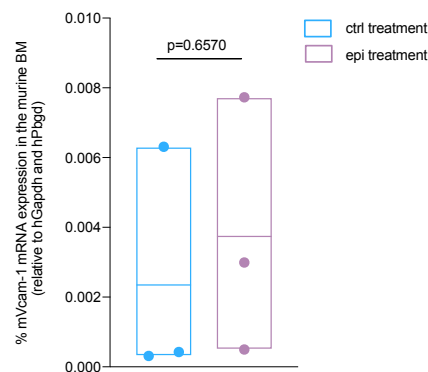


**Figure 12: Effect of EPI on *Vcam-1* mRNA expression in the BM of mice.**

*Vcam-1* mRNA expression was determined by qRT-PCR in the BM of mice one hour after control (blue) or EPI (purple) treatment during day ( $n=3$  mice per group). Data are represented as levels of mRNA relative to the mean expression levels of the two housekeeping genes *PBGD* and *GAPDH*.

Lines represent means with standard deviation. Shapiro-Wilk test for normality, Student-t-test, Mann-Whitney-U-test.

#### **1.1.4. *In vitro* adhesion of AML cells but not HSPCs is influenced by EPI treatment**

In the data presented in the manuscript above, we can see that EPI treatment of recipient mice influences homing of AML cells (Figure 4). We were thus interested to investigate whether this is due to increased adhesion of the transplanted AML cells to the BM stroma. To address this question, we used an adhesion assay (Petit et al., 2005), in which fluorescently labelled AML cells were co-incubated with the murine stromal MS-5 cell line (Figure 13A). After 90 minutes of co-incubation, the non-attached AML cells were removed and the remaining adherent cells were trypsinized and analyzed by FC (Figure 13A). This assay allows us to include different types of treatment with EPI and the corresponding control, i.e. pre-treatment of AML cells before co-incubation with MS-5 cells, pre-treatment of MS-5 cells before co-incubation with AML cells and treatment of both cell types, which are then co-incubated, in order to be able to investigate which cell type is affected by the EPI treatment. In all cases, the duration of the co-incubation was 90 minutes and the concentration of EPI treatment was 10  $\mu$ M (Figure 13A).

The analysis of eight primary AML samples and three AML cells lines indicates that adhesion was enhanced upon EPI treatment during co-incubation in comparison to control treatment both for primary samples and cells lines (Figure 13B). Interestingly, the increase in adhesion of AML cell with the stromal cell line was visible for all types of EPI treatment, but was more pronounced when AML cells were pretreated with catecholamine solution (Figure 13C).

Since we could not observe an influence of CB-derived healthy HSPCs by EPI treatment (Figure 7 of the manuscript), we were interested to analyze the behavior of these cells upon catecholamine treatment in adhesion assays. The analysis of HSPCs derived from four different healthy cord blood (CB) donors showed no difference in the adhesion of the hematopoietic cells to the stroma cell line upon EPI treatment (Figure 13D). The result was similar in all three tested types of catecholamine treatments (Figure 13E).

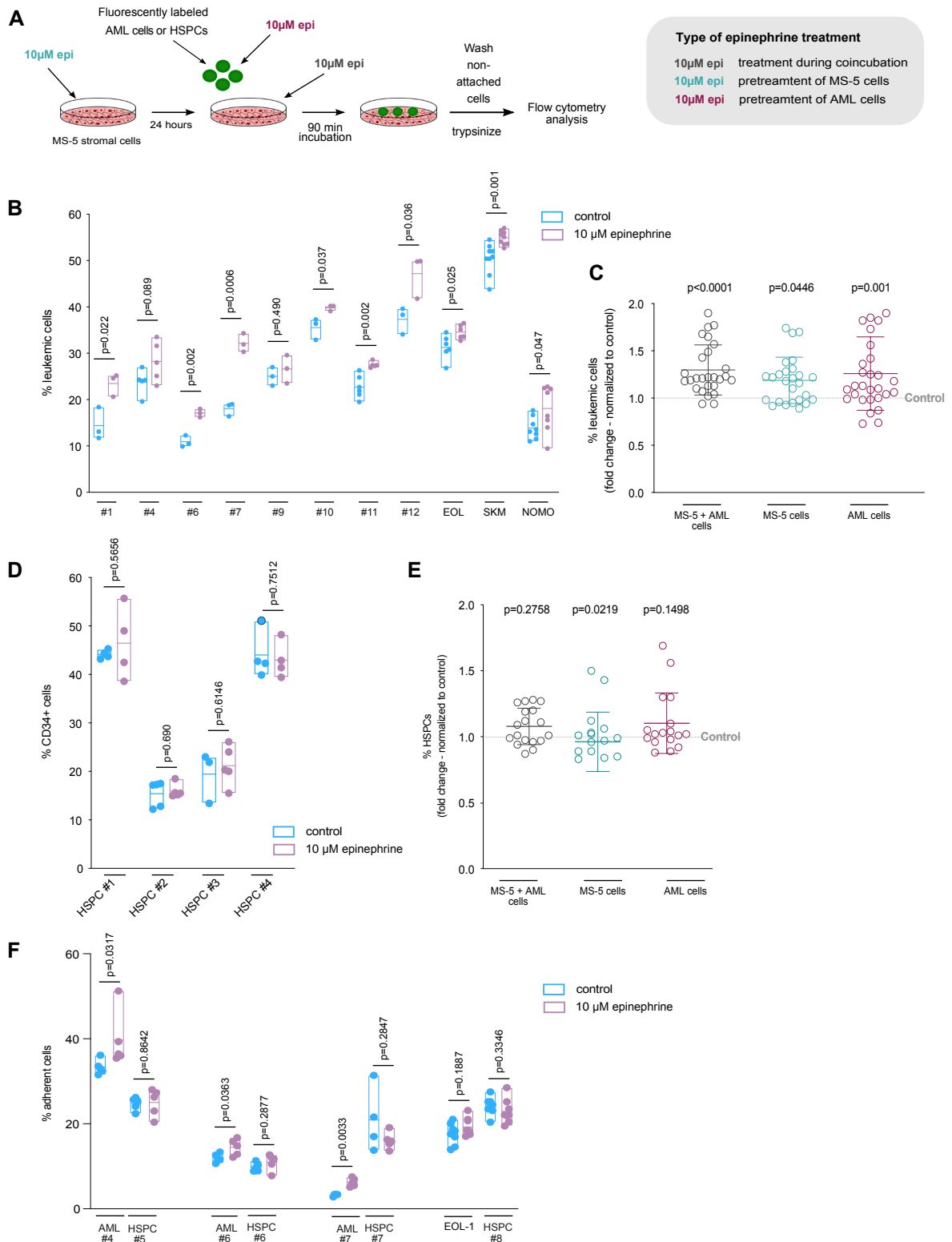


**Figure 13: Effect of EPI treatment on the adhesion of AML cells or HSPCs to stromal cells.**

(A) Schematic overview of the *in vitro* adhesion assay to MS-5 stromal cells. The effect of EPI treatment was investigated at different time-points of the assay (during co-

incubation of AML cells/HSPCs with MS-5 cells, black, pre-treatment of MS-5 cells, blue, and pre-treatment of AML cells/HSPCs, red). **(B)** Adhesion of AML cells to stromal cells was determined after control (blue) and EPI (purple) treatment during co-incubation in three AML cell lines (EOL-1, SKM-1 and NOMO-1) and n=8 primary AML samples (n=3-10 technical replicates per sample and condition). Data are represented as the percentage of leukemic cells amongst retrieved cells and determined by FC. **(C)** Adhesion of AML cells to stromal cells for all three types of EPI treatment was determined. Data are represented as fold change of the percentage of adherent leukemic cells after EPI treatment normalized to control. The same samples than in (B) were used. **(D)** Adhesion of CB derived HSPCs to stromal cells was determined after control (blue) and EPI (purple) treatment during co-incubation in samples derived from four healthy donors (n=4-5 technical replicate per sample and condition). Data are represented as the percentage of leukemic cells amongst retrieved cells and determined by FC. **(E)** Adhesion of CB derived HSPCs to stromal cells for all three types of EPI treatment was determined. Data are represented as fold change of the percentage of adherent HSPCs after EPI treatment normalized to control. The same samples than in (D) were used. **(F)** Adhesion of AML cells and CB derived HSPCs to stromal cells was determined after control (blue) and EPI (purple) treatment during co-incubation in “competition assays”. Samples derived from four healthy donors as well as three primary AML samples and one AML cell line were added together in the same ratio on the MS-5 cells (n=4-5 technical replicates per sample and condition). Data are represented as the percentage of leukemic cells and HSPCs amongst retrieved cells and determined by FC.

In (B, C, D, E and F) lines represent means with standard deviation. Shapiro-Wilk test for normality, Student-t-test, Mann-Whitney-U-test.

Furthermore, we were hypothesizing a possible *in vivo* competition between the transplanted AML cells and endogenous HSPCs for the colonization of and/or the adhesion to the murine BM niche. We tested this hypothesis in this *in vitro* adhesion assay by plating a mixture of the similar proportions of human AML cells and HSPCs. We performed this assay with n=3 primary AML samples that were already studied in the adhesion assay in Figure 13B as well as the EOL-1 cell line. First of all, we could observe that in these competitive adhesion assay settings, both AML cells and HSPCs adhered to different extents to MS-5 cells. In two assays (patients 4 and 6), the

proportion of adherent AML cells was higher than the proportion of adherent HSPCs, whereas for the two other samples the opposite was observed (Figure 13F). This might be linked to the variability of patient as well as healthy donor samples. Moreover, when looking to the adhesion of AML cells under control treatment, we could see that for primary AML cells of patient 4 and 6, the percentage of adherent leukemic cells was very similar in the competitive assay (Figure 13F) when compared to the classical adhesion assay (Figure 13B), indicating that for these AML cells, the presence of HSPCs in the control treatment does not impact their adhesion to the stroma. Contrarily, cells from patient 7 and for the EOL-1 cell line are adhering less in the competitive assay (Figure 13E) in comparison to the classical assay (Figure 13B). Focusing on the effect of EPI treatment, we were able to observe an increase in adhesion of all tested AML cells but none of the tested HSPCs. Notably, by comparing to the control, the ratio of adhered AML cells upon EPI treatment remained constant when comparing the same AML sample in the classical and the competitive adhesion assay (Figure 13B and F).

#### **1.1.5. Effect of EPI treatment on the transcriptome of the MS-5 stromal cell line**

In order to gain insight concerning the impact of adrenergic signaling pathway activation on the transcriptome of BM stromal cells, we performed RNA sequencing on MS-5 cell line as a quick and preliminary experiment. We compared the murine stromal cell line after EPI and control treatment. Principal component analysis (PCA) showed a clear separation of the two groups according to the treatment (Figure 14A), indicating an effect of EPI treatment on the gene expression of the stromal cell line. Amongst genes that were modulated by adrenergic activation, we could find some that were linked to chemotaxis, circulatory, leukocyte, migration and vessel related pathways (Figure 14B). Importantly, this is not an exhausted list of pathways that were influenced by EPI treatment, they were chosen because of their significance in our work.

Unfortunately, no differentially expressed genes of adhesion related pathways were identified after EPI treatment in these experimental settings (data not shown).

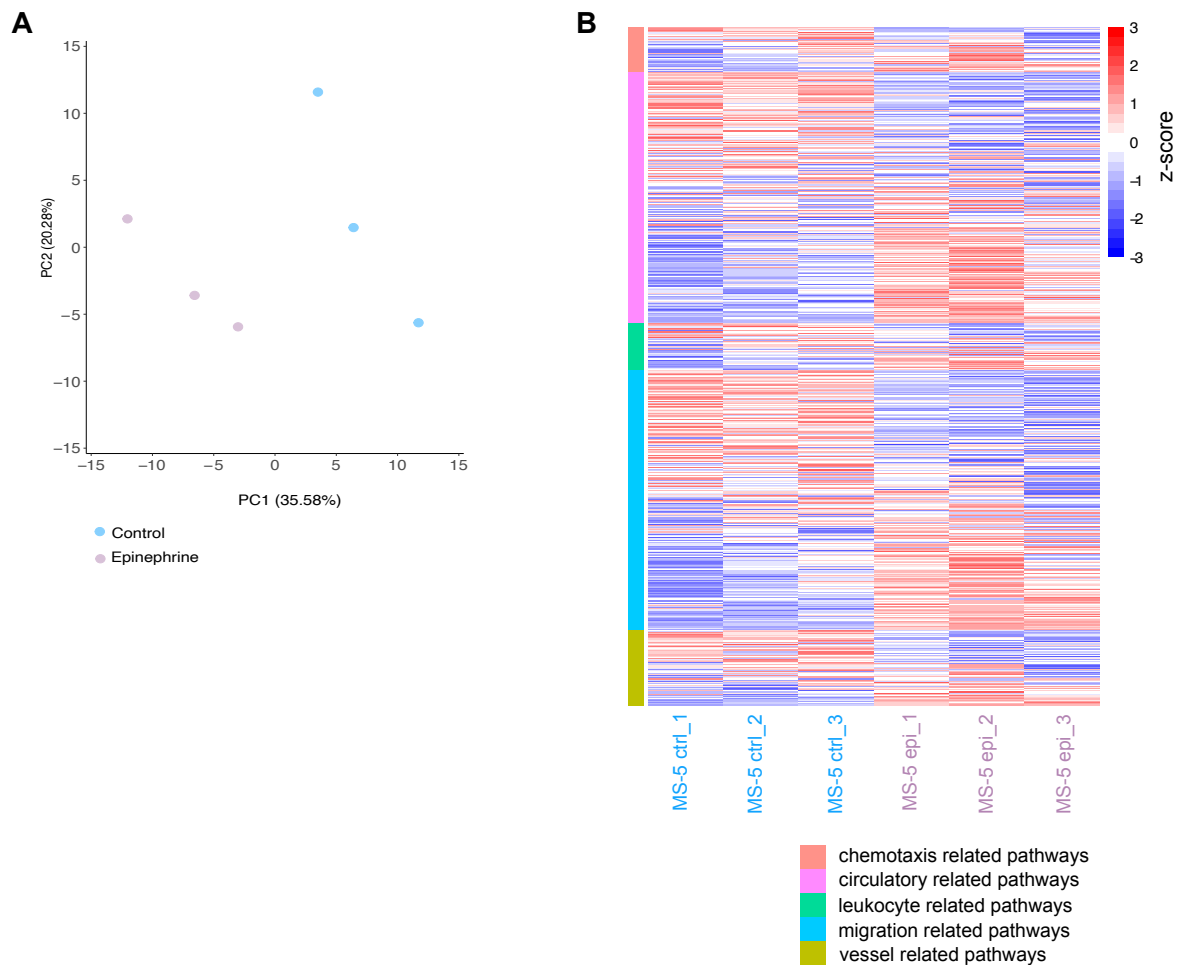


**Figure 14: EPI treatment impacts the transcriptome of the MS-5 cell line.**

**(A)** Principal component analysis (PCA) of MS-5 cells after 24 hours treatment with control (blue) or EPI (violet). **(B)** Heatmap of the genes from the different pathways of interest (see legend and color code below the plot) upon EPI treatment of MS-5 cells. Genes related to the pathways were extracted from the GO database. Row values are centered and scaled.

We focused in more detail on both the chemotaxis (Figure 15A) and migration (Figure 15B) related pathways, since they were particularly relevant to our study. In fact, as we discussed previously in this work, we could see an impact of EPI treatment to the homing of AML cells to the BM. This might be directly linked to chemotaxis and migration mechanisms, in which the stromal cells might play an important role.

In line with this, we could observe that amongst differentially expressed genes (adjusted p.value < 0.05), the majority of them (403/574) were upregulated upon EPI treatment (Figure 15A-B). From the list of significantly upregulated genes, many of



them (*Vegfa*, *Spp1*, *Ccl1*, *itgb7*, *itgb2*) appear as very interesting and will be described more in details latter in the discussion part (Figure 15A-B).

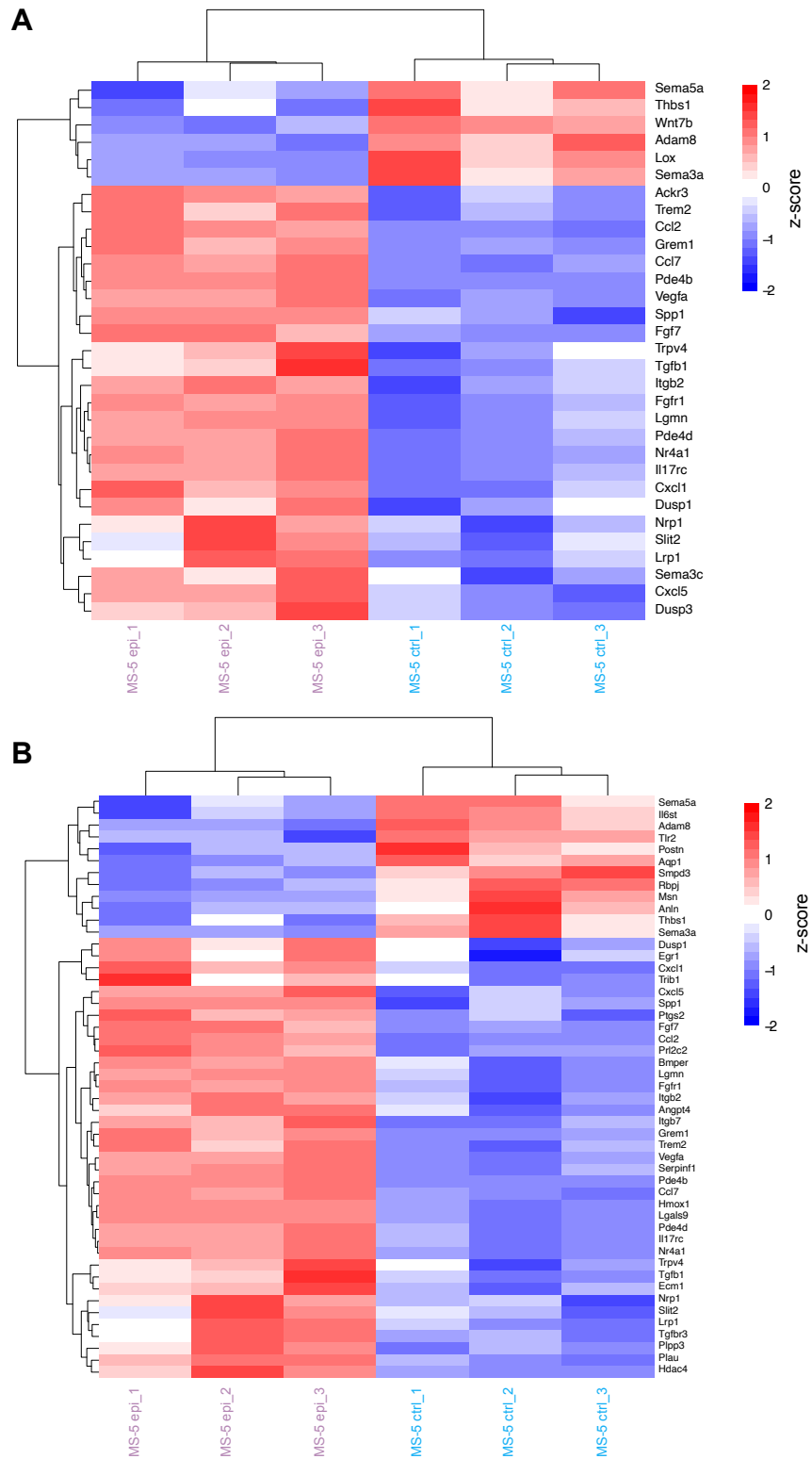


**Figure 15: Differentially regulated genes in MS-5 cells upon epinephrine treatment.**

(A) Heatmap of significantly differentially regulated genes derived from the chemotaxis related pathway. (B) Heatmap of significantly differentially regulated genes derived from the migration related pathway.

**1.1.6. Investigation of EPI treatment on the transcriptome of a primary AML sample and a CB-derived HSPCs sample**

Similarly to the RNA sequencing analysis of MS-5 cells, we also analyzed the effect of EPI on both primary AML cells from one patient and HSPCs from one healthy donor (Figure 16A). PCA shows that even though the respective AML cells and HSPCs nicely cluster together, this is absolutely not the case when comparing the samples treated with the control and the EPI solution, thus indicating no significant effect of EPI on their gene expression (Figure 16A). We could consequently not draw any conclusion from this analysis. This might be explained by a low quality of the RNA sample. Furthermore, it might be necessary to include additional AML and HSPC samples to observe significant differences.

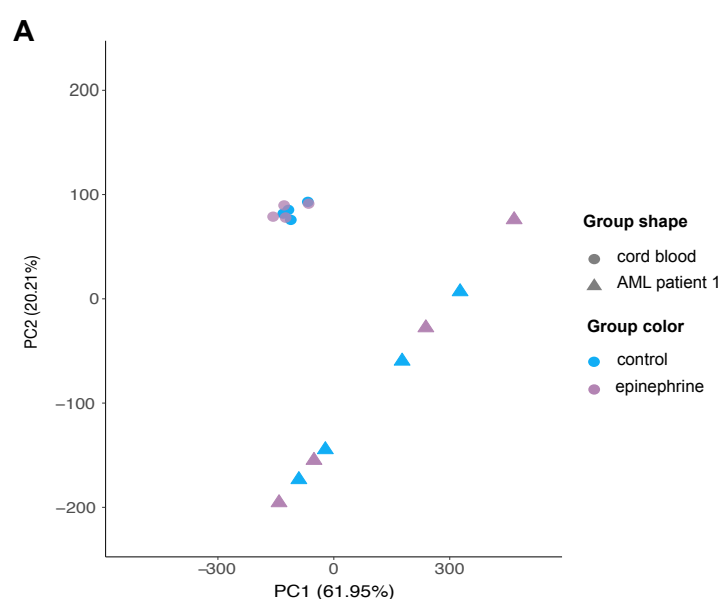


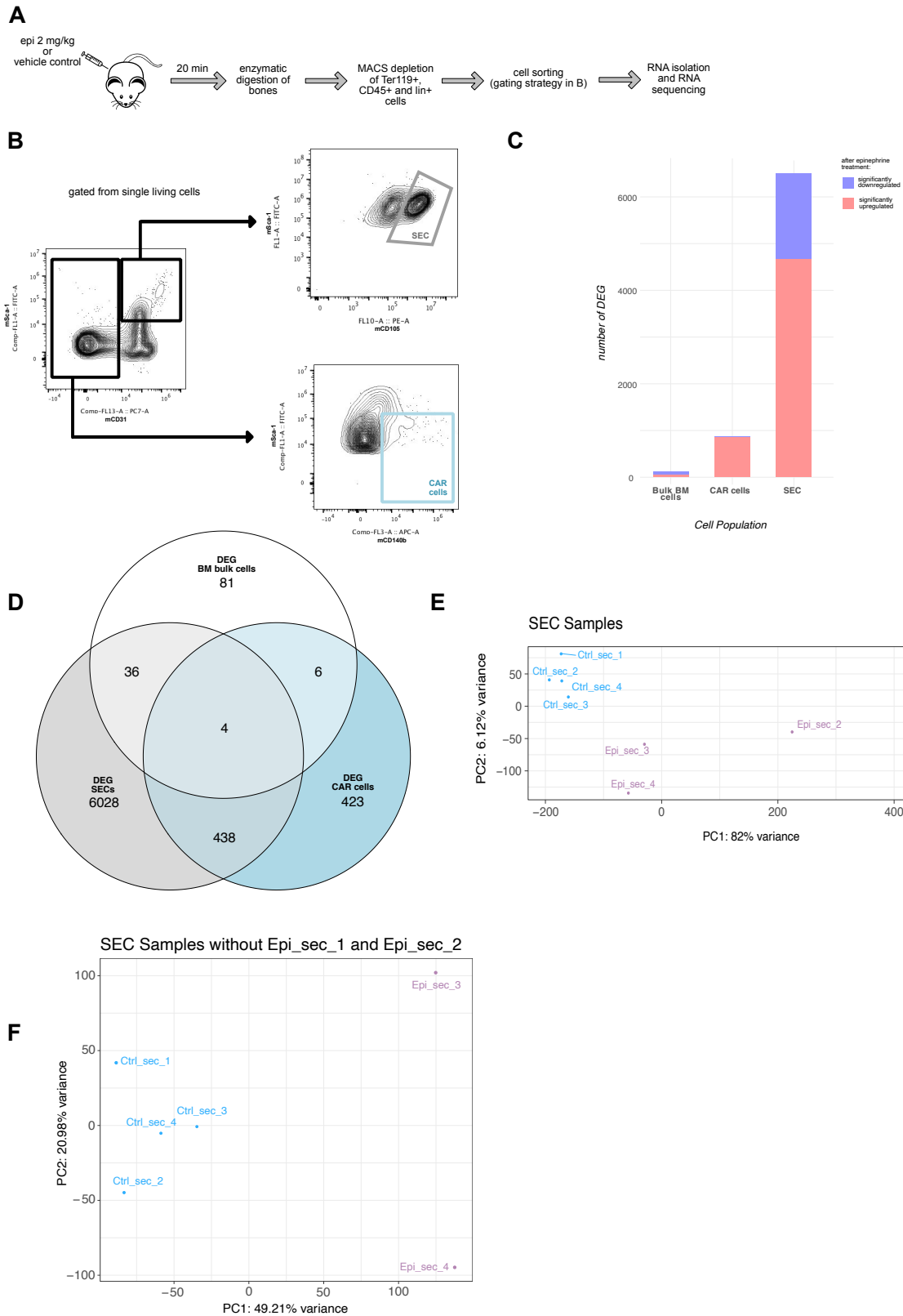
**Figure 16: Effect of EPI on the transcriptome of AML and HSPCs samples.**

**(A)** PCA of CB-derived HSPCs from one healthy donor (circles) and AML cells from patient #1 (triangle) after 24 hours of treatment with control (blue) or EPI (violet).

**1.1.7. EPI particularly influences endothelial cells within the BM microenvironment**

In regard to the very encouraging results obtained while studying the effect of EPI treatment on the transcriptome of mouse stromal cell line (1.1.5) we went one step further and used a more complex and realistic model. In fact, we isolated different types (CAR cells, SECs, AECs, and MSCs) of BM cells from mice treated for 20 minutes either with control or epinephrine solution (Figure 17A-B). Unfortunately, isolated AECs and MSCs could not be further analyzed because of the very low RNA quality and quantity. Of note, we also analyzed a mixture of BM cells (“bulk BM cells”) that did not undergo any FC sorting.

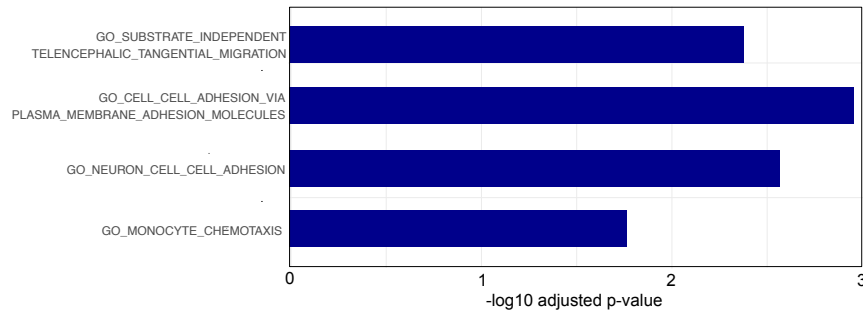
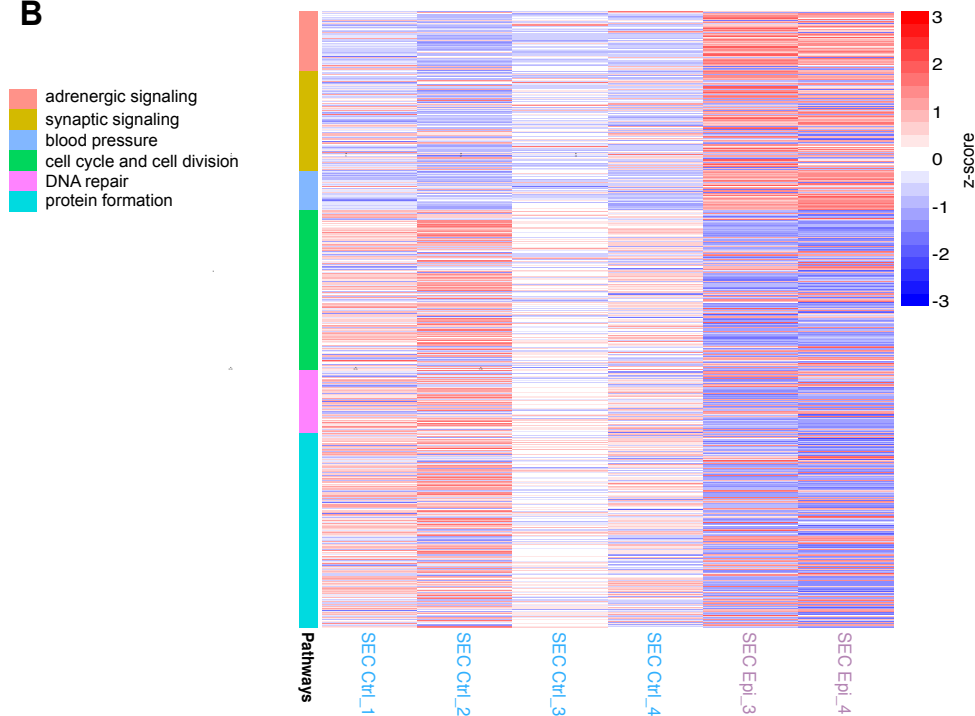
Very interestingly, the number of differentially expressed genes (DEG) between control and EPI samples was very low for the bulk BM cells (127 DEG) and the CAR cells (871 DEG), but reached 6508 DEG for SECs, thus indicating an effect of EPI mainly on these endothelial cells (Figure 17C-D). About half of the DEG for the CAR cells were also common to SECs (Figure 17D). According to these observations, we choose to focus on the effect of EPI on the transcriptome of endothelial cells, thus further analysis will only be shown for this cell type. Two SECs samples that were treated with EPI (Epi\_sec\_1 and Epi\_sec\_2) were of very low quality (about 200,000 versus 50 millions of reads) and were consequently taken out of the analysis. Of note, these samples were also outliers in the PCA (Figure 17E). Nevertheless, the new PCA generated without these two samples still indicated high variability between the remaining EPI samples (Figure 17F).



**Figure 17: Effect of EPI treatment on different types of primary murine BM cells.**

**(A)** Overview of the experimental procedure for the isolation of primary murine BM cells. More details about the protocol are given in the Material and Method section of this thesis. **(B)** Gating strategy for the isolation of CAR cells and SEC. In the first FC plot, cells were already gated on single living cells. Protocol and gating strategy were established with the help of Patrick Helblin (Uni, Ort, Land) and according to previously published work (Gomariz et al., 2018). **(C)** Number of differentially expressed genes (DEG) in each studied category of BM cells. In each group, upregulated genes are represented in red and downregulated genes in blue. **(D)** Venn diagram showing the number of common DEG between the different categories of BM cells. **(E)** PCA of isolated SEC samples after EPI (violet) or control (blue) treatment. All four samples of each group are used in this PCA. **(F)** PCA of isolated SEC samples after EPI (violet) or control (blue) treatment. In contrast to the plot in (E), two outlier samples were removed.

Similar to the analysis performed with MS-5 cells, we also looked at the effect of EPI on genes from pathways containing terms of interest linked to migration, adhesion and chemotaxis since we hypothesized an effect of EPI on the adhesion of AML to endothelial cells, thus favoring their migration into the BM. Unfortunately, we could find only four significantly upregulated pathways containing these terms (Figure 18A) and many downregulated pathways (data not shown). Globally, a vast majority of the DEG were related to pathways containing the following terms of interest: adrenergic signaling, synaptic signaling, blood pressure for the upregulated genes and cell cycle and cell division, DNA repair, and protein formation for the downregulated genes (Figure 18B). This is not surprising and confirms that EPI treatment indeed impacts gene expression in these mice, however, the effect on these pathways is very strong and could consequently shadow and dilute more finely regulated pathways, including those linked to adhesion, migration or chemotaxis.

**A****B**

**Figure 18: Differentially regulated pathways upon EPI treatment in SEC.**

**(A)** Barplot of the pathways significantly upregulated by EPI treatment amongst the pathways containing the following terms of interest: migration, adhesion or chemotaxis. Plotted are the negatives of the log10 of the adjusted (adj.) p-value. Significance was determined by applying a gene set enrichment analysis on our data and then by using a cutoff adj. p-value  $\leq 0.05$ . **(B)** Heatmap of the DEG between SEC samples treated with control (blue) or EPI (violet) of the pathways containing the most represented terms of interest. Genes related to the pathways were defined from the GO database. Row values are centered and scaled.

### 1.3. DISCUSSION

Circadian rhythm and the related adrenergic pathway activation have been widely studied in the context of healthy hematopoiesis and HSPC trafficking, including a central role played by nerve fibers inside the BM microenvironment.

However, knowledge about the adrenergic regulation of malignant hematopoietic cells is still very limited. A vast majority of patients suffering from leukemia experience particularly high stress phases (Levin et al., 2007; Rodin et al., 2013) leading to anxiety and depression that have been described to play a role in patient outcome (Prieto et al., 2005). Consequently, understanding the role of stress and adrenergic signaling in the context of AML will open new perspectives for the treatment of AML patients.

In this study, we took advantage of the xenotransplantation model of human AML to investigate the role of circadian rhythm and adrenergic signaling in different patient backgrounds. The current results indicate that primary AML samples have a faster and stronger course of disease when they were transplanted during the night phase - the activity phase for rodents. This is consistent with previous results reporting a higher engraftment rate when transplanting a human ALL cell line at night (He *et al.*, 2018). Interestingly, similar data were obtained in both studies even if the timepoint of night transplantation was significantly different (ZT (Zeitgeber) 21 in our work vs. ZT13), indicating a conserved effect for the night period. Moreover, we could also show that the effect of night transplantation was maintained in a syngeneic mouse model of MLL-PTD/FLT3-ITD AML, further reinforcing the conserved character of this observation. This model also confers the advantage that the recipient mice are wildtype animals and might provide a less artificial BM microenvironment and also the presence of immune cells.

On a molecular level, we were furthermore able to identify increased levels of stress hormones in the BM at the night timepoint of transplantation, which is consistent with previous findings (Cosentino et al., 2015; Maestroni *et al.*, 1998). We also showed expression of different types of AR mRNA in the AML samples used this work, with a predominance for members of the  $\alpha$ 1-AR subgroup and for  $\beta$ 2-AR, which is also consistent with previous findings (An et al., 2011). Moreover, due to the widely described adrenergic regulation of the BM microenvironment as well as our observation of high catecholamine levels in animals during night we stimulated the adrenergic pathway by treating mice with EPI at day, thus mimicking stress behavior.

As hypothesized, EPI stimulation accelerated leukemia induction and resulted in a higher disease burden only after a single dose of EPI one hour before transplantation. Since EPI has a very quick half-life in the plasma (Gu, 1999), further optimization of the treatment timepoint might lead to even more significant effects. Furthermore, it might be beneficial to analyze the effect of EPI treatment via repeated regular EPI injections in mice in which leukemia is already established, as it was shown in previous studies using solid cancer cells (Barbieri *et al.*, 2019).

Moreover, several epidemiologic studies have been pointing out a protective role of beta-blocker in the development of different types of cancers (Botteri *et al.*, 2013; Chang *et al.*, 2015; Choi *et al.*, 2014; Choy *et al.*, 2016; Grytli *et al.*, 2014; Hanns *et al.*, 2019; Melhem-Bertrandt *et al.*, 2011; Powe *et al.*, 2010). In line with this observation, we could show that treatment at night with propranolol, which is an unselective  $\beta_1/\beta_2$  blocker, decreases the AML burden and increases overall mouse survival. Propranolol is frequently used in common clinical practice, allowing easier translation of these findings to human patients. However, in order to better understand this mechanism, it might be interesting to selectively block different types of Ars in a next step, which would eventually allow identifying the precise signaling pathway that is linked to our phenotype as well as the cell types that are important for this regulation. Consistently, we were able to confirm all our findings in the syngeneic MLL-PTD/FLT3-ITD murine leukemia model thus strengthening the conclusions made from our xenotransplantation model and demonstrating the conserved phenotype of these observations. which emphasizes the importance of this study.

Healthy HSPCs as well as some leukocyte subsets are constantly trafficking between the BM microenvironment and the blood stream. As mentioned before, this process is highly regulated by circadian rhythms and catecholamine levels (He *et al.*, 2018; Méndez-Ferrer *et al.*, 2010a; Méndez-Ferrer *et al.*, 2008). A previous study has shown that homing processes of both AML and B-ALL cells are highly impacted by the timepoint of administration (Scheiermann *et al.*, 2012). Consistently, we could draw similar conclusions in our experimental settings, with higher homing rates at night as well as after EPI treatment in several AML patient samples. In accordance, propranolol treatment reduced both night and EPI-driven increased homing rates, indicating a high dependency of the homing of AML cells on adrenergic cues.



Among the molecules responsible for homing and migration of healthy and leukemic cells to the BM, the chemokine CXCL12 and its receptor CXCR4 are one of the major players. Importantly, increased expression of CXCR4 on AML cells has been correlated to poor prognosis in patients (Cho, 2017; Fiegl, 2009; Sison *et al.*, 2013; Tavor, 2004; Voermans, 2002) (Du *et al.*, 2019). Within the patients used in this work, all investigated patients contained CXCR4 expressing cells, but the proportions were highly heterogenous between patients. The CXCL12/CXCR4 axis is also known to be regulated by diurnal cues via changes in chemokine levels that have been shown to be higher at night in murine BM fluids (Méndez-Ferrer *et al.*, 2010a; Méndez-Ferrer *et al.*, 2008).

Here, we could furthermore show that the impact of CXCR4 blockade on the homing of AML cells is rather low, both in basal conditions and after EPI treatment, while the homing of healthy HSPCs appeared to be more sensitive to CXCL12/CXCR4 regulation. Notably, homing of CB-derived HSPCs was independent of both the timepoint of transplantation as well as adrenergic regulation.

It has previously been described in a preliminary work using human stem cells (Bonde *et al.*, 2005) that intrafemorally transplanted cells do not need the process of homing to reach the BM and reside in the injection site for up to 10 days post transplantation. Transplanting the mice at day and night time-points using IF injections instead of the IV method might thus be of particular interest to gain insight in the hypothesis of the role of an increased homing for the observed enhanced engraftment of mice transplanted at night.

In addition, in this work we also studied the variations of the CXCR4 ligand SDF-1 in our model. It was indeed shown before that circadian release of catecholamines in the BM leads to rhythmic *Sdf-1* downregulation in parallel of the expression of *Cxcr4* in HSCs that is also regulated by circadian cues (Lucas *et al.*, 2008; Méndez-Ferrer *et al.*, 2008). We could reproduce previously published results, i.e. an oscillatory pattern of *Sdf-1* mRNA in the BM reaching a nadir at light onset (Méndez-Ferrer *et al.*, 2010a), and increased *Sdf-1* mRNA levels at our precise time-point of night transplantation in comparison to the day time-point. Nevertheless, EPI treatment of the mice, that we thought would mimic the circadian release of catecholamines, did not affect *Sdf-1* levels. We only investigated two time-points (one and two hours) after EPI treatment and might have missed the downregulation of *Sdf-1* for this reason. Furthermore, it might also be interesting to investigate the levels of SDF-1 protein using an ELISA.

Even though we were able to reproduce the fluctuations in circulating progenitors that have been previously published (Méndez-Ferrer *et al.*, 2008), when comparing the total number of CFU-C at the precise day (5:00 pm, ZT10) and night (4:00 am, ZT21) time-points of transplantation, we could not observe any differences in the number of circulating progenitors. One explanation for these results might reside in the time-points we investigated. Indeed, the two time-points chosen (ZT10 and ZT21) in the previously published work (Méndez-Ferrer *et al.*, 2008) for comparing the numbers of CFU were “located” during the decreasing and the increasing phase of the peak in circulating progenitors and so no significant difference can be observed between these precise time-points (Méndez-Ferrer *et al.*, 2008). To conclude about the role of the circadian rhythm in the numbers of circulating HSPCs in the hypothesis of a competition of AML cells and HSPCs for free niches within the BM microenvironment, the choice of other time-points for transplantation, corresponding to the peak and nadir in number of CFUs (i.e. ZT5 and ZT14), would be more appropriate.

Very interestingly, we were able to note that disturbing the normal light/dark cycle by switching on the light for two hours during the dark phase (thus mimicking the night transplantation conditions) was enough to alter progenitor trafficking and *Sdf-1* mRNA levels. This is in line with previously published work indicating that mice subjected to continuous light as well as jet-lagged animals showed altered and arrhythmic patterns in circulating progenitors (Méndez-Ferrer *et al.*, 2008). This raises the question of the role of the two hours light switch during the night phase on the phenotype observed upon night transplantation of AML cells, and we hypothesize that the differences in engraftment and homing are not only linked to the classical differences between day and night physiology. To conclude about this question, an experimental design in which we would use night vision goggles to avoid switching on the light during the night transplantation procedure might be interesting.

Importantly, our work also indicates that the timepoint of transplantation of human HSPCs into NSG mice or murine lineage negative cells in C57BL/6NCrI mice, respectively, did not influence the engraftment and differentiation into hematopoietic compartments of respective recipient mice. HSPCs were isolated at the same timepoint of the day and were freshly thawed before each transplantation in order to analyze the effect of the microenvironment independent of the effect on hematopoietic cells. These experimental settings are to oppose with a previous study, that describe a difference depending on the timepoint of transplantation of murine lineage negative

BM cells (D'Hondt et al., 2004). Indeed, in their study, the authors isolated lineage negative BM cells before each transplantation and they hypothesized that the difference in engraftment was, at least partially, due to different composition of lineage negative cells between these two timepoints (D'Hondt *et al.*, 2004; Méndez-Ferrer *et al.*, 2010a). From our experiments, we however consequently conclude that the effect of circadian rhythm and catecholamine exposure that are supposedly driven by the BM microenvironment are specific to leukemia cells and do not affect their healthy counterparts. This is of particular interest, since it could facilitate the selective targeting of leukemic cells without affecting normal hematopoiesis.

During the multistep process of homing to the BM, transplanted cells migrate through the blood circulation to the BM where they have to interact with BM endothelial cells. Previous studies indicate that circulating HSPCs rely —among others— on VLA-4/VCAM-1 interactions to adhere firmly to endothelial cells and their ability to extravasate and migrate through the endothelial cell layer (Frenette et al., 1998; Peled, 2000; Petty, 2009; Rettig, 2012). We were particularly interested in studying this interaction in our experimental settings. On the one hand, both HSPCs and AML cells are known to express the VLA-4 integrin (Bae, 2015; Matsunaga, 2003; Vila, 1995), and on the other hand increased CXCL12 levels observed at night phase or under stress conditions have been described to trigger the VLA-4/VCAM-1 interaction (Peled, 2000). We could indeed confirm that both AML and CD34<sup>+</sup> HSPCs samples used in this work showed medium to high proportions of VLA-4 expressing cells. Furthermore, we showed that the affinity of VLA-4 to its receptors was increased upon EPI treatment of AML cells but not of healthy HSPCs. Consistently, VLA-4 blockade of leukemic cells could reduce EPI-driven enhanced homing, pointing out the importance of this integrin in our observed mechanism. Concerning the role of the second actor playing a role in the VLA-4/VCAM-1 interaction, we could not observe any impact of EPI treatment in the expression levels of *Vcam-1* mRNA in the murine BM.

We therefore conclude that the increased levels of CXCL12 observed at night phase and with EPI treatment, activate VLA-4 on CXCR4<sup>+</sup> AML cells, which in turn leads to increased affinity of this integrin molecule to VCAM-1, thus leading to an increase in homing to the BM and engraftment of AML cells. Nevertheless, the reason why EPI treatment in healthy HSPCs does not induce VLA-4 surface expression is still undeciphered. Furthermore, the *in vitro* VLA-4 affinity assay, in which CXCL12

secretion by the microenvironment is missing, suggests the possibility of additional mechanisms involved in the enhancement of VLA-4 affinity upon EPI treatment.

As further steps we study the numerous other molecules described in the context of AML cells homing. For example, VLA-4 does not only binds to VCAM-1 but also to the extracellular ligand fibronectin which is also expressed by many cell types in the BM and was described to play an important role in the migration and maintenance of HSPCs. (Frisch et al., 2008; Wirth et al., 2020) Furthermore, VLA-4 has been found to cooperate with CD44 for binding of HPSCs to fibronectin. (Avigdor *et al.*, 2004; Wirth *et al.*, 2020) Consequently, studying the expression of CD44 in our AML samples as well as investigating the effect of activating the adrenergic signaling pathway on the interaction of fibronectin with the integrin receptor VLA-4 and non-integrin receptor CD44 would be particularly interesting.

Besides adhesion to endothelial cells, the adhesion of transplanted cells to murine BM stromal cells might also play an important role in their homing and engraftment. In the *in vitro* adhesion assay that we used to test this hypothesis we could also observe an increased adhesion capacity of human AML cells, but not human HSPCs.

In line with the CFU assay, here we also investigated the possibility of a competition between HSPCs and AML cells for adhesion to the stroma. In fact, it has been shown that the spatial localization of primary AML cells is restricted to niche elements shared with their normal counterparts, and that normal HSPCs and AML cells compete for the same functional niche (Boyd et al., 2014; Glait-Santar et al., 2015). Competitive adhesion assays showed that no exclusive advantage for AML or HSPCs exists, since both cell types adhere when plated together on murine stromal cells. Moreover, the enhanced adhesion of AML cells observed upon EPI treatment was not accompanied by a decreased adhesion of HSPCs, indicating that the hypothesis of a competition in our settings is invalidated. Here we tested only the classical ratio of 2:1 between the number of hematopoietic cells over the MS-5 plated cells (Petit *et al.*, 2005). Alternatively, we might design the experiment to increase the ratio of hematopoietic cells and to define conditions that would be more appropriate to study competition.

Nevertheless, when drawing conclusions from the adhesion assays, it is important to keep in mind a few technical biases that we could identify. First of all, HSPCs consist in CD34 positive cells isolated from a CB-donor, which is to oppose to AML samples that have very variable proportions of CD34 expressing cells. This is also true for homing and transplantation for long-term experiments, in which CB-derived HSPCs

were used. Furthermore, HSPCs from different donors were used for each assay which brings high variability and could bias the comparisons. It would have been interesting to be able to compare the adhesion of HSPCs from the same CB-donor in classical and competitive adhesion assays, but we were limited by the very small quantity of biological material isolated from one single donor. Pooling CB samples from several donors could be a solution, but it would be necessary to investigate before if cells from one donor may inhibit the adhesion of the others. Furthermore, a simple adhesion assay using the MS-5 cell line to mimic the BM stroma is also a very simplified view of the very complex cellular BM stromal microenvironment including a variety of endothelial, mesenchymal and neural cells (Nombela-Arrieta and Isringhausen, 2016). Together, even though the *in vitro* adhesion assay performed in this study may serve as a preliminary and rapid study of adhesion, it might need optimization to draw more precise conclusions.

It would of course also be interesting to investigate cell migration and the influence of different treatments on the cells by e.g. using a Boyden chamber system. One could imagine designing different migration assays using MS-5 stromal cells (Sadeghi et al., 2020), but also endothelial cells such as HUVEC cells (Nareshkumar et al., 2018) or a BM endothelial cell line, for example BMEC-1 (Möhle et al., 1997). This could be of particular interest to study the CXCR4/CXCL12 chemotaxis pathway.

Even though the MS-5 cell line only offers a very simplified model, we studied the effect of EPI on the MS-5 transcriptome using RNA sequencing which gave encouraging results. We could indeed observe a significant upregulation of many genes involved in migration or chemotaxis.

Amongst these, Vegfa is upregulated in MS-5 after EPI treatment. This pro-angiogenic factor is expressed by many leukemia patients and leads to the induction of angiogenesis and reduction of apoptosis (Backhovens *et al.*, 1987). EPI and NOR were already described as increasing the synthesis of VEGF-A leading to blood vessels with abnormal high permeability and a consequent effect on seeding in bones (Chakroborty *et al.*, 2009; Mulcrone *et al.*, 2017). Moreover, we also found Ccl2 (C-C motif chemokine ligand 2) gene being upregulated after epinephrine treatment. The CCL2/CCR2 (C-C motif chemokine receptor 2) axis was described to be involved in AML cell transmigration, trafficking and proliferation (Macanas-Pirard et al., 2017). In addition, CCR2 expression has been found to be dependent of adrenergic signaling in the heart, leading to recruitment of leukocytes to the heart after acute injury (Grisanti

et al., 2016). In a similar way, this axis might be involved in an enhanced migration of AML cells into the BM upon activation of adrenergic signaling pathways, and it might be worth investigating more into that direction.

Interestingly, we also identified an upregulation of the expression of the osteopontin precursor (Spp1) gene. SPP-1 acts as a cytokine and is involved in enhancing the production of IFN $\gamma$  and IL-12. Furthermore, a correlation between levels of osteopontin in AML core BM biopsies and response to chemotherapy was observed (Treaba et al., 2020). Notably, next to VCMA-1, osteopontin is another ligand for VLA-4 integrin. An enhanced binding of VLA-4 (expressed on AML cells) to osteopontin upon EPI treatment could also participate to the observed mechanism and it would be particularly interesting to study this interaction more in details and to decipher how it conjugates or maybe substitutes the VLA-4/VCAM-1 interaction in our experimental settings.

We also observed up-regulation of several integrins after EPI treatment (Itgb2 and Itgb7), indicating a possible enhanced adhesion and corroborating the results of the adhesion assay. Importantly, the upregulation of these genes as well as all other differentially regulated genes after EPI treatment would have to be confirmed by molecular methods such as qRT-PCR or western blot analysis, before investigating their role in more complex assays.

To study the effect of EPI treatment on the transcriptome in more complex and realistic settings, we used bulk BM, CAR cells and SECs isolated from the BM of mice treated with EPI or the corresponding control. Interestingly, the effect of activating the adrenergic signaling predominantly affected endothelial cells. This is supporting our results from previously described experiments, in which we hypothesized an enhanced interaction of AML cells with the endothelial cell layer upon EPI treatment. The identified DEG in our RNA sequencing analysis mainly indicated genes linked to systemic effects of stress (i.e. adrenergic signaling activation, increase of blood pressure and downregulation of cell cycling processes and protein formation). We could not find a clear upregulation of genes linked to adhesion, migration or chemotaxis process as we would have hypothesized. This might be due to the predominance of the stress linked pathways, but could also be explained by the time point of analysis of our animals 20 minutes after treatment or the way the cells were prepared, as MACS and FC sorting steps are known to be highly stressful for some

cells. Other timepoints should be tested and it would be very interesting to be able to include AECs as well as MSCs, which we had to exclude because of very low quantity and bad quality of RNA in this study.

In conclusion, we have shown that transplanting animals in their active phase leads to faster and stronger AML induction in both xenograft and murine syngeneic leukemia models linked to higher stress molecule levels. Activating adrenergic pathways within the BM microenvironment provides an advantage for AML cells over their healthy counterparts. The critical step is certainly occurring very quickly after transplantation, since we already observe differences in the homing rates of AML cells upon night transplantation or EPI treatment, and might involve both CXCR12/CXCR4 and the VLA-4/VCAM-1 axis. Besides providing a tool to accelerate xenogeneic *in vivo* experiments, these findings open new perspectives both concerning new potential therapeutic agents as well as regarding the impact of stress in a patient's daily life. Further studies are required to gain insights into the precise molecular pathways that regulate the effect of adrenergic signaling and night transplantation in leukemia cells, especially in the light of stress as a process which involves a plethora of physiological responses as well as molecular players. Identifying specific molecules could enable its targeting with blocking agents and open new therapeutic perspectives.

## 5. MATERIALS AND METHODS

### 1.1. PRIMARY AML CELLS AND HEALTHY HSPCs

PB samples from AML patients or healthy donors were collected following informed consent (in accordance with the declaration of Helsinki) approval by the Ethics Review Board of the University Hospital of Basel and Tuebingen and enriched for PBMCs using density gradient centrifugation. Cells were viably frozen in RPMI1640 medium (Sigma-Aldrich, St. Louis, MO, USA) supplemented with 20% fetal calf serum (FCS; Sigma-Aldrich) and 10% dimethyl sulfoxide solution (DMSO; AppliChem, Darmstadt, Germany). For primary samples with blast counts <95%, the magnetic cell separation (MACS) technology was used for CD33 enrichment for samples expressing this surface marker or for depletion of CD19 and CD3. Post-MACS purities exceeded 95% blasts (not shown).

CB CD34<sup>+</sup> HSPCs were purified using the indirect CD34 microbead kit (Miltenyi, Bergisch-Gladbach, Germany) and frozen in FCS supplemented with 10% DMSO.

Before use, cells were thawed in warm RPMI1640 medium supplemented with 10% fetal calf serum and 1% penicillin/streptavidin (P/S, Sigma-Aldrich). CB CD34<sup>+</sup> HSPCs were let for sedimentation for 2 hours in a large quantity of medium (50ml) before centrifugation.

### 1.2. CELL LINES AND CELL CULTURE

AML cell lines (EOL-1, SKM-1, NOMO-1, DSMZ, Braunschweig, Germany) were cultured according to the provider's protocol in RPMI1640 medium supplemented with 10% FCS and 1% P/S.

MS-5 cells (DSMZ) were cultured according to the provider's protocol in alpha-MEM medium (Sigma-Aldrich) supplemented with 10% horse serum (Sigma-Aldrich), 1% P/S (Sigma-Aldrich), 2 mM L-glutamine (Sigma-Aldrich) and 2 mM sodium pyruvate (Sigma-Aldrich). Cells were seeded at  $1 \times 10^6$  cells/ 80 cm<sup>2</sup> and were split when the culture was around 80% confluent using trypsin/EDTA (Ethylenediamine tetraacetic acid, Sigma-Aldrich). Seeded cells were used at passage 12 and were used until maximum passage 25.



### 1.3. XENOTRANSPLANTATION ASSAYS

#### *Catecholamine Project*

NOD.Cg-Prkdc<sup>scid</sup> IL2rg<sup>tmWjl</sup>/Sz (also termed NOD/SCID/IL2R $\gamma$ <sup>null</sup>, NSG) mice were purchased from Jackson Laboratory (Bar Harbor, ME, USA) and bred in-house under pathogen-free conditions according to Swiss federal state regulations (Veterinäramt Basel-Stadt, 2697\_28218, 2697\_32264). Primary AML cells were always freshly thawed before transplantation experiments. Gender-matched 6-10 weeks old animals with or without prior sublethal irradiation were injected via the tail vein with  $1 \times 10^6$  primary AML cells or respectively  $5 \times 10^4$  EOL-1 cells resuspended in 200  $\mu$ L phosphate-buffered saline (PBS, Sigma-Aldrich). Of note, cells were thawed separately but treated equally for the day and the corresponding night experiment to not bias the experiment due to longer time prior to injection. Engraftment was assessed by signs of distress (e.g. decreased food and water consumption, rapid breathing, altered movement) (Jacobsen et al., 2012) or with routine (every 4 to 5 weeks) screening for leukemic cells via BM puncture or blood collection. Engraftment was defined as  $\geq 1\%$  leukemic cells in murine PB and BM (Eppert *et al.*, 2011; Lapidot, 1994). Mice were euthanized at signs of disease (weight loss, ruffled coat, reduced motility or other severe pathology) or detection of engraftment (Konantz *et al.*, 2013; Paczulla *et al.*, 2017; Sanchez *et al.*, 2009). Engraftment percentages in BM, PB, spleen and liver were determined upon final analyses using flow cytometric approaches. Samples were also kept for histopathology and next generation sequencing (NGS) analyses. For transplantation assays with human CD34<sup>+</sup> HSPCs, CB samples were freshly thawed before each experiment. Gender-matched, 6-10 weeks old NSG mice with prior sublethal irradiation were injected via the tail vein with  $1.5 \times 10^5$  CD34<sup>+</sup> cells resuspended in 200  $\mu$ L PBS. Blood was collected via the tail vein every two weeks, starting at 6 weeks post-transplantation and screened for the detection of human CD45 cells among murine cells. 30 weeks post-transplantation, mice were sacrificed and BM, spleen, liver and PB were analyzed. Limiting dilution assays were accomplished by transplanting  $0.5 \times 10^6$  and  $0.1 \times 10^6$  cells intravenously. Homing assays were performed as previously described (Paczulla *et al.*, 2017). In brief, purified AML blasts or human CB derived CD34<sup>+</sup> HSPCs were labeled with CFSE (CellTrace CFSE Cell Proliferation Kit, Invitrogen, Waltham, MA, USA) and

respectively  $1 \times 10^6$  or  $1.5 \times 10^5$  cells per mouse were injected via the tail vein in NSG mice without prior irradiation. 8-12 hours after transplantation mice were euthanized and BM, PB and spleen analyzed by FC recognizing CFSE.

#### *Homing project*

NSG mice were purchased from Jackson Laboratory and bred in-house under pathogen-free conditions according to Swiss federal state regulations (Veterinäramt Basel-Stadt, 2972\_30222). Primary AML cells were always freshly thawed before transplantation experiments. Female 6-10 weeks old animals with prior sublethal irradiation (225 cGy, 24 hours before transplantation) were anesthetized using a ketamin/ (65 mg/kg, Streuli pharma, Uznach, Switzerland) xylasin (13 mg/kg, Streuli pharma) mixture injected intraperitoneally, and the leg with the femur which will undergo transplantation was disinfected with povidone-iodine solution (Betadine, Mundipharma, Frankfurt, Germany). Once the mice were under suitable anesthesia, they were injected intrafemorally with  $5 \times 10^5$  primary AML cells resuspended in 30  $\mu$ L PBS, according to published protocols from our lab (Paczulla *et al.*, 2017; Paczulla *et al.*, 2019). Engraftment was assessed by signs of distress or with routine (week 16, week 26 and week 39) screening for leukemic cells via BM puncture. Mice were euthanized at signs of disease (weight loss, ruffled coat, reduced motility or other severe pathology) or detection of more than 80% of engraftment at the BMP (Konantz *et al.*, 2013; Paczulla *et al.*, 2017; Sanchez *et al.*, 2009). Engraftment percentages in BM, PB and spleen were determined upon final analyses using flow cytometric approaches. Samples were also kept for subsequent histopathology and NGS analyses. When a tumor was present, tumor cells were also analyzed by FC and a piece of the tumor was kept for histopathology. Homing assays were performed as previously described (Paczulla *et al.*, 2017). Purified AML blasts were labeled with CFSE and  $1 \times 10^6$  cells per mouse were injected via the tail vein in male NSG mice without prior irradiation. 16 hours after transplantation, mice were euthanized and BM and PB analyzed by FC recognizing CFSE.

#### 1.4. BONE MARROW PUNCTURE

Routine screening for human leukemic cells into the murine BM was performed via BMP, according to previously described protocols (Chung *et al.*, 2014).

Animals were anesthetized using ketamin/xylasin and leg disinfection as described above. Once the mice were under suitable anesthesia, a 27 G needle was inserted into the femur of the mice and carefully removed. The mice were held so that the leg would not move and an U-100 insulin-syringe (29 G, BD) filled with 30  $\mu$ L sterile PBS was inserted in the same hole. PBS was injected in the femur of the mice and then the needle plunger was gently pulled back to aspirate BM. The procedure permits to aspirate about 5  $\mu$ L of BM, corresponding to around  $0.4-0.8 \times 10^6$  mononuclear cells, that are then transferred into 500  $\mu$ L of PBS. Mice are returned to the housing area, ensuring that they are able to reach food and water, and were kept under particular observation for sign of distress or infection post procedure in the next 24 hours. The procedure was repeated in the opposite femur and mice are punctured for a maximum of three times during their lifespan.

## 1.5. SYNGENEIC MOUSE MODELS

C57BL/6NCrI mice were purchased from Jackson Laboratory and bred in-house under pathogen-free conditions according to Swiss federal state regulation (Veterinäramt Basel-Stadt, 2697\_32264). Splenocytes from a previously described murine leukemia model (MLL-PTD/FLT3-ITD) (Zorko et al., 2012) were used.  $5 \times 10^4$  splenocytes from MLL-PTD/FLT3-ITD mice were transplanted via the tail vein into sublethally irradiated C57BL/6 recipient mice. Mice were monitored for signs of distress as described above. Mice were again euthanized at first signs of disease. Spleen size and weight as well as blood counts (WBC, erythrocytes, hemoglobin and platelets) were determined upon final analysis using an Advia120 Hematology Analyzer using Multispecies version 5.9.0-MS software (Bayer, Leverkusen, Germany).

For the transplantation of murine lineage negative cells, tibias, femurs, hips and the spinal cord were collected from UBC-GFP (Jackson Laboratory) donor mice. These donor mice were euthanized and cells prepared and maintained viably frozen. Cells were then freshly thawed before each transplantation experiment in recipient mice. Lineage negative cells were isolated using the MACS Lineage Cell Depletion Kit for mouse (Miltenyi) according to the manufacturer's protocol. Gender-matched, 6-10 weeks old sublethally irradiated wild-type C57BL/6NCrI recipient animals were injected via tail vein with  $5 \times 10^5$  lineage negative donor cells resuspended in 200  $\mu$ L PBS. For monitoring, blood was collected via tail vein every two weeks, starting at 3

weeks post-transplantation and screened for green fluorescent protein (GFP) positive donor cells. 16 weeks post-transplantation, mice were sacrificed and BM, spleen, liver and PB were analyzed.

## 1.6. DAY/NIGHT TRANSPLANTATION SETTINGS

For the day/night experiments, “day” and “night” mice were transplanted at ZT10 (5 p.m. in our animal facility) and ZT21 (4 a.m.), respectively. “Night” mice were exposed to light one hour before and one hour after transplantation.

## 1.7. EPI AND PROPRANOLOL TREATMENT

Mice were treated intraperitoneally with EPI hydrochloride (2 mg/kg, 100  $\mu$ L in 0.9 M NaCl solution, Sigma-Aldrich) or respectively with propranolol hydrochloride (10 mg/kg, 100  $\mu$ L in 0.9 M NaCl solution, Sigma-Aldrich) one hour before transplantation (Im, 1998). Mice of the control groups were injected similarly with the vehicle solution.

## 1.8. CXCR4 AND VLA-4 BLOCKING

Cells were treated with anti-CXCR4 antibody (10  $\mu$ g/ml,  $1 \times 10^6$  cells/ml, clone 12G5, PharMingen, San Diego, CA, USA) for 45 minutes and were then used for transplantation without including any further wash step (Tavor, 2004). For blocking of CXCR4 using AMD3100 (Sigma-Aldrich), the inhibitor was incubated with the cells at a concentration of 50  $\mu$ M for one hour and was then washed away before transplantation. For VLA-4 blocking, an anti-CD49d antibody was used (clone HP2/1, Biorad, Hercules, CA, USA, 5  $\mu$ g/ml,  $1 \times 10^6$  cells/ml). Cells were incubated with the antibody in PBS for 30 minutes and were washed once prior to transplantation (Peled, 2000).

## 1.9. FLOW CYTOMETRY

*Human cells:* Fluorescence conjugates targeting human CD33, CD34, CD133, CD117, CD45, CD38 (BD Biosciences) and CD3, CD19 (Biolegend, San Diego, CA, USA) were used. For the analysis of human HSPCs transplanted in NSG mice,

fluorescent antibodies against human CD3, CD19, CD33, CD13, CD14, CD15, CD45 and murine CD45 (Biolegend) were used. Antibodies are listed in tables 6 and 7. For CXCR4 and VLA-4 surface expression analysis, anti-CXCR4 antibody (clone 12G5, 10 µg/ml, R&D Systems, Minneapolis, MN, USA) followed by a secondary staining step and a fluorescent antibody against VLA-4 (CD49d, clone ALC1/1, APC, 1 µl antibody per 10<sup>6</sup> cells, Dianova, Hamburg, Germany).

Surface Marker	Conjugate	Clone	Supplier
CD33	PE	WM53	BD Bioscience
CD34	PE	581	BD Bioscience
CD45	FITC	HI30	BD Bioscience
CD38	FITC	HIT2	BD Bioscience
CD34	FITC	581	BD Bioscience
CD34	APC	581	BD Bioscience
CD117	PECy7	104D2	Biolegend
CD133	PECy7	CLONE7	Biolegend
CD31	PECy7	WM59	Biolegend
CD33	APC	WM53	Biolegend
CD19	APC	4G7	Biolegend
CD3	APC	HIT3A	Biolegend

**Table 6: Human Antibodies**

*PE: Phycoerythrin; APC: Allophycocyanin; FITC: fluorescein isothiocyanate; PECy7: Phycoerythrin-Cyanine 7*

*Murine cells:* Fluorescent antibodies against murine CD3, CD19, CD11b, NK1.1, Ly6G, Ly6A/E (Sca-1) and CD117 (c-kit) (Biolegend) were used. Antibodies are listed in table 7.

Analyses were performed on either a BD LSR II Fortessa or Beckman Coulter Cytotflex device. DAPI (4',6-diamindino-2-phenylindole, Carl Roth, Karlsruhe, Germany), SytoxBlue (ThermoFischer, Waltham, MA, USA) or 7-aminoactinomycin D (7-AAD, ThermoFischer) were used to discriminate living and dead cells.

Surface Marker	Conjugate	Clone	Supplier
CD45	PE	30F11	Biolegend
CD45	PB	30F11	Biolegend
CD3	APC	17A2	Biolegend
CD3	FITC	17A2	Biolegend
CD19	APC	1D3/CD19	Biolegend
CD11b	AF700	M1/70	Biolegend
NK1.1	none	Not indicated	Invivomab
LY6G	BV510	1A8	Biolegend
LY6A/E	FITC	D7	Biolegend
LY6A/E	PECy7	D7	eBioscience
CD117	APC	2B8	eBioscience
CD45.1	APC	A20	Biolegend
CD45.2	BV605	104	Biolegend
CD45.2	PE	104	Biolegend
Lineage cocktail	PB		Biolegend
CD31	PECy7	MEC13.3	Biolegend
CD140b	APC	APB5	Biolegend
CD105	biotin	MJ7/18	Biolegend
Streptavidin	PerCP		Biolegend

**Table 7: Murine Antibodies**

*PE: Phycoerythrin; PB: Pacific Blue; APC: Allophycocyanin; FITC: fluorescein isothiocyanate; AF700: Alexa Fluor 700; PECy7: Phycoerythrin-Cyanine 7; BV605: Brilliant Violet 605; PerCP: Peridinin-Chlorophyll-protein*

## 1.10. HISTOPATHOLOGY

Histological studies (hematoxylin and eosin) and immunohistochemical analyses (human CD33; Ventana, Oro Valley, AZ, USA) were performed on formalin-fixed paraffin-embedded organs as described elsewhere (Kunder et al., 2007). Analysis

were performed by Stephan Dirnhofer (University Hospital Basel, Department of Pathology).

### 1.11. qRT-PCR

Total RNA was extracted using the Bioline RNA extraction kit (Isolate II RNA micro kit, Meridian bioscience (Bioline), Cincinnati, OH, USA). FIREScript RT cDNA synthesis kit (Solis Biodyne, Tartu, Estonia) was used to synthesize cDNA. Quantitative RT-PCR was performed using SYBR Green Reagent (Roche, Basel, Switzerland), and the analysis was performed on an ABI Prism 7500 sequence detection system. Primer efficiency was calculated via standard curves for each new primer. *GAPDH* and *PBGD* were used as housekeeping genes to normalize the Ct values, and relative gene expression was quantified using the  $2^{-(\Delta\Delta C_t)}$  method (Livak & Schmittgen...). Primers are listed in table 8.

Primer name	5'-3' sequence
$\alpha$ 1aAR fwd	GTCATGCCCATTTGGGTCTTTC
$\alpha$ 1aAR rev	TCTTGGCTGGAGCATGGGTA
$\alpha$ 1bAR fwd	CCACAACACATCAGCACCTG
$\alpha$ 1bAR rev	AGGCCACAGACAAGATGACTAG
$\alpha$ 1dAR fwd	TGCGCCTGCTCAAGTTCTC
$\alpha$ 1dAR rev	CGGGAACAAGGAGCCGAG
$\alpha$ 2aAR fwd	CCCCTTCACCTACACG
$\alpha$ 2aAR rev	AAACCTCACACGATCCGCTTC
$\alpha$ 2bAR fwd	ATCCCCGATCACTGGCATTTC
$\alpha$ 2bAR rev	AGGAAGACGGTGGTAAAC
$\alpha$ 2cAR fwd	TACTGGTACTTCGGGCAGGT
$\alpha$ 2cAR rev	GTGCGCTTCAGGTTGTA CTC
$\beta$ 1AR fwd	AGGAAAGTTTGGGAAGGGATGG
$\beta$ 1AR rev	CAGAGAGTGTCAAAAACACCTG
$\beta$ 2AR fwd	ATGCCAATGAGACCTGCTGT

β2AR rev	GCTCCACCTGGCTAAGGTTC
β3AR fwd	CCCCACCTTCCTGAAACTC
β3AR rev	AGCATGGAGGGGACAAATGC
RANK fwd	AGCACTCACAGGTATTGTGTCT
RANK rev	AGCAGATCACCATAGGCAGC
RANKL fwd	TGAAGCTCAGCCTTTTGCTC
RANK rev	TTCAGGCTGGATAGAG
VLA-4 fwd	GGATGAAACTCCTGACCAGA
VLA-4 rev	GGAACCACAGCTTCTTTTGG
CXCR4 fwd	AACCAGCGGTTACCATGGAG
CXCR4 rev	GGGCTGTCTAAGTTCAA
PBGD fwd	CGCATCTGGAGTTCAGGAGTA
PBGD rev	CCAGGATGATGGCACTGA
GAPDH fwd	ACCACAGTCCATGCCATCAC
GAPDH rev	TCCACCACCCTGTTGCTGTA

**Table 8: Human primers list**

*Rev: reverse; fwd: forward. Gene abbreviations were already defined previously in this work.*

Primer name	5'-3' sequence
Gapdh fwd	AGTGATGGCATGGACTGTGGTCAT
Gapdh rev	AATGCATCCTGCACCACCAACTGCTT
Pbgd fwd	TGGACCTAGTGAGTGTGTTGC
Pbgd rev	CTTCCTGGTTTCCCCACAAC
Sdf-1 fwd	GAGGAAGGCTGACATCCGTG
Sdf-1 rev	GCAAACCTTAGCATGACCCC
Vcam-1 fwd	ATCCGTAAGTCATGCCGTCC
Vcam-1 rev	AGATCCGGGGGAGATGTCAA

**Table 9: Murine primers list**

*Rev: reverse; fwd: forward. Gene abbreviations were already defined previously in this work.*



## Targeted NGS

NGS analysis was performed both on patient-derived AML cells and corresponding mouse-derived leukemic cells after day/night transplantation obtained by MACS purification of pooled BM samples from all engrafted animals transplanted with one AML patient.

DNA for NGS was isolated using the ZR-Duet DNA/RNA MiniPrep kit (ZymoResearch, Irvine, CA, USA) according to the manufacturer's protocol, and NGS analysis performed as previously described (Paczulla *et al.*, 2017). Patient NGS libraries were prepared using the AML community panel from Thermo Fisher containing 19 genes frequently mutated in AML (see [ampliseq.com](http://ampliseq.com)). Patient libraries were sequenced using the Ion PGM platform and analyzed using the Ion Reporter AML pipeline (version 5.0). The average coverage per sample was ~1.400-fold. Sensitivity for calling a mutation was set at 3%. If a mutation was observed in a "post-transplantation" sample but not reported to be present in the initial patient sample, the mapped reads were manually analyzed to assess whether the mutation was present but with a lower allelic burden than 3%. The sensitivity of such retrospective analysis is dependent on the coverage of the specific region (normally around 0.25%)

NGS experiments were performed by Pontus Lundberg (University Hospital Basel, Diagnostic Hematology).

### 1.12. ENZYME-LINKED IMMUNOSORBENT ASSAYS (ELISA)

BM fluids and plasma samples were collected from NSG mice at different time-points of day and night. For catecholamine ELISAs, samples were stored in 1 mM EDTA and 4 mM sodium metabisulfite to avoid catecholamine degradation.

Catecholamine and corticosterone ELISAs were performed using LND 2-CAT (A-N) Research ELISA (LDN, Nordhorn, Germany) and respectively the Corticosterone ELISA kit (Abcam, Cambridge, United Kingdom) according to the respective manufacturer's protocol.

Absorbance was read using a Synergy HI microplate reader (Biotek Instruments, Winooski, VT, USA) set to 450 nm and with a reference wavelength of 620 nm.

### 1.13. VLA-4 AFFINITY ASSAY

An *in vitro* FC assay was used to explore the affinity of VLA-4 to AML samples and healthy HSPCs. The assay was performed as described elsewhere (Avemaria, 2017). In brief, primary AML samples or HSPCs were freshly thawed and then incubated with LDV tripeptide conjugated to FITC fluorochrome (LDV-FITC, R&D Systems) in medium containing 1 mM CaCl<sub>2</sub>, 1 mM MgCl<sub>2</sub>, 20 mM 4-(2-hydroxyethyl)-1-piperazineethanesulfonic acid (HEPES) containing 1% bovine serum albumin (BSA) for 30 min at 37°C. After incubation, cells were fixed in 4% paraformaldehyde (PFA) solution and washed several times before samples were analyzed via FC on a Beckman Coulter Cytoflex device. LDV binding to AML cells or healthy HSPCs was determined according to the intensity of the FITC fluorochrome.

### 1.14. ADHESION ASSAY

1.5x10<sup>5</sup> MS-5 cells were plated per well in gelatin-coated 24-well plates. After 24 hours of incubation at 37°C, 5%CO<sub>2</sub>, leukemic cells or CB-derived CD34<sup>+</sup> HSPCs were stained with CFSE and 3x10<sup>5</sup> labeled cells were plated per well onto MS-5 cells. After 90 minutes of incubation at 37°C, 5%CO<sub>2</sub>, non-attached cells were removed and adherent cells were dissociated with trypsin-EDTA (Sigma-Aldrich). The percentage of adhered leukemic cells was determined using CFSE-recognizing FC.

Cells were treated with 10 μM EPI hydrochloride or with the respective control solution for 90 min either separately before they were co-incubated or during the co-incubation step.

For competitive adhesion assay, 7.5x10<sup>4</sup> CFSE stained HSPCs and 7.5x10<sup>4</sup> AML cells stained with CellTracker Blue 7-amino-4-chloromethylcoumarin (CMAC) dye (ThermoFischer) according to manufacturer's protocol, were added to the MS-5 cell layer. The assay was performed as described before.

### 1.15. CFU ASSAY FROM MURINE PB

8-12 weeks old NSG mice were sacrificed at the indicated time-point or after the indicated treatment. At least three mice were used for each investigated condition. PB was harvested in sterile conditions by heart puncture. The blood sample was diluted

at a 1:1 ratio with a PBS (Sigma-Aldrich) + 10% FCS (Sigma-Aldrich) + 1% EDTA (Carl Roth) solution. PBMCs were isolated using density gradient centrifugation. Erythrocytes were removed by adding red blood cell lysis buffer (155 mM ammoniumchloride, Carl Roth; 12 mM potassiumhydrogenocarbonate, Carl Roth; 0.1 mM EDTA, Carl Roth).  $2.5 \times 10^5$  cells were plated per well onto 1 mL of ready methylcellulose medium including cytokines (Methocult M3134, StemCell Technology, Vancouver, Canada) in a 12-well cell culture plate, in 2 to 3 replicates per analyzed animal. Plates were incubated 12 to 14 days at 37°C, 5% CO<sub>2</sub> before counting the number of grown colonies using an inverted microscope.

## 1.16. RNA SEQUENCING

### *MS-5 stromal cells*

$6.75 \times 10^5$  MS-5 cells were plated per well in 6-wells plates. After 24 hours of incubation at 37°C, 5%CO<sub>2</sub>, cells were treated with 10 µM epinephrine hydrochloride or in PBS control for 24 hours. Total RNA was extracted from these cells (RNA isolation Biotek kit). The quality and quantity of RNA was verified using the RNA 6000 Pico Assay Chip (Agilent Technologies, Santa Clara, CA, USA) following the manufacturer's protocol and with the help of Philippe Demougin from the "Life Sciences Training Facility in Basel.

cDNA libraries were generated with 10 ng of total RNA using the SMARTer Ultra Low RNA kit for Illumina sequencing (Clontech Laboratories, Mountain View, CA, USA) and sequenced with a NovaSeq 6000 S1 system (Illumina, San Diego, CA, USA).

### *Primary AML cells and CB derived CD34+ HSPCs*

$1 \times 10^6$  primary AML cells from one patient (patient 1) and  $6 \times 10^5$  CB-derived HSPCs were incubated in 4 technical replicates for 24 hours with 10 µM epinephrine hydrochloride or in PBS control. Total RNA was extracted from these cells (PicoPure RNA isolation kit, ThermoFischer). The quality and quantity of RNA was verified as described above. cDNA libraries were again generated with 10 ng of total RNA using the SMARTer Ultra Low RNA kit for Illumina sequencing (Clontech Laboratories) and sequenced with the NovaSeq 6000 S1 system (Illumina).

### *Primary murine BM cells*

8-12 weeks old NSG mice were treated with 2 mg/kg epinephrine hydrochloride or control solution for 20 minutes during the day (4 animals per group). Isolation of BM cells was performed as previously described (Gomariz *et al.*, 2018). In brief, BM was flushed out of tibia and femurs from sacrificed animals and the remaining structure was cut into small fragments and digested with 0.04 g/mL collagenase type 2 (Sigma-Aldrich) in a PBS + 10% FCS + 1% EDTA mixture to which 0.02 mg/mL DNase (Sigma-Aldrich) was added. After filtering of the resulting cell suspension with a 70 µm cell strainer, lineage, CD45 and Ter119 positive cells were depleted using MACS technology. Sorting of AECs, SECs and CAR cells (see gating strategy figure ....) was performed on a FACS Aria III (BD Biosciences) and cells were sorted directly into RLT lysis buffer.  $3 \times 10^5$  bulk BM cells, that did not undergo the sorting process were also used for the analysis. Because of the very few cell numbers obtained from the sorting, RNA extraction was performed with the PicoPure RNA isolation kit (ThermoFischer). The quality and quantity of RNA was verified as described before. Quantity and quality were too low for isolated AECs and were therefore not sent for RNA sequencing. For AECs, SECs, CAR cells and bulk BM samples, cDNA libraries were generated with 2 ng of total RNA using the SMARTer Ultra Low RNA kit for Illumina sequencing (Clontech Laboratories) and sequenced with the NovaSeq 6000 SP system (Illumina).

### *RNA sequencing results analysis*

Paired-end raw Fastq files were trimmed by using the following settings: HEADCROP:3 TRAILING:10 MINLEN:25 for Trimmomatic v2.38, to remove adapter content and bad quality reads. Trimmed fastqs were mapped to the human GRCH37 genome assembly using STAR v2.6.0 (Dobin *et al.*, 2013) using the following settings: --outFilterType BySJout --outFilterMultimapNmax 10 --alignSJoverhangMin 8 --alignSJDBoverhangMin 1 --outFilterMismatchNmax 999 --outFilterMismatchNoverLmax 0.05 --alignIntronMin 20 --alignIntronMax 1000000 --alignMatesGapMax 1000000 --outFilterMatchNmin 16 --quantMode GeneCounts --runThreadN 12. Genes quantified in at least 75% of total samples were kept. DEGs were determined using the R/Bioconductor (Gentleman *et al.*, 2004; Team., 2008) package limma (Ritchie *et al.*, 2015). Genes were considered as significantly regulated with an adjusted p-value threshold at 0.05 (Benjamini-Hochberg method).

For gene set enrichment analysis, the package GAGE (Luo et al., 2009) was used to retrieve from the genes the enriched terms and pathways from the Gene Ontology collection (biological process) (Subramanian et al., 2005) obtained from MSigDB v 7.0. Significance threshold was set to adjusted p-value below 0.05.

### 1.17. STATISTICAL ANALYSIS

Gaussian normality distribution was tested with the help of the Shapiro-Wilk-test. P-values are derived from the application of a two-tailed student t-test, a Mann-Whitney U test, a Welch-test, a ratio paired t-test, linear regression or a Log-Rank test as indicated in the respective figure legends.

Statistical analysis was performed with Prism 7, version 7.0d (GraphPad Software, San Diego, CA, USA).

## 6. CONTRIBUTION TO PUBLICATIONS

### 1.1. STRESS AND CATECHOLAMINE MODULATE THE BONE MARROW MICROENVIRONMENT TO PROMOTE TUMORIGENESIS

Hanns P, Paczulla AM, Medinger M, Konantz M, Lengerke C.

Stress and catecholamines modulate the bone marrow microenvironment to promote tumorigenesis.

Cell Stress. 2019 Jun 4;3(7):221-235. doi: 10.15698/cst2019.07.192. PMID: 31338489; PMCID: PMC6612892.

#### **Abstract**

High vascularization and locally secreted factors make the bone marrow (BM) microenvironment particularly hospitable for tumor cells and bones to a preferred metastatic site for disseminated cancer cells of different origins. Cancer cell homing and proliferation in the BM are amongst other regulated by complex interactions with BM niche cells (e.g. osteoblasts, endothelial cells and mesenchymal stromal cells (MSCs)), resident hematopoietic stem and progenitor cells (HSPCs) and pro-angiogenic cytokines leading to enhanced BM microvessel densities during malignant progression. Stress and catecholamine neurotransmitters released in response to activation of the sympathetic nervous system (SNS) reportedly modulate various BM cells and may thereby influence cancer progression. Here we review the role of catecholamines during tumorigenesis with particular focus on pro-tumorigenic effects mediated by the BM niche.

#### **Contribution**

In this manuscript, Claudia Lengerke (CL) and Pauline Hanns (PH) conceived and organized the review. PH did all the literature research and wrote the manuscript with the help of all co-authors. Furthermore, PH conceived and drew the illustrations.

## 1.2. ABSENCE OF NKG2D LIGANDS DEFINES LEUKAEMIA STEM CELLS AND MEDIATES THEIR IMMUNE EVASION

Paczulla AM, Rothfelder K, Raffel S, Konantz M, Steinbacher J, Wang H, Tandler C, Mbarga M, Schaefer T, Falcone M, Nievergall E, Dörfel D, Hanns P, Passweg JR, Lutz C, Schwaller J, Zeiser R, Blazar BR, Caligiuri MA, Dirnhofer S, Lundberg P, Kanz L, Quintanilla-Martinez L, Steinle A, Trumpp A, Salih HR, Lengerke C.

Absence of NKG2D ligands defines leukaemia stem cells and mediates their immune evasion.

Nature. 2019 Aug;572(7768):254-259. doi: 10.1038/s41586-019-1410-1. Epub 2019 Jul 17. Erratum in: Nature. 2019 Aug 1;: PMID: 31316209; PMCID: PMC6934414.

### **Abstract**

Patients with acute myeloid leukaemia (AML) often achieve remission after therapy, but subsequently die of relapse<sup>1</sup> that is driven by chemotherapy-resistant leukaemic stem cells (LSCs)<sup>2,3</sup>. LSCs are defined by their capacity to initiate leukaemia in immunocompromised mice<sup>4</sup>. However, this precludes analyses of their interaction with lymphocytes as components of anti-tumour immunity<sup>5</sup>, which LSCs must escape to induce cancer. Here we demonstrate that stemness and immune evasion are closely intertwined in AML. Using xenografts of human AML as well as syngeneic mouse models of leukaemia, we show that ligands of the danger detector NKG2D—a critical mediator of anti-tumour immunity by cytotoxic lymphocytes, such as NK cells<sup>6-9</sup>—are generally expressed on bulk AML cells but not on LSCs. AML cells with LSC properties can be isolated by their lack of expression of NKG2D ligands (NKG2DLs) in both CD34-expressing and non-CD34-expressing cases of AML. AML cells that express NKG2DLs are cleared by NK cells, whereas NKG2DL-negative leukaemic cells isolated from the same individual escape cell killing by NK cells. These NKG2DL-negative AML cells show an immature morphology, display molecular and functional stemness characteristics, and can initiate serially re-transplantable leukaemia and survive chemotherapy in patient-derived xenotransplant models. Mechanistically, poly-ADP-ribose polymerase 1 (PARP1) represses expression of NKG2DLs. Genetic or pharmacologic inhibition of PARP1 induces NKG2DLs on the LSC surface but not

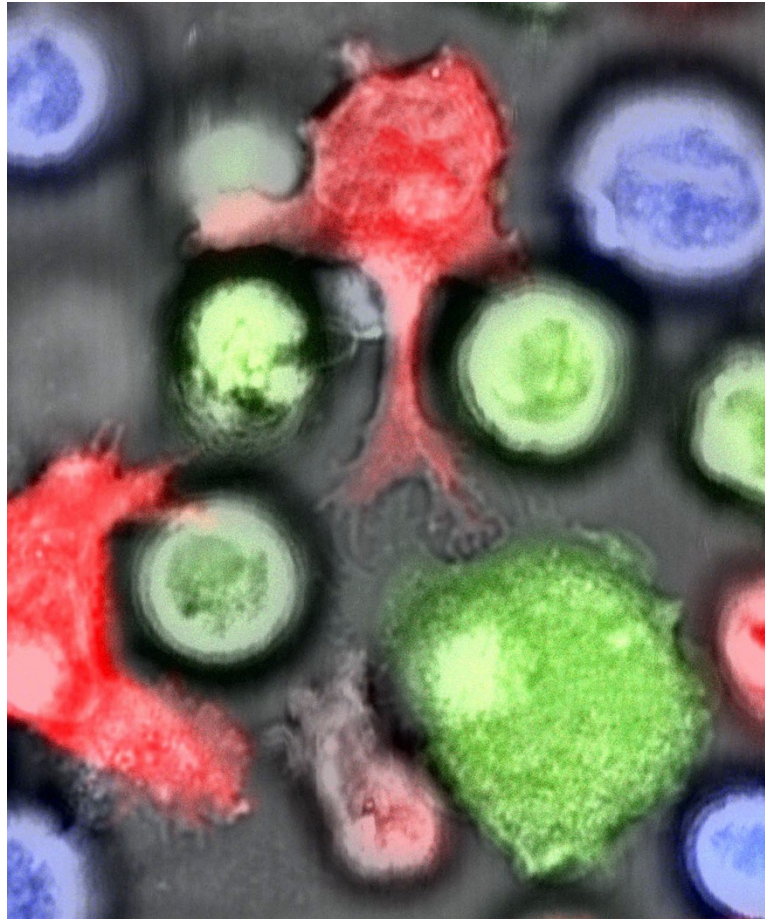
on healthy or pre-leukaemic cells. Treatment with PARP1 inhibitors, followed by transfer of polyclonal NK cells, suppresses leukaemogenesis in patient-derived xenotransplant models. In summary, our data link the LSC concept to immune escape and provide a strong rationale for targeting therapy-resistant LSCs by PARP1 inhibition, which renders them amenable to control by NK cells *in vivo*.

## **Contribution**

In this publication PH helped Anna M. Paczulla (AMP) with the *in vivo* AML transplantation procedures (that also served as training for PH for future transplantation methods) and was also involved in the final analysis of murine recipients of both the xenotransplantation assays and the murine syngeneic transplantations together with AMP and Marcelle Mbarga (MM). PH reviewed the manuscript and the figures during the revision process.

PH also performed the *in vitro* cell culture experiment of co-incubation of both CD34+ and CD34- AML cells with NK cells for the illustration of this publication (see picture below). Christoph Schürch (CS) performed the microscopy work, took the picture and worked on the image.





*Primary AML cells were separated into CD34+ and CD34- cells using magnetic cell sorting (MACS). NK cells from a healthy donor were cultured for three days and CD56+ cells were isolated again using MACS. CD34+ leukemic stem cells were stained with blue cell tracker dye (blue), CD34- leukemic cells with CFSE (green) and NK cells with calcein-APC (red) dye. Cells were mixed in a 1:4 ratio (leukemic cells:NK cells), plated onto poly-L-lysine coated slides and incubated for 3 hours at 37°C, 5% CO<sub>2</sub>. Imaging was performed using an SP5-II-MATRIX fluorescent confocal microscope (Leica Microsystems, 63X Objective).*

### 1.3. MODELING HEMATOPOIETIC DISORDERS IN ZEBRAFISH.

Konantz M, Schürch C, Hanns P, Müller JS, Sauter L, Lengerke C.

Modeling hematopoietic disorders in zebrafish.

Dis Model Mech. 2019 Sep;6;12(9):dmm040360. doi: 10.1242/dmm.040360. PMID: 31519693; PMCID: PMC6765189.

## **Abstract**

Zebrafish offer a powerful vertebrate model for studies of development and disease. The major advantages of this model include the possibilities of conducting reverse and forward genetic screens and of observing cellular processes by *in vivo* imaging of single cells. Moreover, pathways regulating blood development are highly conserved between zebrafish and mammals, and several discoveries made in fish were later translated to murine and human models. This review and accompanying poster provide an overview of zebrafish hematopoiesis and discuss the existing zebrafish models of blood disorders, such as myeloid and lymphoid malignancies, bone marrow failure syndromes and immunodeficiencies, with a focus on how these models were generated and how they can be applied for translational research.

## **Contribution**

In this review, PH summed up the zebrafish models for hematopoietic disorders to draw table 1. PH reviewed the manuscript and helped Martina Konantz (MK) with the poster.

### **1.4. ACUTE MYELOID LEUKEMIA STEM CELLS: THE CHALLENGES OF PHENOTYPIC HETEROGENEITY**

Arnone M, Konantz M, Hanns P, Paczulla Stanger AM, Bertels S, Godavarthy PS, Christopeit M, Lengerke C.

Acute Myeloid Leukemia Stem Cells: The Challenges of Phenotypic Heterogeneity. *Cancers (Basel)*. 2020 Dec 12;12(12):3742. doi: 10.3390/cancers12123742. PMID: 33322769; PMCID: PMC7764578.

## **Abstract**

Patients suffering from acute myeloid leukemia (AML) show highly heterogeneous clinical outcomes. Next to variabilities in patient-specific parameters influencing treatment decisions and outcome, this is due to differences in AML biology. In fact,

different genetic drivers may transform variable cells of origin and co-exist with additional genetic lesions (e.g., as observed in clonal hematopoiesis) in a variety of leukemic (sub)clones. Moreover, AML cells are hierarchically organized and contain subpopulations of more immature cells called leukemic stem cells (LSC), which on the cellular level constitute the driver of the disease and may evolve during therapy. This genetic and hierarchical complexity results in a pronounced phenotypic variability, which is observed among AML cells of different patients as well as among the leukemic blasts of individual patients, at diagnosis and during the course of the disease. Here, we review the current knowledge on the heterogeneous landscape of AML surface markers with particular focus on those identifying LSC, and discuss why identification and targeting of this important cellular subpopulation in AML remains challenging.

## **Contribution**

In this review, I helped Marlon Arnone (MA), MK and Sarah Bertels (SB) with figure conceptions, and reviewed and discussed critical aspects of the manuscript with MA.

### **1.5. SRP54 MUTATIONS INDUCE CONGENITAL NEUTROPENIA VIA DOMINANT-NEGATIVE EFFECTS ON XBP1 SPLICING**

Schürch C, Schaefer T, Müller JS, Hanns P, Arnone M, Dumlin A, Schärer J, Sinning I, Wild K, Skokowa J, Welte K, Carapito R, Bahram S, Konantz M, Lengerke C.

SRP54 mutations induce congenital neutropenia via dominant-negative effects on XBP1 splicing.

Blood. 2021 Mar 11;137(10):1340-1352. doi: 10.1182/blood.2020008115. PMID: 33227812; PMCID: PMC7994924.

#### **Abstract:**

Heterozygous de novo missense variants of SRP54 were recently identified in patients with congenital neutropenia (CN) who display symptoms that overlap with Shwachman-Diamond syndrome (SDS). Here, we investigate *srp54* knockout

zebrafish as the first in vivo model of SRP54 deficiency. *srp54*<sup>-/-</sup> zebrafish experience embryonic lethality and display multisystemic developmental defects along with severe neutropenia. In contrast, *srp54*<sup>+/-</sup> zebrafish are viable, fertile, and show only mild neutropenia. Interestingly, injection of human SRP54 messenger RNAs (mRNAs) that carry mutations observed in patients (T115A, T117Δ, and G226E) aggravated neutropenia and induced pancreatic defects in *srp54*<sup>+/-</sup> fish, mimicking the corresponding human clinical phenotypes. These data suggest that the various phenotypes observed in patients may be a result of mutation-specific dominant-negative effects on the functionality of the residual wild-type SRP54 protein. Overexpression of mutated SRP54 also consistently induced neutropenia in wild-type fish and impaired the granulocytic maturation of human promyelocytic HL-60 cells and healthy cord blood-derived CD34<sup>+</sup> hematopoietic stem and progenitor cells. Mechanistically, *srp54*-mutant fish and human cells show impaired unconventional splicing of the transcription factor X-box binding protein 1 (Xbp1). Moreover, *xbp1* morphants recapitulate phenotypes observed in *srp54* deficiency and, importantly, injection of spliced, but not unspliced, *xbp1* mRNA rescues neutropenia in *srp54*<sup>+/-</sup> zebrafish. Together, these data indicate that SRP54 is critical for the development of various tissues, with neutrophils reacting most sensitively to the loss of SRP54. The heterogenic phenotypes observed in patients that range from mild CN to SDS-like disease may be the result of different dominant-negative effects of mutated SRP54 proteins on downstream XBP1 splicing, which represents a potential therapeutic target.

## **Contribution**

In this publication, PH helped CS to perform some of the zebrafish experiments (set up of breedings and *in situ* hybridization experiments), isolated some of the cord-blood derived CD34<sup>+</sup> HSPCs samples and participated to the counting of neutrophils on zebrafish *in situ* hybridization images.



# REFERENCES

- Abarrategi, A., Mian, S.A., Passaro, D., Rouault-Pierre, K., Grey, W., and Bonnet, D. (2018). Modeling the human bone marrow niche in mice: From host bone marrow engraftment to bioengineering approaches. *J Exp Med* 215, 729-743. 10.1084/jem.20172139.
- Aberger, F., Hutterer, E., Sternberg, C., Del Burgo, P.J., and Hartmann, T.N. (2017). Acute myeloid leukemia - strategies and challenges for targeting oncogenic Hedgehog/GLI signaling. *Cell Commun Signal* 15, 8. 10.1186/s12964-017-0163-4.
- Agliano, A., Martin-Padura, I., Mancuso, P., Marighetti, P., Rabascio, C., Pruneri, G., Shultz, L.D., and Bertolini, F. (2008). Human acute leukemia cells injected in NOD/LtSz-scid/IL-2Rgamma null mice generate a faster and more efficient disease compared to other NOD/scid-related strains. *Int J Cancer* 123, 2222-2227. 10.1002/ijc.23772.
- Ailles, L.E., Gerhard, B., Kawagoe, H., and Hogge, D.E. (1999). Growth characteristics of acute myelogenous leukemia progenitors that initiate malignant hematopoiesis in nonobese diabetic/severe combined immunodeficient mice. *Blood* 94, 1761-1772.
- Aiuti, A.W.I.J., ; Bleul, C.; Springer, T.; Gutierrez-Ramos, J.C, (1997). The chemokine SDF-1 is a chemoattractant for human CD34+ hematopoietic progenitor cells and provides a new mechanism to explain the mobilization of CD34+ progenitors to peripheral blood. *J Exp Med* 185, 111-120. 10.1084/jem.185.1.111.
- Almosailekh, M., and Schwaller, J. (2019). Murine Models of Acute Myeloid Leukaemia. *Int J Mol Sci* 20. 10.3390/ijms20020453.
- An, N., Im, Y.-B., Qudeimat, A.A.M.D., Costa, L.J., Stuart, R.K., and Kang, Y. (2011). Regulation and Functional Role of Beta2-Adrenergic Receptor in Acute Myelogenous Leukemia.
- Arber, D.A., Orazi, A., Hasserjian, R., Thiele, J., Borowitz, M.J., Le Beau, M.M., Bloomfield, C.D., Cazzola, M., and Vardiman, J.W. (2016). The 2016 revision to the

World Health Organization classification of myeloid neoplasms and acute leukemia. *Blood* 127, 2391-2405. 10.1182/blood-2016-03-643544.

Ariëns, E.J., and Simonis, A.M. (1983). Physiological and pharmacological aspects of adrenergic receptor classification. *Biochemical Pharmacology* 32, 1539-1545. doi:10.1016/0006-2952(83)90324-6.

Arnone, M., Konantz, M., Hanns, P., Paczulla Stanger, A.M., Bertels, S., Godavarthy, P.S., Christopeit, M., and Lengerke, C. (2020). Acute Myeloid Leukemia Stem Cells: The Challenges of Phenotypic Heterogeneity. *Cancers (Basel)* 12. 10.3390/cancers12123742.

Arranz, L., Sánchez-Aguilera, A., Martín-Pérez, D., Isern, J., Langa, X., Tzankov, A., Lundberg, P., Muntión, S., Tzeng, Y.-S., Lai, D.-M., et al. (2014). Neuropathy of haematopoietic stem cell niche is essential for myeloproliferative neoplasms. *Nature* 512, 78. doi:10.1038/nature13383.

Asada, N. (2018). Regulation of Malignant Hematopoiesis by Bone Marrow Microenvironment | Oncology. *Frontiers in Oncology*. doi:10.3389/fonc.2018.00119.

Asada, N., Kunisaki, Y., Pierce, H., Wang, Z., Fernandez, N.F., Birbrair, A., Ma'ayan, A., and Frenette, P.S. (2017a). Differential cytokine contributions of perivascular haematopoietic stem cell niches. *Nat Cell Biol* 19, 214-223. 10.1038/ncb3475.

Asada, N., Takeishi, S., and Frenette, P.S. (2017b). Complexity of bone marrow hematopoietic stem cell niche. *International Journal of Hematology* 106, 45-54. doi: 10.1007/s12185-017-2262-9.

Asri, A., Sabour, J., Atashi, A., and Soleimani, M. (2016). Homing in hematopoietic stem cells: focus on regulatory role of CXCR7 on SDF1a/CXCR4 axis. In *EXCLI J*, pp. 134-143. doi: 10.17179/excli2014-585.

Avemaria, F.G.-C., S.; Avci, S; Lapidot, T. (2017). VLA-4 affinity assay for murine bone marrow-derived hematopoietic stem cells. *Bio-protocol* 7. 10.21769/BioProtoc.2134.

Avigdor, A., Goichberg, P., Shivtiel, S., Dar, A., Peled, A., Samira, S., Kollet, O., Hershkoviz, R., Alon, R., Hardan, I., et al. (2004). CD44 and hyaluronic acid cooperate

with SDF-1 in the trafficking of human CD34+ stem/progenitor cells to bone marrow. *Blood* 103, 2981-2989. 10.1182/blood-2003-10-3611.

Avni, B., and Koren-Michowitz, M. (2011). Myeloid sarcoma: current approach and therapeutic options. *Ther Adv Hematol* 2, 309-316. 10.1177/2040620711410774.

Baccin, C., Al-Sabah, J., Velten, L., Helbling, P.M., Grünschläger, F., Hernández-Malmierca, P., Nombela-Arrieta, C., Steinmetz, L.M., Trumpp, A., and Haas, S. (2020). Combined single-cell and spatial transcriptomics reveal the molecular, cellular and spatial bone marrow niche organization. *Nat Cell Biol* 22, 38-48. 10.1038/s41556-019-0439-6.

Backhovens, H., Gheuens, J., and Slegers, H. (1987). Expression of glial fibrillary acidic protein in rat C6 glioma relates to vimentin and is independent of cell-cell contact. *J Neurochem* 49, 348-354. 10.1111/j.1471-4159.1987.tb02872.x.

Bae, M.H.O., S-H., Park, C-J.; Lee, B-R.; Kim, Y. J.; Cho, Y-U.; Jang, S.; Lee, J. H.; Kim, N.; Park, S. H.; Lim, J-H; Seo, E-J.; Lee, K-H. (2015). VLA-4 and CXCR4 expression levels show contrasting prognostic impact (favorable and unfavorable, respectively) in acute myeloid leukemia. *Ann Hematol* 94, 1631-1638. 10.1007/s00277-015-2442-8.

Barbieri, A., Animal Facility Unit, N.I.o.T.o.N.P., Naples, Italy, Bimonte, S., Animal Facility Unit, N.I.o.T.o.N.P., Naples, Italy, Palma, G., Animal Facility Unit, N.I.o.T.o.N.P., Naples, Italy, Luciano, A., Animal Facility Unit, N.I.o.T.o.N.P., Naples, Italy, Rea, D., Animal Facility Unit, N.I.o.T.o.N.P., Naples, Italy, et al. (2019). The stress hormone norepinephrine increases migration of prostate cancer cells in vitro and in vivo. *International Journal of Oncology* 47, 527-534. 10.3892/ijo.2015.3038.

Barron, T.I., Connolly, R.M., Sharp, L., Bennett, K., and Visvanathan, K. (2011). Beta blockers and breast cancer mortality: a population- based study. *J Clin Oncol* 29, 2635-2644. doi: 10.1200/jco.2010.33.5422.

Battula, V.L., Le, P.M., Sun, J.C., Nguyen, K., Yuan, B., Zhou, X., Sonnylal, S., McQueen, T., Ruvolo, V., Michel, K.A., et al. (2017). AML-induced osteogenic



differentiation in mesenchymal stromal cells supports leukemia growth. *JCI Insight* 2. 10.1172/jci.insight.90036.

Behrenbruch, C., Shembrey, C., Paquet-Fifield, S., Molck, C., Cho, H.J., Michael, M., Thomson, B.N.J., Heriot, A.G., and Hollande, F. (2018). Surgical stress response and promotion of metastasis in colorectal cancer: a complex and heterogeneous process. *Clin Exp Metastasis*. doi: 10.1007/s10585-018-9873-2.

Bhadra, U., Thakkar, N., Das, P., and Pal Bhadra, M. (2017). Evolution of circadian rhythms: from bacteria to human. *Sleep Med* 35, 49-61. 10.1016/j.sleep.2017.04.008.

Birbrair, A., and Frenette, P.S. (2016). Niche heterogeneity in the bone marrow. *Ann N Y Acad Sci* 1370, 82-96. 10.1111/nyas.13016.

Bonde, J., Hess, D.A., Maxwell, D.J., Lahey, R., Creer, M.H., Piwnica-Worms, D., and Nolte, J.A. (2005). Comparison of Human Stem Cell Homing after Intravenous or Intra-Femoral Transplantation Using Multimodal In Vivo Imaging of Repopulating Human CD34+ Cells Labeled with Far-Red Fluorescent-Conjugated Nanoparticles.

Bonnet, D., and Dick, J.E. (1997). Human acute myeloid leukemia is organized as a hierarchy that originates from a primitive hematopoietic cell. *Nat Med* 3, 730-737. 10.1038/nm0797-730.

Botteri, E., Munzone, E., Rotmensz, N., Cipolla, C., De Giorgi, V., Santillo, B., Zanelotti, A., Adamoli, L., Colleoni, M., Viale, G., et al. (2013). Therapeutic effect of beta-blockers in triple-negative breast cancer postmenopausal women. *Breast Cancer Res Treat* 140, 567-575. PMID:12356.

Boyd, A.L., Campbell, C.J., Hopkins, C.I., Fiebig-Comyn, A., Russell, J., Ulemek, J., Foley, R., Leber, B., Xenocostas, A., Collins, T.J., and Bhatia, M. (2014). Niche displacement of human leukemic stem cells uniquely allows their competitive replacement with healthy HSPCs. *J Exp Med* 211, 1925-1935. 10.1084/jem.20140131.

Calvani, M., Cavallini, L., Tondo, A., Spinelli, V., Ricci, L., Pasha, A., Bruno, G., Buonvicino, D., Bigagli, E., Vignoli, M., et al. (2018). 3-Adrenoreceptors Control

Mitochondrial Dormancy in Melanoma and Embryonic Stem Cells. *Oxid Med Cell Longev* 2018, 6816508. 10.1155/2018/6816508.

Calvani, M., Pelon, F., Comito, G., Taddei, M.L., Moretti, S., Innocenti, S., Nassini, R., Gerlini, G., Borgognoni, L., Bambi, F., et al. (2015). Norepinephrine promotes tumor microenvironment reactivity through  $\beta$ 3-adrenoreceptors during melanoma progression. *Oncotarget* 6, 4615-4632. 10.18632/oncotarget.2652.

Campbell, J.P., Merkel, A.R., Masood-Campbell, S.K., Elefteriou, F., and Sterling, J.A. (2012). Models of bone metastasis. *J Vis Exp*, e4260. doi: 10.3791/4260.

Cardwell, C.R., Coleman, H.G., Murray, L.J., Entschladen, F., and Powe, D.G. (2013). Beta-blocker usage and breast cancer survival: a nested case-control study within a UK clinical practice research datalink cohort. *Int J Epidemiol* 42, 1852-1861. doi: 10.1093/ije/dyt196.

Chae, Y.K., Dimou, A., Pierce, S., Kantarjian, H., and Andreeff, M. (2014). The effect of calcium channel blockers on the outcome of acute myeloid leukemia. *Leuk Lymphoma* 55, 2822-2829. doi: 10.3109/10428194.2014.901513.

Chakroborty, D., Sarkar, C., Basu, B., Dasgupta, P.S., and Basu, S. (2009). Catecholamines regulate tumor angiogenesis. *Cancer Res* 69, 3727-3730. doi: 10.1158/0008-5472.can-08-4289.

Chang, A., Le, C.P., Walker, A.K., Creed, S.J., Pon, C.K., Albold, S., Carroll, D., Halls, M.L., Lane, J.R., Riedel, B., et al. (2016).  $\beta$ 2-Adrenoceptors on tumor cells play a critical role in stress-enhanced metastasis in a mouse model of breast cancer. *Brain, behavior, and immunity* 57, 106-115. 10.1016/j.bbi.2016.06.011.

Chang, H., Brandwein, J., Yi, Q.L., Chun, K., Patterson, B., and Brien, B. (2004). Extramedullary infiltrates of AML are associated with CD56 expression, 11q23 abnormalities and inferior clinical outcome. *Leuk Res* 28, 1007-1011. 10.1016/j.leukres.2004.01.006.

Chang, P.Y., Huang, W.Y., Lin, C.L., Huang, T.C., Wu, Y.Y., Chen, J.H., and Kao, C.H. (2015). Propranolol Reduces Cancer Risk: A Population-Based Cohort Study. *Medicine (Baltimore)* 94, e1097. doi: 10.1097/md.0000000000001097.

Chen, H., Liu, D., Guo, L., Cheng, X., Guo, N., and Shi, M. (2018). Chronic psychological stress promotes lung metastatic colonization of circulating breast cancer cells by decorating a pre-metastatic niche through activating beta-adrenergic signaling. *J Pathol* 244, 49-60. doi: 10.1002/path.4988.

Cho, B.S.K., H.J.; Konopleva, M. (2017). Targeting the CXCL12/CXCR4 axis in acute myeloid leukemia: from bench to bedside. *Korean J Intern Med* 32, 248-257. 10.3904/kjim.2016.244.

Choi, C.H., Song, T., Kim, T.H., Choi, J.K., Park, J.Y., Yoon, A., Lee, Y.Y., Kim, T.J., Bae, D.S., Lee, J.W., and Kim, B.G. (2014). Meta-analysis of the effects of beta blocker on survival time in cancer patients. *J Cancer Res Clin Oncol* 140, 1179-1188. 10.1007/s00432-014-1658-7.

Choy, C., Raytis, J.L., Smith, D.D., Duenas, M., Neman, J., Jandial, R., and Lew, M.W. (2016). Inhibition of beta2-adrenergic receptor reduces triple-negative breast cancer brain metastases: The potential benefit of perioperative beta-blockade. *Oncol Rep* 35, 3135-3142. doi: 10.3892/or.2016.4710.

Chung, Y.R., Kim, E., and Abdel-Wahab, O. (2014). Femoral bone marrow aspiration in live mice. *J Vis Exp*. 10.3791/51660.

Cole, S.W., Nagaraja, A.S., Lutgendorf, S.K., Green, P.A., and Sood, A.K. (2015). Sympathetic nervous system regulation of the tumour microenvironment. *Nat Rev Cancer* 15, 563-572. doi: 10.1038/nrc3978.

Cosentino, M., Kustrimovic, N., and Marino, F. (2013). Endogenous Catecholamines in Immune Cells: An Overview.

Cosentino, M., Marino, F., and Maestroni, G.J.M. (2015). Sympathoadrenergic modulation of hematopoiesis: a review of available evidence and of therapeutic perspectives. *Frontiers in Cellular Neuroscience* 9, 1-12. doi: 10.3389/fncel.2015.00302.

Costa, M.H.G., de Soure, A.M., Cabral, J.M.S., Ferreira, F.C., and da Silva, C.L. (2018). Hematopoietic Niche - Exploring Biomimetic Cues to Improve the Functionality

of Hematopoietic Stem/Progenitor Cells. *Biotechnol J* 13. doi: 10.1002/biot.201700088.

D'Hondt, L., McAuliffe, C., Damon, J., Reilly, J., Carlson, J., Dooner, M., Colvin, G., Lambert, J.F., Hsieh, C.C., Habibiyan, H., et al. (2004). Circadian variations of bone marrow engraftability. *J Cell Physiol* 200, 63-70. 10.1002/jcp.20032.

Dal Monte, M., Casini, G., Filippi, L., Nicchia, G.P., Svelto, M., and Bagnoli, P. (2013). Functional involvement of  $\beta$ 3-adrenergic receptors in melanoma growth and vascularization. *J Mol Med (Berl)* 91, 1407-1419. 10.1007/s00109-013-1073-6.

Dar, A., Schajnovitz, A., Lapid, K., Kalinkovich, A., Itkin, T., Ludin, A., Kao, W.M., Battista, M., Tesio, M., Kollet, O., et al. (2011). Rapid mobilization of hematopoietic progenitors by AMD3100 and catecholamines is mediated by CXCR4-dependent SDF-1 release from bone marrow stromal cells. *Leukemia* 25, 1286-1296. doi: 10.1038/leu.2011.62.

De Giorgi, V., Grazzini, M., Gandini, S., Benemei, S., Lotti, T., Marchionni, N., and Geppetti, P. (2011). Treatment With  $\beta$ -Blockers and Reduced Disease Progression in Patients With Thick Melanoma. *Archives of Internal Medicine* 171, 779-781. doi: 10.1001/archinternmed.2011.131.

Dethlefsen, C., Hansen, L.S., Lillelund, C., Andersen, C., Gehl, J., Christensen, J.F., Pedersen, B.K., and Hojman, P. (2017). Exercise-Induced Catecholamines Activate the Hippo Tumor Suppressor Pathway to Reduce Risks of Breast Cancer Development. *Cancer Res* 77, 4894-4904. doi: 10.1158/0008-5472.can-16-3125.

Devalon, M.L., Miller, T.D., Squires, R.W., Rogers, P.J., Bove, A.A., and Tyce, G.M. (1989). Dopa in plasma increases during acute exercise and after exercise training. *J Lab Clin Med* 114, 321-327. PMID:2504826.

Diaz, E.S., Karlan, B.Y., and Li, A.J. (2012). Impact of beta blockers on epithelial ovarian cancer survival. *Gynecologic Oncology* 127, 375-378. doi: 10.1016/j.ygyno.2012.07.102.

Dimsdale, J.E., and Moss, J. (2018). Plasma Catecholamines in Stress and Exercise. *JAMA* 243, 340-342. doi: 10.1001/jama.1980.03300300018017.

Ding, L., and Morrison, S.J. (2013). Haematopoietic stem cells and early lymphoid progenitors occupy distinct bone marrow niches. *Nature* 495, 231-235. doi: 10.1038/nature11885.

Ding, L., Saunders, T.L., Enikolopov, G., and Morrison, S.J. (2012). Endothelial and perivascular cells maintain haematopoietic stem cells. *Nature* 481, 457-462. doi: 10.1038/nature10783.

Dobin, A., Davis, C.A., Schlesinger, F., Drenkow, J., Zaleski, C., Jha, S., Batut, P., Chaisson, M., and Gingeras, T.R. (2013). STAR: ultrafast universal RNA-seq aligner. *Bioinformatics* 29, 15-21. doi: 10.1093/bioinformatics/bts635.

Doron, B., Handu, M., and Kurre, P. (2018). Concise Review: Adaptation of the Bone Marrow Stroma in Hematopoietic Malignancies: Current Concepts and Models. *Stem Cells* 36, 304-312. doi: 10.1002/stem.2761.

Du, W., Lu, C., Zhu, X., Hu, D., Chen, X., Li, J., Liu, W., Zhu, J., He, Y., and Yao, J. (2019). Prognostic significance of CXCR4 expression in acute myeloid leukemia. *Cancer Med* 8, 6595-6603. doi: 10.1002/cam4.2535.

Döhner, H., Estey, E., Grimwade, D., Amadori, S., Appelbaum, F.R., Büchner, T., Dombret, H., Ebert, B.L., Fenaux, P., Larson, R.A., et al. (2017). Diagnosis and management of AML in adults: 2017 ELN recommendations from an international expert panel. *Blood* 129, 424-447. doi: 10.1182/blood-2016-08-733196.

Elefteriou, F. (2016). Role of sympathetic nerves in the establishment of metastatic breast cancer cells in bone. *Journal of bone oncology* 5, 132-134. doi: 10.1016/j.jbo.2016.03.003.

Elenkov, I.J., Wilder, R.L., Chrousos, G.P., and Vizi, E.S. (2000). The sympathetic nerve--an integrative interface between two supersystems: the brain and the immune system. *Pharmacological reviews* 52, 595-638. PMID: 11121511.

Ellegast, J.M., Rauch, P.J., Kovtonyuk, L.V., Müller, R., Wagner, U., Saito, Y., Wildner-Verhey van Wijk, N., Fritz, C., Rafiei, A., Lysenko, V., et al. (2016). inv(16) and NPM1mut AMLs engraft human cytokine knock-in mice. *Blood* 128, 2130-2134. doi: 10.1182/blood-2015-12-689356.

Eng, J.W., Reed, C.B., Kokolus, K.M., Pitoniak, R., Utley, A., Bucsek, M.J., Ma, W.W., Repasky, E.A., and Hylander, B.L. (2015). Housing temperature-induced stress drives therapeutic resistance in murine tumour models through beta2-adrenergic receptor activation. *Nat Commun* 6, 6426. doi: 10.1038/ncomms7426.

Eppert, K., Takenaka, K., Lechman, E.R., Waldron, L., Nilsson, B., van Galen, P., Metzeler, K.H., Poepl, A., Ling, V., Beyene, J., et al. (2011). Stem cell gene expression programs influence clinical outcome in human leukemia. *Nat Med* 17, 1086-1093. 10.1038/nm.2415.

Esler, M., Eikelis, N., Schlaich, M., Lambert, G., Alvarenga, M., Kaye, D., El-Osta, A., Guo, L., Barton, D., Pier, C., et al. (2008). Human sympathetic nerve biology: parallel influences of stress and epigenetics in essential hypertension and panic disorder. *Ann N Y Acad Sci* 1148, 338-348. doi: 10.1196/annals.1410.064.

Feuring-Buske, M., Gerhard, B., Cashman, J., Humphries, R.K., Eaves, C.J., and Hogge, D.E. (2003). Improved engraftment of human acute myeloid leukemia progenitor cells in beta 2-microglobulin-deficient NOD/SCID mice and in NOD/SCID mice transgenic for human growth factors. *Leukemia* 17, 760-763. 10.1038/sj.leu.2402882.

Fiegl, M.S., I.; Clise-Dwyer, K.; Burks, J.K.; Mnjoyan, Z.; Andreeff, M. (2009). CXCR4 expression and biologic activity in acute myeloid leukemia are dependent on oxygen partial pressure. *Blood* 113, 1504-1512. 10.1182/blood-2008-06-161539.

Freeman, J.G., Ryan, J.H., Shelburne, C.P., Bailey, D.P., Bouton, A., Narasimhachari, N., Domen, J., Siméon, N., and Courderc, F. (2001). Catecholamines in murine bone marrow derived mast cells. *Journal of Neuroimmunology* 119, 231-238. 10.1016/S0165-5728(01)00384-8.

Frenette, P.S., Subbarao, S., Mazo, I.B., von Andrian, U.H., and Wagner, D.D. (1998). Endothelial selectins and vascular cell adhesion molecule-1 promote hematopoietic progenitor homing to bone marrow. *Proc Natl Acad Sci U S A* 95, 14423-14428. 10.1073/pnas.95.24.14423.

Frisch, B.J., Porter, R.L., and Calvi, L.M. (2008). Hematopoietic niche and bone meet. *Curr Opin Support Palliat Care* 2, 211-217. 10.1097/SPC.0b013e32830d5c12.

Gao, X., Lin, J., Gao, L., Deng, A., Lu, X., Li, Y., Wang, L., and Yu, L. (2015). High expression of c-kit mRNA predicts unfavorable outcome in adult patients with t(8;21) acute myeloid leukemia. *PLoS One* 10, e0124241. 10.1371/journal.pone.0124241.

Gentleman, R.C., Carey, V.J., Bates, D.M., Bolstad, B., Dettling, M., Dudoit, S., Ellis, B., Gautier, L., Ge, Y., Gentry, J., et al. (2004). Bioconductor: open software development for computational biology and bioinformatics. *Genome Biol* 5, R80. 10.1186/gb-2004-5-10-r80.

Glait-Santar, C., Desmond, R., Feng, X., Bat, T., Chen, J., Heuston, E., Mizukawa, B., Mulloy, J.C., Bodine, D.M., Larochelle, A., and Dunbar, C.E. (2015). Functional Niche Competition Between Normal Hematopoietic Stem and Progenitor Cells and Myeloid Leukemia Cells. *Stem Cells* 33, 3635-3642. 10.1002/stem.2208.

Gomariz, A., Helbling, P.M., Isringhausen, S., Suessbier, U., Becker, A., Boss, A., Nagasawa, T., Paul, G., Goksel, O., Székely, G., et al. (2018). Quantitative spatial analysis of haematopoiesis-regulating stromal cells in the bone marrow microenvironment by 3D microscopy. *Nat Commun* 9, 2532. 10.1038/s41467-018-04770-z.

Gong, J.K. (1978). Endosteal marrow: a rich source of hematopoietic stem cells. *Science* (New York, N.Y.).

Greenbaum, A., Hsu, Y.M.S., Day, R.B., Schuettpelz, L.G., Christopher, M.J., Borgerding, J.N., Nagasawa, T., and Link, D.C. (2013). CXCL12 Production by Early Mesenchymal Progenitors is Required for Hematopoietic Stem Cell Maintenance. *Nature* 495, 227-230. doi: 10.1038/nature11926.

Griessinger, E., Vargaftig, J., Horswell, S., Taussig, D.C., Gribben, J., and Bonnet, D. (2018). Acute myeloid leukemia xenograft success prediction: Saving time. *Exp Hematol* 59, 66-71.e64. 10.1016/j.exphem.2017.12.002.

Grisanti, L.A., Traynham, C.J., Repas, A.A., Gao, E., Koch, W.J., and Tilley, D.G. (2016).  $\beta$ 2-Adrenergic receptor-dependent chemokine receptor 2 expression

regulates leukocyte recruitment to the heart following acute injury. *Proc Natl Acad Sci U S A* 113, 15126-15131. 10.1073/pnas.1611023114.

Grytli, H.H., Fagerland, M.W., Fossa, S.D., and Tasken, K.A. (2014). Association between use of beta-blockers and prostate cancer-specific survival: a cohort study of 3561 prostate cancer patients with high-risk or metastatic disease. *Eur Urol* 65, 635-641. 10.1016/j.eururo.2013.01.007.

Gu, X.S., F.E.; Simons, K.J. (1999). Epinephrine absorption after different routes of administration in an animal model. *Biopharm Drug Dispos* 20, 401-405. 10.1002/1099-081x(199911)20:8<401::aid-bdd204>3.0.co;2-l.

Guilak, F., Cohen, D.M., Estes, B.T., Gimble, J.M., Liedtke, W., and Chen, C.S. (2009). Control of stem cell fate by physical interactions with the extracellular matrix. *Cell Stem Cell* 5, 17-26. doi: 10.1016/j.stem.2009.06.016.

Haladyna, J.N., Yamauchi, T., Neff, T., and Bernt, K.M. (2015). Epigenetic modifiers in normal and malignant hematopoiesis. *Epigenomics* 7, 301-320. 10.2217/epi.14.88.

Han, J.A., An, J., and Ko, M. (2015). Functions of TET Proteins in Hematopoietic Transformation. *Mol Cells* 38, 925-935. 10.14348/molcells.2015.0294.

Hanns, P., Paczulla, A.M., Medinger, M., Konantz, M., and Lengerke, C. (2019). Stress and catecholamines modulate the bone marrow microenvironment to promote tumorigenesis. *Cell Stress* 3, 221-235. 10.15698/cst2019.07.192.

Hanoun, M., Zhang, D., Mizoguchi, T., Pinho, S., Pierce, H., Kunisaki, Y., Lacombe, J., Armstrong, S.A., Dührsen, U., and Frenette, P.S. (2014). Acute myelogenous leukemia-induced sympathetic neuropathy promotes malignancy in an altered hematopoietic stem cell niche. *Cell Stem Cell* 15, 365-375. doi: 10.1016/j.stem.2014.06.020.

Hanson, E.D., Sakkal, S., Evans, W.S., Violet, J.A., Battaglini, C.L., McConell, G.K., and Hayes, A. (2018). Altered stress hormone response following acute exercise during prostate cancer treatment. *Scand J Med Sci Sports* 28, 1925-1933. doi: 10.1111/sms.13199.



Hassan, S., Karpova, Y., Baiz, D., Yancey, D., Pullikuth, A., Flores, A., Register, T., Cline, J.M., D'Agostino, R., Jr., Danial, N., et al. (2013). Behavioral stress accelerates prostate cancer development in mice. *J Clin Invest* 123, 874-886. doi: 10.1172/jci63324.

He, W., Holtkamp, S., Hergenhan, S.M., Kraus, K., de Juan, A., Weber, J., Bradfield, P., Grenier, J.M.P., Pelletier, J., Druzd, D., et al. (2018). Circadian Expression of Migratory Factors Establishes Lineage-Specific Signatures that Guide the Homing of Leukocyte Subsets to Tissues. *Immunity* 49, 1175-1190 e1177. 10.1016/j.immuni.2018.10.007.

Heidt, T., Sager, H.B., Courties, G., Dutta, P., Iwamoto, Y., Zaltsman, A., von Zur Muhlen, C., Bode, C., Fricchione, G.L., Denninger, J., et al. (2014). Chronic variable stress activates hematopoietic stem cells. *Nat Med* 20, 754-758. 10.1038/nm.3589.

Hein, L., and Kobilka, B.K. (1995). Adrenergic receptor signal transduction and regulation. *Neuropharmacology* 34, 357-366. doi: 10.1016/0028-3908(95)00018-2.

Her, Z., Yong, K.S.M., Paramasivam, K., Tan, W.W.S., Chan, X.Y., Tan, S.Y., Liu, M., Fan, Y., Linn, Y.C., Hui, K.M., et al. (2017). An improved pre-clinical patient-derived liquid xenograft mouse model for acute myeloid leukemia. *J Hematol Oncol* 10, 162. 10.1186/s13045-017-0532-x.

Hieble, J.P., Bondinell, W.E., and Ruffolo, R.R., Jr. (1995). Alpha- and beta-adrenoceptors: from the gene to the clinic. 1. Molecular biology and adrenoceptor subclassification. *J Med Chem* 38, 3415-3444. PMID: 7658428.

Hoggatt, J., and Scadden, D.T. (2012). The stem cell niche: tissue physiology at a single cell level. *The Journal of clinical investigation* 122, 3029-3034. doi: 10.1172/JCI60238.

Howlader, N.N., A.M., Krapcho, M., Miller, D., Brest, A., Yu, M., Ruhl, J., Tatalovich, Z., Mariotto, A., Lewis, D.R., Chen, H.S., et al. (2019). SEER Cancer Statistics review. National Cancer Institute.

Hu, W., Zhen, X., Xiong, B., Wang, B., Zhang, W., and Zhou, W. (2008). CXCR6 is expressed in human prostate cancer in vivo and is involved in the in vitro invasion of

PC3 and LNCap cells. *Cancer Sci* 99, 1362-1369. doi: 10.1111/j.1349-7006.2008.00833.x.

Hulsurkar, M., Li, Z., Zhang, Y., Li, X., Zheng, D., and Li, W. (2017). Beta-adrenergic signaling promotes tumor angiogenesis and prostate cancer progression through HDAC2-mediated suppression of thrombospondin-1. *Oncogene* 36, 1525-1536. doi: 10.1038/onc.2016.319.

Huntly, B.J., and Gilliland, D.G. (2005). Leukaemia stem cells and the evolution of cancer-stem-cell research. *Nat Rev Cancer* 5, 311-321. 10.1038/nrc1592.

Im, Y.B.W., J. S.; Suh, H. W.; Huh, S. O.; Kim, Y. H.; Song, D. K. (1998). Differential effect of adrenaline and noradrenaline on the hepatic expression of immediate early genes in mice. *J Auton Pharmacol* 18 (3), 149-155. 10.1046/j.1365-2680.1998.1830149.x.

Imperato, A.A., L.; Casolini, P.; Zocchi, A.; Puglisi-Allegra, S. (1992). Repeated stressful experiences differently affect limbic dopamine release during and following stress. *Brain Research* 577, 194-199. [https://doi.org/10.1016/0006-8993\(92\)90274-D](https://doi.org/10.1016/0006-8993(92)90274-D).

Inra, C.N., Zhou, B.O., Acar, M., Murphy, M.M., Richardson, J., Zhao, Z., and Morrison, S.J. (2015). A perisinusoidal niche for extramedullary haematopoiesis in the spleen. *Nature* 527, 466-471. 10.1038/nature15530.

Ishikawa, F., Yoshida, S., Saito, Y., Hijikata, A., Kitamura, H., Tanaka, S., Nakamura, R., Tanaka, T., Tomiyama, H., Saito, N., et al. (2007). Chemotherapy-resistant human AML stem cells home to and engraft within the bone-marrow endosteal region. *Nat Biotechnol* 25, 1315-1321. 10.1038/nbt1350.

Jacamo, R., Chen, Y., Wang, Z., Ma, W., Zhang, M., Spaeth, E.L., Wang, Y., Battula, V.L., Mak, P.Y., Schallmoser, K., et al. (2014). Reciprocal leukemia-stroma VCAM-1/VLA-4-dependent activation of NF- $\kappa$ B mediates chemoresistance. *Blood* 123, 2691-2702. 10.1182/blood-2013-06-511527.

Jacobsen, K.R., Kalliokoski, O., Teilmann, A.C., Hau, J., and Abelson, K.S. (2012). Postsurgical food and water consumption, fecal corticosterone metabolites, and

behavior assessment as noninvasive measures of pain in vasectomized BALB/c mice. *J Am Assoc Lab Anim Sci* 51, 69-75.

Jin, L., Hope, K.J., Zhai, Q., Smadja-Joffe, F., and Dick, J.E. (2006). Targeting of CD44 eradicates human acute myeloid leukemic stem cells. *Nat Med* 12, 1167-1174. doi: 10.1038/nm1483.

Jones, D.H., Nakashima, T., Sanchez, O.H., Kozieradzki, I., Komarova, S.V., Sarosi, I., Morony, S., Rubin, E., Sarao, R., Hojilla, C.V., et al. (2006). Regulation of cancer cell migration and bone metastasis by RANKL. *Nature* 440, 692-696. doi: 10.1038/nature04524.

Jung, Y., Wang, J., Song, J., Shiozawa, Y., Havens, A., Wang, Z., Sun, Y.X., Emerson, S.G., Krebsbach, P.H., and Taichman, R.S. (2007). Annexin II expressed by osteoblasts and endothelial cells regulates stem cell adhesion, homing, and engraftment following transplantation. *Blood* 110, 82-90. doi: 10.1182/blood-2006-05-021352.

Kaapu, K.J., Murtola, T.J., Maattanen, L., Talala, K., Taari, K., Tammela, T.L., and Auvinen, A. (2016). Prostate cancer risk among users of digoxin and other antiarrhythmic drugs in the Finnish Prostate Cancer Screening Trial. *Cancer Causes Control* 27, 157-164. doi: 10.1007/s10552-015-0693-2.

Kan, C., Vargas, G., Pape, F.L., and Clézardin, P. (2016). Cancer Cell Colonisation in the Bone Microenvironment. *International journal of molecular sciences* 17. doi: 10.3390/ijms17101674.

Keyhani, A., Huh, Y.O., Jendiroba, D., Pagliaro, L., Cortez, J., Pierce, S., Pearlman, M., Estey, E., Kantarjian, H., and Freireich, E.J. (2000). Increased CD38 expression is associated with favorable prognosis in adult acute leukemia. *Leuk Res* 24, 153-159. doi: 10.1016/s0145-2126(99)00147-2.

Khwaja, A., Bjorkholm, M., Gale, R.E., Levine, R.L., Jordan, C.T., Ehninger, G., Bloomfield, C.D., Estey, E., Burnett, A., Cornelissen, J.J., et al. (2016). Acute myeloid leukaemia. *Nat Rev Dis Primers* 2, 16010. doi: 10.1038/nrdp.2016.10.

Kiel, M.J., Yilmaz, O.H., Iwashita, T., Terhorst, C., and Morrison, S.J. (2005). SLAM family receptors distinguish hematopoietic stem and progenitor cells and reveal endothelial niches for stem cells. *Cell* 121, 1109-1121. doi: 10.1016/j.cell.2005.05.026.

Kikuchi, N., Nishiyama, T., Sawada, T., Wang, C., Lin, Y., Watanabe, Y., Tamakoshi, A., and Kikuchi, S. (2017). Perceived Stress and Colorectal Cancer Incidence: The Japan Collaborative Cohort Study. *Scientific reports* 7, 40363-40363. doi: 10.1038/srep40363.

Kim, S.Y., S-S., Hong, J., Shin, D.-Y., Koh, Y., M., B.J., and Kim, I. (2020). Characterization and Prognosis of Secondary Acute Myeloid Leukemia in an Asian Population: AML With Antecedent Hematological Disease Confers Worst Outcomes, Irrespective of Cytogenetic Risk. *Anticancer Research*.

Kim, T.H., Gill, N.K., Nyberg, K.D., Nguyen, A.V., Hohlbauch, S.V., Geisse, N.A., Nowell, C.J., Sloan, E.K., and Rowat, A.C. (2016). Cancer cells become less deformable and more invasive with activation of beta-adrenergic signaling. *J Cell Sci* 129, 4563-4575. doi: 10.1242/jcs.194803.

Kim-Fuchs, C., Le, C.P., Pimentel, M.A., Shackelford, D., Ferrari, D., Angst, E., Hollande, F., and Sloan, E.K. (2014). Chronic stress accelerates pancreatic cancer growth and invasion: a critical role for beta-adrenergic signaling in the pancreatic microenvironment. *Brain Behav Immun* 40, 40-47. doi: 10.1016/j.bbi.2014.02.019.

King, M.B., G.; Wheatley, D.; France, R.; Howie, J.; Porter, M.; Heaney, D.; Wilson, A.; Bostock, J. (1993). Stress management in general practice. *Occas Pap R Coll Gen Pract*, iv-vi, 1-42.

Klco, J.M., Spencer, D.H., Miller, C.A., Griffith, M., Lamprecht, T.L., O'Laughlin, M., Fronick, C., Magrini, V., Demeter, R.T., Fulton, R.S., et al. (2014). Functional heterogeneity of genetically defined subclones in acute myeloid leukemia. *Cancer Cell* 25, 379-392. doi: 10.1016/j.ccr.2014.01.031.

Kohm, A.P., and Sanders, V.M. (2000). Norepinephrine: a messenger from the brain to the immune system. *Immunology Today* 21, 539-542. doi: 10.1016/S0167-5699(00)01747-3.

Konantz, M., Andre, M.C., Ebinger, M., Grauer, M., Wang, H., Grzywna, S., Rothfuss, O.C., Lehle, S., Kustikova, O.S., Salih, H.R., et al. (2013). EVI-1 modulates leukemogenic potential and apoptosis sensitivity in human acute lymphoblastic leukemia. *Leukemia* 27, 56-65. 10.1038/leu.2012.211.

Konantz, M., Schürch, C., Hanns, P., Müller, J.S., Sauter, L., and Lengerke, C. (2019). Modeling hematopoietic disorders in zebrafish. *Dis Model Mech* 12. 10.1242/dmm.040360.

Kropfl, J.M., Stelzer, I., Mangge, H., Pekovits, K., Fuchs, R., Allard, N., Schinagl, L., Hofmann, P., Dohr, G., Wallner-Liebmann, S., et al. (2014). Exercise-induced norepinephrine decreases circulating hematopoietic stem and progenitor cell colony-forming capacity. *PLoS One* 9, e106120. doi: 10.1371/journal.pone.0106120.

Kuci, Z., Seitz, G., Kuci, S., Kreyenberg, H., Schumm, M., Lang, P., Niethammer, D., Handgretinger, R., and Bruchelt, G. (2006). Pitfalls in detection of contaminating neuroblastoma cells by tyrosine hydroxylase RT-PCR due to catecholamine-producing hematopoietic cells. *Anticancer Res* 26, 2075-2080. PMID: 16827147.

Kumar, R., Godavarthy, P.S., and Krause, D.S. (2018). The bone marrow microenvironment in health and disease at a glance. *J Cell Sci* 131. 10.1242/jcs.201707.

Kunder, S., Calzada-Wack, J., Holzlwimmer, G., Müller, J., Kloss, C., Howat, W., Schmidt, J., Hofler, H., Warren, M., and Quintanilla-Martinez, L. (2007). A comprehensive antibody panel for immunohistochemical analysis of formalin-fixed, paraffin-embedded hematopoietic neoplasms of mice: analysis of mouse specific and human antibodies cross-reactive with murine tissue. *Toxicol Pathol* 35, 366-375. 10.1080/01926230701230296.

Kunisaki, Y., Bruns, I., Scheiermann, C., Ahmed, J., Pinho, S., Zhang, D., Mizoguchi, T., Wei, Q., Lucas, D., Ito, K., et al. (2013). Arteriolar niches maintain haematopoietic stem cell quiescence. *Nature* 502, 637-643. 10.1038/nature12612.

Kunisaki, Y., and Frenette, P.S. (2014). Influences of vascular niches on hematopoietic stem cell fate. *Int J Hematol* 99, 699-705. 10.1007/s12185-014-1580-4.

Lamkin, D.M., Sloan, E.K., Patel, A.J., Chiang, B.S., Pimentel, M.A., Ma, J.C., Arevalo, J.M., Morizono, K., and Cole, S.W. (2012). Chronic stress enhances progression of acute lymphoblastic leukemia via  $\beta$ -adrenergic signaling. *Brain Behav Immun* 26, 635-641. 10.1016/j.bbi.2012.01.013.

Lane, S.W., Scadden, D.T., and Gilliland, D.G. (2009). The leukemic stem cell niche: current concepts and therapeutic opportunities. *Blood* 114, 1150-1157. 10.1182/blood-2009-01-202606.

Lanier, L.L., Testi, R., Bintl, J., and Phillips, J.H. (1989). Identity of Leu-19 (CD56) leukocyte differentiation antigen and neural cell adhesion molecule. *J Exp Med* 169, 2233-2238. 10.1084/jem.169.6.2233.

Lapidot, T., Fajerman, Y., and Kollet, O. (1997). Immune-deficient SCID and NOD/SCID mice models as functional assays for studying normal and malignant human hematopoiesis. *J Mol Med (Berl)* 75, 664-673. 10.1007/s001090050150.

Lapidot, T.S., C.; Vormoor, J.; Murdoch, B.; Hoang, T.; Caceres-Cortes, J., Minden, M.; Paterson, B.; Caligiuri, M. A.; Dick, J.E.; (1994). A cell initiating human acute myeloid leukaemia after transplantation into SCID mice. *Nature* 367, 645-648.

Le, C.P., Nowell, C.J., Kim-Fuchs, C., Botteri, E., Hiller, J.G., Ismail, H., Pimentel, M.A., Chai, M.G., Karnezis, T., Rotmensz, N., et al. (2016). Chronic stress in mice remodels lymph vasculature to promote tumour cell dissemination. *Nat Commun* 7, 10634. doi: 10.1038/ncomms10634.

Lemeshow, S., Sorensen, H.T., Phillips, G., Yang, E.V., Antonsen, S., Riis, A.H., Lesinski, G.B., Jackson, R., and Glaser, R. (2011). beta-Blockers and survival among Danish patients with malignant melanoma: a population-based cohort study. *Cancer Epidemiol Biomarkers Prev* 20, 2273-2279. doi: 10.1158/1055-9965.epi-11-0249.

Leone, G., Mele, L., Pulsoni, A., Equitani, F., and Pagano, L. (1999). The incidence of secondary leukemias. *Haematologica* 84, 937-945.

Levesque, J.-P.W., I. G. (2016). Cell Adhesion Molecules in Normal and Malignant Hematopoiesis: from Bench to Bedside. *Current stem cell reports*

Levin, T.T., Li, Y., Riskind, J., and Rai, K. (2007). Depression, anxiety and quality of life in a chronic lymphocytic leukemia cohort. *Gen Hosp Psychiatry* 29, 251-256. 10.1016/j.genhosppsy.2007.01.014.

Levine, R.L. (2013). Molecular pathogenesis of AML: translating insights to the clinic. *Best Pract Res Clin Haematol* 26, 245-248. 10.1016/j.beha.2013.10.003.

Lin, Q., Wang, F., Yang, R., Zheng, X., Gao, H., and Zhang, P. (2013). Effect of chronic restraint stress on human colorectal carcinoma growth in mice. *PLoS One* 8, e61435. doi: 10.1371/journal.pone.0061435.

Lisovsky, M., Estrov, Z., Zhang, X., Consoli, U., Sanchez-Williams, G., Snell, V., Munker, R., Goodacre, A., Savchenko, V., and Andreeff, M. (1996). Flt3 ligand stimulates proliferation and inhibits apoptosis of acute myeloid leukemia cells: regulation of Bcl-2 and Bax. *Blood* 88, 3987-3997.

Livingstone, E., Hollestein, L.M., van Herk-Sukel, M.P., van de Poll-Franse, L., Nijsten, T., Schadendorf, D., and de Vries, E. (2013). beta-Blocker use and all-cause mortality of melanoma patients: results from a population-based Dutch cohort study. *Eur J Cancer* 49, 3863-3871. doi: 10.1016/j.ejca.2013.07.141.

Lord, B.I.T., N. G., and Hendry, J.H. (1975). The relative spatial distributions of CFUs and CFUc in the normal mouse femur. . *Blood*.

Lucas, D., Battista, M., Shi, P.A., Isola, L., and Frenette, P.S. (2008). Mobilized hematopoietic stem cell yield depends on species-specific circadian timing. *Cell Stem Cell* 3, 364-366. 10.1016/j.stem.2008.09.004.

Luo, W., Friedman, M.S., Shedden, K., Hankenson, K.D., and Woolf, P.J. (2009). GAGE: generally applicable gene set enrichment for pathway analysis. *BMC Bioinformatics* 10, 161. 10.1186/1471-2105-10-161.

Lutgendorf, S.K., DeGeest, K., Dahmouh, L., Farley, D., Penedo, F., Bender, D., Goodheart, M., Buekers, T.E., Mendez, L., Krueger, G., et al. (2011). Social isolation

is associated with elevated tumor norepinephrine in ovarian carcinoma patients. *Brain Behav Immun* 25, 250-255. doi: 10.1016/j.bbi.2010.10.012.

Macanas-Pirard, P., Quezada, T., Navarrete, L., Broekhuizen, R., Leisewitz, A., Nervi, B., and Ramírez, P.A. (2017). The CCL2/CCR2 Axis Affects Transmigration and Proliferation but Not Resistance to Chemotherapy of Acute Myeloid Leukemia Cells. *PLoS One* 12, e0168888. 10.1371/journal.pone.0168888.

Mach, D.B., Rogers, S.D., Sabino, M.C., Luger, N.M., Schwei, M.J., Pomonis, J.D., Keyser, C.P., Clohisy, D.R., Adams, D.J., O'Leary, P., and Mantyh, P.W. (2002). Origins of skeletal pain: sensory and sympathetic innervation of the mouse femur. *Neuroscience* 113, 155-166. doi: 10.1016/S0306-4522(02)00165-3.

Madden, K.S., Szpunar, M.J., and Brown, E.B. (2013). Early impact of social isolation and breast tumor progression in mice. *Brain Behav Immun* 30 *Suppl*, S135-141. doi: 10.1016/j.bbi.2012.05.003.

Maestroni, G.J., Cosentino, M., Marino, F., Togni, M., Conti, A., Lecchini, S., and Frigo, G. (1998). Neural and endogenous catecholamines in the bone marrow. Circadian association of norepinephrine with hematopoiesis? *Exp Hematol* 26, 1172-1177.

Magnon, C., Hall, S.J., Lin, J., Xue, X., Gerber, L., Freedland, S.J., and Frenette, P.S. (2013). Autonomic nerve development contributes to prostate cancer progression. *Science* 341, 1236361. 10.1126/science.1236361.

Maryanovich, M., Takeishi, S., and Frenette, P.S. (2018). Neural Regulation of Bone and Bone Marrow. *Cold Spring Harb Perspect Med* 8. 10.1101/cshperspect.a031344.

Matsunaga, T.T., N.; Sato, T.; Takimoto, R.; Tanaka, I.; Fujimi, A.; Akiyama, T.; Kuroda, H.; Kawano, Y.; Kobune, M.; Kato, J.; Hirayama, Y.; Sakamaki, S.; Kohda, K.; Miyake, K.; Niitsu, Y. (2003). Interaction between leukemic-cell VLA-4 and stromal fibronectin is a decisive factor for minimal residual disease of acute myelogenous leukemia. *Nat Med* 9, 1158-1165. <https://doi.org/10.1038/nm909>.

McCourt, C., Coleman, H.G., Murray, L.J., Cantwell, M.M., Dolan, O., Powe, D.G., and Cardwell, C.R. (2014). Beta-blocker usage after malignant melanoma diagnosis and



survival: a population-based nested case-control study. *Br J Dermatol* 170, 930-938. doi: 10.1111/bjd.12894.

Melhem-Bertrandt, A., Chavez-Macgregor, M., Lei, X., Brown, E.N., Lee, R.T., Meric-Bernstam, F., Sood, A.K., Conzen, S.D., Hortobagyi, G.N., and Gonzalez-Angulo, A.M. (2011). Beta-blocker use is associated with improved relapse-free survival in patients with triple-negative breast cancer. *J Clin Oncol* 29, 2645-2652. doi: 10.1200/jco.2010.33.4441.

Molinoff, P.B. (1984). Alpha- and beta-adrenergic receptor subtypes properties, distribution and regulation. *Drugs* 28 *Suppl* 2, 1-15. doi: 10.2165/00003495-198400282-00002.

Montoya, A., Amaya, C.N., Belmont, A., Diab, N., Trevino, R., Villanueva, G., Rains, S., Sanchez, L.A., Badri, N., Otoukesh, S., et al. (2017). Use of non-selective  $\beta$ -blockers is associated with decreased tumor proliferative indices in early stage breast cancer. In *Oncotarget*, pp. 6446-6460. 10.18632/oncotarget.14119.

Moreno-Smith, M., Lutgendorf, S.K., and Sood, A.K. (2010). Impact of stress on cancer metastasis. *Future oncology (London, England)* 6, 1863-1881. doi: 10.2217/fon.10.142.

Morrison, S.J., and Scadden, D.T. (2014). The bone marrow niche for haematopoietic stem cells. *Nature* 505, 327. doi:10.1038/nature12984.

Mulcrone, P.L., Campbell, J.P., Clément-Demange, L., Anbinder, A.L., Merkel, A.R., Brekken, R.A., Sterling, J.A., and Elefteriou, F. (2017). Skeletal Colonization by Breast Cancer Cells Is Stimulated by an Osteoblast and  $\beta$ 2AR-Dependent Neo-Angiogenic Switch. *Journal of Bone and Mineral Research* 32, 1442-1454. doi: 10.1002/jbmr.3133.

Muthu, K., Iyer, S., He, L.K., Szilagyi, A., Gamelli, R.L., Shankar, R., and Jones, S.B. (2007). Murine Hematopoietic Stem cells and Progenitors Express Adrenergic Receptors. *J Neuroimmunol* 186, 27-36. doi: 10.1016/j.jneuroim.2007.02.007.

Méndez-Ferrer, S., Battista, M., and Frenette, P.S. (2010a). Cooperation of  $\beta$ 2- and  $\beta$ 3-adrenergic receptors in hematopoietic progenitor cell mobilization. *Annals of the*

New York Academy of Sciences 1192, 139-144. doi: 10.1111/j.1749-6632.2010.05390.x.

Méndez-Ferrer, S., Chow, A., Merad, M., and Frenette, P.S. (2009). Circadian rhythms influence hematopoietic stem cells. *Curr Opin Hematol* 16, 235-242. 10.1097/MOH.0b013e32832bd0f5.

Méndez-Ferrer, S., Lucas, D., Battista, M., and Frenette, P.S. (2008). Haematopoietic stem cell release is regulated by circadian oscillations. *Nature* 452, 442-447. doi: 10.1038/nature06685.

Méndez-Ferrer, S., Michurina, T.V., Ferraro, F., Mazloom, A.R., Macarthur, B.D., Lira, S.A., Scadden, D.T., Ma'ayan, A., Enikolopov, G.N., and Frenette, P.S. (2010b). Mesenchymal and haematopoietic stem cells form a unique bone marrow niche. *Nature* 466, 829-834. 10.1038/nature09262.

Möhle, R., Moore, M.A., Nachman, R.L., and Rafii, S. (1997). Transendothelial migration of CD34+ and mature hematopoietic cells: an in vitro study using a human bone marrow endothelial cell line. *Blood* 89, 72-80.

Nadri, S., Soleimani, M., Mobarra, Z., and Amini, S. (2008). Expression of dopamine-associated genes on conjunctiva stromal-derived human mesenchymal stem cells. *Biochem Biophys Res Commun* 377, 423-428. doi: 10.1016/j.bbrc.2008.09.148.

Nagaraja, A.S., Dood, R.L., Armaiz-Pena, G., Kang, Y., Wu, S.Y., Allen, J.K., Jennings, N.B., Mangala, L.S., Pradeep, S., Lyons, Y., et al. (2017). Adrenergic-mediated increases in INHBA drive CAF phenotype and collagens. *JCI Insight* 2. doi: 10.1172/jci.insight.93076.

Nagaraja, A.S., Dorniak, P.L., Sadaoui, N.C., Kang, Y., Lin, T., Armaiz-Pena, G., Wu, S.Y., Rupaimoole, R., Allen, J.K., Gharpure, K.M., et al. (2016). Sustained adrenergic signaling leads to increased metastasis in ovarian cancer via increased PGE2 synthesis. *Oncogene* 35, 2390-2397. doi: 10.1038/onc.2015.302.

Narayanan, D., and Weinberg, O.K. (2020). How I investigate acute myeloid leukemia. *Int J Lab Hematol* 42, 3-15. 10.1111/ijlh.13135.

Nareshkumar, R.N., Sulochana, K.N., and Coral, K. (2018). Inhibition of angiogenesis in endothelial cells by Human Lysyl oxidase propeptide. *Sci Rep* 8, 10426. 10.1038/s41598-018-28745-8.

Nicolini, F.E., Cashman, J.D., Hogge, D.E., Humphries, R.K., and Eaves, C.J. (2004). NOD/SCID mice engineered to express human IL-3, GM-CSF and Steel factor constitutively mobilize engrafted human progenitors and compromise human stem cell regeneration. *Leukemia* 18, 341-347. 10.1038/sj.leu.2403222.

Nilsson, S.K., Johnston, H.M., Whitty, G.A., Williams, B., Webb, R.J., Denhardt, D.T., Bertonecello, I., Bendall, L.J., Simmons, P.J., and Haylock, D.N. (2005). Osteopontin, a key component of the hematopoietic stem cell niche and regulator of primitive hematopoietic progenitor cells. *Blood* 106, 1232-1239. doi: 10.1182/blood-2004-11-4422.

Nilsson, S.K.J., H. M., and Coverdale, J.A. (2001). Spatial localization of transplanted hemopoietic stem cells: inferences for the localization of stem cell niches. . *Blood*.

Nombela-Arrieta, C., and Isringhausen, S. (2016). The Role of the Bone Marrow Stromal Compartment in the Hematopoietic Response to Microbial Infections. *Front Immunol* 7, 689. 10.3389/fimmu.2016.00689.

Nombela-Arrieta, C., Pivarnik, G., Winkel, B., Canty, K.J., Harley, B., Mahoney, J.E., Park, S.Y., Lu, J., Protopopov, A., and Silberstein, L.E. (2013). Quantitative imaging of haematopoietic stem and progenitor cell localization and hypoxic status in the bone marrow microenvironment. *Nat Cell Biol* 15, 533-543. 10.1038/ncb2730.

Notta, F., Doulatov, S., and Dick, J.E. (2010). Engraftment of human hematopoietic stem cells is more efficient in female NOD/SCID/IL-2Rgc-null recipients. *Blood* 115, 3704-3707. 10.1182/blood-2009-10-249326.

Obradović, M.M.S., Hamelin, B., Manevski, N., Couto, J.P., Sethi, A., Coissieux, M.M., Müntz, S., Okamoto, R., Kohler, H., Schmidt, A., and Bentires-Alj, M. (2019). Glucocorticoids promote breast cancer metastasis. *Nature* 567, 540-544. 10.1038/s41586-019-1019-4.

Orenberg, E.K., Pfenndt, E.A., and Wilkinson, D.I. (1983). Characterization of  $\alpha$ - and  $\beta$ -Adrenergic Agonist Stimulation of Adenylate Cyclase Activity in Human Epidermal Keratinocytes In Vitro. *Journal of Investigative Dermatology* 80, 503-507. doi: 10.1111/1523-1747.ep12535068.

Orkin, S.H., and Zon, L.I. (2008). Hematopoiesis: an evolving paradigm for stem cell biology. *Cell* 132, 631-644. 10.1016/j.cell.2008.01.025.

Paczulla, A.M., Dirnhofer, S., Konantz, M., Medinger, M., Salih, H.R., Rothfelder, K., Tsakiris, D.A., Passweg, J.R., Lundberg, P., and Lengerke, C. (2017). Long-term observation reveals high-frequency engraftment of human acute myeloid leukemia in immunodeficient mice. *Haematologica* 102, 854-864. 10.3324/haematol.2016.153528.

Paczulla, A.M., Rothfelder, K., Raffel, S., Konantz, M., Steinbacher, J., Wang, H., Tandler, C., Mbarga, M., Schaefer, T., Falcone, M., et al. (2019). Absence of NKG2D ligands defines leukaemia stem cells and mediates their immune evasion. *Nature* 572, 254-259. 10.1038/s41586-019-1410-1.

Papaemmanuil, E., Gerstung, M., Bullinger, L., Gaidzik, V.I., Paschka, P., Roberts, N.D., Potter, N.E., Heuser, M., Thol, F., Bolli, N., et al. (2016). Genomic Classification and Prognosis in Acute Myeloid Leukemia. *N Engl J Med* 374, 2209-2221. 10.1056/NEJMoa1516192.

Parker, W.P., Lohse, C.M., Zaid, H.B., Chevillie, J.C., Boorjian, S.A., Leibovich, B.C., and Thompson, R.H. (2017). Evaluation of beta-blockers and survival among hypertensive patients with renal cell carcinoma. *Urol Oncol* 35, 36.e31-36.e36. doi: 10.1016/j.urolonc.2016.08.013.

Partecke, L.I., Speerforck, S., Kading, A., Seubert, F., Kuhn, S., Lorenz, E., Schwandke, S., Sendler, M., Kessler, W., Trung, D.N., et al. (2016). Chronic stress increases experimental pancreatic cancer growth, reduces survival and can be antagonised by beta-adrenergic receptor blockade. *Pancreatology* 16, 423-433. doi: 10.1016/j.pan.2016.03.005.

Pearce, D.J., Taussig, D., Zibara, K., Smith, L.L., Ridler, C.M., Preudhomme, C., Young, B.D., Rohatiner, A.Z., Lister, T.A., and Bonnet, D. (2006). AML engraftment in the NOD/SCID assay reflects the outcome of AML: implications for our understanding of the heterogeneity of AML. *Blood* 107, 1166-1173. 10.1182/blood-2005-06-2325.

Pedersen, L., Idorn, M., Olofsson, G.H., Lauenborg, B., Nookaew, I., Hansen, R.H., Johannesen, H.H., Becker, J.C., Pedersen, K.S., Dethlefsen, C., et al. (2016). Voluntary Running Suppresses Tumor Growth through Epinephrine- and IL-6-Dependent NK Cell Mobilization and Redistribution. *Cell Metab* 23, 554-562. doi: 10.1016/j.cmet.2016.01.011.

Peled, A.K., O.; Ponomaryov, T.; Petit, I.; Franitza, S.; Grabovsky, V.; Slav, M. M.; Nagler, A.; Lider, O.; Alon, R.; Zipori, D.; Lapidot, T. (2000). The chemokine SDF-1 activates the integrins LFA-1, VLA-4, and VLA-5 on immature human CD34+ cells: role in transendothelial/stromal migration and engraftment of NOD/SCID mice. *Blood* 95, 3289-3296. <https://doi.org/10.1182/blood.V95.11.3289>.

Perrone, M.G., Notarnicola, M., Caruso, M.G., Tutino, V., and Scilimati, A. (2008). Upregulation of beta3-adrenergic receptor mRNA in human colon cancer: a preliminary study. *Oncology* 75, 224-229. 10.1159/000163851.

Petit, I., Goichberg, P., Spiegel, A., Peled, A., Brodie, C., Seger, R., Nagler, A., Alon, R., and Lapidot, T. (2005). Atypical PKC-zeta regulates SDF-1-mediated migration and development of human CD34+ progenitor cells. *J Clin Invest* 115, 168-176. 10.1172/JCI21773.

Petty, J.M.L., C. C.; Weiss, D. J.; Poynter, M. E.; Suratt, B. T. (2009). Crosstalk between CXCR4/SDF-1 and VLA-4/VCAM-1 pathways regulates neutrophil retention in the bone marrow. *J Immunol* 182, 604-612. 10.4049/jimmunol.182.1.604.

Pinho, S., and Frenette, P.S. (2019). Haematopoietic stem cell activity and interactions with the niche. *Nat Rev Mol Cell Biol* 20, 303-320. 10.1038/s41580-019-0103-9.

Pittenger, M.F., Mackay, A.M., Beck, S.C., Jaiswal, R.K., Douglas, R., Mosca, J.D., Moorman, M.A., Simonetti, D.W., Craig, S., and Marshak, D.R. (1999). Multilineage

potential of adult human mesenchymal stem cells. *Science* 284, 143-147. 10.1126/science.284.5411.143.

Plesa, A., Dumontet, C., Mattei, E., Tagoug, I., Hayette, S., Sujobert, P., Tigaud, I., Pages, M.P., Chelghoum, Y., Baracco, F., et al. (2017). High frequency of CD34+CD38-/low immature leukemia cells is correlated with unfavorable prognosis in acute myeloid leukemia. *World J Stem Cells* 9, 227-234. 10.4252/wjsc.v9.i12.227.

Powe, D.G., Voss, M.J., Zanker, K.S., Habashy, H.O., Green, A.R., Ellis, I.O., and Entschladen, F. (2010). Beta-blocker drug therapy reduces secondary cancer formation in breast cancer and improves cancer specific survival. *Oncotarget* 1, 628-638. doi: 10.18632/oncotarget.101009.

Prieto, J.M., Atala, J., Blanch, J., Carreras, E., Rovira, M., Cirera, E., Espinal, A., and Gasto, C. (2005). Role of depression as a predictor of mortality among cancer patients after stem-cell transplantation. *J Clin Oncol* 23, 6063-6071. 10.1200/jco.2005.05.751.

Puglisi-Allegra, S.I., A.; Angelucci, L.; Cabib, S. (1991). Acute stress induces time-dependent responses in dopamine mesolimbic system. *Brain Res.* 19 (554), 217-222. doi: 10.1016/0006-8993(91)90192-x.

Puram, R.V., Kowalczyk, M.S., de Boer, C.G., Schneider, R.K., Miller, P.G., McConkey, M., Tothova, Z., Tejero, H., Heckl, D., Jaras, M., et al. (2016). Core Circadian Clock Genes Regulate Leukemia Stem Cells in AML. *Cell* 165, 303-316. 10.1016/j.cell.2016.03.015.

Qiao, G., Chen, M., Bucsek, M.J., Repasky, E.A., and Hylander, B.L. (2018). Adrenergic Signaling: A Targetable Checkpoint Limiting Development of the Antitumor Immune Response. *Front Immunol* 9, 164. doi: 10.3389/fimmu.2018.00164.

Qin, J., Jin, F., Li, N., Guan, H., Lan, L., Ni, H., and Wang, Y. (2015). Adrenergic receptor  $\beta$ 2 activation by stress promotes breast cancer progression through macrophages M2 polarization in tumor microenvironment. In *BMB Rep*, pp. 295-300. doi: 10.5483/BMBRep.2015.48.5.008.

Quek, L., Otto, G.W., Garnett, C., Lhermitte, L., Karamitros, D., Stoilova, B., Lau, I.J., Doondeea, J., Usukhbayar, B., Kennedy, A., et al. (2016). Genetically distinct

leukemic stem cells in human CD34- acute myeloid leukemia are arrested at a hemopoietic precursor-like stage. *J Exp Med* 213, 1513-1535. 10.1084/jem.20151775.

Rains, S.L., Amaya, C.N., and Bryan, B.A. (2017). Beta-adrenergic receptors are expressed across diverse cancers. *Oncoscience* 4, 95-105. doi: 10.18632/oncoscience.357.

Rang, H., Dale, M., Ritter, J., and Flower, R. (2007). *Rang & Dale's Pharmacology E-Book - 6th Edition*.

Raspadori, D., Damiani, D., Lenoci, M., Rondelli, D., Testoni, N., Nardi, G., Sestigiani, C., Mariotti, C., Birtolo, S., Tozzi, M., and Lauria, F. (2001). CD56 antigenic expression in acute myeloid leukemia identifies patients with poor clinical prognosis. *Leukemia* 15, 1161-1164. 10.1038/sj.leu.2402174.

Reagan, M.R., and Rosen, C.J. (2016). Navigating the bone marrow niche: translational insights and cancer-driven dysfunction. *Nature Reviews Rheumatology* 12, 154-168. doi: 10.1038/nrrheum.2015.160.

Reinisch, A., Thomas, D., Corces, M.R., Zhang, X., Gratzinger, D., Hong, W.J., Schallmoser, K., Strunk, D., and Majeti, R. (2016). A humanized bone marrow ossicle xenotransplantation model enables improved engraftment of healthy and leukemic human hematopoietic cells. *Nat Med* 22, 812-821. 10.1038/nm.4103.

Rettig, M.P.A., G.; DiPersio, J. F, (2012). Mobilization of hematopoietic stem and progenitor cells using inhibitors of CXCR4 and VLA-4. *Leukemia* 26, 34-53. 10.1038/leu.2011.197.

Rieger, M.A., Hoppe, P.S., Smejkal, B.M., Eitelhuber, A.C., and Schroeder, T. (2009). Hematopoietic cytokines can instruct lineage choice. *Science* 325, 217-218. doi: 10.1126/science.1171461.

Ritchie, M.E., Phipson, B., Wu, D., Hu, Y., Law, C.W., Shi, W., and Smyth, G.K. (2015). limma powers differential expression analyses for RNA-sequencing and microarray studies. *Nucleic Acids Res* 43, e47. 10.1093/nar/gkv007.

Roccaro, A.M., Sacco, A., Purschke, W.G., Moschetta, M., Buchner, K., Maasch, C., Zboralski, D., Zöllner, S., Vonhoff, S., Mishima, Y., et al. (2014). SDF-1 inhibition targets the bone marrow niche for cancer therapy. *Cell reports* 9, 118-128. doi: 10.1016/j.celrep.2014.08.042.

Rodin, G., Yuen, D., Mischitelle, A., Minden, M.D., Brandwein, J., Schimmer, A., Marmar, C., Gagliese, L., Lo, C., Rydall, A., and Zimmermann, C. (2013). Traumatic stress in acute leukemia. *Psychooncology* 22, 299-307. 10.1002/pon.2092.

Rombouts, E.J., Pavic, B., Löwenberg, B., and Ploemacher, R.E. (2004). Relation between CXCR-4 expression, Flt3 mutations, and unfavorable prognosis of adult acute myeloid leukemia. *Blood* 104, 550-557. 10.1182/blood-2004-02-0566.

Rombouts, W.J., Blokland, I., Löwenberg, B., and Ploemacher, R.E. (2000a). Biological characteristics and prognosis of adult acute myeloid leukemia with internal tandem duplications in the Flt3 gene. *Leukemia* 14, 675-683. 10.1038/sj.leu.2401731.

Rombouts, W.J., Broyl, A., Martens, A.C., Slater, R., and Ploemacher, R.E. (1999). Human acute myeloid leukemia cells with internal tandem duplications in the Flt3 gene show reduced proliferative ability in stroma supported long-term cultures. *Leukemia* 13, 1071-1078. 10.1038/sj.leu.2401446.

Rombouts, W.J., Martens, A.C., and Ploemacher, R.E. (2000b). Identification of variables determining the engraftment potential of human acute myeloid leukemia in the immunodeficient NOD/SCID human chimera model. *Leukemia* 14, 889-897. 10.1038/sj.leu.2401777.

Rongvaux, A., Willinger, T., Martinek, J., Strowig, T., Gearty, S.V., Teichmann, L.L., Saito, Y., Marches, F., Halene, S., Palucka, A.K., et al. (2014). Development and function of human innate immune cells in a humanized mouse model. *Nat Biotechnol* 32, 364-372. 10.1038/nbt.2858.

Roodman, G.D. (2004). Mechanisms of Bone Metastasis. *New England Journal of Medicine* 350, 1655-1664. doi: 10.1056/NEJMra030831.



Rupp, H.D., K.S.; Dhalla, N.S. (1994). Mechanisms of cardiac cell damage due to catecholamines: significance of drugs regulating central sympathetic outflow. *J Cardiovasc Pharmacol* 24 (1), S16-24. doi: 10.1097/00005344-199424001-00004.

Rupp, H.J., R. (1995). Excess catecholamines and the metabolic syndrome: Should central imidazoline receptors be a therapeutic target? *Medical Hypotheses* 44, 217-225. [https://doi.org/10.1016/0306-9877\(95\)90139-6](https://doi.org/10.1016/0306-9877(95)90139-6).

Sadeghi, L., Arvidsson, G., Merrien, M., M Wasik, A., Görgens, A., Smith, C.I.E., Sander, B., and Wright, A.P. (2020). Differential B-Cell Receptor Signaling Requirement for Adhesion of Mantle Cell Lymphoma Cells to Stromal Cells. *Cancers (Basel)* 12. 10.3390/cancers12051143.

Sanchez, P.V., Perry, R.L., Sarry, J.E., Perl, A.E., Murphy, K., Swider, C.R., Bagg, A., Choi, J.K., Biegel, J.A., Danet-Desnoyers, G., and Carroll, M. (2009). A robust xenotransplantation model for acute myeloid leukemia. *Leukemia* 23, 2109-2117. 10.1038/leu.2009.143.

Sanders, V.M., and Kohm, A.P. (2002). Sympathetic nervous system interaction with the immune system. In *International Review of Neurobiology*, (Academic Press), pp. 17-41. doi: 10.1016/S0074-7742(02)52004-3.

Sarkaria, S.M., Decker, M., and Ding, L. (2018). Bone Marrow Micro-Environment in Normal and Deranged Hematopoiesis: Opportunities for Regenerative Medicine and Therapies. *Bioessays* 40. doi: 10.1002/bies.201700190.

Sarry, J.E., Murphy, K., Perry, R., Sanchez, P.V., Secreto, A., Keefer, C., Swider, C.R., Strzelecki, A.C., Cavelier, C., Récher, C., et al. (2011). Human acute myelogenous leukemia stem cells are rare and heterogeneous when assayed in NOD/SCID/IL2R $\gamma$ -deficient mice. *J Clin Invest* 121, 384-395. 10.1172/JCI41495.

Scanzano, A., and Cosentino, M. (2015). Adrenergic regulation of innate immunity: a review. *Front Pharmacol* 6, 171. doi: 10.3389/fphar.2015.00171.

Scheiermann, C., Kunisaki, Y., Lucas, D., Chow, A., Jang, J.E., Zhang, D., Hashimoto, D., Merad, M., and Frenette, P.S. (2012). Adrenergic nerves govern circadian

leukocyte recruitment to tissues. *Immunity* 37, 290-301. doi: 10.1016/j.immuni.2012.05.021.

Scheller, E.L., Khandaker, S., Learman, B.S., Cawthorn, W.P., Anderson, L.M., Pham, H.A., Robles, H., Wang, Z., Li, Z., Parlee, S.D., et al. (2018). Bone marrow adipocytes resist lipolysis and remodeling in response to beta-adrenergic stimulation. *Bone*. doi: 10.1016/j.bone.2018.01.016.

Schepers, K., Campbell, T.B., and Passegue, E. (2015). Normal and leukemic stem cell niches: insights and therapeutic opportunities. *Cell Stem Cell* 16, 254-267. doi: 10.1016/j.stem.2015.02.014.

Schmidt, C.K., K. (1996). Beta-endorphin and catecholamine concentrations during chronic and acute stress in intensive care patients. *European Journal of Medical Research* 1, 528-532.

Schofield, R. (1978). The relationship between the spleen colony-forming cell and the haemopoietic stem cell. *Blood Cells* 4, 7-25.

Schuurhuis, G.J., Heuser, M., Freeman, S., Béné, M.C., Buccisano, F., Cloos, J., Grimwade, D., Haferlach, T., Hills, R.K., Hourigan, C.S., et al. (2018). Minimal/measurable residual disease in AML: a consensus document from the European LeukemiaNet MRD Working Party. *Blood* 131, 1275-1291. doi: 10.1182/blood-2017-09-801498.

Seidel, J., Niggemann, B., Punzel, M., Fischer, J., Zanker, K.S., and Dittmar, T. (2007). The neurotransmitter GABA is a potent inhibitor of the stromal cell-derived factor-1alpha induced migration of adult CD133+ hematopoietic stem and progenitor cells. *Stem Cells Dev* 16, 827-836. doi: 10.1089/scd.2007.0004.

Shafat, M.S., Gnaneswaran, B., Bowles, K.M., and Rushworth, S.A. (2017). The bone marrow microenvironment - Home of the leukemic blasts. *Blood Rev* 31, 277-286. doi: 10.1016/j.blre.2017.03.004.

Shallis, R.M., Wang, R., Davidoff, A., Ma, X., and Zeidan, A.M. (2019). Epidemiology of acute myeloid leukemia: Recent progress and enduring challenges. *Blood Rev* 36, 70-87. doi: 10.1016/j.blre.2019.04.005.

Sharma, M., Afrin, F., Satija, N., Tripathi, R.P., and Gangenahalli, G.U. (2011). Stromal-derived factor-1/CXCR4 signaling: indispensable role in homing and engraftment of hematopoietic stem cells in bone marrow. *Stem Cells Dev* 20, 933-946. doi: 10.1089/scd.2010.0263.

Shen, H.M., Sha, L.X., Kennedy, J.L., and Ou, D.W. (1994). Adrenergic receptors regulate macrophage secretion. *Int J Immunopharmacol* 16, 905-910. doi: 10.1016/0192-0561(94)90045-0.

Shi, X., He, B.L., Ma, A.C., Guo, Y., Chi, Y., Man, C.H., Zhang, W., Zhang, Y., Wen, Z., Cheng, T., and Leung, A.Y. (2015). Functions of *idh1* and its mutation in the regulation of developmental hematopoiesis in zebrafish. *Blood* 125, 2974-2984. doi: 10.1182/blood-2014-09-601187.

Shiozawa, Y., Eber, M.R., Berry, J.E., and Taichman, R.S. (2015). Bone marrow as a metastatic niche for disseminated tumor cells from solid tumors. *BoneKey Reports* 4. doi: 10.1038/bonekey.2015.57.

Shiozawa, Y., Havens, A.M., Jung, Y., Ziegler, A.M., Pedersen, E.A., Wang, J., Lu, G., Roodman, G.D., Loberg, R.D., Pienta, K.J., and Taichman, R.S. (2008). Annexin II/annexin II receptor axis regulates adhesion, migration, homing, and growth of prostate cancer. *J Cell Biochem* 105, 370-380. doi: 10.1002/jcb.21835.

Shiozawa, Y., Pedersen, E.A., Havens, A.M., Jung, Y., Mishra, A., Joseph, J., Kim, J.K., Patel, L.R., Ying, C., Ziegler, A.M., et al. (2011). Human prostate cancer metastases target the hematopoietic stem cell niche to establish footholds in mouse bone marrow. *In J Clin Invest*, pp. 1298-1312. doi: 10.1172/jci43414.

Shiozawa, Y., Pedersen, E.A., Patel, L.R., Ziegler, A.M., Havens, A.M., Jung, Y., Wang, J., Zalucha, S., Loberg, R.D., Pienta, K.J., and Taichman, R.S. (2010). GAS6/AXL axis regulates prostate cancer invasion, proliferation, and survival in the bone marrow niche. *Neoplasia (New York, N.Y.)* 12, 116-127. PMID: 20126470.

Sipkins, D.A., Wei, X., Wu, J.W., Runnels, J.M., Côté, D., Means, T.K., Luster, A.D., Scadden, D.T., and Lin, C.P. (2005). In vivo imaging of specialized bone marrow

endothelial microdomains for tumour engraftment. *Nature* 435, 969-973. doi: 10.1038/nature03703.

Sison, E.A., McIntyre, E., Magoon, D., and Brown, P. (2013). Dynamic chemotherapy-induced upregulation of CXCR4 expression: a mechanism of therapeutic resistance in pediatric AML. *Mol Cancer Res* 11, 1004-1016. 10.1158/1541-7786.MCR-13-0114.

Sloan, E.K., Priceman, S.J., Cox, B.F., Yu, S., Pimentel, M.A., Tangkanangnukul, V., Arevalo, J.M.G., Morizono, K., Karanikolas, B.D.W., Wu, L., et al. (2010). The sympathetic nervous system induces a metastatic switch in primary breast cancer. *Cancer research* 70, 7042-7052. doi: 10.1158/0008-5472.CAN-10-0522.

Song, Y., Gan, Y., Wang, Q., Meng, Z., Li, G., Shen, Y., Wu, Y., Li, P., Yao, M., Gu, J., and Tu, H. (2017). Enriching the Housing Environment for Mice Enhances Their NK Cell Antitumor Immunity via Sympathetic Nerve-Dependent Regulation of NKG2D and CCR5. *Cancer Res* 77, 1611-1622. doi: 10.1158/0008-5472.can-16-2143.

Sood, A.K., Armaiz-Pena, G.N., Halder, J., Nick, A.M., Stone, R.L., Hu, W., Carroll, A.R., Spannuth, W.A., Deavers, M.T., Allen, J.K., et al. (2010). Adrenergic modulation of focal adhesion kinase protects human ovarian cancer cells from anoikis. *J Clin Invest* 120, 1515-1523. doi: 10.1172/jci40802.

Spiegel, A., Shivtiel, S., Kalinkovich, A., Ludin, A., Netzer, N., Goichberg, P., Azaria, Y., Resnick, I., Hardan, I., Ben-Hur, H., et al. (2007). Catecholaminergic neurotransmitters regulate migration and repopulation of immature human CD34+ cells through Wnt signaling. *Nat Immunol* 8, 1123-1131. doi: 10.1038/ni1509.

Spoos, A.C., Lubbert, M., Wierda, W.G., and Burger, J.A. (2007). CXCR4 is a prognostic marker in acute myelogenous leukemia. *Blood* 109, 786-791. 10.1182/blood-2006-05-024844.

Stevenson, L.W., Laks, H., Terasaki, P.I., Kahan, B.D., and Drinkwater, D.C. (1988). Cardiac transplantation. Selection, immunosuppression, and survival. *West J Med* 149, 572-582.

Strell, C., Niggemann, B., Voss, M.J., Powe, D.G., Zanker, K.S., and Entschladen, F. (2012). Norepinephrine promotes the beta1-integrin-mediated adhesion of MDA-MB-

231 cells to vascular endothelium by the induction of a GRO $\alpha$  release. *Mol Cancer Res* 10, 197-207. doi: 10.1158/1541-7786.mcr-11-0130.

Subramanian, A., Tamayo, P., Mootha, V.K., Mukherjee, S., Ebert, B.L., Gillette, M.A., Paulovich, A., Pomeroy, S.L., Golub, T.R., Lander, E.S., and Mesirov, J.P. (2005). Gene set enrichment analysis: a knowledge-based approach for interpreting genome-wide expression profiles. *Proc Natl Acad Sci U S A* 102, 15545-15550. 10.1073/pnas.0506580102.

Sugiyama, T.K., H.; Noda, M.; Nagasawa, T. (2006). Maintenance of the hematopoietic stem cell pool by CXCL12-CXCR4 chemokine signaling in bone marrow stromal cell niches. *Immunity* 25, 977-988. 10.1016/j.immuni.2006.10.016.

Sun, Y., Wan, J., Song, Q., Luo, C., Li, X., Luo, Y., Huang, X., Ding, R., Li, H., Hou, Y., et al. (2021). Prognostic Significance of CD56 Antigen Expression in Patients with. *Biomed Res Int* 2021, 1929357. 10.1155/2021/1929357.

Sun, Y.X., Fang, M., Wang, J., Cooper, C.R., Pienta, K.J., and Taichman, R.S. (2007). Expression and activation of alpha v beta 3 integrins by SDF-1/CXC12 increases the aggressiveness of prostate cancer cells. *Prostate* 67, 61-73. doi: 10.1002/pros.20500.

Sun, Y.X., Schneider, A., Jung, Y., Wang, J., Dai, J., Cook, K., Osman, N.I., Koh-Paige, A.J., Shim, H., Pienta, K.J., et al. (2005). Skeletal localization and neutralization of the SDF-1(CXCL12)/CXCR4 axis blocks prostate cancer metastasis and growth in osseous sites in vivo. *J Bone Miner Res* 20, 318-329. doi: 10.1359/jbmr.041109.

Taichman, R.S.R., M. J., and Emerson, S.G. (1996). Human osteoblasts support human hematopoietic progenitor cells in vitro bone marrow cultures. *Blood*.

Taussig, D.C., Vargaftig, J., Miraki-Moud, F., Griessinger, E., Sharrock, K., Luke, T., Lillington, D., Oakervee, H., Cavenagh, J., Agrawal, S.G., et al. (2010). Leukemia-initiating cells from some acute myeloid leukemia patients with mutated nucleophosmin reside in the CD34(-) fraction. *Blood* 115, 1976-1984. 10.1182/blood-2009-02-206565.

Tavor, S.P., I.; Porozov, S.; Avigdor, A.; Dar, A.; Leider-Trejo, L.; Shemtov, N.; Deutsch, V.; Naparstek, E.; Nagler, A.; Lapidot, T. (2004). CXCR4 regulates migration

and development of human acute myelogenous leukemia stem cells in transplanted NOD/SCID mice. *Cancer research* 64, 2817-2824. 10.1158/0008-5472.can-03-3693.

Team., R.C. (2008). *A language and environment for statistical computing*. R Foundation for Statistical Computing, Vienna, Austria

Thaker, P.H., Han, L.Y., Kamat, A.A., Arevalo, J.M., Takahashi, R., Lu, C., Jennings, N.B., Armaiz-Pena, G., Bankson, J.A., Ravoori, M., et al. (2006). Chronic stress promotes tumor growth and angiogenesis in a mouse model of ovarian carcinoma. *Nat Med* 12, 939-944. doi: 10.1038/nm1447.

Traggiai, E., Chicha, L., Mazzucchelli, L., Bronz, L., Piffaretti, J.C., Lanzavecchia, A., and Manz, M.G. (2004). Development of a human adaptive immune system in cord blood cell-transplanted mice. *Science* 304, 104-107. 10.1126/science.1093933.

Treaba, D.O., Bonal, D.M., Chorzalska, A.D., Schorl, C., Hopkins, K., Reagan, J.L., Rintels, P., Quesenberry, P.J., and Dubielecka, P.M. (2020). Levels of Osteopontin ( SPP1 ), Osteonectin ( SPARC ) and Biglycan ( BGN ) in Acute Myeloid Leukemia Bone Marrow Biopsies Post-Induction Therapy Define the Status of Osteogenic Niche and Show Inverse Correlation with Therapeutic Response. *Blood*.

Vaiselbuh, S.R., Edelman, M., Lipton, J.M., and Liu, J.M. (2010). Ectopic human mesenchymal stem cell-coated scaffolds in NOD/SCID mice: an in vivo model of the leukemia niche. *Tissue Eng Part C Methods* 16, 1523-1531. 10.1089/ten.tec.2010.0179.

Van Acker, H.H., Capsomidis, A., Smits, E.L., and Van Tendeloo, V.F. (2017). CD56 in the Immune System: More Than a Marker for Cytotoxicity? *Front Immunol* 8, 892. 10.3389/fimmu.2017.00892.

Vick, B., Rothenberg, M., Sandhöfer, N., Carlet, M., Finkenzeller, C., Krupka, C., Grunert, M., Trumpp, A., Corbacioglu, S., Ebinger, M., et al. (2015). An advanced preclinical mouse model for acute myeloid leukemia using patients' cells of various genetic subgroups and in vivo bioluminescence imaging. *PLoS One* 10, e0120925. 10.1371/journal.pone.0120925.

Vila, L.T., X.; Campos, L.; Sabido, O.; Archimbaud, E. (1995). Expression of VLA molecules on acute leukemia cells: relationship with disease characteristics. *Exp Hematol* 23.

Villatoro, A., Konieczny, J., Cuminetti, V., and Arranz, L. (2020). Leukemia Stem Cell Release From the Stem Cell Niche to Treat Acute Myeloid Leukemia. *Front Cell Dev Biol* 8, 607. 10.3389/fcell.2020.00607.

Visnjic, D., Kalajzic, Z., Rowe, D.W., Katavic, V., Lorenzo, J., and Aguila, H.L. (2004). Hematopoiesis is severely altered in mice with an induced osteoblast deficiency. *Blood* 103, 3258-3264. 10.1182/blood-2003-11-4011.

Voermans, C.v.H., W. P. M.; de Jong, I.; Gerritsen, W.R.; van Der Schoot, C. E. (2002). Migratory behavior of leukemic cells from acute myeloid leukemia patients. *Leukemia* 16, 650-657. 10.1038/sj.leu.2402431.

Weberpals, J., Jansen, L., Carr, P.R., Hoffmeister, M., and Brenner, H. (2016). Beta blockers and cancer prognosis - The role of immortal time bias: A systematic review and meta-analysis. *Cancer Treat Rev* 47, 1-11. doi: 10.1016/j.ctrv.2016.04.004.

website, C.R.L. (consulted 30.07.2021). SCID mice. <https://www.criver.com/products-services/research-models-services/animal-models/mice/immunodeficient-mice/scid-mice?region=36169>.

Wei, Q., and Frenette, P.S. (2018). Niches for Hematopoietic Stem Cells and Their Progeny. *Immunity* 48, 632-648. doi: 10.1016/j.immuni.2018.03.024.

Westwood, J.A., Darcy, P.K., and Kershaw, M.H. (2013). Environmental enrichment does not impact on tumor growth in mice. *F1000Res* 2, 140. doi: 10.12688/f1000research.2-140.v1.

Wirth, F., Lubosch, A., Hamelmann, S., and Nakchbandi, I.A. (2020). Fibronectin and Its Receptors in Hematopoiesis. *Cells* 9. 10.3390/cells9122717.

Wunderlich, M., Chou, F.S., Link, K.A., Mizukawa, B., Perry, R.L., Carroll, M., and Mulloy, J.C. (2010). AML xenograft efficiency is significantly improved in NOD/SCID-

IL2RG mice constitutively expressing human SCF, GM-CSF and IL-3. *Leukemia* 24, 1785-1788. 10.1038/leu.2010.158.

Xu, C., Gao, X., Wei, Q., Nakahara, F., Zimmerman, S.E., Mar, J., and Frenette, P.S. (2018). Stem cell factor is selectively secreted by arterial endothelial cells in bone marrow. *Nat Commun* 9, 2449. 10.1038/s41467-018-04726-3.

Xu, S., Li, X., Zhang, J., and Chen, J. (2015). Prognostic value of CD56 in patients with acute myeloid leukemia: a meta-analysis. *J Cancer Res Clin Oncol* 141, 1859-1870. 10.1007/s00432-015-1977-3.

Yap, A., Lopez-Olivo, M.A., Dubowitz, J., Pratt, G., Hiller, J., Gottumukkala, V., Sloan, E., Riedel, B., and Schier, R. (2018). Effect of beta-blockers on cancer recurrence and survival: a meta-analysis of epidemiological and perioperative studies. *Br J Anaesth* 121, 45-57. doi: 10.1016/j.bja.2018.03.024.

Yu, V.W., Saez, B., Cook, C., Lotinun, S., Pardo-Saganta, A., Wang, Y.H., Lymperi, S., Ferraro, F., Raaijmakers, M.H., Wu, J.Y., et al. (2015). Specific bone cells produce DLL4 to generate thymus-seeding progenitors from bone marrow. *J Exp Med* 212, 759-774. 10.1084/jem.20141843.

Zahalka, A.H., Arnal-Estape, A., Maryanovich, M., Nakahara, F., Cruz, C.D., Finley, L.W.S., and Frenette, P.S. (2017). Adrenergic nerves activate an angio-metabolic switch in prostate cancer. *Science* 358, 321-326. 10.1126/science.aah5072.

Zhang, C.C., and Lodish, H.F. (2008). Cytokines regulating hematopoietic stem cell function. *Curr Opin Hematol* 15, 307-311. doi: 10.1097/MOH.0b013e3283007db5.

Zhang, J., Deng, Y.-t., Liu, J., Wang, Y.-q., Yi, T.-w., Huang, B.-y., He, S.-s., Zheng, B., and Jiang, Y. (2016). Norepinephrine induced epithelial–mesenchymal transition in HT-29 and A549 cells in vitro. *Journal of Cancer Research and Clinical Oncology* 142, 423-435. doi: 10.1007/s00432-015-2044-9.

Zhang, L., Gajewski, T.F., and Kline, J. (2009). PD-1/PD-L1 interactions inhibit antitumor immune responses in a murine acute myeloid leukemia model. *Blood* 114, 1545-1552. 10.1182/blood-2009-03-206672.



Zhang, W., Ching Lo, H., Xiang, and Zhang, H.F. (2017). Mapping bone marrow niches of disseminated tumor cells. *Science China Life Science* 60, 1125-1132. doi: 10.1007/s11427-017-9180-5.

Zizioli, D., Mione, M., Varinelli, M., Malagola, M., Bernardi, S., Alghisi, E., Borsani, G., Finazzi, D., Monti, E., Presta, M., and Russo, D. (2019). Zebrafish disease models in hematology: Highlights on biological and translational impact. *Biochim Biophys Acta Mol Basis Dis* 1865, 620-633. 10.1016/j.bbadis.2018.12.015.

Zorko, N.A., Bernot, K.M., Whitman, S.P., Siebenaler, R.F., Ahmed, E.H., Marcucci, G.G., Yanes, D.A., McConnell, K.K., Mao, C., Kalu, C., et al. (2012). Mll partial tandem duplication and Flt3 internal tandem duplication in a double knock-in mouse recapitulates features of counterpart human acute myeloid leukemias. *Blood* 120, 1130-1136. 10.1182/blood-2012-03-415067.

# APPENDIX: CV

**PROFESSIONAL EXPERIENCE**

Since September 2017	PhD student position: "Investigation of catecholamine-based mechanisms regulating acute myeloid leukemia in a mouse xenotransplantation model" University hospital Basel (Switzerland), Department of Biomedicine, Team Stem Cells and Hematopoiesis, Prof. C. Lengerke
February 2017 - September 2017	Master student position: "Charakterization of double transgenic Evi1/RAS- induced zebrafish leukemia models"; University hospital Basel (Switzerland), Departement of Biomedicine, Team „Stem Cells and Hematopoiesis“, Prof. C. Lengerke
2015 (4 Months)	Intern Position: Quality insurance and production of homeopathic drugs; Boiron SA, Illkirch-Graffenstaden (France)
2014 (4 Weeks)	Intern Position: "Tumor cells xenograft in Zebrafish embryos to study the metastatic process <i>in vivo</i> " INSERM U1109 Hautepierre (France), „Micro-Environmental Niche in Tumorigenesis and Targeted Therapy“, Dr. J. Goetz
2008 - 2015	Different temporary work experiences Waitress in restaurants (Ferme-Auberge de la Tirelire Cosswiller, Le Relais de Wasselonne), Baby-Sitting, private tutoring.

**EDUCATION**

2014 - 2017	Engineering degree in Biotechnology with honors (Ecole Supérieure de Biotechnologie de Strasbourg), Illkirch-Graffenstaden Tri-national school including courses in the university of Basel (Switzerland) and Freiburg-im-Breisgau (Germany) Multidisciplinary courses in biology and biotechnology, engineering sciences, languages and social and economic sciences.
2016 - 2017	Master 2 in drug design and conception (Pharmacy Faculty) Strasbourg Study of biological and chemical characteristics if drug molecules and its action on target molecules, identification of potential therapeutic targets
2012 - 2014	Two years university degree in Biology and Chemistry, Université de Strasbourg Biology, Biochemistry, Metabolism, Organic Chemistry, Thermodynamics
2012	Baccalauréat in Sciences (Life Sciences, Chemistry and Mathematics) with honors, Lycée Général et Technologique Leclerc, Saverne

**SOFT SKILLS**

Languages	French (native speaker), English (business fluent, TOIEC: 920, 2016), German (fluent), Spanisch (elementary)		
Animal experimentation	LTK-Module 1: Training in animal experimentation, recognized as FELASA B (Federation of European Laboratory Animal Sciences Association)		
Project Management	8-Module Workshop: Project management for researchers with Dr. D. Krstic		

**COMPUTER SKILLS**

<b>General</b>	Word, Excel, PowerPoint, Inkscape, Affinity Designer	Flow cytometry Image processing Programming Citation	FlowJo (good) Fiji/Image J (good) Prism (very good) Mendeley/Endnote (very good)
<b>Data processing</b>	Prism (very good)		

## Pauline HANNS



**Contact**

 +33 6 66 94 99 24

 [pauline.hanns@unibas.ch](mailto:pauline.hanns@unibas.ch)

 3, impasse des Rossignols  
68680 KEMBS  
FRANCE

**Personal data**

**Date of Birth:** 17.06.1994

**Nationality:** French

**Familial status:** married,  
1 Child

## SCIENTIFIC METHODS

Molecular biology	RNA/DNA isolation, RNA/DNA purification, DNA gel extraction, PCR, reverse transcription, qPCR, ELISA, CRISPR/CAS9
Cell Biology	Isolation and cultivation of human primary leukemia cells/ cell lines, isolation of cord blood-derived hematopoietic stem cells, magnetic-activated cell sorting, colony forming unit assay, adhesion assay with bone marrow stromal cells, cytospins, flow cytometry, affinity assay
Mouse-Handling	Blood collection, injection methods (intraperitoneal, intravenous, intrafemoral), bone marrow puncture, organ collection
Zebrafisch-Handling	Crossing, embryo sorting, kidney marrow and blood collection, tail clip genotyping, eye/heart cell transplantation, imaging (confocal and fluorescent microscopes)

## PARTICIPATION TO CONFERENCES

2017 Frankfurt am Main	"Characterization of HRAS-induced myeloid neoplasia in zebrafish", 46. Annual scientific meeting of ISEH (International society for experimental hematology), Poster presentation
2018 Vienna	"Investigation of catecholamine-based mechanisms regulating leukemia induction in a xenotransplantation model of human acute myeloid leukemia", Annual scientific meeting of DGHO (Deutsche Gesellschaft für Hämatologie und medizinische Onkologie), Poster presentation price
2018 San Diego	"Catecholamine exposure accelerates in vivo leukemogenesis in acute myeloid leukemia patient derived xenografts" 60. Annual scientific meeting of ASH (American Society for Hematology), Poster presentation
2019 Orlando	"Night transplantation and catecholamine exposure accelerates in vivo leukemia development by enhancing bone marrow homing capacity in leukemic cells" und "Investigation of homing capacity as prognostic marker in human acute myeloid leukemia" 61. Annual scientific meeting of ASH (American Society for Hematology), Poster presentations

## PERSONAL INTERESTS

Member and ex-president of a newly created association which tends to help women and children over the world (Golden Z Les Louissettes, Saverne-Metz-Strasbourg)

Jogging, Cooking and Baking, Long-distance bicycling trip

## REFEREES

### Prof. Dr. Claudia Lengerke

Universitätsspital Basel, Department Biomedicine  
Hebelstrasse 20, BASEL  
And  
Universitätsklinikum Tübingen  
Otfried-Müller-Strasse 10, TÜBINGEN  
+49 70712982770  
claudia.lengerke@unibas.ch

### Prof. Dr. Georges ORFANOUDAKIS

ESBS school director in 2017  
UMR7242 Biotechnologie et Signalisation  
Cellulaire – ESBS  
300, boulevard Sébastien Brant  
67412 ILLKIRCH  
+33 3 68 85 47 65  
georges.orfanoudakis@unistra.fr

### Supervised by Dr. Martina Konantz

Universitätsspital Basel, Department Biomedicine  
Hebelstrasse 20, BASEL  
+41 613 28 55 87  
martina.konantz@unibas.ch